Optimization of an industrial L-lysine producing Corynebacterium glutamicum strain

Kjeldsen, Kjeld Raunkjær; Nielsen, Jens

Publication date:
2009

Document Version
Publisher's PDF, also known as Version of record

Optimization of an industrial L-lysine producing *Corynebacterium glutamicum* strain

Industrial Ph.D. Thesis

Kjeld Raunkjær Kjeldsen

Center for Microbial Biotechnology
Department of Systems Biology
Technical University of Denmark

and

Agro&Ferm A/S

2008

Preface

This research work was carried out at Center for Microbial Biotechnology, the Technical University of Denmark and at Agro&Ferm A/S, during June 2005-June-2008 under the supervision of Professor Jens Nielsen. The project was an Industrial PhD project.

I would like to express my thanks to Jens Nielsen for guiding me through the PhD study, and for many fruitful discussions and brilliant ideas. Without his convincing and engaged supervision I am sure this project would not have been the same.

I would like to express my thanks to my colleagues at CMB. It has been a pleasure to be part of the CMB family, and I have had the opportunity to work with many of you. I would like to thank Ana Oliveira and Michael Rørdam Andersen for helping at the construction of the genome-scale model. I would like to thank Anni Jensen, Anna Lantz and Jette Tykjær for assistance at metabolic flux estimations.

I would also like to thank my colleagues at Agro&Ferm A/S. Many of you have assisted this work by sample taking and other experimental work. I would like to express a special thank to CEO, Vagn Hundebøll for giving me the opportunity to do a PhD project. And I would like to thank Manager of R&D, Henrik Pedersen for many fruitful discussions about this project and future perspectives.

Last but not least I would like to thank my friends and my family for support and encouragement throughout this Ph.D. study. They were behind me throughout and I thank them sincerely.

Kjeld Raunkjær Kjeldsen
June 2008

Content

Summary

Optimization of lysine production in an industrial relevant lysine producing *Corynebacterium glutamicum* strain was done using a combination of mathematically modelling, metabolic engineering and metabolic flux estimation.

A mathematical model of the metabolic network of *C. glutamicum* based on genomic information, and based on the wealth of biochemical information which is available for this organism due to its long history as a commercial relevant organism was constructed and validated against earlier published data. The model comprising 446 reactions and 411 metabolites was extensively validated against earlier published data. The model was used to analyze the metabolic network during lysine production, and based on this a number of biochemical hypotheses were suggested to improve lysine production in *C. glutamicum*. The first prediction made by the model was that a high ATP production under high lysine production resulted in a limitation in lysine production. This was the case at high lysine yield (>55%) and low growth. Secondly, the model predicted a limitation in lysine production when the succinylase branch of the lysine synthetic pathway was preferred over the dehydrogenase branch. The result was a decrease in maximal theoretical lysine yield from 0.75 mmol lysine · (mmol glucose)$^{-1}$ to 0.57 mmol lysine · (mmol glucose)$^{-1}$ due to a relatively higher activity of the TCA cycle because of the involvement of the TCA intermediate Succinyl-CoA. The higher TCA cycle activity was suboptimal for lysine production because of a loss of carbon due to CO_2 –production. Thirdly, the model predicted a correlation between a high pentose phosphate pathway flux and high lysine production. The fourth prediction made from the analysis of the *in silico* model was that there is a correlation between increasing anaplerotic net flux and increasing lysine production.

Various metabolic engineering strategies were tested in a high producing *C. glutamicum* strain Based on the findings in the metabolic network reconstruction and based on results reported in literature three parts of the metabolism were selected for metabolic engineering. As predicted by the *in silico* model the pentose phosphate pathway is a target as it may lead to an increase in the NADPH formation. The two NADPH generating enzymes glucose-6-phosphate dehydrogenase (*zwf*) and 6-phosphogluconate dehydrogenase (*gnd*) were up-regulated, and both modifications were seen to have a positive effect on lysine yield of 5% and 6%, respectively, indicating that NADPH was in fact limiting under high lysine producing conditions. The enzyme pyruvate carboxylase was also selected for up-regulations to increase the anaplerotic net flux, which is believed to be beneficial for lysine production based on findings in literature and predictions by the *in silico* model. This modification resulted in a decrease in lysine production and did not fit the initial expectations. Five enzymes in the lysine synthetic pathway were selected for up-regulation based on results found in literature. The enzymes were aspartate kinase (*lysC*), dihydrodipicolate syntase (*dapA*), succinylaminoketopimelate transaminase (*dapC*), diaminopimelate epimerase (*dapF*) and lysine permerase (*lysE*). Only the strain with an up-regulated aspartate kinase activity showed a significant effect on the overall lysine yield, and this effect was negative. In this study it was seen that although metabolic engineering strategies had earlier shown to be beneficial for lysine production in *C. glutamicum* strains, many of these strategies could not be transferred directly to a high producing industrial strain.

Finally, estimations of *in vivo* fluxes under growth and lysine production in complex medium and during batch and fed-batch fermentation were conducted. For the industrial strain, *C. glutamicum* KK-11, a higher flux through the pentose phosphate pathway was seen compared to earlier published data. In addition to flux estimations during balanced growth present in the batch phase of the fermentation the method was employed on samples from the fed-batch phase of the fermentation. These results were used to identify metabolic changes when the physiological state of the cells was changed. The tendencies identified employing this method was an increase in the pentose phosphate pathway flux, a decrease in the TCA flux, and an increase in the anaplerotic net flux. Another *C. glutamicum* strain, ATCC 21253, earlier used in flux estimation studies were also included in the flux estimation study. This strain was found to have lower pentose phosphate pathway flux compared to the industrial strain. And during the change from batch to fed-batch fermentation the tendencies were different than what was seen for the industrial strain. The pentose phosphate pathway flux was increased as seen for the industrial strain, but the TCA flux was increased and the anaplerotic net flux decreased.

Dansk Sammenfatning

Optimering af lysin produktion i en industriel relevant *Corynebacterium glutamicum* stamme blev udført ved at anvende en kombination af matematisk modellering, "metabolic engineering" og estimering af intracellulære metaboliske fluxe.

En matematisk model af det metaboliske netværk i *C. glutamicum* blev lavet baseret på tilgængelige information fra genomet for denne organisme, samt ved at anvende den imponerende mængde af tilgængelig biologisk og biokemisk information. Modellen blev valideret mod tidligere publicerede data. Modellen består af 446 reaktioner samt 411 metabolitter. Modellen blev anvendt til at analysere det metaboliske netværk for *C. glutamicum* under forskellige vækst- og lysin producerende betingelser, og baseret på dette blev en række biologiske hypoteser til at øge lysindannelsen i denne organisme foreslået. Den første hypotese gik ud på at der under stor lysinproduktion og lav vækst blev dannet et overskud af ATP, og at dette overskud fører til en reduktion i lysinproduktionen. Modellen forudså at dette var et problem når lysinudbyttet er over 55%. Den anden forudsigelse lavet ved brug af modellen var at der er en begrænsning i lysinsyntese-vejen når succinylase-vejen blev foretrukket frem for dehydrogenase-vejen. Resultatet var ifølge modellen at det teoretiske maksimale udbytte faldt fra 75% til 57% på grund af en højere aktivitet af TCA cyklus for at producere succinyl-CoA, som indgår som led i lysindannelsen når syccinyl-vejen bliver brugt. En højere TCA cyklus aktivitet er suboptimal for lysinsyntese fordi der mistes kulstof til CO_2 –produktion. Modellen forudså desuden en sammenhæng mellem en højere flux gennem pentose fosfat-vejen og en højere lysinproduktion. Dette var ifølge modellen også tilfældet for et højre anaplerotisk netfluks.

Forskellige "metabolic engineering" strategier til forøgelse af lysin udbyttet i en højt producerende *C. glutamicum* stamme blev testet. Baseret til dels på simulerings resultater fra den metaboliske matematiske model og resultater fra den videnskabelige litteratur tre dele af metabolismen blev udvalgt til metabolic engineering. Den matematiske model forudså at en forøget flux gennem pentose fosfat-vejen ville øge lysineudbyttet, angiveligt fordi NADPH vil blive begrænsende ved høje lysinudbytter. De to NADPH genererende enzymer glucose-6-phosphate dehydrogenase (*zwf*) of 6-phosphogluconate dehydrogenase (*gnd*) blev udvalgt til opregulering. Begge modifikationer gav et positivt resultat med henholdsvis 5% og 6% bedre udbytter, hvilket indikerede at NADPH var begrænsende for lysinproduktionen i denne stamme. Enzymet pyruvate decarboxylase (*pyc*) blev ligeledes udvalgt til opregulering fordi en øget anaplerotic netflux har vist sig at være korreleret med øget lysinproduktion, både baseret på resultater fra litteraturen og den matematiske models forudsigelser. Resultaterne var dog ikke som forventet, idet effekten var negativ. Fem reaktioner i lysinsyntese-vejen blev overudtrykt. Disse blev valgt baseret på tidligere resultater rapporteret i litteraturen. De fem reaktioner var aspartate kinase (*lysC*), dihydrodipicolate syntase (*dapA*), succinylaminoketopimelate transaminase (*dapC*), diaminopimelate epimerase (*dapF*) og lysine permerase (*lysE*). Kun stammen med en overudtrykt aspartate kinase viste en effekt, og denne effekt var negativ på lysinudbyttet. I dette studie blev det set at selvom nogle "metabolic engineering" strategier har vist sig at have positiv effekt i nogle stammer kan dette ikke altid overføres direkte til en industriel stamme.

Estimering af *in vivo* fluxe under vækst og lysinproduktion i komplekst medium og under både batch og fed-batch fermentering blev udført. For den industrielle stamme, *C. glutamicum* KK-11,

blev der set en betydeligt højere flux gennem pentose phosphat-vejen end der normalt ses for *C. glutamicum* stammer. Foruden flux estimering under balanceret vækst der ses under den eksponentielle vækstfase, blev der ligeledes lavet flux estimering for prøver udtaget under fed-batch fasen. Disse resultater blev brugt til at identificere flux ændringer som følge af den fysiologiske ændring der skete i cellerne som et resultat af at kulturen gik fra batch til fed-batch fermentering. Resultaterne viste at fluxen gennem pentose fosfat-vejen blev forøget, mens fluxen gennem TCA cyklus gik ned og den anaplerotiske netflux gik op. En anden *C. glutamicum* stamme, ATCC 21253, blev ligeledes analyseret med denne metode. Denne stamme, der producerer lysin, men i mindre grad end den industrielle stamme, viste andre tendenser end den industrielle stamme. Fluxen gennem pentose fosfat-vejen gik op i fed-batch fasen, som det var tilfældet for den indusrielle stamme, mens TCA cyklus fluxen gik op og den anaplerotiske net flux gik ned hvilket var modsat hvad der var set for den industrielle stamme.

Chapter 1

1. Introduction

Bacteria belonging to the genus *Corynebacterium* are due to their ability to produce and secrete a number of industrially important amino acids and nucleotides used in industrial production processes, in particular for large scale production of the amino acids glutamate and lysine.

Lysine is produced in an aerobic fermentation process using the bacterium *Corynebacterium glutamicum* or *Escherichia coli*. Lysine is an essential amino acid for animals, and since the content of lysine often is suboptimal in corn, barley and wheat, the feedstuffs traditionally used as the major ingredients for animal feed, this amino acid often becomes limiting for feed efficiency. Supplementing lysine in concentrations between 0.5% and 1% to the feed leads to an optimized protein utilization of the feed which improves the growth of especially pigs and poultry with up to 20%. In addition to the economical benefit from the increased productivity, less nitrogen is released to the environment, which is an issue that has received a lot of attention in recent years.

As lysine-production costs have been lowered due to a continuous optimization of the process, the lysine price has followed this development and the demand has increased leading to an annual production of 1,100,000 tones lysine,HCl annually (Feedinfo.com). Since the demand for white meat from pigs and poultry is increasing in a combination with environmental issues, a further increase in lysine demand of about 8% per year is expected (Feedinfo.com). In spite of increased lysine demands worldwide, further development of the lysine production process, including strain development is essential to be competitive in the lysine production-business.

A biotechnological production process like lysine production with *C. glutamicum*, employ self reproducing living organisms, which serves as living cell factories for the conversion of chemicals involving a complex network of enzymes, substrates and products inside and outside the cell. The development and optimization of production strains by random mutagenesis followed by extensive screening programs to find and isolate superior mutants have been shown to be a successful strategy. However, with the rapid development of methods for metabolic engineering this has opened new possibilities for strain improvements by targeted genetic modifications. Today, experimental protocols for almost any genetic manipulation in *C. glutamicum* are available. The challenge is not how to apply the genetic manipulations - but where to apply them.

The major challenge in this respect is that living organisms are complex systems with thousands of reactions and multiple variables interacting with each other. Using traditional reductionistic approaches focusing on the generation of information about individual cellular components is often not enough when such complex networks needs to be analyzed. A more holistic approach needs to be applied focusing on the system rather than the individual reactions.

With the developments in genomics there has been an increased focus on the behavior of complete biological systems, which has led to the development of systems biology. Biological data from different levels of the metabolism, i.e. genome, fluxome, transcriptome, metabolome, proteome and interactome are integrated in order to analyze an organism. To cope with the large amount of data

generated the development of mathematical models describing the biological systems has played a major role in systems biology. With the large sequencing-effort that has been conducted recently, whole genomes are now made available, including the *C. glutamicum* genome. This information can be used to make mathematical models which can serve as platforms for whole cell models able to predict cellular phenotypes.
Within the field of metabolic engineering the prediction power of mathematical models can be used to find and select targets for metabolic engineering strategies.

Corynebacterium – A working horse in amino acid production

The production of amino acids is in terms of quantity the third most important within white biotechnology, only surpassed by ethanol- and antibiotics production (Leuchtenberger *et al.*, 2005). The two most important amino acids in this respect are L-glutamate and L-lysine with a marked value exceeding $1.5 billion annually (Demain and Adrio, 2008), both of which is produced by various species of the genera *Corynebacterium* and *Brevibacterium*. In addition to lysine and glutamate *Corynebacterium* has also been used as a platform for the production of other amino acids such as L-threonine (Shiio, 1990; Kase and Nakayama, 1974; Shiio *et al.*, 1991), L-methionine (Nakayama *et al.*, 1973; Kase and Nakayama, 1975), L-serine (Eggeling, 2007), L-histidine (Araki *et al.*, 1974), L-valine (Ruklisha *et al.*, 2007), L-tryptophan (Ikeda, 2006), L-phenylalanine and L-tyrosine (Ikeda and Katsumata, 1992), L-leucine (Pátek, 2007) and L-isoleucine (Guillout *et al.*, 2002).

Industrial L-lysine production

The first steps towards industrial production of lysine were done in Japan in the 1950s when Kyowa Hakko Co., Ltd., Tokyo started a research program aiming at finding a microorganim able to produce glutamate. One of the results from this was the isolation of a microorganism *Micrococcus glutamicus*, later renamed to *C. glutamicum*, which was able to produce glutamate (Kinoshita *et al.*, 1957; Udaka, 1960). During the following mutagenesis and screening program lysine producing mutants were discovered (Kinoshita *et al.*, 1958), and the foundation for lysine production was made. Within a few years the first large scale lysine production facility was in use.
Since then lysine fermentation processes have been developed for the very large scale as the demand for a cost effective production has increased as product-prices have decreased. Today lysine production involves fermentation in very large fermentation tanks, often exceeding hundreds of cubic meters, which makes it challenging to obtain homogeneity in the fermenter and to maintain sufficient mass-transfer rates. Normally traditional stirred-tank reactors are used since they allow for a high specific power intake, which makes it possible to obtain high oxygen transfer rates (Kelle *et al.*, 2005). The fermentation process consists of multiple steps with several propagation steps to obtain sufficient biomass for the main fermentation process. The number of propagation steps can vary, but usually 1:10 steps between each propagation step is applied (Hermann, 2003). To optimize lysine yield and productivity the process is normally run as a fed-batch or repeated fed-batch process. Attempts have been made to develop a continuous process (Hirao *et al.*, 1989). However, due to numerous practical aspects such as sterility and strain stability in industrial scale, continuous production is generally not applied (Kelle *et al.*, 2005).

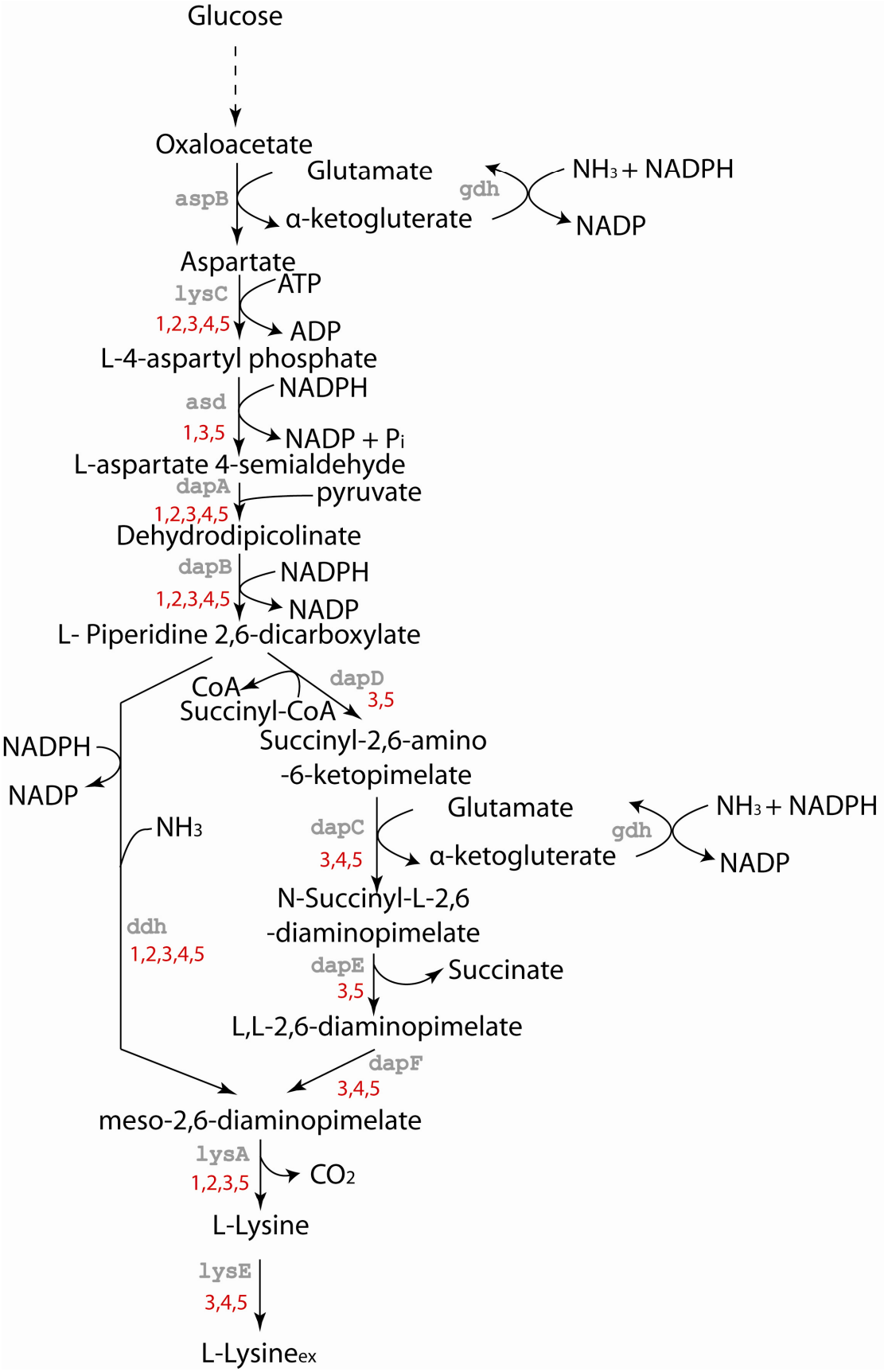

Figure 1.1: Lysine biosynthetic pathway in *Corynebacterium glutamicum*, including gene-names (grey letters) and patent and patent applications (red numbers) claming an improved lysine production through modification of the lysine biosynthetic pathway in *C. glutamicum*. The information on patents and the companies behind the patents (1: Archer Daniels Midland, 2: Ajinomoto, 3: BASF, 4: Degussa (now Evonik); 5: Kyowa Hakko Kogyo) was taken from Kelle *et al.* (2005).

The lysine synthetic pathway in C. glutamicum

An overview of the lysine synthetic pathway in *C. glutamicum* can be seen in figure 1.1. Lysine is produced in seven or ten steps from its precursor oxaloacetate, depending on which route is used. The first step in the lysine synthetic pathway is the conversion of oxaloacetate to aspartate by adding an amino-group from glutamate, catalyzed by the *aspB*-gene-product. Aspartate is phosphorylated to L-4-aspartyl phosphate by the reaction catalyzed by the *lysC*-gene-product, which is further converted to L-aspartate 4-semialdehyde via *asd*. L-4-aspartyl phosphate is further converted to dehydrodipicolinate by *dapA*. In the next step L-piperidine 2,6-dicarboxylate is made by *dapB*. At the level of L-piperidine 2,6-dicarboxylate there are two possibilities for the conversion to meso-2,6-diaminopimelate, the last step before lysine. Either the direct reaction adding the second amino-group in one single step is used (*ddh*), known as the dehydrogenase variant, or four successive reactions, named the succinyl variant, is used. The succinylase variant involves the *dapD*-, *dapC*-, *dapE*- and *dapF*-gene-products, and using this variant the TCA intermediate succinyl-Coa is involved. The final step is the decarboxylation of meso-2,6-diaminopimelate to lysine (*lysA*), which finally is exported out of the cell by lysine permerase (*lysE*).

Due to the commercial importance of lysine production in *C. glutamicum*, the lysine synthetic pathway has received a lot of attention, which has led to an impressive list of patents and patent applications (Figure 1.1).

Maximal lysine yield for C. glutamicum

The calculation of the maximal theoretical lysine yield on substrate for *C. glutamicum* is interesting because it gives an estimate for the existing potential for a given strain. Earlier stoichiometric calculations found that the maximum lysine yield on glucose was 0.75 mol · mol^{-1} for this organism when no biomass was produced (Stephanopoulos and Vallino, 1991). Recently a maximum yield of 0.82 mol · mol^{-1} was proposed (Wittmann and Becker, 2007). In this calculation the action of a cycle between three enzymes: pyruvate carboxylase (EC 6.4.1.1), malate dehydrogenase (EC 1.1.1.37) and malic enzyme (EC 1.1.1.40) formed a transhydrogenase-like reaction contributing significant to the NADPH supply. However, based on biochemical information the operation of such a cycle can be discussed (Petersen *et al.*, 2000). For both yield calculations no activity of the TCA cycle was included and the dehydrogenase variant (*ddh*) of the lysine synthesis pathway was exclusively used. This would in practice not be the case during the fermentation process of lysine, and in addition to that biomass needs to be produced, why a discussion of theoretical possible yields is rather useless without considering the context of the whole metabolism of the organism, including reactions involved in biomass formation. This type of calculations needs a more complex network of reactions, information and estimations. This will give more reliable information about the maximum achievable yield, and in addition to this it can provide information about reactions and flux-distributions during optimal lysine production. The maximum yields for the production strains used today are not public due to competitive issues. However, yields up to 55% have been reported in literature (Shiio *et al.*, 1987), and it can be expected that the intensive effort that have been made recent years have increased this even further.

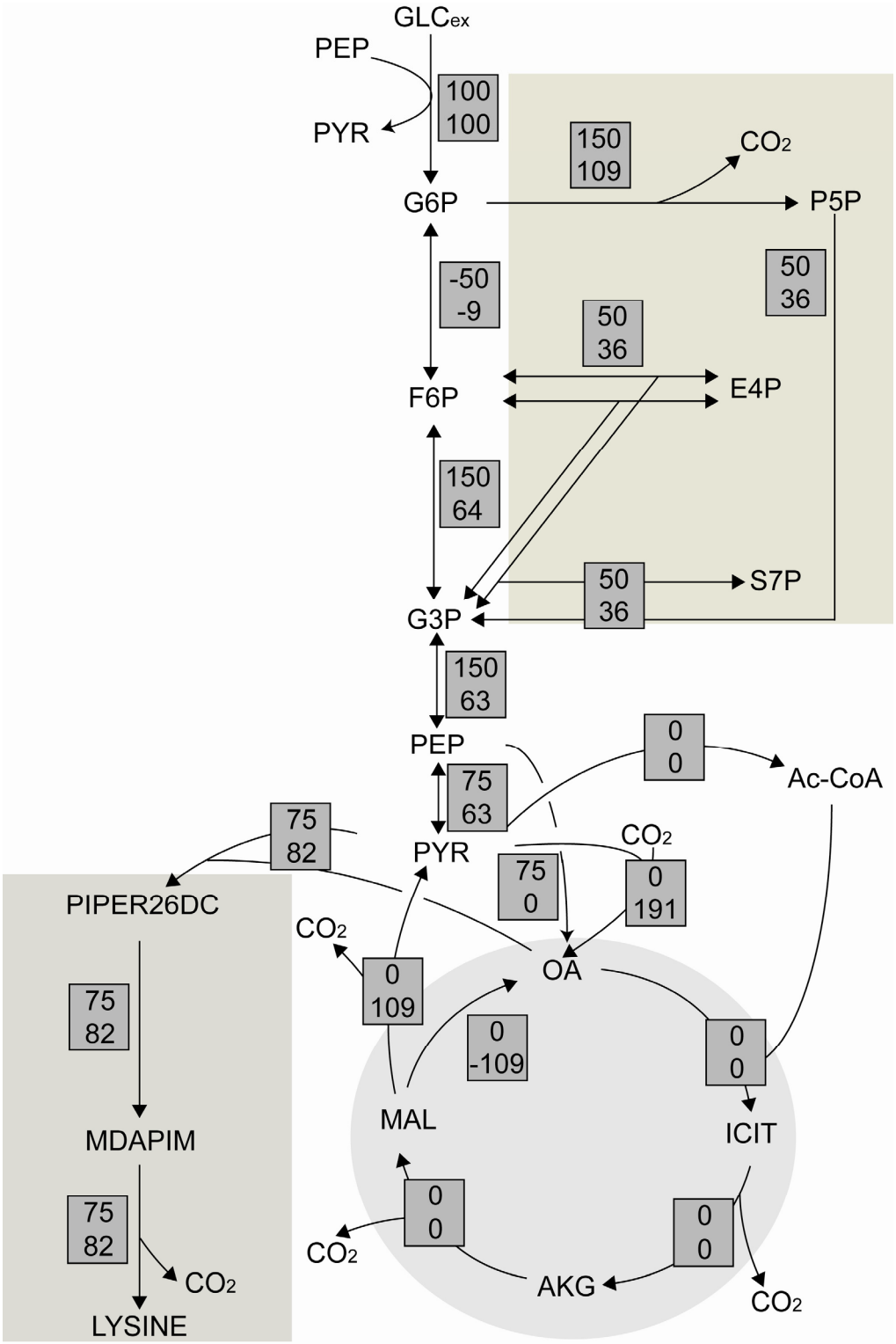

Figure 1.2: Metabolic flux distribution in *Corynebacterium glutamicum* with maximal theoretical lysine yield on glucose. All fluxes are given as relative molar fluxes to the glucose uptake in mol · $(mol)^{-1}$ × 100. Upper values: Stephanopoulos and Vallino (1991); lower values: Wittmann and Becker (2007). Abbreviations: GLC_{ex}: extracellular glucose; G6P: glucose-6-phosphate; F6P: fructose-6-phosphate; P5P: pentose-5-phosphate; E4P: erythose-4-phosphate; S7P: sedoheptulose-7-phosphate; G3P: glyceraldehyde phosphate; PEP: phosphoenolpyruvate; PYR: pyruvate; Ac-CoA: acetyl CoA; ICIT: isocitrate; AKG: α-ketogluterate; SUCC: succinate; OA: oxaloacetate; PIPER26DC: L-piperidine 2,6-dicarboxylate; MDAPIM: meso-2,6-diaminopimelate.

Production strain development

Lysine producing strains of *C. glutamicum* have continuously been improved since the development of the first large scale process for the production of this compound. Classical mutagenesis followed by screening has been proven very successful in this respect, and recently more rational approaches using recombinant DNA technologies, in some cases in combination with systems biology, have been applied with success. This later part later will be reviewed more in detail in chapter 2.

Outline and background for PhD thesis

This thesis is based on work performed during an industrial PhD project. The project has been carried out in a collaboration between the lysine producer Agro&Ferm A/S and Center for Microbial Biotechnology (CMB), BioSys, DTU. The aim of the project was to improve lysine production in a *C. glutamicum* production strain.

This thesis is divided into chapters where the first chapters introduce the subject and methods used and the following describes the work performed during this PhD study.

Chapter 1 gives an introduction to the thesis, and gives and introduction to *C. glutamicum* and commercial lysine production. Chapter 2 introduces the methods used in this work. Flux balance analysis, genome scale modeling, flux analysis and metabolic engineering in *C. glutamicum* are presented. Chapter 3 is a review on the biochemistry of *C. glutamicum*, and this chapter is making the basis for the reconstruction of the metabolic network of *C. glutamicum* presented in chapter 4.

The chapters 4-6 are manuscripts presenting the scientific work of this thesis. Chapter 4 (manuscript A) presents the reconstruction and validation of the *C. glutamicum* metabolic network. Chapter 5 (Manuscript B) presents a comparison of several different metabolic engineering strategies implemented in a *C. glutamicum* production strain for improving lysine production and evaluation of the different strategies applied. In chapter 6 (Manuscript C) flux analysis in complex media on two *C. glutamicum* production strains is presented.

Finally chapter 7 summarizes the work and comments on future perspectives for improving lysine production in *C. glutamicum*.

References

Araki,K., Kato,F., Aral,Y., and Nakayama,K. (1974) Histidine production by auxotrophic histidine analog-resistant mutants of Corynebacterium glutamicum. Agricultural and Biological Chemistry **38**, 837.

Demain,A.L. and Adrio,J.L. (2008) Contributions of microorganisms to industrial biology. Molecular Biotechnology **38**, 41-55.

Eggeling,L. (2007) L-Serine and Glycine. In Amino Acid Biosynthesis - Pathway, Regulation and Metabolic Engineering (Edited by Wendisch,V.F.) pp. 259-272. Springer-Verlag, Berlin-Heidelberg.

Guillout,S., Rodal,A.A., Lessard,P.A., and Sinskey,A.J. (2002) Methods for producing L-isoleucine. USA patent [US 6451564 B1].

Hermann,T. (2003) Industrial production of amino acids by coryneform bacteria. Journal of Biotechnology **104**, 155-172.

Hirao,T., Nakano,T., Azuma,T., Sugimoto,M., and Nakanishi,T. (1989) L-Lysine production in continuous culture of an L-lysine hyperproducing mutant of *Corynebacterium glutamicum*. Applied Microbiology and Biotechnology **32**, 269-273.

Ikeda,M. (2006) Towards bacterial strains overproducing L-tryptophan and other aromatics by metabolic engineering. Applied Microbiology and Biotechnology **69**, 615-626.

Ikeda,M. and Katsumata,R. (1992) Metabolic engineering to produce tyrosine or phenylalanine in a tryptophan producing *Corynebacterium glutamicum* strain. Applied and Environmental Microbiology **58**, 781-785.

Kase,H. and Nakayama,K. (1974) Studies on L-threonine fermentation. 4. Mechanism of L-threonine and L-lysine production by analog-resistant mutants of *Corynebacterium glutamicum*. Agricultural and Biological Chemistry **38**, 993-1000.

Kase,H. and Nakayama,K. (1975) Fermentation production of L-methionine and regulation of L-methionine biosynthesis in *Corynebacterium glutamicum*. 3 L-methionine production by mehionine analog-resistant mutants of *Corynebacterium glutamicum*. Agricultural and Biological Chemistry **39**, 153-160.

Kelle,R., Hermann,T., and Bathe,B. (2005) L-Lysine production. In Handbook of *Corynebacterium glutamicum* (Edited by Eggeling,L. and Bott,M.) pp. 465-488. CRC Press, Boca Raton.

Kinoshita,S., Nakayama,K., and Kitada,S. (1958) Method of producing L-lysine by fermentation. USA Patent [2979439].

Kinoshita,S., Udaka,S., and Shimono,M. (1957) Studies on the amino acid fermentation. Part I. Production of L-glutamic acid by various microorganisms. The Journal of General and Applied Microbiology **3**, 193-205.

Leuchtenberger,W., Huthmacher,K., and Drauz,K. (2005) Biotechnological production of amino acids and derivatives: current status and prospects. Applied Microbiology and Biotechnology **69**, 1-8.

Nakayama,K., Sagamira,I., and Araki,K. (1973) Process for producing L-methionine. USA Patent [3729381].

Pátek,M. (2007) Branched-Chain Amino Acids. In Amino Acid Biosynthesis - Pathways, Regulation and Metabolic Engineering (Edited by Wendisch,V.F.) pp. 128-162. Springer-Verlag, Berlin-Heidelberg.

Petersen,S., de Graff,A.A., Eggeling,L., Mollney,M., Wiechert,W., and Sahn,H. (2000) In vivo quantification of parallel and bidirectional fluxes in the anaplerosis of *Corynebacterium glutamicum*. Journal of Biological Chemistry. **275**, 35932-35941.

Ruklisha,M., Paegle,L., and Denina,I. (2007) L-Valine biosynthesis during batch and fed-batch cultivations of *Corynebacterium glutamicum*: Relationship between changes n bacterial growth rate and intracellular metabolism. Process Biochemistry **42**, 634-640.

Shiio,I. (1990) Threonine production by dihydrodipicolinate syntase-defective mutants of *Brevibacterium flavum*. Biotechnology Advances **8**, 97-103.

Shiio,I., Toride,Y., Yokota,A., Sugimoto,S., and Kawamura,K. (1991) Process for the production of L-threonine by fermentation. USA Patent [5077207].

Shiio,I., Yokota,A., and Sugimoto,M. (1987) Effect of pyruvate kinase deficiency on L-lysine productivities of mutants with feed-back resistant aspartokinase. Agricultural and Biological Chemistry **51**, 2485-2493.

Stephanopoulos,G. and Vallino,J.J. (1991) Network rigidity and metabolic engineering in metabolite overproduction. Science **252**, 1675-1681.

Udaka,S. (1960) Screening method for microorganisms accumulating metabolites and its use in the isolation of *Micrococcus glutamis*. Journal of Bacteriology **79**, 754-755.

Wittmann,C. and Becker,J. (2007) The L-lysine story: From metabolic pathways to industrial production. In Amino Acid Biosynthesis - Pathway, Regulation and Metabolic Engineering (Edited by Wendisch,V.F.) pp. 39-70. Springer-Verlag, Berlin.

Chapter 2

2. Flux balance analysis and metabolic engineering

Biological systems are complex, and knowledge about pathways, regulation and metabolic capability of the system is essential in order to design efficient cell factories. It is often necessary to analyze the system as a whole. This may be approached by using mathematical modeling as a tool. By modeling the metabolic network using information available about the whole biological system as a context, it is possible to design an improved metabolic network, i.e. by suggesting changes in the genotype (Covert *et al.*, 2001b; Palsson, 2000). Recent developments in genome sequencing and annotation, and an increasing amount of biological information in public databases have made reconstruction of metabolic networks relatively straightforward (Price *et al.*, 2003; Åkesson *et al.*, 2004).

Stoichiometri and structure of biochemical reaction networks

The interconnectivity of metabolites in a network of biological reactions is given by reaction equations, defining the stoichiometric conversion of substrates into products for each reaction

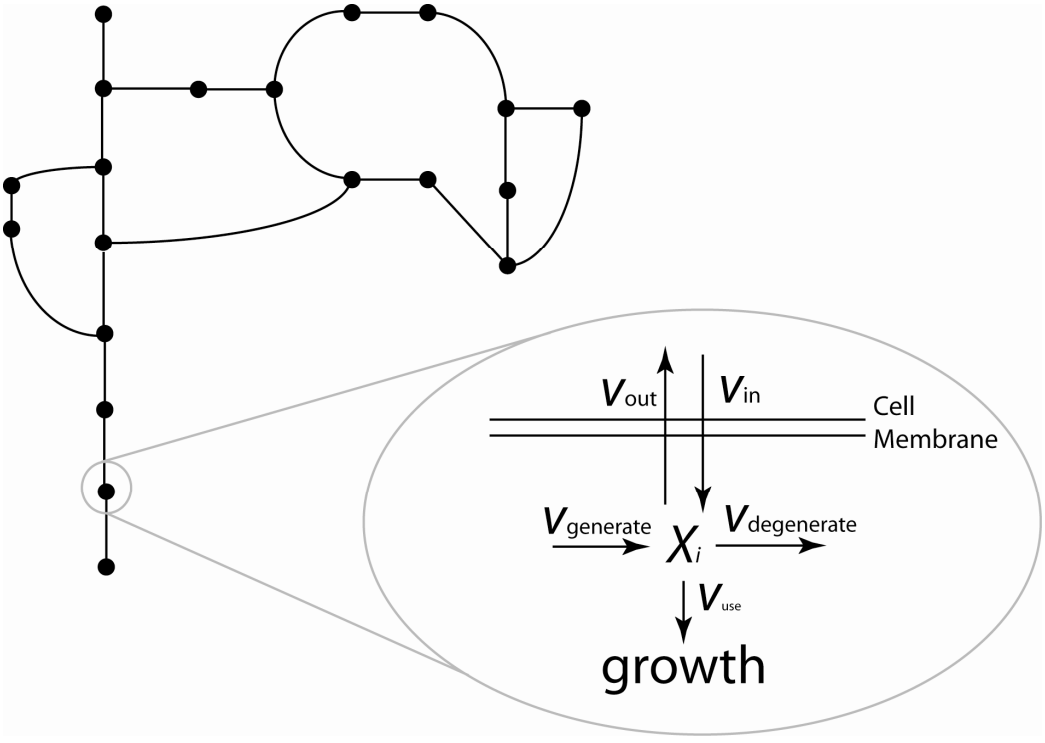

Figure 2.1: Mass balance around the metabolite *i* in a metabolic system. X_i: the concentration of metabolite *i*; $v_{generate}$: flux towards the generation of the metabolite *i*; $v_{degenerate}$: flux of metabolite *i* degenerated; v_{use}: flux of the metabolite *i* used for metabolic requirements (growth and maintenance); v_{in}: flux of the metabolite *i* into the system; v_{out}: flux of the metabolite *i* out of the system.

(Schilling *et al.*, 1999). Reactions are enzymatic reactions converting a substrate into a product, or transport reactions moving metabolites between different parts of the system, intracellular, extracellular or between different compartments. The result of active reactions in the biological system is fluxes serving to dissipate or generate metabolites. Following the law of conservation of mass, a balance describing the reaction rate of a particular metabolite through a particular reaction can be written:

(eq. 2.1) $$\frac{dX_{met}}{dt} = r_{met} - \mu X_{met}$$

where the difference between the rate of production and consumption of a particular metabolite is equivalent to the changes in concentration of that particular metabolite over time. In eq. (2.1) X_{met} is the concentration vector for the intracellular metabolite, and r_{met} is a vector containing the net rates of formation of the intracellular metabolite for each single reaction of the network. The last term on the right hand side accounts for dilution due to biomass growth. In figure 2.1 equation (2.1) is illustrated showing the mass balance around the metabolite *i* in a metabolic system. The consuming fluxes of metabolite *i* is divided into the flux towards metabolic requirements (V_{use}), the flux towards export from the cell (V_{out}), and the flux towards the degeneration reactions ($V_{degeneration}$). Two fluxes are serving to increase the concentration of X_i: import from outside the cell ($V_{in)}$ and reactions serving to generate the metabolite ($V_{generate}$). At steady state the concentrations of all metabolites are constant, and the reaction rate of the specific fluxes generating a metabolite must be equivalent to the reaction rate of the fluxes that consumes the metabolite. Since time constants associated with growth are much larger than those associated with kinetic reactions, it is reasonable to place the metabolic system in a pseudo-steady state (Stephanopoulos *et al.*, 1998), which allow us to neglect metabolite accumulation leading to:

(eq. 2.2) $$0 = r_{met} - \mu X_{met}$$

Because metabolite concentrations generally are low compared to netflux rates of metabolites the last term, corresponding to the dilution due to growth, can generally be neglected (Stephanopoulos *et al.*, 1998). In this case it is possible to reduce the system to a homogeneous linear equation, which in matrix notation is written as:

(eq. 2.3) $$0 = r_{met} = S \cdot v$$

The stoichiometric matrix *S* is an *m x n* matrix where *m* is the number of metabolites and *n* is the number of reactions or fluxes taking place within the metabolic network. The vector *v* refers to the reaction rate of each individual reaction or flux in the metabolic network. Metabolic models usually also include constraints, which will lead to the definition of a solution space in which the solution to the network equation must lie (Price *et al.*, 2003). Constraints in a model are dealt with by introducing constraint equations to the metabolic network, which can assign a direction of a given reaction (reversibility or irreversibility) according to known thermodynamic constraints. These equations are typically of the form $\alpha_i \leq v_i \leq \beta_i$, where α_i and β_i are the feasible lower and upper limit of the reaction rate v_i, respectively. In practice the upper and lower limits are set to arbitrarily high values when a reaction is reversible without any regulation, whereas α_i is set to zero when a reaction is irreversible. Constrain reactions can also be used to set a maximum flux through a given reaction based on biochemical information.

Flux balance analysis

The above described equation system is usually underdetermined due to the fact that the number of unknown fluxes exceeds the number of metabolites in the network, leading to a number of possible solutions, and hence, no unique solution (Bonarius *et al.*, 1997) (Figure 2.2A). By the introduction of constraints to the network, leading to the definition of a solution space in which the solution to the network equation must lie (Price *et al.*, 2003) this problem can be handled. To cope with this, linear programming optimization can be used to maximize (or minimize) for a certain metabolite objective (e.g. growth or product formation), and seeking its maximal (or minimal) value within the stoichiometrically defined domain. This procedure is often referred to as flux balance analysis (FBA) (Palsson, 2006). FBA is based on fundamental physiochemical constraints on metabolic networks, and it only requires information about stoichiometri of metabolic pathways and the metabolic demands. Furthermore, it is possible to include additional information about the metabolic network when it is available. FBA can be used to investigate the capabilities of a reconstructed biological network only based on systematic mass balances of the network, and some biological constraints based on knowledge about the biological system. In this way some limits are defined for the metabolic behavior of the biological system, and within these limits "optimal" steady-state solutions can be found using linear optimization techniques (Covert *et al.*, 2001b). This limitation is often referred to as a "solution space" in literature. Setting individual fluxes it is possible to constrain the magnitude and direction of a particular reaction, hence limiting the number of feasible reactions. These equality and inequality constraints define the closed solution space (Covert *et al.*, 2001b). FBA uses linear programming optimization techniques to determine the optimal flux distribution within a network by minimizing or maximizing a particular objective function. The suggested optimization problem can then be solved using linear programming (Bertsimas and Tsitsiklis, 1997). A presentation of a defined solution space and a particular solution (optimal) is presented in figure 2.2. FBA have successfully been used for prediction of outcomes of gene-knockout experiments (Edwards and Palsson, 2000), prediction of phenotypic behavior during different oxygen availabilities (Varma *et al.*, 1993b), obtaining quantitative genotype-phenotype

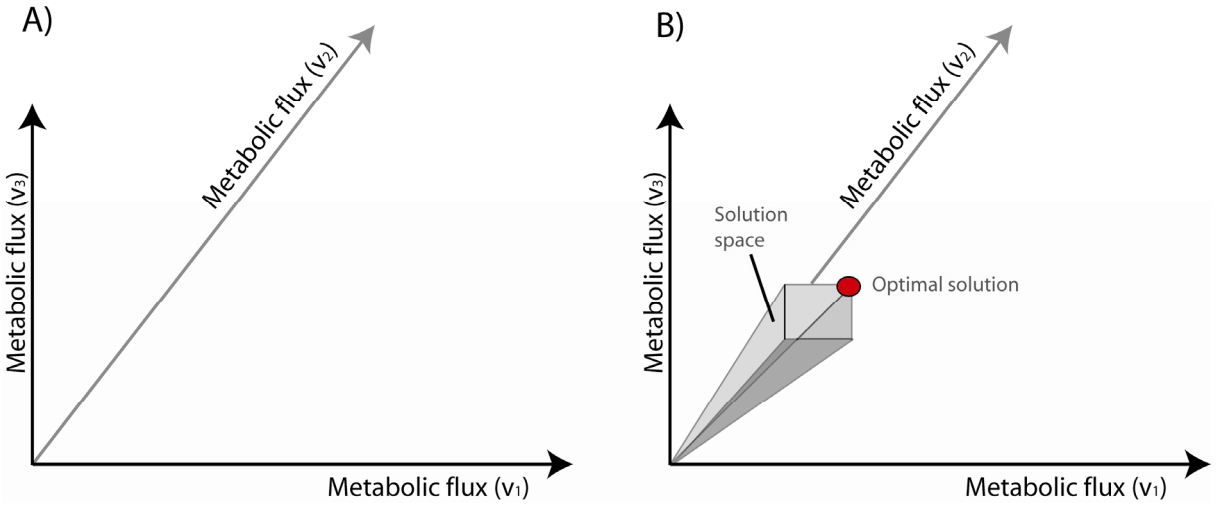

Figure 2.2: Constrain based analysis of metabolic networks. **(A)**: An unbounded space where every possible flux distribution for every reaction is possible. This often makes the linear problem infeasible. **(B)**: Presentation of the defined solution space which has been defined by applying constraints such as system stoichiometri, thermodynamics (reversibility of reactions) and maximum capacity of the system. Within this defined solution space the optimal steady-state solution to the flux vector is found.

relationship (Edwards *et al.*, 2001) and predicting gene targets for enhancing production of biological compounds (Burgard *et al.*, 2003). FBA can also be used to predict maximal growth rates or maximal production of a given metabolite in terms of yield on substrate.

Applications of flux balance analysis

FBA have been widely applied as a tool in analyzing the metabolic capabilities of metabolic networks – in particular for organisms relevant for industrial production of biochemicals. Some of the work reported so far in this respect has been the evaluation of metabolic networks for the production of anaerobic fermentation products (Papoutsakis, 1984; Papoutsakis and Meyer, 1985); the metabolic capabilities of *Escherichia coli* (Varma *et al.*, 1993a; Förberg *et al.*, 1988); the metabolic network of *C. glutamicum* for the potential and limitations in amino acid production (Hollander, 1994; Vallino and Stephanopoulos, 1993; Vallino and Stephanopoulos, 1994a; Vallino and Stephanopoulos, 1994b); and the metabolic capacity of *Bacillus subtilis* for the production of purine nucleotides, riboflavin, and folic acid (Sauer *et al.*, 1998).

Recently the availability of annotated genome sequences has enabled the reconstruction of genome-scale metabolic networks (Covert *et al.*, 2001a). Genomes of a large number of organisms have up till today been sequenced and annotated, and more will come within the neatest future. To date (April, 2008) 619 bacterial and 82 eukaryote genomes have been completed and 1753 bacterial and 914 eukaryotic genome projects are ongoing (www.genomesonline.org). In addition most of this sequence data is made available in public databases making it relatively straightforward to extract genome information from many organisms. This information can be used to make stoichiometric models of biological networks. Genome-scale metabolic models have already been constructed for a number of micro-organisms such as *Saccharomyces cerevisiae* (Förster *et al.*, 2003), *Escherichia coli* (Reed *et al.*, 2003), *Lactococcus lactis* (Oliviera *et al.*, 2005), *Staphylococcus aurerus* (Heinemann *et al.*, 2005), *Streptomyces coelicolor* (Borodina *et al.*, 2005), *Helicobacter pylori* (Schilling *et al.*, 2002), *Haemophilus influenzae* (Schilling and Palsson, 2000), *Methanosarcina barkeri* (Feist *et al.*, 2006) and *Lactobacillus plantarum* (Teusink *et al.*, 2006).

To improve the prediction power of the FBA models the stoichiometric genome-scale model can be combined with additional biological knowledge. This can be accomplished by incorporation of data from high-throughput techniques such as transcriptomics (Covert *et al.*, 2004; Åkesson *et al.*, 2004) or fluxomics (Herrgård *et al.*, 2006), and combining this with the constrain-based method (Price *et al.*, 2003). It is also possible to incorporate regulatory constraints, representing temporary flux constraints mediated by specific environmental conditions, rather than physiochemical constraints. This approach has been applied by Covert and co-workers (Covert *et al.*, 2001b). Covert et al. (2001b) introduced transcriptional regulatory events as time-dependent constrains, which led to an additional constraining of the metabolic network, and consequently made it possible to predict dynamic flux profiles for microbial growth. Using the same methods the steady-state solution space of a FBA model could be reduced (Covert and Palsson, 2003). Recent results on integration of gene expression data into a *S. cerevisiae* genome-scale model showed a significant improvement in prediction power during batch fermentations (Åkesson *et al.*, 2004), leading to the conclusion that this approach looks promising for improving FBA models. However, it needs to be emphasized that this approach also has some disadvantages as discussed by Åkesson et al. (2004), i.e. the fact that gene expression and metabolic fluxes does not always correlate (Yang *et al.*, 2002).

The incorporation of experimentally determined flux values into FBA models has also been applied for improving the prediction power of the models. Herrgård *et al*. (2006) used this approach, and was able to improve the performance of an *E. coli* FBA model.

The considerable interest in the redirection of metabolic fluxes to improve or develop production strains for industrial production of biochemicals, has led to the development of metabolic engineering (Bailey, 1991). Today, experimental protocols for almost any genetic manipulation in a wide variety of industrial relevant organisms are available. The challenge is therefore not how to apply genetic manipulations - but where to apply them. Besides from a convenient overview of the organism and its capabilities, stoichiometric models in a combination with FBA can be used in this respect. The prediction of phenotypic behavior during different environmental and genetic conditions has been presented (Edwards and Palsson, 2000; Edwards *et al.*, 2001; Oliviera *et al.*, 2005), and this can directly be used to test biological hypotheses (Patil *et al.*, 2004), and consequently predict metabolic engineering strategies as in the case of improving bioethanol-production in *S. cerevisiae* (Bro *et al.*, 2006).

Reconstruction of the metabolic network

The first step of the reconstruction of a metabolic network is in principle, to make a list of reactions present in the organism. This is done by gathering information about the organism from the sequenced genome, relevant literature from biochemical textbooks and scientific papers, and finally by searching reaction databases (Figure 2.3). The backbone in reconstruction of a metabolic network is the annotated genome. Normally, the reconstruction of a given metabolic network begins with a thorough examination of the genome(Covert *et al.*, 2001a). The first step in this examination is the annotation where all open reading frames (ORFs) are identified from the sequence of the genome, and these ORFs are searched against databases using special designed algorithms for comparing DNA-sequences as i.e. BLAST (McGinnis and Madden, 2004) or FASTA (Shpaer *et al.*, 1996). Using these databases one is able to extract and utilize information about already identified ORFs from other organisms. Based on this search and comparison, the function and presence of a large number of ORFs can be identified. Depending on which organism is object to the construction there is a number of options for helpful internet-resources, which can be used. Some organisms have organism-specific databases (i.e. *E. coli* and yeast) whereas others are included in more general databases, like KEGG (Kanehisa *et al.*, 2006) or BioCyc (Karp *et al.*, 2005). Finally, there are some general databases like MetaCyc (Caspi *et al.*, 2006) making an overview over all biological pathways, which can be used to find "missing links" in the biological network. From these databases valuable information can be found about an organism, and user friendly interfaces have made it relatively straightforward to get a quick overview. To complement the database resources, available literature is used to confirm the individual reactions or the network.
When all reactions and transport mechanisms have been identified the second step of the reconstruction is to make a dynamic mass balance for the metabolites in the metabolic network. The mass balance is defined in terms of flux through each reaction and the stoichiometri of that reaction. The result is a set of differential equations, which can be simplified to Eq. 2.3 as shown earlier in this chapter.

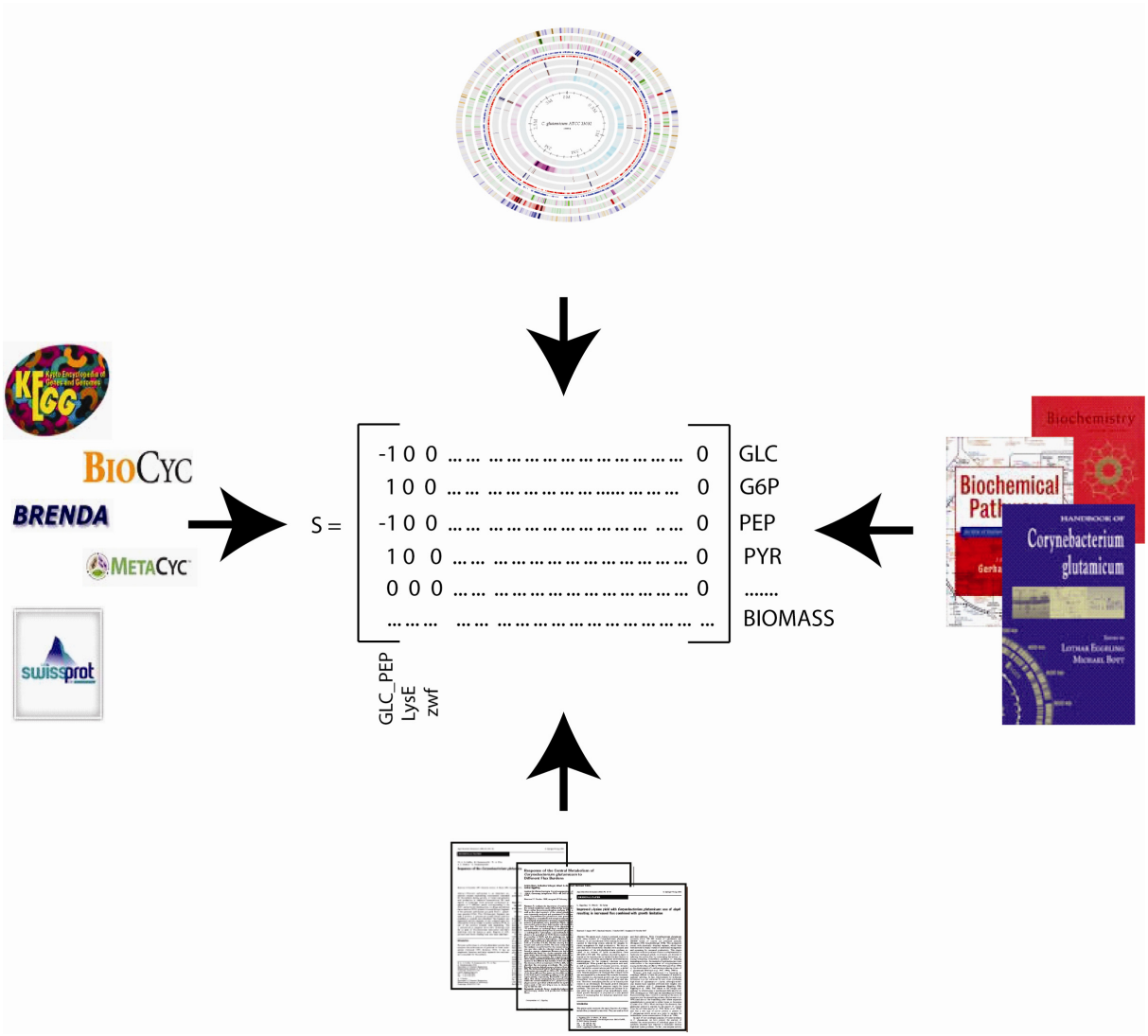

Figure 2.3: Construction of the metabolic network. Based on information from the annotated genome, relevant literature from biochemical textbooks and scientific papers and metabolic pathway and reaction databases it is possible to construct a metabolic network representing the overall set of metabolic reactions occurring in the cell.

The third step is to define the solution space (Figure 2.2) wherein the optimal solution must lie. This is done by reviewing literature. Here relevant biochemical books, organism specific books and recent papers can be used. Some constraints that are typically used is physiochemical data (i.e. reversibility of each individual reaction), or information about the maximum capacity of given reactions. Another important part of a metabolic network, which is used for constraining the model, is the composition of the macromolecules of the organism. This part of the reconstruction work can be quite difficult because it often is necessary to collect information from many different resources, and these resources are not always comparable due to different environmental conditions (media, substrate, oxygen availability, pH, fermentation strategy etc.). And in some cases it is not possible to find quantitative data for some components.

When the metabolic network has been created some validation needs to be done. Either by comparing simulations with published experimental data, or by designing and carrying out own

experiments. From published data and own experimental work some constraints can be set in order to fit the metabolic model to the real behavior of the organism, i.e. when pathways or enzymes are preferred compared to others or if futile cycles is present in the organism.

Metabolic flux analysis

The identification and quantification of metabolic reactions in an organism is a central element in metabolic engineering (Bailey, 1991; Stephanopoulos, 1999). The determination and study of metabolic fluxes *in vivo* has been termed metabolic flux analysis (Stephanopoulos, 1999), and the great scientific interest within this field has led to the development of a number of methods, which can be applied for metabolic flux analysis. One of the major challenges in flux analysis is the fact that the total number of fluxes exceeds the number of fluxes that can be measured. In some cases for small metabolic models it is, however, possible to measure sufficient fluxes to estimate all the other fluxes, and among measurable fluxes are typically the glucose uptake rate or product formation (Christensen and Nielsen, 1999b). This approach is often referred to as metabolite balancing. From a given bioreaction network stoichiometri, intracellular fluxes are reconstructed so as to satisfy the measured rates of extracellular metabolite accumulation or depletion (Stephanopoulos, 1999). No reaction kinetics needs to be taken into account, and the metabolic fluxes can be estimated using linear algebraic equations. Some examples where this approach has been applied for the estimation of fluxes is in *C. glutamicum* during growth and lysine production (Vallino and Stephanopoulos, 1993; Vallino and Stephanopoulos, 1994a; Vallino and Stephanopoulos, 1994b), in *Penicillum chrysogenum* for antibiotic production (Jørgenen *et al.*, 1995), and in the industrial important yeast *S. cerevisiae* (Nissen *et al.*, 1997). However, if the biological network contains more than one pathway leading to the same metabolite, this method can not be applied to discriminate between the different pathways. Using isotopic labeled substrates (i.e. ^{13}C-labelled glucose) this challenge can be handled (Christensen and Nielsen, 1999a). This methodology named isotopic balancing utilizes the asymmetry which often is present at splits between different pathways leading to the same end-product. When substrates labeled with i.e. ^{13}C at specific carbon locations is used, the ratio between the labeling states of metabolites can be used to determine the flux of the competing pathways (Stephanopoulos *et al.*, 1998). The number of different labeling states depends on the number of C-atoms present in the given metabolite. A metabolite with n carbon-atoms has 2^n possible labeling states. As an example a C-3 molecule would have eight different labeling states (Table 2.1). The different combinations of labeling states are called isotope isomers or isotopomers.

Metabolite balancing is limited to the estimation of absolute fluxes, i.e. the absolute carbon entering a metabolite pool also has to leave the pool, whereas isotope balancing enables estimation of relative fluxes. Combining the two methods it is possible to estimate all fluxes within the system (Christensen and Nielsen, 1999b), as it have been illustrated in studies of *C. glutamicum* (Marx *et al.*, 1996) and *P. chrysogenum* (Christensen and Nielsen, 2000).

^{13}C-labelling experiments

Since the primary metabolism in many cases is able to generate all precursors needed for biochemical reactions within the microbial cell, the use of ^{13}C-labelling substrate for flux analysis in such systems has been widely applied. In particular ^{13}C-glucose has been used intensively because it through catabolic reactions is incorporated into all cellular compounds. The labeling patterns of the compounds synthesized by the organism are governed by the labeling pattern of the precursor, which is governed by the labeling pattern of the substrate etc. These labeling patterns can be used to elucidate the flux distribution in the cell as described in Christensen and Nielsen (1999a). Due to practical reasons not all compounds are suitable for labeling analysis. Amino acids from the hydrolyzed protein fraction of the cell are often preferred in this respect (Christensen and Nielsen, 1999a), mainly because these compounds are present in high quantities in cell extracts and biomass hydrolysates, and because the flux through the pool of amino acids is low compared to the total amino acid pool, which makes sampling procedures and the following measurements less difficult. Those characteristics are in contrast to those of the precursors present in the central metabolites where concentrations are small compared to the flux, making sampling and analysis much more challenging. Knowing the precursor-amino acid relationship, it is possible to deduce the labeling pattern of the precursors from the central metabolism from the labeling pattern of the amino acids (Christensen and Nielsen, 1999a), and hence predict the metabolic flux distributions.

Table 2.1: The different isotopomers of a C_3 molecule. Shaded circles are ^{13}C and white circles are ^{12}C.

Isotopic composition
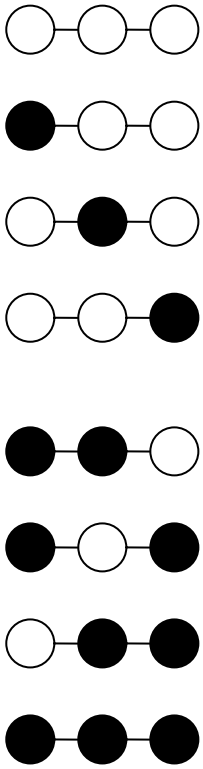

Reciprocal labeling

As mentioned above labeling experiments based on specific labeled substrates are very powerful for elucidating and analyzing flux distributions of biological networks. However, an important feature that can not be addressed by the methods mentioned above is the uptake and conversion of other carbon sources than the labeled substrate. In some experiments it may be necessary to add unlabelled co-substrates to the medium, i.e. if the behavior of an organism in complex media needs to be studied, or if the strain has certain auxotrophies. And if one wants to study the uptake, degradation and conversion of these compounds, alternative methods need to be applied. Reciprocal labeling can be used for this purpose as discussed by Christensen (2001). The idea in reciprocal labeling is that instead of using labeled substrate with only one ^{13}C (i.e. [1-^{13}C]glucose), substrate labeled in all positions is used (i.e. [U-$^{13}C_6$]glucose). A high ^{13}C-background is generated, and this way the contribution from the non-labeled substrate can be elucidated from the ^{12}C-labeling, hence making it possible to determine the role of the non-labeled co-substrate (Christensen, 2001).

Current status for metabolic engineering activities in C. glutamicum

Since the development and prevalence of metabolic engineering for improving product yields and productivity, *C. glutamicum* has undergone a large number of metabolic engineering strategies, of which the major milestones will be reviewed here. The metabolic engineering efforts have been focusing on various parts of the metabolism, of which the more important can be overviewed in figure 2.3.

Metabolic engineering of reactions within the lysine pathway

The lysine synthetic pathway of *C. glutamicum* has been the main focus of many metabolic engineering strategies presented so far. Many of these studies have focused on optimizing the flux through this pathway by altering enzymes or enzyme activities of this pathway. A reaction and gene which have received a lot of attention in this respect is the aspartate kinase (*lysC*) due to its importance in the regulation of flux towards lysine-, methionine- and threonine- biosynthesis. In the wild type strain this reaction is feed back inhibited by lysine and threonine, making this reaction a key step in regulation of the biosynthesis of lysine (Kelle *et al.*, 2005). In most *C. glutamicum* strains overproducing lysine at a production scale the *lysC*-gene is known to have mutations causing feed back resistance. The best described mutations in this respect is T311I (Ohnishi *et al.*, 2002), and S301Y and S301F (Lu and Liao, 1997). The effect of the feedback resistant *lysC*-gene was shown in a study where the wild type *lysC*-gene was replaced by a mutated gene in a wild type background leading to lysine accumulation, which was not seen for the wild type strain (Cremer *et al.*, 1991; Eggeling *et al.*, 1998). Furthermore, an increase in lysine production was observed when the mutated *lysC*-gene was over-expressed in the lysine producing strain *C. glutamicum* DG 52-5, (Cremer *et al.*, 1991; Eggeling *et al.*, 1998). These results showed the importance of this reaction in lysine production. However, no effect was seen when the same strategy was applied in a high level lysine producing strain *C. glutamicum* MH20-22B (Eggeling *et al.*, 1998). A possible explanation for this disagreement between the results is that *C. glutamicum* DG 52-5 is a low-level producer whereas *C. glutamicum* MH20-22B is a high level producer (Eggeling *et al.*, 1998), and it can be expected that some of the limitations present in MH20-22B are not present in DG 52-5.

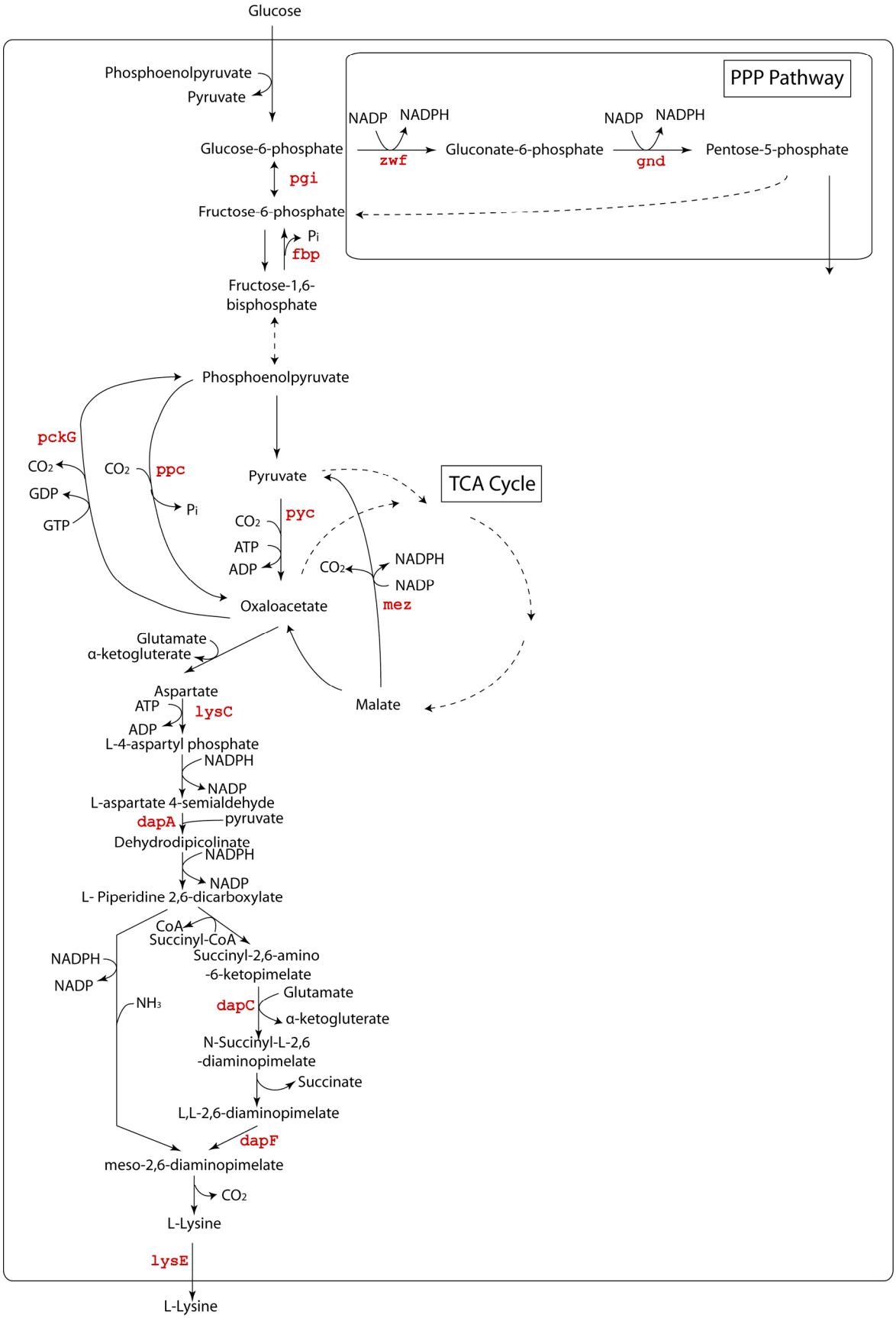

Figure 2.4: Overview of important targets for metabolic engineering for optimizing *C. glutamicum* for lysine production. Dashed lines represent multiple reactions. For abbreviations see text.

Another gene in the lysine synthetic pathway which has been identified to be involved in lysine productivity is dihydrodipicolinate syntase (*dapA*). Over-expression of this gene led to production of lysine in a wild type strain (Cremer *et al.*, 1991). In addition an increase in lysine production was seen when the same strategy was applied on DG 52-5 (Cremer *et al.*, 1991; Eggeling *et al.*, 1998) and MH20-22B (Eggeling *et al.*, 1998). In another lysine producer, *C. glutamicum* ATCC 21253, up-regulation of *lysC* showed positive lysine production whereas *dapA* showed no effect (Hua *et al.*, 2000). The simultaneous up-regulation of *dapA* and *lysC* resulted in further increase in lysine production, compared to the situation where the genes were up-regulated individually (Eggeling *et al.*, 1998).

This strategy was not applied in the study of Hua *et al*. (2000). In addition to *lysC* and *dapA* both Eggeling *et al*. (1998) and Cremer *et al*. (1991) up-regulated the genes *asd* (aspartosemialdehyde dehydrogenase), *dapB* (dihydrodipicolinate), *ddh* (diamonopimelate dehydrogenase), *lysA* (diaminopimelate decarboxylase) without effect, and for *ddh* a negative effect on lysine accumulation was seen in the study of Eggeling *et al.* (1998).

The succinyl branch of the lysine pathway has also been investigated in order to find bottlenecks. Over-expression of *dapF* or *dapC* in a lysine producer (*C. glutamicum* DSM5715) increased lysine accumulation (Hartmann *et al.*, 2003), whereas it have been shown that disruption of *dapE* had no effect on lysine production in *C. glutamicum* ATCC 21253 (Shaw-Reid *et al.*, 1999).
The efflux of lysine from the cytosol of the bacterium is done by the transport protein lysine permerase (*LysE*)(Bellmann *et al.*, 2001; Vrljic *et al.*, 1996). This exporter is tightly controlled in the wild type strain, making this an obvious candidate for optimization of lysine production. Vrljic *et al.* (1996) improved the efflux of lysine in the wild type strain (ATCC 13032) five fold by over-expressing *lysE*, identifying this as a key reaction in optimization of lysine producers.

Metabolic engineering of NADPH metabolism

In *C. glutamicum* the co-factor NADPH has been object to a lot of attention due to its role in lysine synthesis where four moles of NADPH is consumed for the synthesis of one molecule of lysine (Marx *et al.*, 1997). A detailed insight into the NADPH metabolism has been made through ^{13}C metabolic flux analysis, which has been conducted under various physiological conditions (Becker *et al.*, 2005; Becker *et al.*, 2007; Dominguez *et al.*, 1998; Kiefer *et al.*, 2004; Marx *et al.*, 1996; Marx *et al.*, 1997; Marx *et al.*, 1999; Petersen *et al.*, 2000; Petersen *et al.*, 2001; Sonntag *et al.*, 1995; Wendisch *et al.*, 2000; Wittmann and Heinzle, 2001; Wittmann and Heinzle, 2002; Wittmann *et al.*, 2004). These results have demonstrated that the NADPH supply and consumption are fairly flexible (Marx *et al.*, 1997; Marx *et al.*, 1999), and it varies depending on the carbon source used (Dominguez *et al.*, 1998; Kiefer *et al.*, 2004; Wendisch *et al.*, 2000; Wittmann *et al.*, 2004), the physiological state of the cells (Marx *et al.*, 1997), and the genetic background of the cells including introduction of genetic modifications (Becker *et al.*, 2005; Becker *et al.*, 2007; Marx *et al.*, 1999; Petersen *et al.*, 2001; Wittmann and Heinzle, 2002). In many cases an apparent NADPH excess have been reported (Dominguez *et al.*, 1998; Marx *et al.*, 1996; Sonntag *et al.*, 1995; Wittmann and Heinzle, 2001; Wittmann and Heinzle, 2002; Wittmann *et al.*, 2004). The presence of additional not yet identified NADPH consuming reactions not included in the models used for estimating the metabolic fluxes have been proposed as an explanation for this apparent NADPH excess in the metabolic flux analysis experiments (Wittmann *et al.*, 2004). In addition to this it needs to be taken into account that when the data mentioned above is extrapolated to industrial lysine producers

where lysine yields are significantly higher than what is reported here, it can be expected that NADPH is in fact limiting during maximal lysine production.

In *C. glutamicum* NADPH can be generated by four different reactions: glucose-6-phosphate dehydrogenase (*zwf*); 6-phosphogluconate dehydrogenase (*gnd*); isocitrate dehydrogenase (*icd*); and malic enzyme (*mez*). Carbon flux analysis revealed the critical importance of the PPP during lysine synthesis (Figure 2.5), why the two NADPH-generating enzymes present within the PPP, *zwf* and *gnd*, have received a lot of attention. Enzyme studies demonstrated that both enzymes are strongly inhibited by NADPH (Moritz *et al.*, 2000), which may explain why no successful studies on over-expression of the wild type variants of these genes have been reported so far. However, feed-back insensitive variants of both the *zwf*-gene-product (Becker *et al.*, 2007) and the *gnd*-gene-product (Ohnishi *et al.*, 2005) have been identified, and individual over-expression of these gene-products in lysine producing *C. glutamicum* strains have resulted in increased lysine production (Becker *et al.*, 2007; Ohnishi *et al.*, 2005). Another strategy to increase the flux through the PPP is by removing the competing reaction to glucose-6-phosphate, glucose-6-phospoglucose isomerase (*pgi*), was proposed (Dunican *et al.*, 2001) and further studies showed an increased PPP flux and consequently an increased lysine yield (Marx *et al.*, 2003). Based on flux analysis studies the deregulation of another gene-target , fructose 1,6-bisphosphatase (*fdp*), was proposed for increasing the PPP flux (Kiefer *et al.*, 2004; Wittmann *et al.*, 2004). Over-expression of this gene in a lysine producing *C. glutamicum* strain (wild type background introduced with a $lysC^{T311I}$ mutation) led to an increased lysine yield on glucose, fructose and sucrose (Becker *et al.*, 2005). In another study over-expression of *fdp* in a *C. glutamicum* strain (wild type background introduced with defined mutations (pyc^{P458S}, hom^{V59A}, $lysC^{T311I}$, zwf^{A243T})) led to improved lysine yields when glucose and fructose mixtures, or sucrose was used as carbon source, while no effect was seen on the modification when glucose or fructose was used (Georgi *et al.*, 2005). By metabolic flux analysis Becker et al. (2005) was able to identify a 19% increase in the PPP flux in the strain with an over-expressed *fdp*-reaction indicating that the increased lysine yield was in fact due to an increase in NADPH supply.

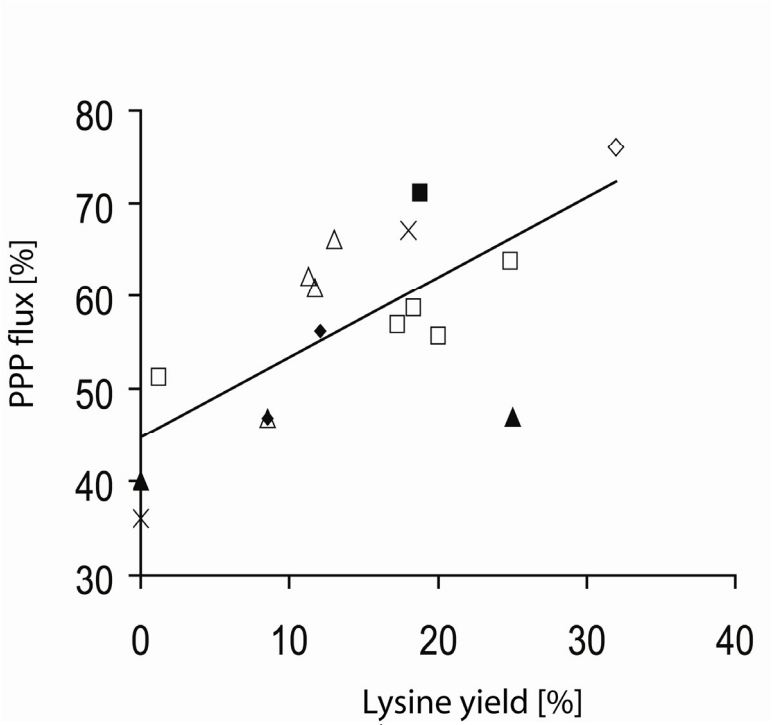

Figure 2.5: Lysine yield (mol lysine · (mol glucose)$^{-1}$) versus metabolic flux through the pentose phosphate pathway (PPP) normalised to total substrate uptake. Studies included are: Wittmann and Heinzle (2001) (closed squares); Wittmann and Heinzle (2002) (open squares); Sonntag *et al*. (1995) (closed triangles); Marx *et al*. (1997) (crosses); Marx *et al*. (1999) (open diamonds); Becker *et al*. (2005) (closed diamonds); and Becker *et al*. (2007) (open triangles).

Another NADPH generating reaction, malic enzyme (*mez*), has been suggested as a target for improving lysine production (Dominguez *et al.*, 1998). It was proposed that this reaction together with NAD-dependent-malate dehydrogenase (*mdh*) and pyruvate carboxylase (*pyc*) was able to make a cycling between pyruvate, oxaloacetate and malate, forming NADPH by the use of NADH and ATP. Recently, the effect on lysine yield of over-expression *mez* in a lysine producing *C. glutamicum* was tested (Georgi *et al.*, 2005). No effect on lysine yield were observed when *mez* was over-expressed in a lysine producing *C. glutamicum* strain (wild type background introduced with defined mutations (pyc^{P458S}, hom^{V59A}, $lysC^{T311I}$, zwf^{A243T})) when glucose, fructose, glucose and fructose or sucrose was used as substrate, although enzyme activities observed were about three fold higher as compared to negative controls (Georgi *et al.*, 2005). The physiological role of *mez* in *C. glutamicum* is thought to be during growth on gluconeogenic carbon sources such as acetate or citrate (Netzer *et al.*, 2004) or lactate (Gourdon *et al.*, 2000). Gourdon *et al*. (2000) generalized the role of *mez* to be involved in NADPH generation during growth on substrates with low PPP flux. With the results from Georgi *et al*. (2005) in mind and observations from glucose grown cells where no detectable flux was seen for *mez* in a wild type strain (Petersen *et al.*, 2000), it can be concluded that this reaction is controlled tightly, and more sophisticated strategies needs to be applied.

The last NADPH generating reaction identified so far in *C. glutamicum*, isocitrate dehydrogenase (*icd*), was earlier characterized (Eikmanns *et al.*, 1995). This reaction is part of the TCA cycle, and based on stoichiometric considerations NADPH generation using this reaction is not as efficient (1 NADPH per CO_2) as when the two reactions in the PPP is used (2 NADPH per CO_2). Therefore, *icd* has not been included in metabolic engineering strategies for lysine production so far.

An alternative strategy to optimize NADPH metabolism for lysine production was evaluated in a study by Marx *et al*. (1999). The background for this strategy is the fact that two of the four NADPH-molecules consumed for the biosynthesis of one molecule of lysine are associated with the incorporation of amine to α-ketoglutarate forming glutamate. This reaction is catalyzed by the NADPH-dependent glutamate dehydrogenase (*gnd*) in *C. glutamicum*. Marx *et al*. (1999) substituted this gene with a gene coding for the NADH-dependent glutamate dehydrogenase, which essentially decreased the demand for NADPH for biomass- and lysine-production. However, the response of this genetic modification was not increased lysine production. In stead a decrease in lysine yield was seen, whereas biomass- and CO_2 yields increased significantly. The study of Marx *et al*. (1999) demonstrated that the cells adjust fluxes to the reduced NADPH demand, and in this case the potentially available increase in NADPH did not result in increased lysine production.

From the work done so far on NADPH metabolism in *C. glutamicum* it can be concluded that lysine production most likely is limited by NADPH supply when lysine production is high, and the PPP is the major pathway for NADPH supply in this organism.

Metabolic engineering of the anaplerotic reactions

In *C. glutamicum* there are a number of potential reactions involved in the supply of oxaloacetate, which is the direct precursor for lysine. ^{13}C-flux analysis has revealed the importance of these reactions, since a correlation between lysine yield and the anaplerotic netflux is seen (Figure 2.6). In order to increase the anaplerotic flux various strategies have been suggested and tested. The carboxylation of phosphoenolpyruvate catalyzed by phosphoenolpyruvate carboxylase (*ppc*), was proposed as a promising target for metabolic engineering based on carbon flux simulations (Stephanopoulos and Vallino, 1991; Vallino and Stephanopoulos, 1993). When this gene was over-expressed or inactivated in the lysine producing *C. glutamicum* strains MH20-22H, no effect was seen on lysine production (Gubler *et al.*, 1994; Peters-Wendisch *et al.*, 1993; Eggeling *et al.*, 1998). In another strain, *C. glutamicum* DG 52-5, a positive effect was observed on over-expressing *ppc* (Cremer *et al.*, 1991; Eggeling *et al.*, 1998).

Another oxaloacetate generating reaction which have received attention is the carboxylation of pyruvate catalyzed by pyruvate carboxylase (*pyc*) (Peters-Wendisch *et al.*, 1998). This reaction is considered the major anaplerotic reaction in *C. glutamicum* (Petersen *et al.*, 2000). Over-expression of this gene has, as it was the case for *ppc*, given different results with respect to lysine production. In the lysine producing strain *C. glutamicum* DG 52-5 over-expression resulted in an increase in lysine production, whereas inactivation of the *pyc*-gene resulted in a negative response (Peters-Wendisch *et al.*, 2001). In another study applying the same strategy in two different strains (*C. glutamicum* ATCC 21253 and ATCC 21799) no significant effect was seen on the final lysine production (Koffas *et al.*, 2002). Data from Koffas *et al*. (2002) indicated the presence of a limitation in the lysine pathway somewhere downstream oxaloacetate, and it was suggested that

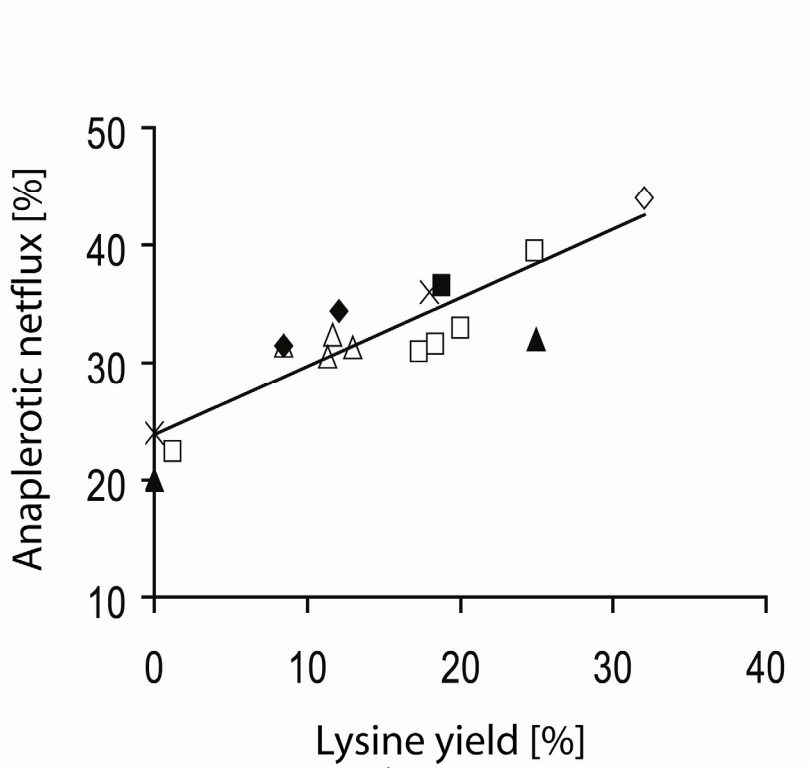

Figure 2.6: Lysine yield (mol lysine · (mol glucose)$^{-1}$) versus anaplerotic netflux normalised to total substrate uptake. Studies included are: Wittmann and Heinzle (2001) (closed squares); Wittmann and Heinzle (2002) (open squares); Sonntag *et al*. (1995) (closed triangles); Marx *et al*. (1997) (crosses); Marx *et al*. (1999) (open diamonds); Becker *et al*. (2005) (closed diamonds); and Beckers *et al*. (2007) (open triangles).

simultaneous over-expression of *lysC* and *pyc* could increase lysine production. This hypothesis was confirmed in a later study where a *C. glutamicum* ATCC 21253 with over-expressed *pyc* and *lysC* increased lysine production (Koffas *et al.*, 2003). Recently, the point mutation C1372T in the *pyc*-gene sequence were identified to be beneficial for lysine production (Ohnishi *et al.*, 2002).
From the results presented above, and the learning from ^{13}C-flux analysis (Figure 2.6) it can be concluded that an increased netflux towards oxaloacetate is beneficial for lysine production. An alternative to increasing the flux of the carboxylation reactions is decreasing the decarboxylating reactions. Two reactions decarboxylating oxaloacetate are present in *C. glutamicum*, phosphoenolpyruvate carboxykinase (*pckG*) (Riedel *et al.*, 2001) and oxaloacetate decarboxylase (*odx*) (Jetten and Sinskey, 1995). The activity of *pckG* was found to be counteractive to lysine production, since a decrease was seen for a strain with increased activity of the enzyme, and since an increase was seen in a strain where *pckG* was inactivated (Petersen *et al.*, 2001; Riedel *et al.*,

2001). The role for the second decarboxylation reaction, *odx*, has not yet been thoroughly investigated with respect to lysine production. However, based on ^{13}C-flux analysis, the flux from oxaloacetate to pyruvate, and therefore also *odx* activity, is insignificant under normal conditions (Petersen *et al.*, 2000; Petersen *et al.*, 2001), why the expected effect of an inactivation would be limited or absent.

The last reaction involved in anaplerotic fluxes in *C. glutamicum* is *mez*, which have been discussed earlier.

Utilization of alternative substrates

The major part of the variable costs in lysine production is the carbon source (Seibold *et al.*, 2006). Most work on developing production strains has therefore been focusing on improving product yields. However, another strategy which has been persued is designing *C. glutamicum* strains able to utilize cheap raw materials.

C. glutamicum is unable to metabolize lactose and galactose, and is therefore unable to utilize dairy based waste-products, such as whey. By inserting the lactose operon (*lacYZ*) from *E. coli* containing lactose permerase and β-galactosidase a non lysine producing *C. glutamicum* was able to grow on lactose as the only carbon source (Brabetz *et al.*, 1991). However, in the study of Brabetz *et al*. (1991) the galactose part of the disaccharide was not utilised, and an accumulation of this compound was observed in the fermentation broth. In a later study galactose accumulation was abolished by making a double mutant containing both the lactose operon from *Lactobacillus delbrueckii* susp. *bulgarisus* and the galactose operon (*galMKTE*) from a *Lactococcus lactis* subsp. *cremoris* MG13063 coding for the enzymes responsible for galactose catabolism in this organism (aldose-1-epimerase, galactokinase, UDP-glucose-1-P-uridylyltransferase, UDP-galactose-4-epimerase) (Barret *et al.*, 2004). Barret *et al*. (2004) used this strategy on a lysine producing *C. glutamicum* strain which was able to produce lysine on a whey based medium. Despite the increased catabolic flexibility of the mutants, slower growth rates and strain instability was observed.

Another substrate which has received some attention as a potential substrate for lysine production is starch. Starch hydrolysates from corn, wheat or cassava are today one of the major substrates for lysine production (Seibold *et al.*, 2006). However, for practical and economical reasons it would be beneficial if *C. glutamicum* could directly metabolize soluble starch (Seibold *et al.*, 2006). By introducing the *amyE* gene from *Streptomyces griseus* into a lysine producing *C. glutamicum* Seibold *et al*. (2006) was able to construct a mutant excreting α-amylase, and able to grow and produce lysine on a starch based medium.

With the recent developments in utilizing lignocellulosic biomass from agricultural waste in bioprocesses, a palette of interesting alternative substrates has emerged. These substrates are often complex and contain a wide variety of different carbon sources (Aristidou and Penttilä, 2000), many of which are not utilizable for *C. glutamicum*. The composition of lignicellulosic biomass varies depending on the biomass source, but in general the carbohydrate fraction typically consists of 40% glucose (Aristidou and Penttilä, 2000). However, the pentose fraction is rather significant, the two major fractions being xylose (5-20%) and arabinose (1-5%) (Aristidou and Penttilä, 2000). *C. glutamicum* is unable to utilize both pentoses. Introducing two *E. coli* genes *xylA* and *xylB*, a *C.*

glutamicum strain was able to utilize xylose (Kawaguchi *et al.*, 2006). Later, the same strategy was used on arabinose, where the *E. coli* genes *araA*, *araB* and *araD* with success was introduced into a *C. glutamicum* strain making it able to utilize this carbohydrate (Kawaguchi *et al.*, 2008). In both cases the strains used were not lysine producing strains why the application for this still needs to be proven.

Although the examples mentioned above are very good starting points, further metabolic engineering efforts and process optimization needs to be done to enable efficient and sustainable production of lysine on alternative substrates.

Systems biology in improving metabolic engineering in *C. glutamicum*

Systems biology can be used for the elucidations of cell function and physiology through integrated use of genomic and physiological data. The use of systems biology for improving metabolic engineering strategies is not a new concept and some of the early examples using flux balance analysis (FBA) for predicting metabolic engineering strategies have already been mentioned earlier in this chapter (Vallino and Stephanopoulos, 1993; Stephanopoulos and Vallino, 1991). With the sequencing and annotation of the whole genome of the wild type strain *C. glutamicum* ATCC 13032 (Ikeda and Nakagawa, 2003; Kalinowski *et al.*, 2003), the development in systems biology has been intensified. Transciptome analysis using DNA microarrays has been developed (Wendisch, 2003) and provided valuable insights into gene expression under various conditions in *C. glutamicum*. Also protocols for proteome analysis have been developed (Hermann *et al.*, 2001), and results from this have given some insight into *C. glutamicum* microbiology. However, the method which has contributed the most to understanding *C. glutamicum* metabolism is metabolic flux analysis by ^{13}C based methods (Becker *et al.*, 2005; Becker *et al.*, 2007; Dominguez *et al.*, 1998; Kiefer *et al.*, 2004; Marx *et al.*, 1996; Marx *et al.*, 1997; Marx *et al.*, 1999; Petersen *et al.*, 2000; Petersen *et al.*, 2001; Sonntag *et al.*, 1995; Wendisch *et al.*, 2000; Wittmann and Heinzle, 2001; Wittmann and Heinzle, 2002; Wittmann *et al.*, 2004). Development of methods for parallel integration of high-throughput genomic and physiological data sets has facilitated the application of a holistic approach allowing links between different parts of cell physiology, such as transcriptome and fluxome to be elucidated (Krömer *et al.*, 2004). It is expected that such systematic approaches can be used to predict metabolic engineering strategies for designing optimized *C. glutamicum* strains for lysine production, as it has been seen for bioethanol production in *S. cerevisieae* (Bro *et al.*, 2006).

With the developments in *C. glutamicum* genomics a new methodology has been developed named "genome breeding"(Ohnishi *et al.*, 2003; Ohnishi *et al.*, 2002). In this approach a "minimal mutation strain" is created by carrying our comparative genomic analysis between a high level producing mutant and the wild type strain to identify those mutations beneficial for production of the desired bioproduct. Those mutations are then transferred to a wild type background. This way a production strain is made without unnecessary and counter-productive mutations normally obtained by random mutagenesis. Using this methodology a high producing strain was generated (Ohnishi *et al.*, 2002), and one important feature in this new strain was that it was able to grow and produce lysine at higher temperatures (40°C) when compared to the production strain (30°C) obtained by classical mutagenesis (Ohnishi *et al.*, 2003).

References

Åkesson,M., Förster,J., and Nielsen,J. (2004) Integration of gene expression data into genome-scale metabolic models. Metabolic Engineering **6**, 285-293.

Aristidou,A.A. and Penttilä,M. (2000) Metabolic engineering applications for renewable resource utilization. Current Opinion in Biotechnology **11**, 187-198.

Bailey,J.E. (1991) Towards a science of metabolic engineering. Science **252**, 1668-1675.

Barret,E., Stanton,C., Zelder,O., Fitzgerald,G., and Ross,R.P. (2004) Heterologous expression of lactose- and galactose-utilizing pathways from lactic acid bacteria in *Corynebacterium glutamicum* from production of lysine in whey. Applied and Environmental Microbiology **70**, 2861-2866.

Becker,J., Klopprogge,C., Herold,A., Zelder,O., Bolten,C.J., and Wittmann,C. (2007) Metabolic flux engineering of L-lysine production in *Corynebacterium glutamicum* - over expression and modification of G6P dehydrogenase. Journal of Biotechnology **132**, 99-109.

Becker,J., Klopprogge,C., Zelder,O., Heinzle,E., and Wittmann,C. (2005) Amplified expression of fructose 1,6.bisphosphate in *Corynebacterium glutamicum* increases in vivo flux through the pentose phosphate pathway and lysine production on different carbon sources. Applied and Environmental Microbiology **71**, 8587-8596.

Bellmann,A., Vrljic,M., Patek,M., Sahm,H., and Krämer,R. (2001) Expression control and specificity of the basic amino acid exporter *LysE* of *Corynebacterium glutamicum*. Microbiology **147**, 1765-1774.

Bertsimas,D. and Tsitsiklis,J.N. (1997) Introduction to Linear Optimization. Athena Scientific, Belmont.

Bonarius,H.P.J., Schmid,G., and Tramper,J. (1997) Flux analysis of underdetermined metabolic networks: the quest for the missing constraints. Trends in Biotechnology **15**, 308-314.

Borodina,I., Krabben,P., and Nielsen,J. (2005) Genome-scale analysis of *Streptomyces coelicolor* A3(2) metabolism. Genome Research **15**, 820-829.

Brabetz,W., Liebl,W., and Schleifer,K.H. (1991) Studies on the utilization of lactose by *Corynebacterium glutamicum*, bearing the lactose operon of *Escherichia coli*. Archives of Microbiology **155**, 607-612.

Bro,C., Regenberg,B., Förster,J., and Nielsen,J. (2006) *In silico* aided metabolic engineering of *Saccharomyces cerevisae* for improved bioethanol production. Metabolic Engineering **8**, 102-111.

Burgard,A.P., Pharkya,P., and Maranas,C.D. (2003) OptKnock: A bilevel programming framework for identifying gene knockout strategies for microbial strain optimization. Biotechnology and Bioengineering **84**, 647-657.

Caspi,R., Foerster,H., Fulcher,C.A., Hopkinson,R., Ingraham,J., Kaipa,P., Krummenacker,M., Paley,S., Pick,J., Rhee,S.Y., Tissier,C., Zhang,P., and Karp,P.D. (2006) MetaCyc: a multiorganism database of metabolic pathways and enzymes. Nucleic Acids Research **34**, 511-516.

Christensen,B. (2001) Metabolic Network Analysis: Principles, Methodologies and Applications. PhD-Thesis: BioCentrum-DTU, Technical University of Denmark, Lyngby.

Christensen,B. and Nielsen,J. (1999a) Isotopomer analysis using GC-MS. Metabolic Engineering **1**, 282-290.

Christensen,B. and Nielsen,J. (1999b) Metabolic network analysis. Advances in Biochemical Engineering **66**, 209-231.

Christensen,B. and Nielsen,J. (2000) Metabolic network analysis of *Penicillum chrysogenum* using 13C-labelled glucose. Biotechnology and Bioengineering **68**, 652-659.

Covert,M.W., Knight,E.M., Reed,J.L., Herrgard,M.J., and Palsson,B.O. (2004) Integrated high-throughput and computational data elucidates bacterial networks. Nature **429**, 92-96.

Covert,M.W. and Palsson,B.O. (2003) Constraints-based models: regulation of gene expression reduces the steady-state solution space. Journal of Theoretical Biology **221**, 309-325.

Covert,M.W., Schilling,C.H., Famili,I., Edwards,J.S., Goryanin,I.I., Selkov,E., and Palsson,B.O. (2001a) Metabolic modeling of microbial strains *in silico*. TRENDS in Biochemical Science **26**, 179-186.

Covert,M.W., Schilling,C.H., and Palsson,B.O. (2001b) Regulation of gene expression in flux balance models of metabolism. Journal of Theoretical Biology **213**, 73-88.

Cremer,J., Eggeling,L., and Sahm,H. (1991) Control of the lysine biosynthesis sequence in *Corynebacterium glutamicum* as analysed by overexpression of the individual corresponding genes. Applied and Environmental Microbiology **57**, 1746-1752.

Dominguez,H., Rollin,C., Guyonvarch,A., Guerquin-Kern,J.L., Cocaign-Bousquet,M., and Lindley,N.D. (1998) Carbon-flux distribution in the central metabolic pathways of *Corynebacterium glutamicum* during growth on fructose. European Journal of Biochemistry **254**, 96-102.

Dunican,L.K., McCormack,A., Stapelton,C., Burke,K., O'Donohue,M., Marx,A., and Möckel,B. (2001) Cloning and uses of a novel nucleotide sequence coding for a glucose-6-phosphate isomerase (*pgi*) from bacteria. European Patent [EP 1087015].

Edwards,J.S., Ibarra,R.U., and Palsson,B.Ø. (2001) *In silico* predictions of *Escherichia coli* metabolic capabilities are consistent with experimental data. Nature Biotechnology **19**, 125-130.

Edwards,J.S. and Palsson,B.Ø. (2000) The *Escherichia coli* MG1655 *in silico* metabolic genotype: Its definition, characteristics, and capabilities. PNAS **97**, 5528-5533.

Eggeling,L., Oberle,S., and Sahm,H. (1998) Improved L-lysine yield with *Corynebacterium glutamicum*: use of *dapA* resulting in increased flux combined with growth limitation. Applied Microbiology and Biotechnology **49**, 24-30.

Eikmanns,B.J., Rittmann,D., and Sahm,H. (1995) Cloning, sequence analysis, expression, and inactivation of the *Corynebacterium glutamicum icd* gene encoding isocitrate dehydrogenase and biochemical characterization of the enzyme. Journal of Bacteriology **177**, 774-782.

Feist,A.M., Scholten,J.C.M., Palsson,B.O., Brockman,F.J., and Ideker,T. (2006) Modelling methanogenesis with a genome-scale metabolic reconstruction of *Methanosarcina barkeri*. Molecular Systems Biology **2**, 1-14.

Förberg,C., Eliaeson,T., and Häggström,L. (1988) Correlation of theoretical and experimental yields of phenylalanine from non-growing cells of a rec *Escherichia coli* strain. Journal of Biotechnology **7**, 319-332.

Förster,J., Famili,I., Fu,P., Palsson,B.Ø., and Nielsen,J. (2003) Genome-scale reconstruction of the *Saccharomyces cerevisiae* metabolic network. Genome Research **13**, 244-253.

Georgi,T., Rittmann,D., and Wendisch,V.F. (2005) Lysine and glutamate production by *Corynebacterium glutamicum* on glucose, fructose and sucrose: Roles of malic enzyme and fructose-1,6-bisphosphatase. Metabolic Engineering **7**, 291-301.

Gourdon,P., Baucher,M.F., Lindley,N.D., and Guyonvarch,A. (2000) Cloning of the malic enzyme gene from *Corynebacterium glutamicum* and role of the enzyme in lactate metabolism. Applied and Environmental Microbiology **66**, 2981-2987.

Gubler,M.E., Park,S.M., Jetten,M.S., and Stephanopoulos,G. (1994) Effects of phosphoenolpyruvate carboxylase deficiency on metabolism and lysine production in *Corynebacterium glutamicum*. Applied Microbiology and Biotechnology **40**, 857-863.

Hartmann,M., Tauch,A., Eggeling,L., Bathe,B., Mockel,B., Puhler,A., and Kalinowski,J. (2003) Identification and characterization of the last two unknown genes, *dapC* and *dapF*, in the succinylase branch of the -lysine biosynthesis of *Corynebacterium glutamicum*. Journal of Biotechnology **104**, 199-211.

Heinemann,M., Kümmel,A., Ruinatscha,R., and Panke,S. (2005) *In silico* genome-scale reconstruction and validation of the *Staphylococcus aureus* metabolic network. Biotechnology and Bioengineering **92**, 850-864.

Hermann,T., Pfefferle,W., Baumann,C., Busker,E., Schaffer,S., Bott,M., Sahm,H., Dusch,N., Kalinowski,J., Pühler,A., Bendt,A.K., Krämer,R., and Burkovski,A. (2001) Proteome analysis of *Corynebacterium glutamicum*. Electrophoresis **22**, 1712-1723.

Herrgård,M.J., Fong,S.S., and Palsson,B.O. (2006) Identification of Genome-scale metabolic network models using experimentally measured flux profiles. PLoS Computationel Biology **2**, 676-686.

Hollander,J.A. (1994) Potential metabolic limitations in lysine production by *Corynebacterium glutamiucm* as revealed by metabolic network analysis. Applied Microbiology and Biotechnology **42**, 508-515.

Hua,Q., Yang,C., and Shimizu,K. (2000) Metabolic control analysis for lysine synthesis using *Corynebacterium glutamicum* and experimental verification. Journal of Bioscience and Bioengineering **90**, 184-192.

Ikeda,M. and Nakagawa,S. (2003) The *Corynebacterium glutamicum* genome: features and impacts on biotechnological processes. Applied Microbiology and Biotechnology **62**, 99-109.

Jetten,M.S.M. and Sinskey,A.J. (1995) Purification and properties of oxaloacetate decarboxylase from *Corynebacterium glutamicum*. Antonie van Leeuwenhoek **67**, 221-227.

Jørgenen,H.S., Nielsen,J., Villadsen,J., and Møllgaard,H. (1995) Metabolic flux distributions in *Penicillium chrysogenum* during fed-batch cultivations. Biotechnology and Bioengineering **46**, 117-131.

Kalinowski,J., Bathe,B., Bartels,D., Bischoff,N., Bott,M., Burkovski,A., Dusch,N., Eggeling,L., Eikmanns,B.J., and Gaigalat,L. (2003) The complete *Corynebacterium glutamicum* ATCC 13032 genome sequence and its impact on the production of -aspartate-derived amino acids and vitamins. Journal of Biotechnology **104**, 5-25.

Kanehisa,M., Goto,S., Hattori,M., Aoki-Kinoshita,K.F., Itoh,M., Kawashima,S., Katayama,T., Araki,M., and Hirakawa,M. (2006) From genomics to chemical genomics: new developments in KEGG. Nucleic Acids Research **34**, 354-357.

Karp,P.D., Ouzounis,C.A., Moore-Kochlacs,C., Goldovsky,L., Kaipa,P., Ahrén,D., Tsoka,S., Darzentas,N., Kunin,V., and López-Bigas,N. (2005) Expansion of the BioCyc collection of pathway/genome databases to 160 genomes. Nucleic Acids Research **33**, 6083-6089.

Kawaguchi,H., Sasaki,M., Vertes,A.A., Inui,M., and Yukawa,H. (2008) Engineering of an L-arabinose metabolic pathway in *Corynebacterium glutamicum*. Applied Microbiology and Biotechnology **77**, 1053-1062.

Kawaguchi,H., Vertes,A.A., Okino,S., Inui,M., and Yukawa,H. (2006) Engineering of a xylose metabolic pathway in *Corynebacterium glutamicum*. Applied and Environmental Microbiology **72**, 3418-3428.

Kelle,R., Hermann,T., and Bathe,B. (2005) L-Lysine production. In Handbook of Corynebacterium glutamicum (Edited by Eggeling,L. and Bott,M.) pp. 465-488. CRC Press, Boca Raton.

Kiefer,P., Heinzle,E., Zelder,O., and Wittmann,C. (2004) Comparative metabolic flux analysis of lysine-producing *Corynebacterium glutamicum* cultured on glucose or fructose. Applied and Environmental Microbiology **70**, 229-239.

Koffas,M.A.G., Jung,G.Y., Aon,J.C., and Stephanopoulos,G. (2002) Effect of pyruvate carboxylase overexpression on the physiology of *Corynebacterium glutamicum*. Applied and Environmental Microbiology **68**, 5422-5428.

Koffas,M.A.G., Jung,G.Y., and Stephanopoulos,G. (2003) Engineering metabolism and product formation in *Corynebacterium glutamicum* by coordinated gene overexpression. Metabolic Engineering **5**, 32-41.

Krömer,J.O., Sorgenfrei,O., Klopprogge,K., Heinzle,E., and Wittmann,C. (2004) In-depth profiling of lysine-producing *Corynebacterium glutamicum* by combined analysis of the transcriptome, metabolome, and fluxome. Journal of Bacteriology **186**, 1769-1784.

Lu,J.-H. and Liao,C.-C. (1997) Site-directed mutagenesis of the aspartikinase gene *lysC* and its characterization in *Brevibacterium flavum*. Letters in Applied Microbiology **24**, 211-213.

Marx,A., de Graaf,A.A., Wiechert,W., Eggeling,L., and Sahm,H. (1996) Determination of the fluxes in the central metabolism of *Corynebacterium glutamicum* by nuclear magnetic resonance spectroscopy combined with metabolite balancing. Biotechnology and Bioengineering **49**, 111-129.

Marx,A., Eikmanns,B.J., Sahm,H., de Graaf,A.A., and Eggeling,L. (1999) Response of the central metabolism in *Corynebacterium glutamicum* to the use of an NADH-Dependent glutamate dehydrogenase. Metabolic Engineering **1**, 35-48.

Marx,A., Hans,S., Möckel,B., Bathe,B., and de Graaf,A.A. (2003) Metabolic phenotype of phosphoglucose isomerase mutants of *Corynebacterium glutamicum*. Journal of Biotechnology **104**, 185-197.

Marx,A., Striegel,K., de Graaf,A.A., Sahm,H., and Eggeling,L. (1997) Response of the central metabolism of *Corynebacterium glutamicum* to different flux burdens. Biotechnology and Bioengineering **56**, 168-180.

McGinnis,S. and Madden,T.L. (2004) BLAST: at the core of a powerful and diverse set of sequence analysis tools. Nucleic Acids Research **32**, 20-25.

Moritz,B., Striegel,K., de Graff,A.A., and Sahm,H. (2000) Kinetic properties of the glucose-6-phosphate and 6-phosphogluconate dehydrogenases from *Corynebacterium glutamicum* and their application for predicting pentose phosphate pathway flux in vivo. European Journal of Biochemistry **267**, 3442-3452.

Netzer,R., Krause,M., Rittmann,D., Peters-Wendisch,P., Eggeling,I., Wendisch,V.F., and Sahm,H. (2004) Roles of pyruvate kinase and malic enzyme in *Corynebacterium glutamicum* for growth on carbon source requiring gluconeogenesis. Archives of Microbiology **182**, 354-363.

Nissen,T.L., Schulze,U., Nielsen,J., and Villadsen,J. (1997) Flux distributions in anaerobic, glucose-limited continuous cultures of *Saccharomyces cerevisiae*. Microbiology **143**, 203-218.

Ohnishi,J., Hayashi,M., Mitsuhashi,S., and Ikeda,M. (2003) Efficient 40°C fermentation of L-lysine by a new *Corynebacterium glutamicum* mutant developed by genome breeding. Applied Microbiology and Biotechnology **62**, 69-75.

Ohnishi,J., Kakahira,R., Mitsuhashi,S., Kakita,S., and Ikeda,M. (2005) A novel *gnd* mutation leading to increased L-lysine production in *Corynebacterium glutamicum*. FEMS Microbiology Letters **242**, 265-274.

Ohnishi,J., Mitsuhashi,S., Hayashi,M., Ando,S., Yokoi,H., and Ikeda,M. (2002) A novel methology employing *Corynebacterium glutamicum* genome information to generate a new L-lysine-producing mutant. Applied Microbiology and Biotechnology **58**, 217-223.

Oliveira,A.P., Nielsen,J., and Förster,J. (2005) Modelling *Lactococcus lactis* using a genome-scale flux model. BMC Microbiology **5,** 39.

Palsson,B.O. (2000) The challenges of *in silico* biology. Nature Biotechnology **18**, 1147-1150.

Palsson,B.O. (2006) Systems Biology - Properties of Reconstructed Networks. Cambridge University Press, New York, USA

Papoutsakis,E.T. (1984) Equations and calculations for fermentations of butyric acid bacteria. Biotechnology and Bioengineering **26**, 174-184.

Papoutsakis,E.T. and Meyer,C.L. (1985) Equations and calculations of product yield and preferred pathways for butanediol and mixed-acid fermentations. Biotechnology and Bioengineering **27**, 50-66.

Patil,K.R., Åkesson,M., and Nielsen,J. (2004) Use of genome-scale microbial models for metabolic engineering. Current Opinion in Biotechnology **15**, 64-69.

Peters-Wendisch,P., Eikmanns,B.J., Thierbach,G., Bachmann,B., and Sahm,H. (1993) Phosphoenolpyruvate carboxylase in *Corynebacterium glutamicum* is dispensable for growth and lysine production. FEMS Microbiology Letters **112**, 269-274.

Peters-Wendisch,P.G., Kreutzer,C., Kalinowski,J., Patek,M., Sahm,H., and Eikmanns,B.J. (1998) Pyruvate carboxylase from *Corynebacterium glutamicum*: characterization, expression and inactivation of the *pyc* gene. Microbiology **144**, 915-927.

Peters-Wendisch,P.G., Schiel,B., Wendisch,V.F., Katsoulidis,E., Mockel,B., Sahm,H., and Eikmanns,B.J. (2001) Pyruvate carboxylase is a major bottleneck for glutamate and lysine production by *Corynebacterium glutamicum*. Journal of Molecular Microbiology and Biotechnology **3**, 295-300.

Petersen,S., de Graff,A.A., Eggeling,L., Mollney,M., Wiechert,W., and Sahn,H. (2000) *In vivo* quantification of parallel and bidirectional fluxes in the anaplerosis of *Corynebacterium glutamicum*. Journal of Biological Chemistry. **275**, 35932-35941.

Petersen,S., Mack,C., de Graaf,A.A., Riedel,C., Eikmanns,B.J., and Sahm,H. (2001) Metabolic consequences of altered phosphoenolpyruvate carboxykinase activity in *Corynebacterium glutamicum* reveal anaplerotic regulation mechanisms *in vivo*. Metabolic Engineering **3**, 344-361.

Price,N.D., Papin,J.A., Schilling,C.H., and Palsson,B.Ø. (2003) Genome-scale microbial *in silico* models: the constrain-based approach. Trends in Biotechnology **21**, 162-169.

Reed,J.R., Vo,T.D., Schilling,C.H., and Palsson,B.Ø. (2003) An expanded genome-scale model of *Escherichia coli* K-12 (iJR904 GSM/GPR). Genome Research **4**.

Riedel,C., Rittmann,D., Dangel,P., Möckel,B., Sahn,H., and Eikmanns,B.J. (2001) Characterization, expression, and inactivation of the phosphoenolpyruvate carboxykinase gene from *Corynebacterium glutamicum* and significance of the enzyme for growth and amino acid production. Journal of Molecular Microbiology and Biotechnology **3**, 573-583.

Sauer,U., Cameron,D.C., and Bailey,J.E. (1998) Metabolic capacity of *Bacillus subtilis* for the production of purine nucleotides, riboflavin, and folic acid. Biotechnology and Bioengineering **59**, 227-238.

Schilling,C.H., Covert,M.W., Famili,I., Church,G.M., Edwards,J.S., and Palsson,B.Ø. (2002) Genome-scale metabolic model of *Helicobacter pylori* 26695. Journal of Bacteriology **184**, 4582-4593.

Schilling,C.H. and Palsson,B.O. (2000) Assessment of the metabolic capabilities of *Haemophilus influenzae* Rd through a genome-scale pathway analysis. Journal of Theoretical Biology **203**, 249-283.

Schilling,C.H., Schuster,S., Palsson,B.O., and Heinrich,R. (1999) Metabolic pathway analysis: basic concepts and scientific applications in the post-genomic era. Biotechnology Progress **15**, 296-303.

Seibold,G., Auchter,M., Berens,S., Kalinowski,J., and Eikmanns,B.J. (2006) Utilization of soluble starch by a recombinant *Corynebacterium glutamicum* strain: Growth and lysine production. Journal of Biotechnology **124**, 381-391.

Shaw-Reid,C.A., McCormick,M.M., Sinskey,A.J., and Stephanopoulos. (1999) Flux through the tetrahydrodipicolinate succinylase pathway is dispensable for L-lysine production in *Corynebacterium glutamicum*. Applied Microbiology and Biotechnology **51**, 325-333.

Shpaer,E.G., Robinson,M., Yee,D., Candlin,J.D., Mines,R., and Hunkapiller,T. (1996) Sensitivity and selectivity in protein similarity searches: A comparison of Smith-Waterman in hardware to BLAST and FASTA. Genomics **38**, 179-191.

Sonntag,K., Schwinde,J.W., de Graaf,A.A., Marx,A., Eikmanns,B.J., Wiechert,W., and Sahm,H. (1995) 13C NMR studies of the fluxes in the central metabolism of *Corynebacterium glutamicum* during growth and overproduction of amino acids in batch cultures. Applied Microbiology and Biotechnology **44**, 489-495.

Stephanopoulos,G. (1999) Metabolic fluxes and metabolic engineering. Metabolic Engineering **1**, 1-11.

Stephanopoulos,G. and Vallino,J.J. (1991) Network rigidity and metabolic engineering in metabolite overproduction. Science **252**, 1675-1681.

Stephanopoulos,G.N., Aristidou,A.A., and Nielsen,J. (1998) Metabolic Engineering - Principles and Methodologies. Academic Press, San Diego, USA.

Teusink,B., Wiersma,A., Molenaar,D., Francke,C., de Vos,W.M., Siezen,R.J., and Smid,E.J. (2006) Analysis of growth of *Lactobacillus plantarum* WCFS1 on a complex medium using a genome-scale model. Journal of Biological Chemistry **281**, 40041-40048.

Vallino,J.J. and Stephanopoulos,G. (1993) Metabolic flux distribution in *Corynebacterium glutamicum* during growth and lysine overproduction. Bioprocess Engineering **41**, 633-646.

Vallino,J.J. and Stephanopoulos,G. (1994a) Carbon flux distributions at the glucose 6-phosphate branch point in *Corynebacterium glutamicum* during lysine overproduction. Biotechnology Progress **10**, 327-334.

Vallino,J.J. and Stephanopoulos,G. (1994b) Carbon flux distribution at the pyruvate branch point in *Corynebacterium glutamicum* during lysine overproduction. Biotechnology Progress **10**, 320-326.

Varma,A., Boesch,B.W., and Palsson,B.O. (1993a) Biochemical production capabilities of *Escherichia coli*. Biotechnology and Bioengineering **42**, 59-73.

Varma,A., Boesch,B.W., and Palsson,B.O. (1993b) Stoichiometric interpretation of *Escherichia coli* glucose catabolism under various oxygenation rates. Applied and Environmental Microbiology **59**, 2465-2473.

Vrljic,M., Sahm,H., and Eggeling,L. (1996) A new type of transporter with a new type of cellular function: l-lysine export from *Corynebacterium glutamicum*. Molecular Microbiology **22**, 815-826.

Wendisch,V.F. (2003) Genome-wide expression analysis in *Corynebacterium glutamicum* using DNA microarrays. Journal of Biotechnology **104**, 273-285.

Wendisch,V.F., de Graaf,A.A., Sahm,H., and Eikmanns,B.J. (2000) Quantitative determination of metabolic fluxes during co-utilization of two carbon sources: Comparative analyses with *Corynebacterium glutamicum* during growth on acetate and/or glucose. Journal of Bacteriology **182**, 3088-3096.

Wittmann,C. and Heinzle,E. (2001) Application of MALDI-TOF MS to lysine-producing *Corynebacterium glutamicum*: A novel approach for metabolic flux analysis. European Journal of Biochemistry **268**, 2441-2455.

Wittmann,C. and Heinzle,E. (2002) Genealogy profiling through strain improvement by using metabolic network analysis: metabolic flux genealogy of several generations of lysine-producing Corynebacteria. Appled and Environmental Microbiology **68**, 5843-5859.

Wittmann,C., Kiefer,P., and Zelder,O. (2004) Metabolic fluxes in *Corynebacterium glutamicum* during lysine production with sucrose as carbon source. Applied and Environmental Microbiology **70**, 7277-7287.

Yang,C., Hua,Q., and Shimizu,K. (2002) Integration of the information from gene expression and metabolic fluxes for the analysis of the regulatory mechanisms in *Synechocystis*. Applied Microbiology and Biotechnology **58**, 813-822.

Chapter 3

3. Microbiology and biochemistry of *Corynebacterium glutamicum*

In this chapter a short introduction to the microbiology of *Corynebacterium glutamicum* is given, followed by a review of biochemistry of *C. glutamicum.* The review is used as the basis for the later reconstruction of the *C. glutamicum* metabolic network which is presented in chapter 4. Abbreviations used in this chapter are also used for the model reconstruction.

Microbiology of Corynebacterium glutamicum

C. glutamicum is a gram-positive, non-sporulating, non-motile, ellipsoidal bacteria (Abe *et al.*, 1967). It is aerobic and catalase-positive (Liebl, 2005) and most strains form pale yellow colonies, but some cream-white variants are also known to occur (Abe *et al.*, 1967). The type strain *Corynebacterium glutamicum* ATCC 13032 (alternative designations: DSM 20300, IMET 10482, and NCIB 10025) was originally isolated from sewage. Other strains have been isolated from soils, soils contaminated with bird faeces, sewage and manure (Liebl, 2005). *C. glutamicum* is able to utilize various carbon sources i.e. sugars such as glucose and fructose (Dominguez *et al.*, 1997) and sucrose (Dominguez and Lindley, 1996), and organic acids such as acetate (Gerstmeier *et al.*, 2003), lactate and pyruvate (Cocaign-Bousquet *et al.*, 1993) and gluconate (Lee *et al.*, 1998). In addition to this it is able to co-metabolize substrates of which some examples have been reported in literature i.e. lactate and acetate, glucose and pyruvate, glucose and lactate (Cocaign-Bousquet *et al.*, 1993), and acetate and glucose (Wendisch *et al.*, 2000). Cocaign-Bousquet *et al*., (1993) found simultaneous consumption kinetics during co-metabolism of sugars and organic acids. This lack of diauxic growth patterns is quite rarely reported in literature.

C. glutamicum is able to take up and utilize the inorganic nitrogen sources ammonia and ammonium (Burkovski, 2003a). In addition to that some organic sources can be used as nitrogen donors i.e. urea (Siewe *et al.*, 1998), glutamine (Siewe *et al.*, 1995), glutamate (Kronemeyer *et al.*, 1995) and serine (Netzer *et al.*, 2004). It is generally known that other amino acids such as alanine, aspargine, and threonine also can be used. The *C. glutamicum* parent strain is prototrophic for all amino acids and vitamins, except for biotin (Liebl, 2005). Some amino acid production strains derived by strain improvement programs have obtained some amino acid auxotropies such as threonine, methionine, leucine and isoleucine, and in some cases also vitamin auxotrophies such as thiamine and 4-amino benzoic acid have been reported (Abe *et al.*, 1967).

C. glutamicum grow well in complex media such as brain heart infusion broth (Difco), LB5G broth (0.5% yeast extract, 1% tryptone, 0.5% glucose and 0.5% NaCl; pH 7.2-7.4)) (Vallino and Stephanopoulos, 1993); *Corynebacterium* medium: (1% casein peptone, 0.5% yeast extract, 0.5% glucose and 0.5% NaCl; pH 7.2-7.4) (Deutze Sammling von Microorganismen und Zellkulturen GmbH (DSMZ)) or similar tryptone, peptone, yeast extract based medium. Also less expensive components can be used for complex media preparations such as corn steep liquor (CSL) or soybean meal hydrolysate. Those types of complex raw materials are normally used on industry

scale fermentations. Defined media have also been developed for this organism (Marx *et al.*, 1996; Moritz *et al.*, 2000; Petersen *et al.*, 2000; Vallino and Stephanopoulos, 1993). This type of media is used in experiments where complex compounds can compromise the results, i.e. in flux analysis.

The *C. glutamicum* ATCC 13032 parent strain have been reported to grow well at 40°C (Ohnishi *et al.*, 2003), whereas optimal temperatures for amino acid producing strains typically have been reported between 25 and 37°C (Abe *et al.*, 1967). Traditionally cultivation temperature for lysine fermentations is 30-34°C (Hermann, 2003). Optimum pH is in the range of 7.2-7.4 (DSMZ). *C. glutamicum* has a high demand for oxygen and an efficient oxygen supply is important for efficient growth and lysine production.

The Corynebacterium glutamicum genome

The genome of *C. glutamicum* ATCC 13032 have been sequenced by at least three independent research groups of which two are now available via open databases (Ikeda and Nakagawa, 2003; Kalinowski *et al.*, 2003). Recently another strain, *C. glutamicum* R (Inui *et al.*, 2004), was sequenced, published and made available in public databases (Yukawa *et al.*, 2007). In addition to this, genome sequence projects have been conducted for closely related organisms such as *Corynebacterium efficiens* YS-314 (Nishio *et al.*, 2003), *Corynebacterium jeikeium* K411 (Tauch *et al.*, 2005) and *Corynebacterium diphtheriae* NCTC 13129 (Ceredeño-Tárraga *et al.*, 2003). Based on this intensive genome analysis it could be concluded that the size of the *C. glutamicum* genome is 3.3 kb and the following annotations have revealed about 3000 ORFs. The G+C content is 54% of the *C. glutamicum* genome.

Biochemistry of C. glutamicum

Substrate uptake and utilization

C. glutamicum is able to utilize a variety of sugars, sugar alcohols and organic acids as carbon sources, either as a single substrate or during co-metabolism. The sugars fructose, glucose and sucrose are all mainly taken up by specific PTS systems (Moon *et al.*, 2005), which phosphorylates these sugars to either glucose-6-phosphate or fructose-6-phosphate by the conversion of phosphoenolpyruvate to pyruvate. In the case of sucrose only the glucose part is phosphorylated using this system (Dominguez *et al.*, 1997). Phosphorylation of fructose is only possible using the PTS-system, why internal fructose is transported out of the cell by a unknown transport-mechanism, followed by transport and phosphorylation using the PTS-system (Dominguez *et al.*, 1997; Dominguez and Lindley, 1996). The presence of an mannose specific PTS-system have also been suggested and confirmed by complementation in *E. coli* (Lee *et al.*, 1993). However, the physiological role of this system in *C. glutamicum* is complex since it has been found to also be involved in fructose transport (Kiefer *et al.*, 2004), and glucose transport during osmotic stress (Gourdon *et al.*, 2003). Growth of *C. glutamicum* in the presence of mannose as the only carbon source is lower than for growth on glucose (Parche *et al.*, 2001). Parche *et al*. (2001) also tested maltose as a carbon source and found growth similar to glucose grown cells. The presence of an alternative glucose uptake system has been identified, and in addition to this a glucose kinase (*glk*) is present in the organism (Park *et al.*, 2000), making an alternative to the PTS-system for glucose

utilization. A number of organic acids have been investigated as substrate for *C. glutamicum*. Lactate can be used as a single carbon source or in co-metabolism with other substrates (Cocaign-Bousquet and Lindley, 1995). Both D- and the L-lactate can be utilized, and lactate enters the metabolism via lactate dehydrogenase converting lactate to pyruvate (Bott and Niebisch, 2003). Acetate can be used as a single carbon source or in co-metabolism with other carbon sources (Wendisch *et al.*, 2000), and enters the TCA cycle as Acetyl-CoA after the combined activities of acetate kinase (*ackA*) and phosphotransacetylase (*pta*) (Reinscheid *et al.*, 1999). Propionate can be used as a single carbon source or in a combination with other carbon sources (Claes *et al.*, 2002), and enters the metabolism forming pyruvate and succcinate by reaction with oxaloacetate. Pyruvate metabolism is involved in the respiratory energy metabolism (Bott and Niebisch, 2003). It can be used as a single carbon source or in co-metabolism (Cocaign-Bousquet *et al.*, 1993). The organic acid gluconate enters the organism by the use of a gluconate permerase. Subsequently it is phosphorylated by gluconate kinase (*gntK*) forming 6-phosphogluconate, which is an intermediate in the pentose phosphate pathway (Lee *et al.*, 1998; Frunzke *et al.*, 2008). Recently citrate have been evaluated as a substrate for *C. glutamicum*, and it was seen that this substrate could be utilized either as the only carbon source or simultaneous with glucose (Polen *et al.*, 2007).

Nitrogen metabolism

Nitrogen uptake and the regulation of nitrogen metabolism have been investigated and reviewed intensively in *C. glutamicum* (Burkovski, 2003a; Burkovski, 2003b). The organism is able to utilize inorganic nitrogen as ammonium or ammonia, or as organic nitrogen in the presence of urea or amino acids. Ammonia or ammonium can be taken op either by diffusion when concentrations are high or by active uptake systems when concentrations are lower (Meier-Wagner *et al.*, 2001; Siewe *et al.*, 1996). This is also the case for urea (Siewe *et al.*, 1998). Some amino acids can also serve as nitrogen donors for *C. glutamicum*. L-glutamine (Siewe *et al.*, 1995), L-glutamate (Kronemeyer *et al.*, 1995) and L-serine (Netzer *et al.*, 2004) have been studied in this respect, and in addition to these L-alanine, L-aspargine and L-threonine are generally accepted to serve as potential nitrogen sources for *C. glutamicum*, although no systematic studies have been conducted so far. The major route of ammonium assimilation at high concentrations in *C. glutamicum* is through glutamate dehydrogenase (*gdh*: EC 1.4.1.4) (Eq. 3.1). At lower ammonium concentrations (≤0.1 mM) the high affinity system GS/GOGAT is used instead involving two sequential reactions catalysed by glutamine syntase (*glnA*: EC 6.3.1.2), Eq. 3.2, and glutamate syntase (*gltBD*: EC 1.4.1.13), Eq. 3.3, (Jakoby *et al.*, 1997). The difference between the net result of the GS/GOGAT and gnd is the consumption of one mole of ATP, making this system less energy efficient. During relevant fermentation conditions ammonium concentrations are always high (≥ 0.5 mM), which makes gdh most significant for ammonium assimilation during amino acid production.

Eq. 3.1 (*gdh*): α-ketogluterate + NADPH + NH_4^+ → glutamate + $NADP^+$

Eq. 3.2 (*glnA*): glutamate + ATP + NH_4^+ → glutamine + ADP + P_i

Eq. 3.3 (*gltBD*): glutamine + α-ketogluterate + NADPH → 2 glutamate + $NADP^+$

When inside the cell urea is hydrolysed by the enzyme urease (*ureA*: EC 3.5.1.5) (Siewe *et al.*, 1998) yielding two molecules of ammonia and one molecule of carbon dioxide. Ammonia is further assimilated into glutamate or glutamine as described above.

Phosphorous metabolism

In bacterial cells phosphorous occurs in inorganic form, mostly orthophosphate (P_i), pyrophosphate (PP_i) or polyphosphates ($polyP_i$), and in organic form mostly as a component in a number of biomass components, the most important being RNA and DNA. In addition phosphorous plays a central role in energy metabolism since biochemical energy obtained by the oxidation of substrates is used to form ATP from ADP and P_i. The most important source of phosphorous for *C. glutamicum* is phosphate (PO_4^{3+}). The presence of three different systems (*pitA*, *nptA*, and *pst*) for the uptake of inorganic phosphorous have been proposed in *C. glutamicum* based on the annotated genome (Ishige *et al.*, 2003).The pitA-system is a low affinity transporter with a high capacity using the proton motive force, and is preferably used when phosphorous concentrations are high. The nptA-system is a Na^+-dependent symporter transport system. The last system is an ABC-type ATP-driven high affinity transport system, probably used during conditions where phosphorous concentrations are low since this system is strongly upregulated during phosphorous starvation conditions (Ishige *et al.*, 2003).

Sulfur metabolism

Sulfur is used as a constituent of a large number of biomass components, methionine and cysteine being the most dominant. The main source of sulfur for micro-organisms in nature and in fermentations is the inorganic compound sulfate (SO_4^{2-}), which will be the main focus here. Sulfate enters the cell via an ATP-dependent transport-system, and is reduced to the bio-available sulfide (H_2S) via a sequence of steps (Lee, 2005). These steps involves an activation to adenosine-5'-phosphosulphate (APS) followed by a reduction to sulfite (SO_3^{2-}), and a further reduction step to sulfide. An alternative pathway which has been proposed due to its presence in other bacteria is the phosphorylation of APS to 3'-phosphoadenosine 5'phosphosulphate (PAPS), which is reduced to sulfite. However, the presence or this pathway has not yet been confirmed, and the apparent lack of the gene encoding the enzyme catalyzing the first reaction in the annotated genome indicates that only the first pathway is in fact present in *C. glutamicum* (Lee, 2005). An alternative to the assimilation of inorganic sulfur is the degradation of sulfur containing amino acids. Cysteine can be degraded to pyruvate, H_2S, and NH_3 by cysteine desulfhydrase (*aecD*) (Rossol and Pühler, 2003). Methionine degradation is not well investigated. Based on genome data it is likely that it is a three step pathway forming α-ketobutyrate, methanethiol, and NH_3. Another variant involves an additional step yielding α-keto-γ-thiobutyrate and glutamate from methionine and α-ketobutyrate. However, no biological evidence has yet been presented for these pathways.

Central Carbon Metabolism

The Glycolysis

After sugars has been taken up and phosphorylated they enter the glycolytic pathway or the pentose phosphate pathway (see later in this chapter) (Figure 3.1). The point for the metabolic flux towards either glycolysis or pentose phosphate pathway is at the metabolite glucose-6-phosphate, which earlier have been identified as a branch point for central metabolism in *C. glutamicum* (Vallino and

Stephanopoulos, 1994). The first step in glycolysis is catalysed by the enzyme glucose-6-phosphate isomerase (*pgi*) catalysing the reversible reaction between glucose-6-phosphate and fructose-6-phosphate (Marx *et al.*, 2003). Fructose-6-phosphate is further converted to fructose-1,6-bisphosphate via 6-phosphofructokinase (*pfkA*) (Sugimoto and Shiio, 1989b). During gluconegenesis the enzyme fructose-1,6-bisphosphatase (*fbp*) is essential catalysing the reverse reaction of *pfkA* (Rittmann *et al.*, 2003). The further conversion of fructose-1,6-bisphosphate is catalysed by glyceraldehydes-3-phosphate dehydrogenase (*fda*) forming dihydroxyacetone phosphate and glycaldehyde 3-phosphate (von der Osten *et al.*, 1989). The generated dihydroxyacetone phosphate is converted to glycaldehyde 3-phosphate by triosephosphate isomerase (*tpiA*), and glycaldehyde 3-phosphate is further converted to 1,3-biphosphoglycerate by glycaldehyde 3-phosphate dehydrogenase (*gapA*) using NAD^+ as a co-enzyme (Eikmanns, 1992; Omumasaba *et al.*, 2004). The presence of an NADPH dependent glycaldehyde 3-phosphate dehydrogenase (*gapB*) have also been confirmed and investigated (Omumasaba *et al.*, 2004). Omumasaba *et al*. (2004) investigated the role of both enzymes and found that *gapA* was essential for growth on glucose, whereas the deletion of *gapB* did not have any effect. During growth on organic acids (lactate, acetate and pyruvate) growth was seen for both Δ*gapA*- and Δ*gapB*-mutants, although a more abundant negative effect was observed for the Δ*gapB*-mutant. These results indicate that *gapA* is reversible, and strictly used during growth on glucose, whereas *gapB* only is active during gluconeogenic growth, where this pathway is more effective than *gapA*. The next reaction is the reversible reaction converting 1,3-biphosphoglycerate to 3-phosphoglycerate coupled to phosphorylation of ADP to ATP, catalysed by 3-phosphoglycerate kinase (*pgk*) (Eikmanns, 1992). Based on the annotated genome 3-phosphoglycerate is converted to 2-phosphoglycerate by

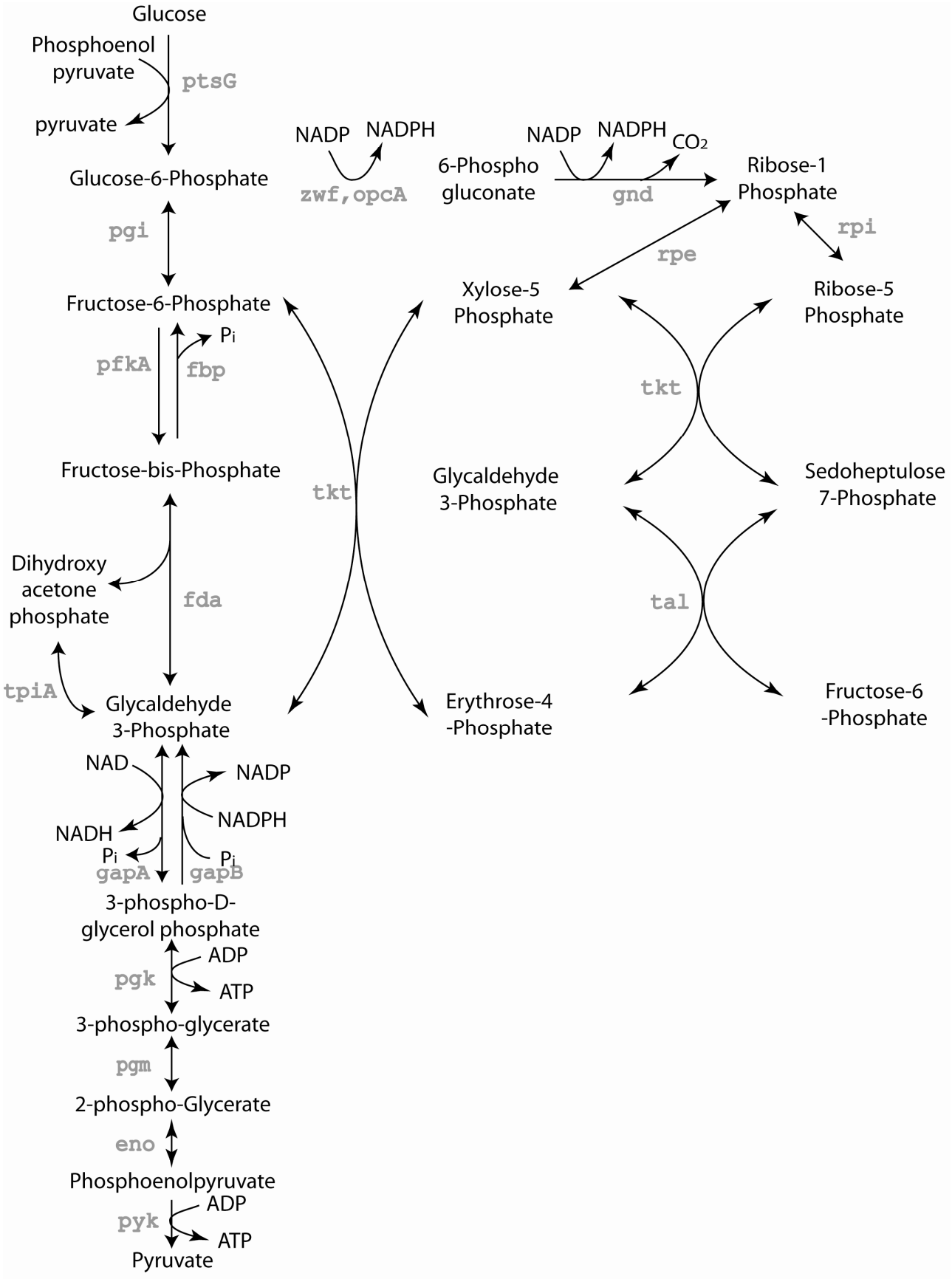

Figure 3.1: Glycolysis and pentose phosphate pathway in *C. glutamicum*. Genes and enzymes involved: *ptsG*: EC 2.7.1.69 (PTS-permerase); *pgi*: EC 5.3.1.9 (glucose-6-phosphate isomerase); *pfkA*: EC 2.7.1.11 (6-phosphofructokinase); *fbp*: EC 3.1.3.11 (fructose-bisphosphatase); *fda*: EC 4.1.2.13 (fructose-bisphosphate aldolase); *tpiA*: EC 5.3.1.1 (trisose-phosphate isomerise); *gapA*: EC 1.2.1.12 (glycaldehyde-3-phosphate dehydrogenase); *gapB*: EC 1.2.1.12 (glycaldehyde-3-phosphate dehydrogenase); *pgk*: EC 2.7.2.3 (phosphoglycerate kinase); *pgm*: EC 5.4.2.1 (phosphoglycerate mutase); *eno*: EC 4.2.1.11 (enolase); *zwf*: EC 1.1.149 (glucose-6-phosphate dehydrogenase); *gnd*: EC 1.1.1.44 (phosphogluconate dehydrogenase); *rpe*: EC 5.1.3.1 (ribose-phosphate 3 isomerase); *rpi*: EC 5.3.1.6

phosphoglycerate mutase (*pgm*), which is a reversible reaction, and 2-phosphoglycerate is further converted to phosphoenolpyruvate by another reversible reaction catalysed by enolase (*eno*). None of these enzymes have yet been purified and characterised in *C. glutamicum*. In the last reaction of the glycolysis phosphoenolpyruvate is converted to pyruvate by pyruvate kinase (*pyk*), a reaction which is coupled to phosphorylation of ADP to ATP (Jetten *et al.*, 1994). Phosphoenolpyruvate and pyruvate is involved in a number of anaploretic reactions and in the PTS-sugar uptake system. This will be discussed more in detail elsewhere.

The Pentose Phosphate Pathway

The initial reactions of the pentose phosphate pathway is the formation of 6-phosphogluconate from glucose-6-phosphate by glucose-6-phosphate dehydrogenase (*zwf,opcA*) (Sugimoto and Shiio, 1987a), followed by a conversion to ribulose-6-phosphate by 6-phosphogluconate dehydrogenase (*gnd*) (Sugimoto and Shiio, 1987b), with the formation of two moles of NADPH from $NADH^+$ and the formation of one mole of CO_2 (Figure 3.1) Glucose-6-phosphate dehydrogenase consists of two subunits (*zwf* and *opcA*), forming a heteromultimeric complex, and both *zwf,opcA*- and *gnd*-gene-products are inhibited by NADPH (Moritz *et al.*, 2000). The rest of the reactions and enzymes involved in the pentose phosphate pathway have not been investigated in detail in *C. glutamicum*. However, based on the genome annotation and available experimental data for *C. glutamicum* (Sugimoto and Shiio, 1989a; Ikeda *et al.*, 1998) and the related *Corynebacterium ammoniagenses* (Kamada *et al.*, 2001; Kamada *et al.*, 2003), an unravelling of this pathway can be conducted (Figure 3.1). Ribulose-5-phosphate can be converted to either ribose-5-phosphate or xulose-5-phosphate by ribose-5-phosphate isomerase (*rpi*) or ribulose-5-phosphate isomerase (*rpe*), respectively. Both are reversible reactions. The *tkt*-gene-product transketolase is able to catalyse two reactions: xulose-5-phosphate + ribulose-5-phosphate ↔ glycaldehyde 3-phosphate + sedohepulose 7-phosphate and xulose-5-phosphate + erythose 4-phosphate ↔ glycaldehyde 3-phosphate + fructose-6-phosphate. The transaldolase (*tal*) catalyses the reaction glycaldehyde 3-phosphate + sedohepulose 7-phosphate ↔ erythose 4-phosphate + fructose-6-phosphate. These reactions catalysed by transketolase and transaldolase create a reversible link between the glycolysis and the pentose phosphate pathway. However, little is known about the distribution between these reactions in *C. glutamicum*.

TCA cycle

The replenishment of carbon into the TCA cycle is mediated by acetyl-CoA (Figure 3.2). During growth on carbohydrates acetyl-CoA is generated by oxidative decarboxylation of pyruvate yielding Acetyl-CoA, CO_2 and NAD^+. In *C. glutamicum* this reaction is catalysed by the pyruvate dehydrogenase complex (Schwinde *et al.*, 2001; Cocaign-Bousquet and Lindley, 1995). This enzyme complex is composed of three subunits (de Kok *et al.*, 1998). The activity of two of these subunits (*lpd*) (Schwinde *et al.*, 2001) and (*aceE*) (Schreiner *et al.*, 2005) have been confirmed by experimental work. Presence of the third subunit in *C. glutamicum* has been proposed from genome annotation where an ORF sharing similarity to the gene (*aceF*) encoding this enzyme in *E. coli* has been found. The first compound in the TCA cycle citrate is generated as a condensation of acetyl-CoA and oxaloacetate. The enzyme citrate synthase (*gltA*) catalyses this reaction (Eikmanns *et al.*, 1994). The next reaction step is reversible isomerization of citrate to isocitrate catalysed by the enzyme aconitase (*acn*) (Krug *et al.*, 2005). Isocitrate dehydrogenase (*icd*) further catalyzes the conversion of isocitrateto 2-oxoglutarate and CO_2 by the reduction of $NADP^+$ (Audette *et al.*, 1999; Eikmanns *et al.*, 1995). 2-oxoglutarate can then be aminated to form glutamate (this reaction step is

described elsewhere), or be converted to succinyl-CoA, another TCA intermediate, and NADH via the 2-oxoglutarate dehydrogenase complex. The 2-oxoglutamate dehydrogenase complex share some similarity to the pyruvate dehydrogenase complex described above. One of the subunits (*lpd*) is even shared between the two enzyme complexes. The two existing subunits (*odhA* and *sucB*) have both been identified in *C. glutamicum* by experiments (Kataoka *et al.*, 2006; Usuda *et al.*, 1996). Succinyl-CoA synthase catalyses the next reaction in the TCA cycle converting succinyl-CoA to succinate and CoA yielding one ATP (Zhao and Lin, 2002). The further conversion of succinate to fumarate is done by the membrane bound succinate dehydrogenase enzyme complex, which consists of three subunits *sdhA*, *sdhB* and *sdhC*. This complex is part of the respiratory chain in *C. glutamicum* (Bott and Niebisch, 2003), which will be described more in detail elsewhere. Fumerate is converted to malate via the reversible reaction catalysed by the enzyme fumerase (*fumC*) (Genda *et al.*, 2006). The last reaction in the TCA cycle is the conversion between malate and oxaloacetate. This reaction can be conducted via two different reactions: the NAD dependent malate dehydrogenase (*mdh*) or the membrane associated malate:quinone oxidoreduktase (*mqo*) (Molenaar *et al.*, 2000), both of which are part of the respiratory chain of *C. glutamicum* (Bott and Niebisch, 2003). However, due the energetically unfavourable properties of the *mdh* reactions, the *mqo* reaction will be preferred during standard growth conditions, and *mdh* will only occur during low oxaloacetate and/or high malate concentrations (Molenaar *et al.*, 1998). During growth on carbon sources entering the central metabolism as acetyl-CoA (i.e. acetate, ethanol or fatty acids) the glyoxylate cycle must be active in order to obtain sufficient amounts of oxaloacetate to fulfil anaplerotic function of the organism (Gerstmeier *et al.*, 2003). Using the glyoxylate cycle three reactions of the TCA cycle are bypassed (Figure 3.2). Isocitrate is converted directly to succinate and glyoxylate via isocitrate lyase (*aceA*), and glyoxylate is further converted to malate using a Acetyl-CoA yielding CoA via malate syntase (*aceB*) (Reinscheid *et al.*, 1994). Activity of the glyoxylate cycle is tightly controlled at a transcriptional level, and is down regulated during growth on carbohydrates (Reinscheid *et al.*, 1994; Wendisch *et al.*, 2004).

***

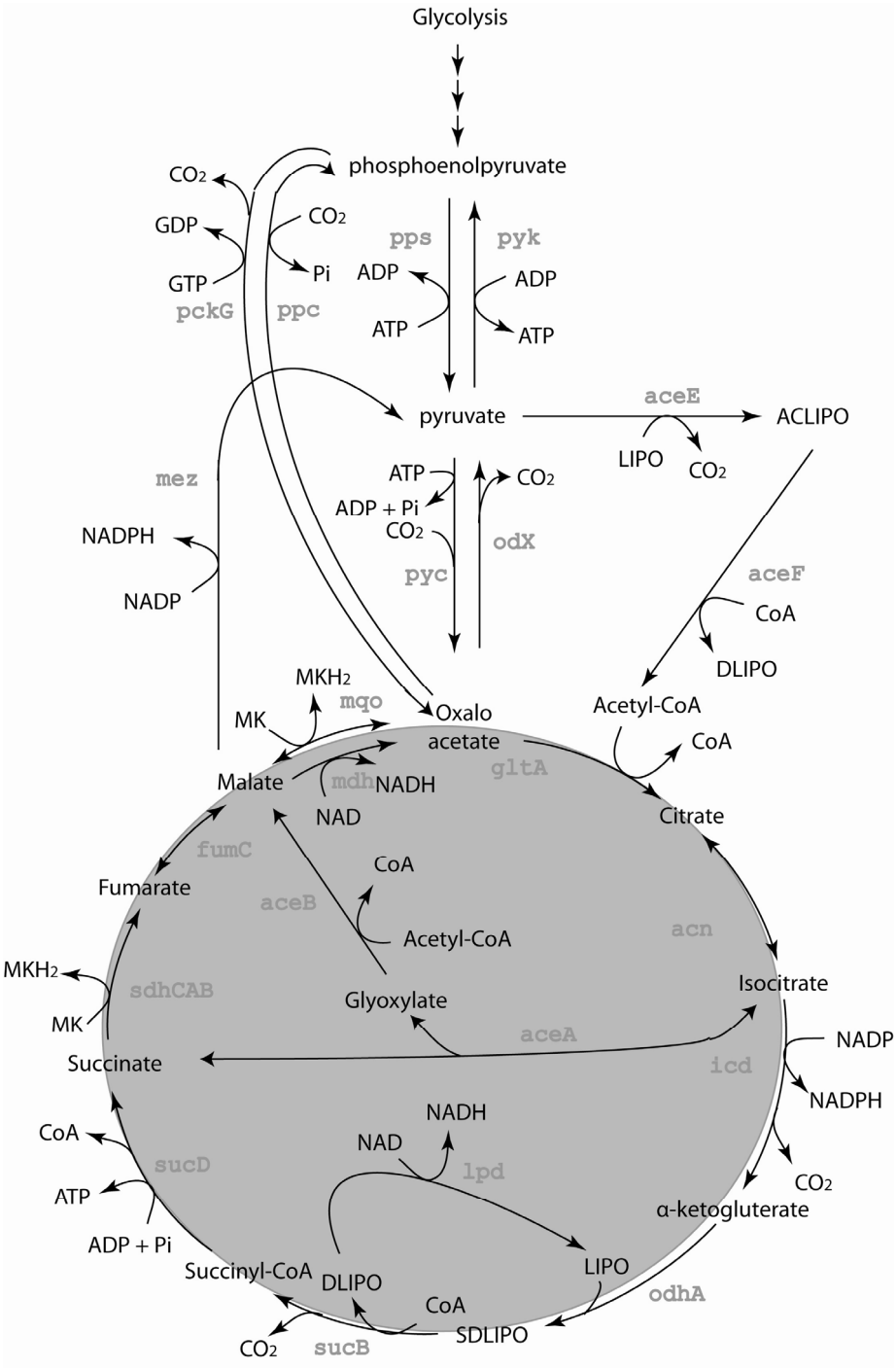

Figure 3.2: TCA cycle and anaploretic reactions in *C. glutamicum*. Genes and enzymes involved*: pckG*: EC 4.1.1.32 (phosphoenolpyruvate carboxykinase (GTP)); *ppc*: EC 4.1.1.31 (phosphoenolpyruvate carboxylase); *pps*: EC 2.7.9.2 (phosphoenolpyruvate syntase); *pyk*: 2.7.1.40 (pyruvate kinase); *pyc*: EC 6.4.1.1 (pyruvate carboxylase); *odX*: EC 4.1.1.3 (oxaloacetate decarboxylase); *aceE*: EC 1.2.4.1 (pyruvate dehydrogenase); *aceF*: EC 2.3.1.12; *gltA*: 2.3.3.1 (citrate syntase); *acn*: EC 4.2.1.3 (aconitate hydratase); *icd*: EC 1.1.1.42 (isocitrate dehydrogenase); *odhA*: EC 1.2.4.2 (oxoglutarate dehydrogenase); *sucB*: EC 2.3.1.61; *sucD*: EC 6.2.1.5 (succinate-CoA ligase); *sdhCAB*: EC 1.3.5.1 (succinate dehydrogenase); *fumC*: EC4.2.1.2 (fumerate hydratase); *mdh*: EC 1.1.1.37 (malate dehydrogenase); *mqo*: EC 1.1.99.16 (malate dehydrogenase); *aceA*: 4.1.3.1 (isocitrate lyase); *aceB*: EC 2.3.3.9 (formerly EC 4.1.3.2) (malate syntase); *mez*: EC 1.1.140 (malic enzyme).

Anaplerotic reactions around the phosphoenolpyruvate-pyruvate-oxaloacetate node

The phosphoenolpyruvate-pyruvate-oxaloacetate node has been given a lot of attention due to its central position in the metabolism directing carbon towards the TCA-cycle. *C. glutamicum* possess a number of enzymes and reactions around this node (Figure 3.2). Two C3-carboxylating enzymes: pyruvate carboxylase (*pyc*) (Peters-Wendisch *et al.*, 1998) and phosphoenolpyruvate carboxylase (*ppc*) (Eikmanns *et al.*, 1989); three C4-decarboxylating enzymes malic enzyme (*mez*) (Gourdon *et al.*, 2000), oxaloacetate decarboxylase (*Odx*) (Jetten and Sinskey, 1995); phosphoenolpyruvate carboxykinase (*pckG*) (Jetten and Sinskey, 1993); and the ATP-yielding pyruvate kinase (*pyk*) (Jetten *et al.*, 1994) are present. However, the level of activity of these enzymes, and consequently the flux-distributions, are highly dependent on the substrate(s) utilized by the organism (Petersen *et al.*, 2000; Peters-Wendisch *et al.*, 1998; Gourdon *et al.*, 2000; Dominguez *et al.*, 1998). Based on the annotated genome another two enzymes are present at this node: Phosphoenolpyruvate syntase (*pps*; EC 2.7.9.2) and malate dehydrogenase (*mdh2*; EC 1.1.1.82). However, the presence of these enzymes in *C. glutamicum* has until today not been shown experimentally. During growth on carbohydrates *pyc* and *ppc* are essential as anaplerotic enzymes (Peters-Wendisch *et al.*, 1998), and those are also the dominating pathways during growth and lysine synthesis on carbohydrates, with *pyc* being the most significant (90%) (Petersen *et al.*, 2000; Park *et al.*, 1997). Although the role of *mez*, *Odx* and *pckG* have been excluded during anaploreis (Peters-Wendisch *et al.*, 1998), some activity of these enzymes are still seen during utilization of carbohydrates (Petersen *et al.*, 2001; Petersen *et al.*, 2000; Gourdon *et al.*, 2000; Jetten and Sinskey, 1995), why the significance of these enzymes can not be neglected. However, based on data from Petersen *et al.* (2000) the only C4-decarboxylating reaction contributing with a significant flux is *pckG*. The consequence of this flux is a GTP consuming futile cycle in which pyruvate is converted to oxaloacetate (via *pyc*), oxaloacetate is converted to phosphoenolpyruvate (via *pckG*) and phosphoenolpyruvate is converted back to pyruvate (via *pyk*). Petersen *et al*. (2000) suggested that this cycling between the C4- and C3-pool serves as a fine tuning within the central metabolism to balance anaplerosis with catabolism, and to be able to make rapid responses to alterations in the environment.

***

Respiratory Energy Metabolism

C. glutamicum has a respiratory energy metabolism, with oxygen as the terminal electron donor. Reducing equivalents obtained by oxidation of various substrates are transferred to a menaquinone via eight different dehydrogenases which have been identified from the annotated genome (Bott and Niebisch, 2003)(Figure 3.3). These are NADH dehydrogenase (*ndh*), succinate dehydrogenase (*sdhCAB*), malate:quinone oxidoreductase (*mqo*), pyruvate:quinone oxidoreductase (*poxB*), L-lactate dehydrogenase (*lldD*), D-lactate dehydrogenase (*dld2*), glycerol-3-phosphate dehydrogenase (*glpD*), and proline dehydrogenase (*putA*). From menaquinone the electrons are transferred to oxygen via either the cytochrome bc_1–aa_3 supercomplex (*qcrCAB*, *ctaCDEF*) (Niebisch and Bott, 2003) or via cytochrome *bd* menaquinol oxidase (*cydAB*) (Kusumoto *et al.*, 2000). In addition to oxygen, nitrate can serve as an electron acceptor in *C. glutamicum* by reduction to nitrite via nitrate

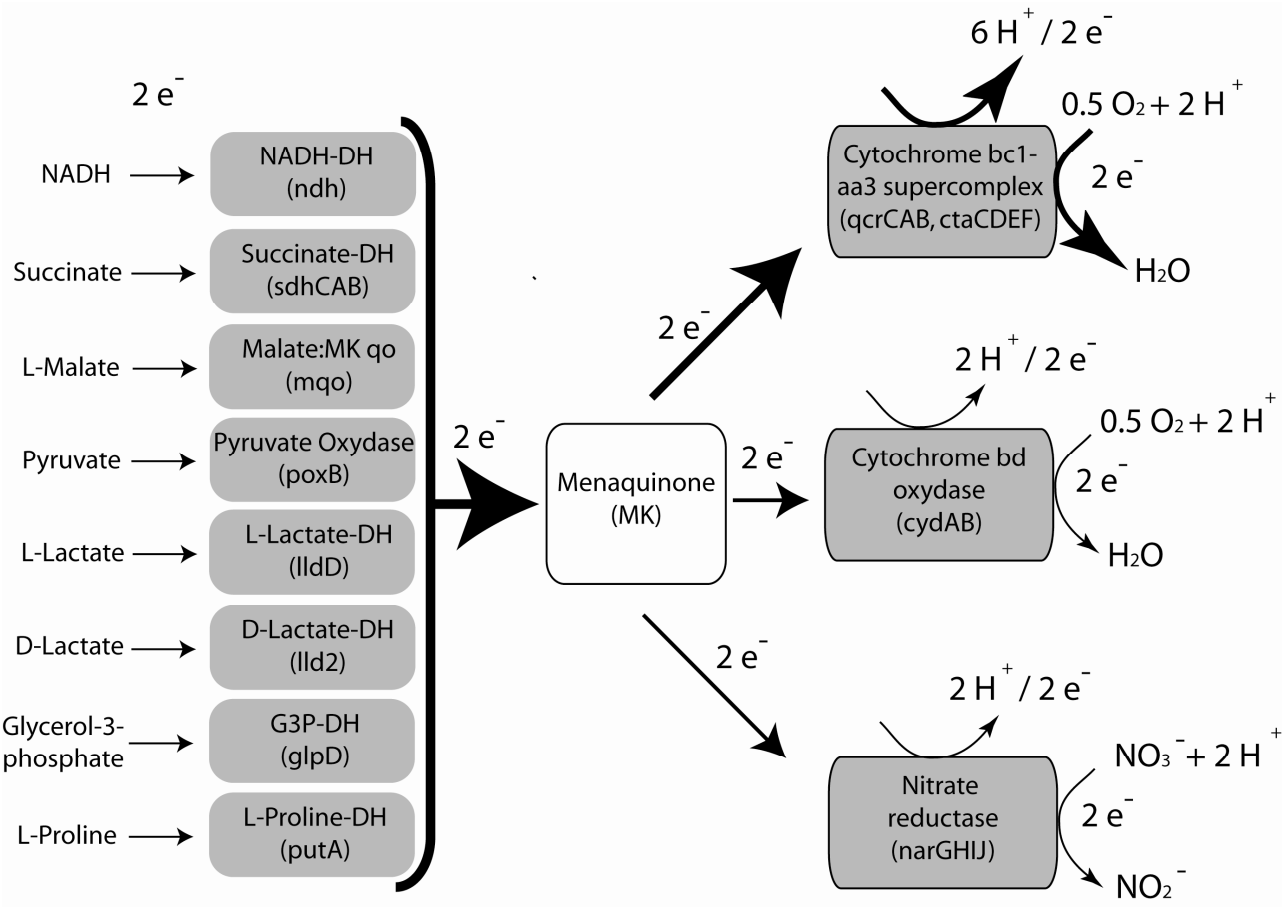

Figure 3.3: Proposed model of the respiratory chain of *C. glutamicum*. The number of electrons and protons presumable transferred is indicated. The route involving cytochrome bc_1–aa_3 supercomplex is used under normal conditions. Modified after Bott and Niebisch (2003).

reductase (*narGHIJ*) (Bott and Niebisch, 2003). The physiological role of nitrate reductase is yet unknown and no reports about anaerobic growth with nitrate as terminal electron acceptor has been published so far. The final step in oxidative phosphorylation is the generation of ATP via the F_1F_0-ATP synthase (*atpIBEFHAGDC*) driven by an electrochemical proton gradient across the cytoplasmic membrane. According to generally accepted values the number of protons transferred across the membrane per electron (H^+/e^-) is three for the cytochrome bc_1–aa_3 supercomplex

(Nicholls and Ferguson, 1992), and one for cytochrome *bd* menaquinol oxidase (Stryer, 1995a). Production of one molecule of ATP by the F_1F_0-ATP synthase requires transport of three to four protons, consequently leading to a maximum P/O-value of 1.5-2 when the cytochrome bc_1–aa_3 supercomplex is used for electron transfer and 0.5-2/3 when cytochrome *bd* menaquinol oxidase is used (Bott and Niebisch, 2003).Under normal conditions the more efficient cytochrome bc_1–aa_3 supercomplex is used, and mutants lacking this complex have been shown to have severe growth defects (Niebisch and Bott, 2001; Niebisch and Bott, 2003).

Biomass components

Amino acid biosynthesis

The wild-type strain of *C. glutamicum* ATCC 13032 is prototrophic with respect to all amino acids. In many cases the synthesis of the individual amino acids has been investigated quite thoroughly in *C. glutamicum*, and not surprisingly the lysine and glutamate synthesis pathways are among the most well characterised pathways in this organism.

Glutamate family (glutamate, glutamine, arginine and proline)

The major route of ammonia assimilation in *C. glutamicum* is the incorporation of ammonia/ammonium to glutamate or glutamine through either glutamate dehydrogenase (*gdh*) or through the GS/GOGAT system, both of which have been presented in the "nitrogen metabolism"-part of this chapter. From glutamate proline is synthesized from glutamate via three gene-products λ-glytamylkinase (*proB*), λ-glytamyl phosphate reductase (*proA*) and Δ1-pyrroline-5-carboxylate reductase (*proC*) (Ankri *et al.*, 1996; Serebrijski *et al.*, 1995)(Figure 3.4). In addition L-glutamate 5-semialdehyde is converted to (S)-1-Pyrroline-5-carboxylate via a non-enzymatic reaction. *proB* and *proC* are essential for growth, whereas Δ*proA* mutants are able to grow slowly, suggesting an alternative to the *proA* pathway (Ankri *et al.*, 1996). Ankari *et al.* (1996) suggested that the *asd*-gene present in the lysine synthetic pathway was involved in this bypass. In addition to being a biomass component, proline is also used as a compatible solute during osmotic stress, resulting in an accumulation of intracellular proline under such conditions (Guillouet and Engasser, 1995).

The arginine synthetic pathway has not been investigated as thoroughly as it is the case for most other amino acid pathways in *Corynebacterium*, in spite of the fact that strains of *Corynebacterium* have been and still are used for production of L-arginine (Utagawa, 2004; Lu, 2006). Arginine is synthesised from glutamate and Acetyl-CoA in a series of reactions where eight genes are involved: *argR*; *argB; argC; argD*; *argJ*; *argF*; *argG*; *argH* (Utagawa, 2004). The proposed arginine pathway in *C. glutamicum* is summarised in figure 3.5. The gene-product from *argB* (N-acetylglucokinase) is inhibited by arginine making this enzyme the control point of this pathway (Utagawa, 2004).

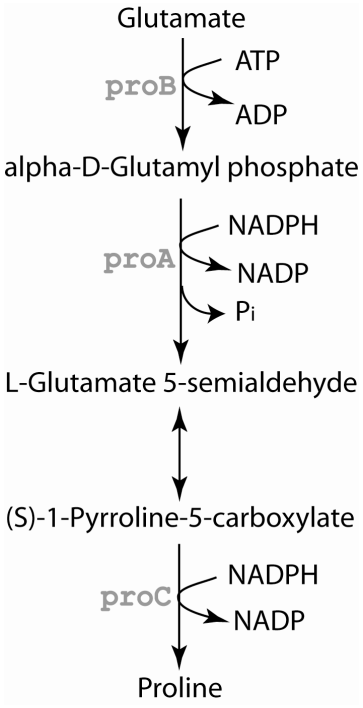

Figure 3.4: The consensus biosynthetic pathway of proline in *C. glutamicum*. Genes and enzymes involved: *proB*: EC 2.7.2.11 (λ-glytamylkinase); *proA*: EC 1.2.1.41 (λ-glytamyl phosphate reductase); *proC*: EC 1.5.1.2 (Δ1-pyrroline-5-carboxylate reductase).

The branched chain amino acids (isoleucine, valine, leucine)

The synthesis of the three branched amino acids isoleucine, leucine and valine is tightly correlated due to the fact that a number of enzymes are shared in the biosynthetic pathways of these compounds (Radmacher *et al.*, 2002). Also the synthesis of the vitamin D-pantothenate is sharing some of these enzymes, since the intermediate 2-oxoisovalerate is used in the first step of the synthesis of this compound (Sahm and Eggeling, 1999) in competition with leucine and valine biosynthesis. Isoleucine and valine biosynthesis (and in principle also leucine and pantothenate) share three enzymes, and one enzyme is shared between all three branched chain amino acids (Figure 3.6). Isoleucine is synthesized from threonine. The first step is catalyzed by threonine ammonialyase (*ilvA*) yielding 2-oxobutanate. From here the next three reactions are shearing enzymes with the valine- and leucine biosynthetic pathways: *ilvBN*, *ilvC*, *ilvD* and *ilvE* yielding the gene-products acetohydroxyacid synthase, isomero reductase, dihydroxyacid dehydratase and transaminase B, respectively. During this sequence of reactions a pyruvate is consumed in addition to a NADPH and one amine-group which is transferred from glutamate by the formation of 2-oxogluterate. Both valine and leucine biosynthesis are initiated by the condensation of two moles of pyruvate. Via three steps the intermediate 2-oxoisovalerate is synthesized producing one mole of CO_2 and consuming NADPH. From this compound valine is synthesized by transferring an amine from glutamate catalyzed by the *ilvE* gene-product. Leucine is synthesized from 2-oxoisovalerate via another four reactions catalyzed by the enzymes 2-isopropylmalate synthase, 3-isopropylmalate dehydratase, isopropylmalate dehydrogenase and finally transaminase B, which are gene-products from *leuA*, *leuCD*, *leuBP* and *ilvE,* respectively. Due to the complexity of this system a tight control must be present in order to maintain sufficient concentrations of each single metabolite without

overproducing others. Isoleucine synthesis is controlled at the first reaction step (*ilvA*) by feedback inhibition by isoleucine, whereas valine has the opposite effect. Using this mechanism the organism is able to balance the isoleucine and valine biosynthesis by restricting the synthesis of 2-oxobutanoate when isoleucine is in excess and by promoting 2-oxobutanoate synthesis when valine is in excess (Möckel *et al.*, 1992). The activity of the gene-product of *ilvBN* is increased by 2-oxobutanoate, which is due to a higher transcription of this gene (Keilhauer *et al.*, 1993). Valine on the other hand decreases the activity of the *ilvBN* gene-product (Eggeling *et al.*, 1987). As 2-oxoisovalerate is precursor for leucine, valine and panthenoate there is a tight regulation of enzymes at this point. Leucine is a strong feed-back inhibitor of the *leuA* (Patek *et al.*, 1994) and *leuB* (Patek *et al.*, 1998) gene-products, which catalyses the first and the third reaction in the leucine synthesis pathway.

***

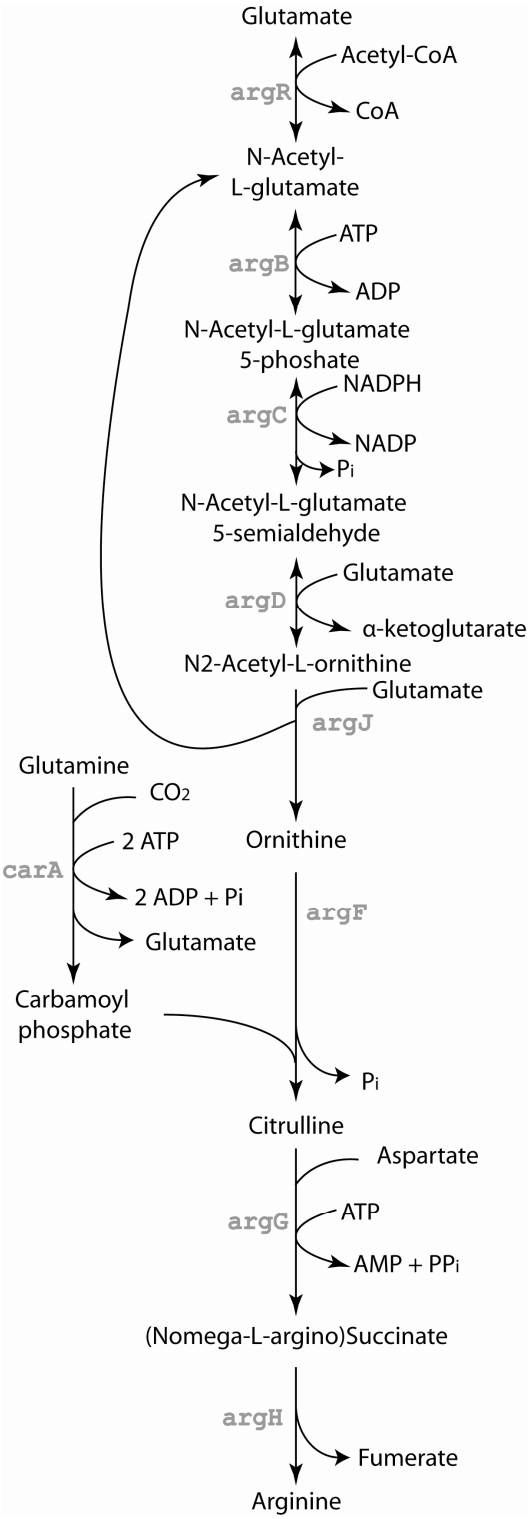

Figure 3.5: Arginine synthetic pathway in *C. glutamicum* based on the annotated genome and Utawa (2004). Genes and enzymes involved: *argR*: EC 2.3.1.1 (N-acetylglutamate synthase); *argB*: EC 2.7.2.8 (Acetylglutamate kinase); *argC*: EC 1.2.1.38 (N-acetyl-gamma-glutamyl-phosphate reductase); *argD*: EC 2.6.1.11 (Acetylornithine transaminase); *argJ*: EC 2.3.1.35 (Glutamate N-acetyltransferase); carA: EC 6.3.5.5 (carbamoyl-phosphate syntase) *argF*: EC 2.1.3.3 (Ornithine carbamoyltransferase); *argG*: EC 6.3.4.5 (Argininosuccinate synthase); *argH*: EC 4.3.2.1 (Argininosuccinate lyase)

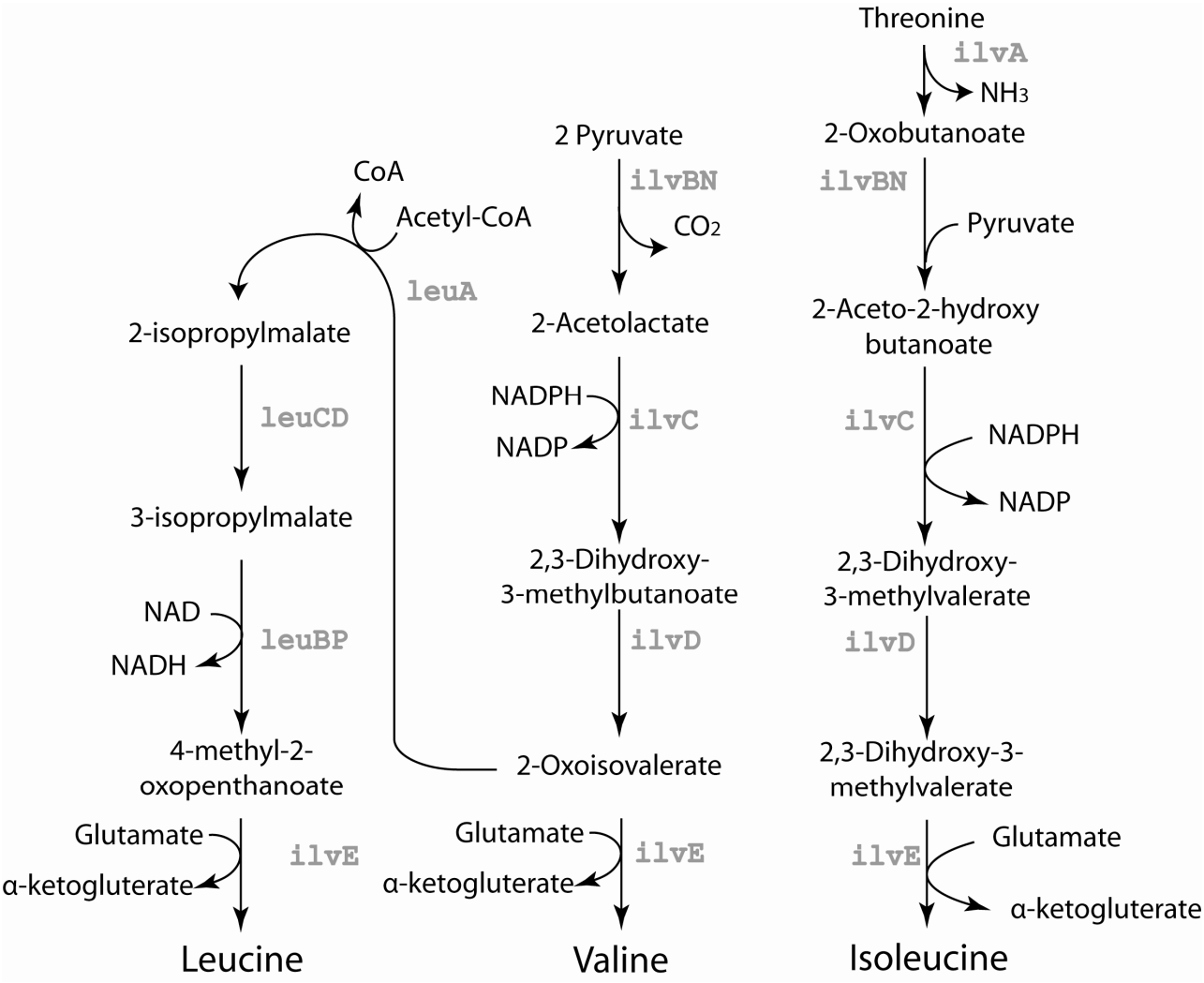

Figure 3.6: Biosynthetic pathways of the branched amino acids, L-leucine, L-valine and L-isoleucine in *C. glutamicum*. Genes and enzymes involved: *ilvA*: EC 4.3.1.19 (formerly EC 4.2.1.16) (threonine-ammonia lyase); *ilvBN*: EC 2.2.1.16 (acetohydroxy-acid syntase); *ilvC*: EC 1.1.1.86 (ketol-acid reductoisomerase); *ilvD*: EC 4.2.1.9 (dihydroxy-acid dehydratase); *ilvE*: EC 2.6.1.42 (transaminase B); *leuA*: EC 2.3.3.13 (isopropylmalate syntase); *leuCD*: EC 4.2.1.33 (isopropylmalate dehydratase); *leuBP*: EC 1.1.1.85 (isopropylmalate dehydrogenase).

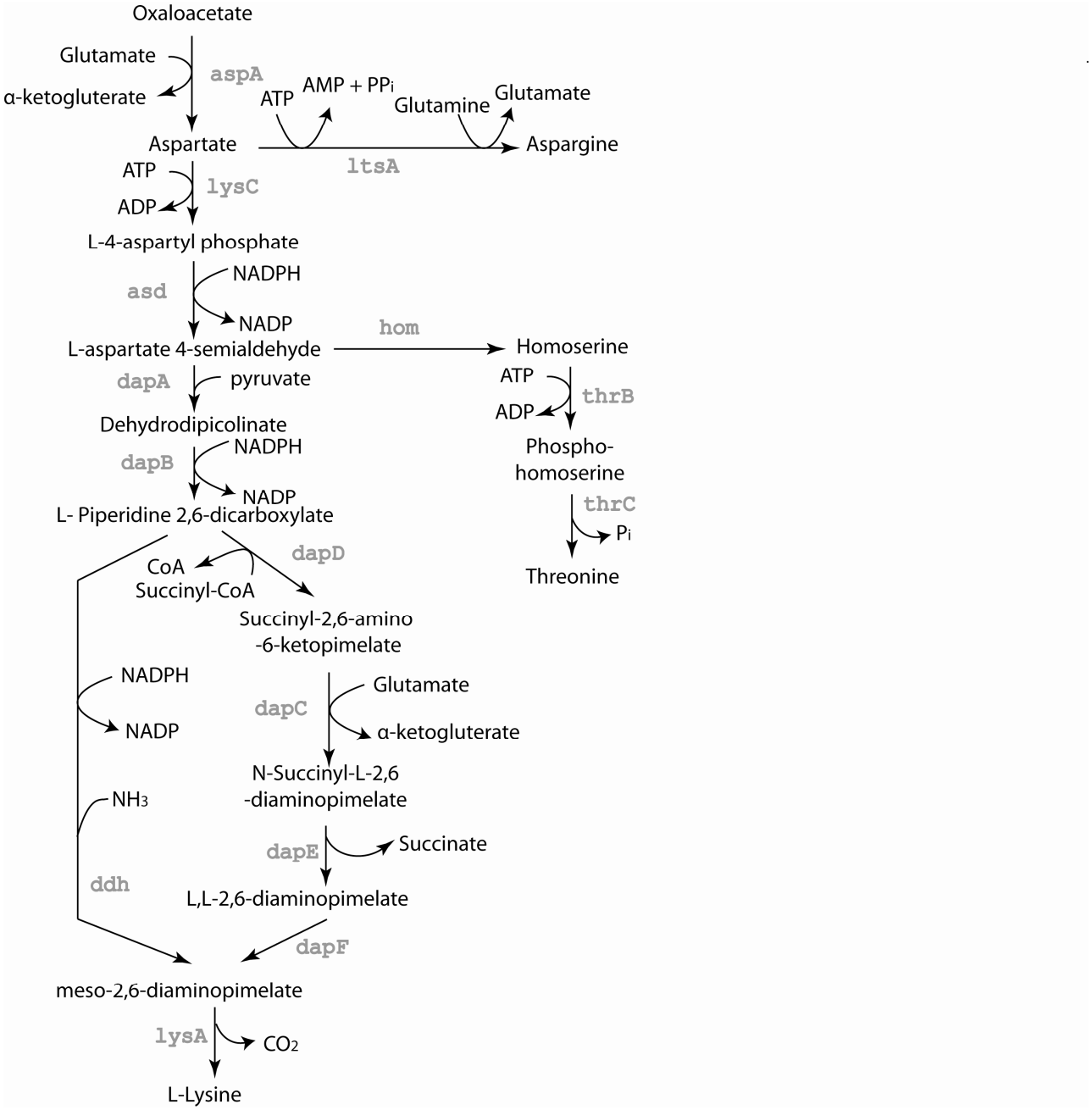

Figure 3.7: Biosynthetic pathways of aspartate family amino acids, L-aspartate, L-aspargine, L-threonine and L-lysine in *C. glutamicum*. Genes and enzymes involved: *aspB*: EC: 2.6.1.1 (aspartate transaminase); *ltsA*: EC 6.3.5.4 (aspargine syntase); *lysC*: EC 2.7.2.4 (aspartate kinase); *asd*: 1.2.1.11 (aspartate semialdehyde dehydrogenase); *dapA*: EC 4.2.1.52 (dihydrodipicolinate synthase); *dapB*: EC 1.3.1.26 (dihydrodipicolinate reductase); *dapD*: EC2.3.1.117 (2,3,4,5-tetrahydropyridine-2,6-dicarboxylate N-succinyltransferase); *dapC*: EC 2.6.1.17 (succinyl-amino-ketopimelate transaminase); *dapE*: EC 3.5.1.18 (succinyl-diaminopimelate desuccinylase); *dapF*: EC 5.1.1.7 (diaminopimelate epimerase); *lysA*: EC 4.1.1.20 (diaminopimelate decarboxylase); *ddh*: EC 1.4.1.16 (diaminopimelate dehydrogenase); *hom*: EC 1.1.1.3 (homoserine dehydrogenase); *thrB*: EC 2.7.1.39 (homoserine kinase); *thrC*: EC 4.2.3.1 (threonine synthase).

The aspartate family (aspartate, aspargine, threonine, lysine, methionine)
All amino acids part of the aspartate family are synthesized from aspartate. Due to the commercial importance of a number of these amino acids, and the high potential of *C. glutamicum* to produce some of these amino acids, these synthetic pathways have been thoroughly investigated. Aspartate is synthesized from oxaloacetate via aspartate transaminase (*aspB*: EC 2.6.1.1). Aspargine biosynthesis has not been given a lot of attention compared to the rest of the aspartate family amino acids. Based on the annotated genome two aspargine synthase enzymes are present in *C. glutamicum*: *ltsA* (EC 6.3.5.4) and *NCgl2116* (EC 6.3.1.1). However, none of these enzymes have been characterized so far.

The initial reactions of the lysine-, threonine- and methionine pathways are shared. From aspartate, aspartylphosphate is synthesized via aspartate kinase (*lysC*). Aspartylphosphate is then further converted to aspartatesemialdehyde by aspartatesemialdehyde dehydrogenase (*asd*). Aspartatesemialdehyde is further converted either towards threonine and methionine (*hom)* or towards lysine synthesis (*dapA*). In *C. glutamicum* there are two possible lysine pathways (Figure 3.7). Via *dapA* and *dapB* dehydrodipicolinate and L-piperidine 2,6-dicarboxylate is synthesized. From here meso-2,6-diaminopimelate is synthesized either directly via *ddh*, called the dehydrogenase variant, or via four reactions catalyzed by gene-products from *dapD*, *dapC*, *dapE* or *dapF*, known as the succinylase variant (Schrumpf *et al.*, 1991). The final step in the lysine synthesis is carried out by the *lysA* gene-product diaminopimelate decarboxylase. Due to the large commercial interest in lysine the pathway for this amino acid has been intensively investigated. A detailed review on the lysine synthetic pathway and various strategies for improving this pathway is given in chapter 2.

At the split between threonine/methionine and lysine synthesis some metabolic control is present in order to balance amino acid synthesis for biomass production without overproduction. The *hom* gene-product homoserine dehydrogenase is inhibited by threonine and isoleucine (Miyajima *et al.*, 1968). From homoserine, threonine is synthesized via two reactions: *thrB* and *thrC* (Willis *et al.*, 2005). The *thrB* gene-product homoserine kinase is strongly inhibited by threonine, whereas the other aspartate family amino acids shows slightly inhibitory effects when concentrations exceeds 10 mM (Miyajima *et al.*, 1968). The last enzyme in the threonine synthesis pathway threonine syntase (*thrC*) is scarcely inhibited by amino acids of the aspartate family and strongly inhibited by cysteine and the tripeptide glutathione (Miyajima *et al.*, 1968).

The last aspartate family amino acid is methionine, and two possible pathways are present leading to this amino acid in *C. glutamicum* (Lee and Hwang, 2003)(Figure 3.8). The first reaction in the biosynthesis of this compound is catalyzed by homoserine acetyltransferase (*metX*) (Park *et al.*, 1998), converting homoserine into *O*-acetylhomoserine using Acetyl-CoA as an acyl donor. *O*-acetylhomoserine is further converted to homocysteine either by one step via the *metY*-gene-product homoserine *O*-acetyltransferase using inorganic sulfur as sulfur source, or by two steps involving *metB* and *metC* with cystathionine as an intermediate and using cysteine as sulfur source. Both pathways are equally functional in the organism (Hwang *et al.*, 2002). Homocysteine is converted to methionine by a reaction donating a methyl group from 5,10-methenylenetetrahydrofolate (MTHF) to the compound. This reaction can be catalyzed by two different gene-products: *metE* or *metH*, *metE* being B_{12}-dependent whereas this is not the case for *metH* (Rückert *et al.*, 2003). MTHF for this reaction is formed from serine and tetrahydrofolate (THF) in two steps yielding glycine as a by-product involving gene-products from *glyA* and *metF*. From methionine *S*-adnosylmethionine (SAM) can be synthesized in a single step (*metK*) consuming one ATP. SAM is

an essential molecule and is involved in methylation reactions and polyamine biosynthesis (Lee, 2005). Methionine biosynthesis is strictly regulated by inhibition and repression by methionine itself, and by other compounds i.e. threonine, homocysteine and SAM (Lee and Hwang, 2003).

The pyruvate family (alanine)
Based on the annotated genome of *C. glutamicum* there is no alanine dehydrogenases present in this organism. The only alanine synthesizing pathways identified (based on annotated genome) to date are valine-pyruvate transaminase (*NCgl0388*: EC 2.6.1.66) and alanine racemase (*alrK:* EC 5.1.1.1) catalyzing the formation of alanine and 2-keto-isovalerate from valine and pyruvate and D-alanine from L-alanine, respectively.

The serine family (serine, glycerine, cysteine)
Serine is in *C. glutamicum* synthesized in three steps from 3-phosphoglycerate via the gene-products *serA* (phosphoglycerate dehydrogenase), *serC* (phosphoserine transaminase) and *serB* (phosphoserine phosphatase) (Peters-Wendisch *et al.*, 2005) (Figure 3.9). Only 16 % of synthesized

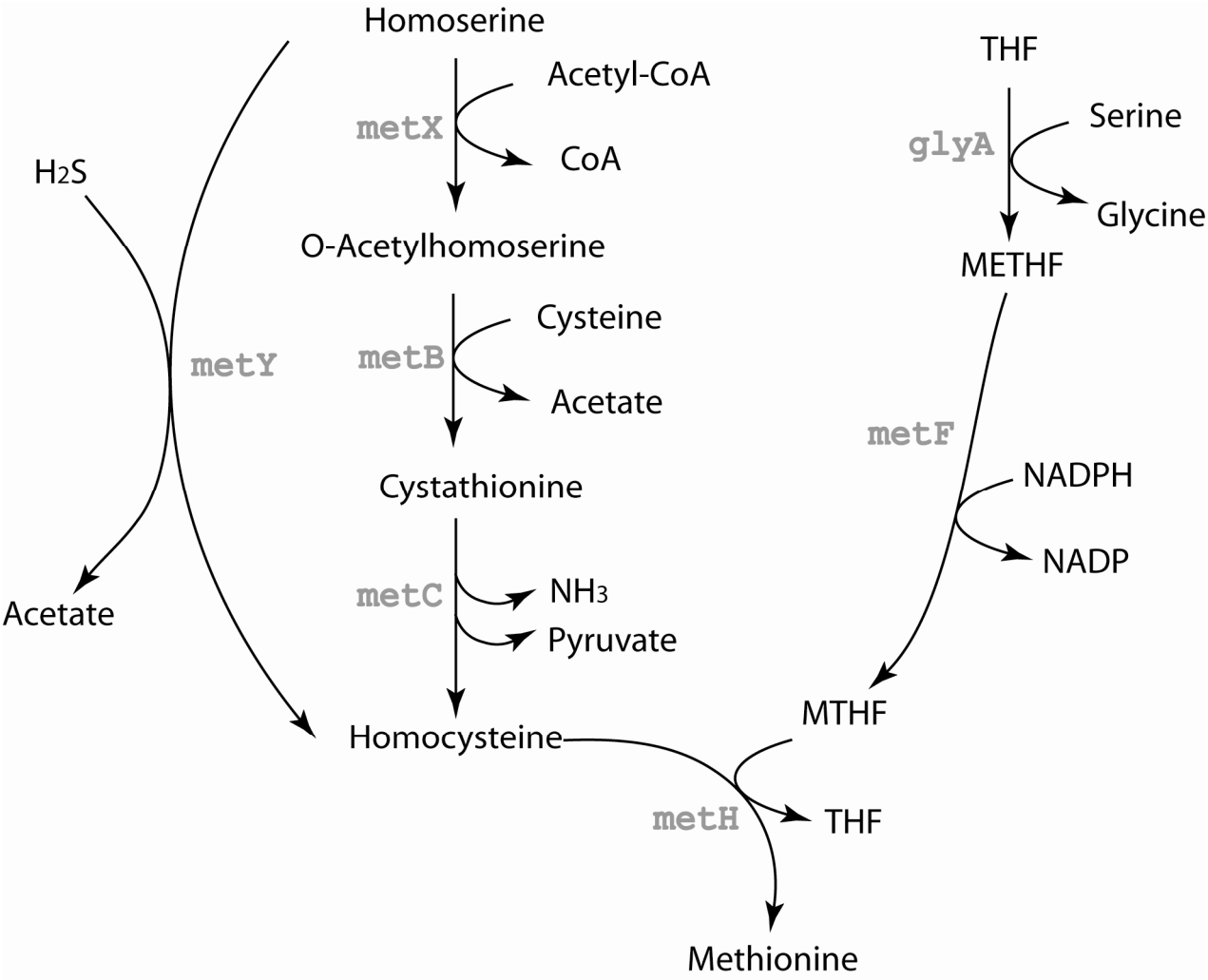

Figure 3.8: Biosynthetic pathways of methionine in *C. glutamicum*. Genes and enzymes involved: *metX*: EC 2.3.1.31 (homoserine acetyltransferase); *metB*: EC 2.5.1.48 (cystathionine gamma-synthase); *metC*: EC 4.4.1.8 (cystathionine beta-lyase); *metY*: EC 2.5.1.49 (O-acetylhomoserine aminocarboxypropyltransferase); *metH*: EC 2.1.1.13 (methionine synthase); *glyA*: EC 2.1.2.1 (glycine hydroxymethyltransferase); *metF*: EC 1.7.99.5 (5,10-methylenetetrahydrofolate reductase). Abbreviations: THF: Tetrahydrofolate; METHF: 5,10-Methenylenetetrahydrofolate; MTHF: 5-Methyltetrahydrofolate.

L-serine is incorporated into protein to support biomass formation (Marx *et al.*, 1996). The rest is used in glycine- or cysteine synthesis (see next sections) or can be converted to pyruvate via *sdaA* (L-serine aminase) (Netzer *et al.*, 2004). Based on the results of Netzer *et al*. (2004) the flow towards amino acid synthesis is thought to contribute the most to the drain of serine under normal conditions since the *sdaA* gene-product has a low affinity to serine. Serine synthesis is controlled by feed-back inhibition by serine at the first step of the pathway (Peters-Wendisch *et al.*, 2002).
Two routes for the synthesis of glycine are present in *C. glutamicum* both of which are catalyzed by the same gene-product *glyA* (glycine hydroxymethyltransferase): via serine and tetrahydrofolate (THF) yielding glycine and 5,10-methenylenetetrahydrofolate (MTHF) or by degrading threonine to glycine and acetaldehyde (Simic *et al.*, 2002) (Figure 3.9).

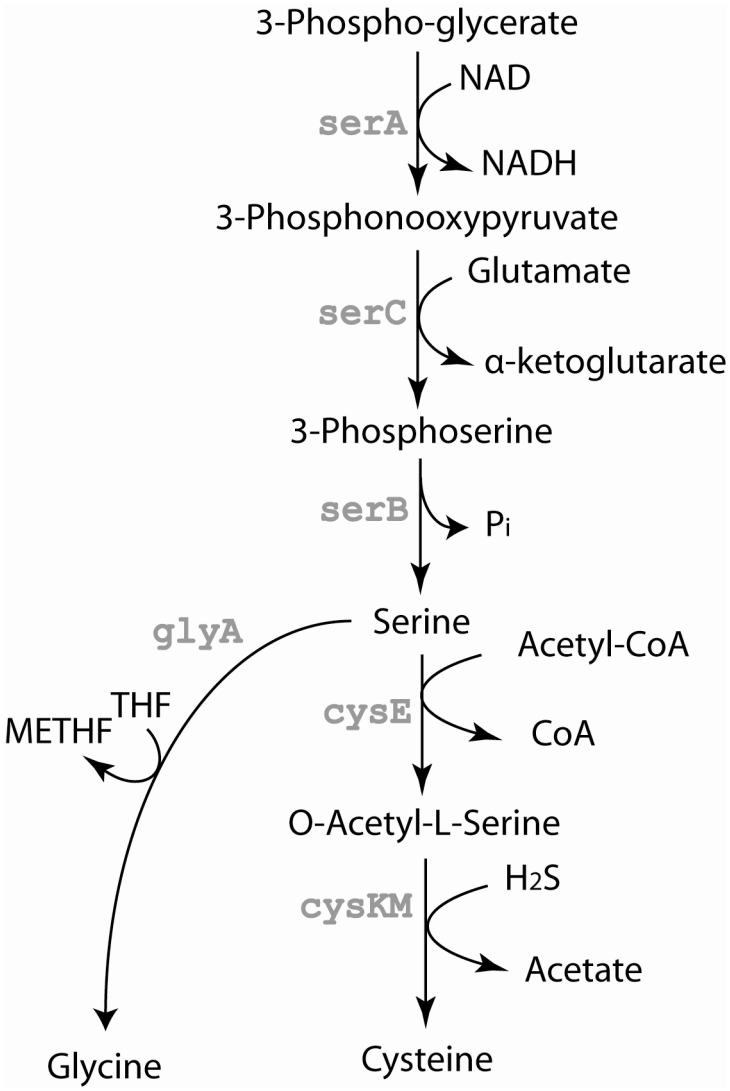

Figure 3.9: Biosynthetic pathways of the serine family amino acids serine, glycine and cysteine in *C. glutamicum*. Genes and enzymes involved: *serA*: EC 1.1.1.95 (phosphoglycerate dehydrogenase); *serC*: EC 2.6.1.52 (phosposerine transaminase); *serB*: EC 3.1.3.3 (phosphoserine phosphatase); *cysE*: EC 2.3.1.30 (serine acetyltransferase); *cysKM*: EC 2.5.1.47 (cysteine syntase); *glyA*: EC 2.1.2.1 (Glycine hydroxymethyltransferase). Abbreviations: THF: Tetrahydrofolate; METHF: 5,10-Methenylenetetrahydrofolate.

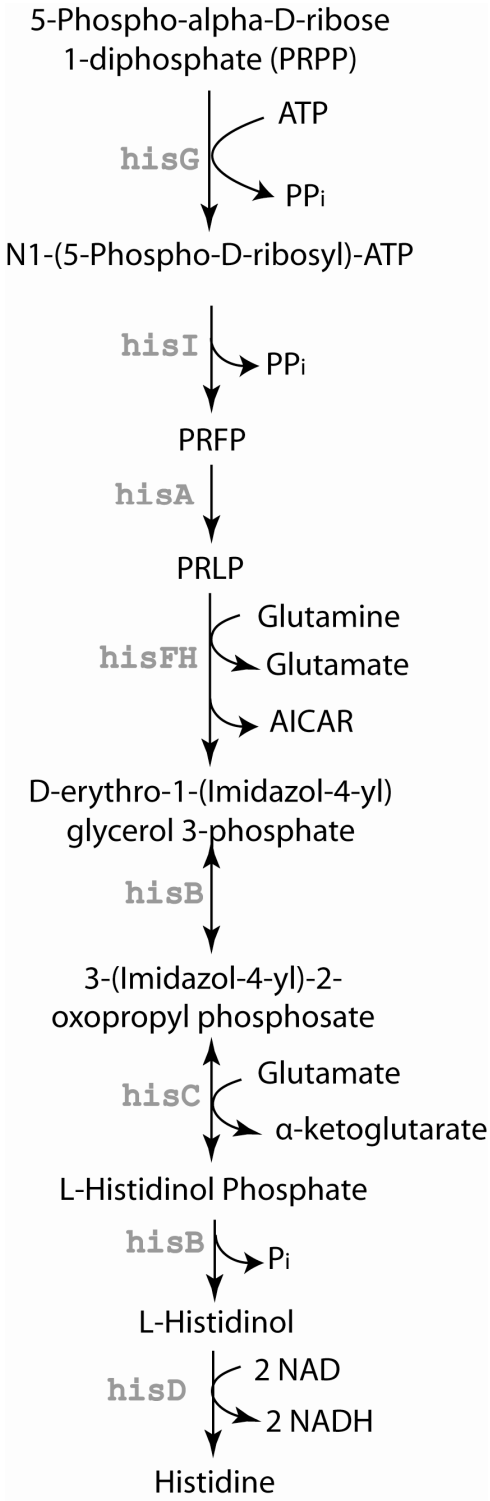

Figure 3.10: The histidine biosynthetic pathway in *Corynebacterium glutamicum*. Gene-products: *hisG* (EC 2.4.2.17: ATP phosphoribosyltransferase); *HisI* (EC 3.6.1.31: phosphoribosyl-ATP diphosphatase); *HisA* (5.3.1.16: 1-(5-phosphoribosyl)-5- ((5-phosphoribosylamino)methylideneamino)imidazole-4-carboxamide isomerase); *HisFH* (EC 2.4.2.17: ATP phosphoribosyltransferase); *HisB* (EC 4.2.1.19: imadazoleglycerol-phosphate dehydratase and EC 3.1.3.15: histidinol-phosphatase); *HisC* (EC 2.6.1.9: histidinol-phosphate transferase); *HisD* (EC 1.1.1.23: histidinol dehydrogenase). PRFP: 5-(5-Phospho-D-ribosylaminoformimino)-1-(5-phosphoribosyl)-imidazole-4-carboxamide; PRLP: N-(5'-Phospho-D-1'-ribulosylformimino)-5-amino-1-(5"-phospho-D-ribosyl)-4-imidazolecarboxamide.

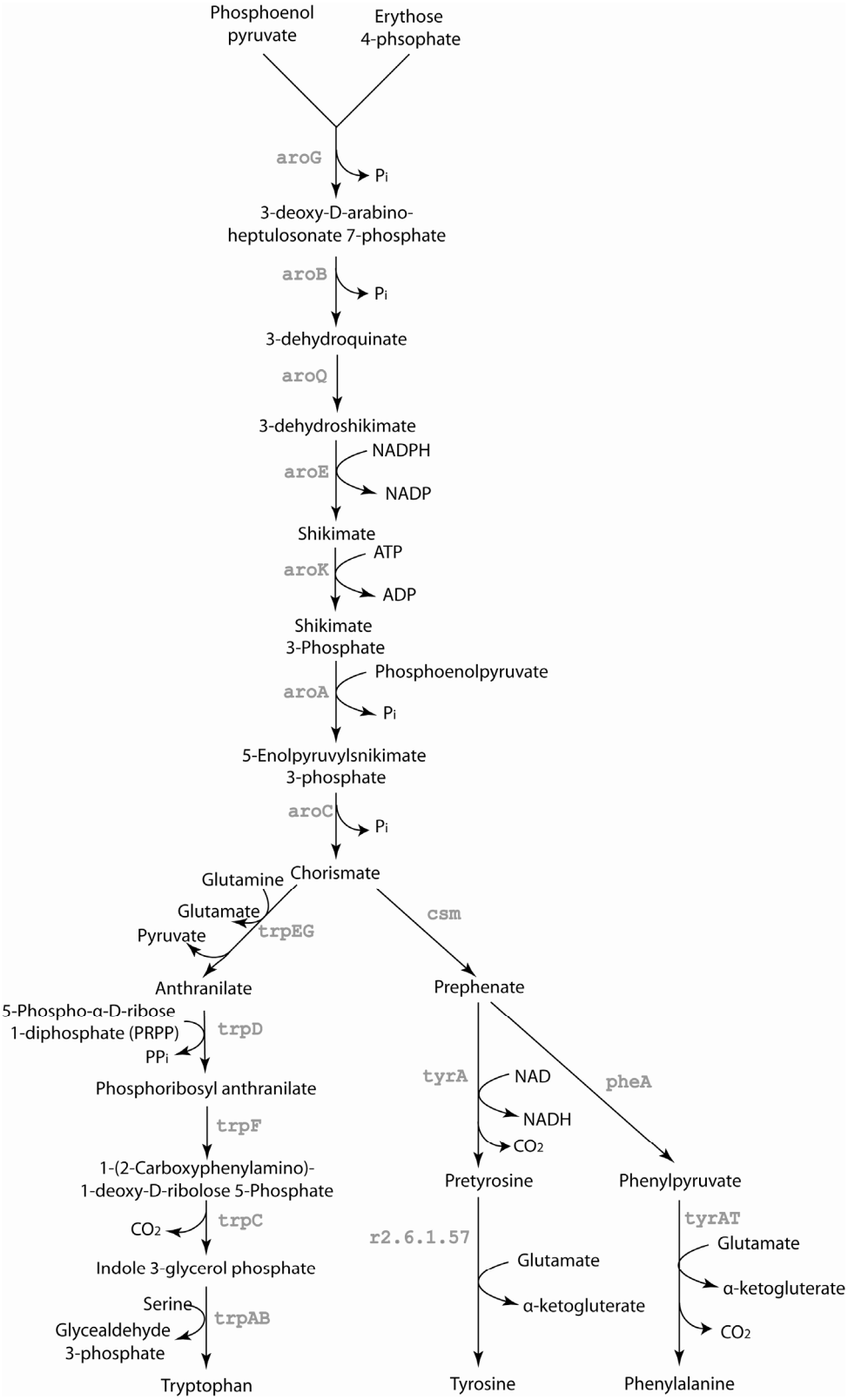

Figure 3.11: The synthetic pathways of the aromatic amino acids, tryptophan, tyrosine and phenylanaline, in *C. glutamicum*. Genes and enzymes involved: *aroG*: EC 2.5.1.54 (3-deoxy-7-phosphoheptulonate synthase); *aroB*: EC 4.2.3.4 (3-dehydroquinate synthase); *aroQ*: 4.2.1.10 (3-dehydroquinate dehydratase); *aroE*: EC 1.1.1.25 (shikimate dehydrogenase); *aroK*: EC 2.7.1.71 (shikimate kinase); *aroA*: EC 2.5.1.19 (3-phosphoshikimate 1-carboxyvinyltransferase); *aroC*: EC 4.2.3.5 (chorismate synthase); *trpEG* EC 4.1.3.27 (anthranilate synthase); *trpD*: EC 2.4.2.18 (anthranilate phosphoribosyltransferase); *trpC*: EC 4.1.1.48 (indole-3-glycerol-phosphate synthase); *trpAB*: EC 4.2.1.20 (tryptophan synthase); *csm*: EC 5.4.99.5 (chorismate mutase); *tyrAT*: EC 1.3.1.12 (prephenate dehydrogenase); r2.6.1.57: EC 2.6.1.57 (aromatic-amino-acid transaminase); *pheA*: EC 4.2.1.51 (prephenate dehydratase).

Cysteine is synthesized in two steps (Figure 3.9). In the first step *O*-acetylserine is synthesized from serine using acetyl-CoA as an acetyl donor by the *cysE* gene-product serine acetyltransferase (Wada *et al.*, 2002). *O*-acetyltransferase is converted to cysteine by the incorporation of sulphide (H_2S) via *CysK* (Wada *et al.*, 2004). It is also speculated that thiosulphate can be used as sulfur source using the *cysM* gene-product (*O*-acetylserine sulfhydrylase B) and an additional protein not yet identified to form cysteine (Lee, 2005). Cysteine can be degraded to pyruvate, NH_3 and H_2S by cysteine desulfhydrase (*aecD*) (Wada *et al.*, 2002).

Histidine

Histidine biosynthesis in *C. glutamicum* has not yet been fully elucidated. However, based on annotated genomic data and some experimental data it seems clear that the histidine pathway in this organism does not differentiate from most other prokaryotic organisms. In this respect the histidine pathway in *C. glutamicum* consists of 10 enzymatic reactions catalyzed by 8 different gene-products requiring phosphor-ribosyl-pyrophosphate (PRPP) and ATP (Jung *et al.*, 1998; Alifano *et al.*, 1996; Mormann *et al.*, 2006). The eight genes and gene-products involved in histidine synthesis are *hisA*, *hisB*, *hisC*, *hisD*, *hisF*, *hisG*, *hisH* and *hisI*, where the *hisI*, *hisB* and *hisD* gene-products are isoenzymes each catalysing two reactions within the pathway (Alifano *et al.*, 1996). The *hisF* and *hisH* gene-products form an enzyme-complex (Jung *et al.*, 1998). From figure 3.10 an overview of the reaction pathway and gene-products of histidine synthesis can be seen.

The aromatic family (Tryptophan, tyrosine and phenylalanine)

The biosynthesis of all the aromatic amino acids begins with the formation of the precursor chorismate. Chorismate is synthesized in seven enzymatic steps beginning with the condensation of phosphoenolpyruvate and erythose 4-phosphate. This reaction step is catalyzed by feedback sensitive 3-deoxy-D-*arabino*-heptulosonate 7-phosphate synthase (*aroG*) yielding 3-deoxy-D-*arabino*-heptulosonate 7-phosphate. This enzyme is slightly inhibited by tyrosine and phenylalanine when these amino acids are singly present, while the enzyme is strongly synergistically inhibited when both amino acids are present (Shiio *et al.*, 1974). From 3-deoxy-D-*arabino*-heptulosonate 7-phosphate chorismate is synthesised from six enzymatic reactions none of which have been reported to be subject to any kind of regulation. The reactions are catalyzed by *AroB, AroQ, AroE, AroK, AroA* and *AroC* (Figure 3.11). Chorismate can be converted to either anthranilate (precursor for tryptophan) or prephenate (precursor for tyrosine and phenylalanine) by the enzymes anthranilate synthase (*trpEG*) and chorismate mutase (*csm*), respectively. Both pathways are subject to control by inhibiting the end-products. In the tryptophan synthetic pathway anthranilate is further synthesized to phosphoribosyl anthranilate via *TrpD*, which is feedback inhibited by tryptophan (O'Gara and Dunican, 1995). The next two steps are known to form a multifunctional protein consisting of *TrpF* and *TrpC* forming indole 3-glycerolphosphate via 1-(2-carboxyphenylamino)-1-deoxy-D-ribulose 5-phosphate. In the last step tryptophan is formed by the *TrpAB* enzyme complex. In addition to the enzymatic inhibition mentioned above negative transcriptional control of all enzymes in the tryptophan branch has been reported at high tryptophan concentrations (Sugimoto and Shiio, 1977). Tyrosine is synthesized from prephenate via pretyrosine by two enzymatic reactions: *TyrA* and pretyrosine dehydrogenase (Fazel and Jensen, 1979b). Phenylalanine is synthesized from prephenate via phenylpyruvate. Prephenate dehydratase (*pheA*) catalyze the first step of this pathway (Follettie and Sinskey, 1986), whereas the last step is catalyzed by tyrosine aminotransferase (*tyrAT*) (Fazel and Jensen, 1979a).

Nucleotide Metabolism and Biosynthesis

Nucleotides in the forms of ribonucleotides and deoxyribonucleotides are the building blocks of DNA and RNA. In addition to be part of these important macromolecules for biomass, nucleotides also serve as constituents for a number of co-factors (e.g. CoA, FAD, NAD and NADP). Some nucleotides are also used for specific purposes in cellular metabolism as it is the case for ATP in energy metabolism. Nucleotides consist of a nitrogenous base, a sugar and one or more phosphate groups. Depending on weather it is a ribonucleotide

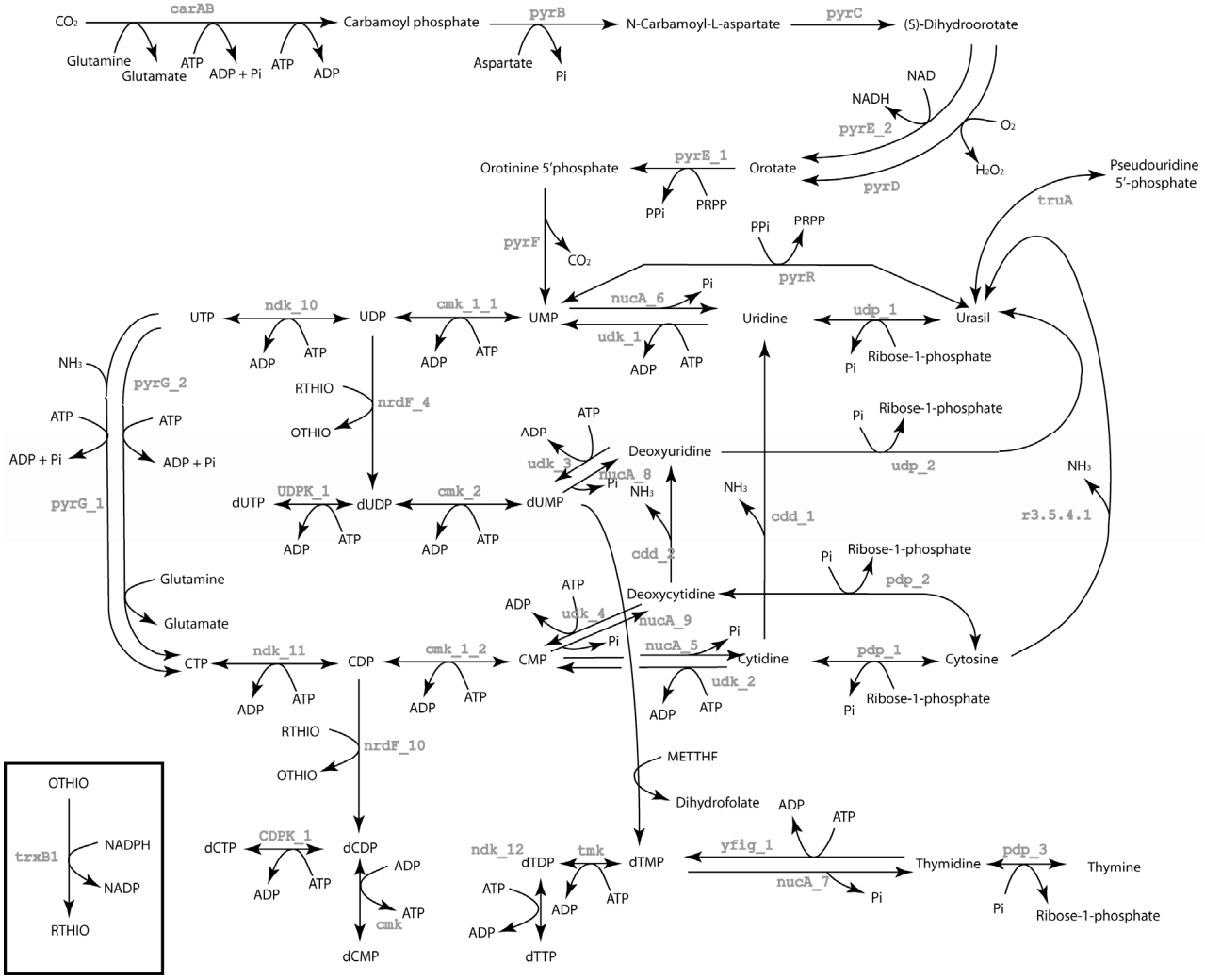

Figure 3.12: The pyrimidine metabolic pathways based on annotated genomic data. Gray text indicates tentative gene names.

or a deoxyribonucleotide the sugar group is a ribose or a deoxyribose, respectively. The nitrogenous bases are derivatives of purine or pyrimidine. The purines in DNA are adenine and guanine, and the pyrimidines are thymine and cytosine. In RNA thymine is replaced by the pyrimidine uracil. The nucleotide metabolism in *C. glutamicum* has not been thoroughly investigated. The related *Corynebacterium ammoniagenes* has been used for the production of some nucleotides, such as inosine, IMP, GTP, and ATP, why some work on this bacteria have been done. However, information is still sparse. Based on the annotated genome the biosynthetic pathways for purines and pyrimidines were reconstructed (Figure 3.12 and Figure 3.13)

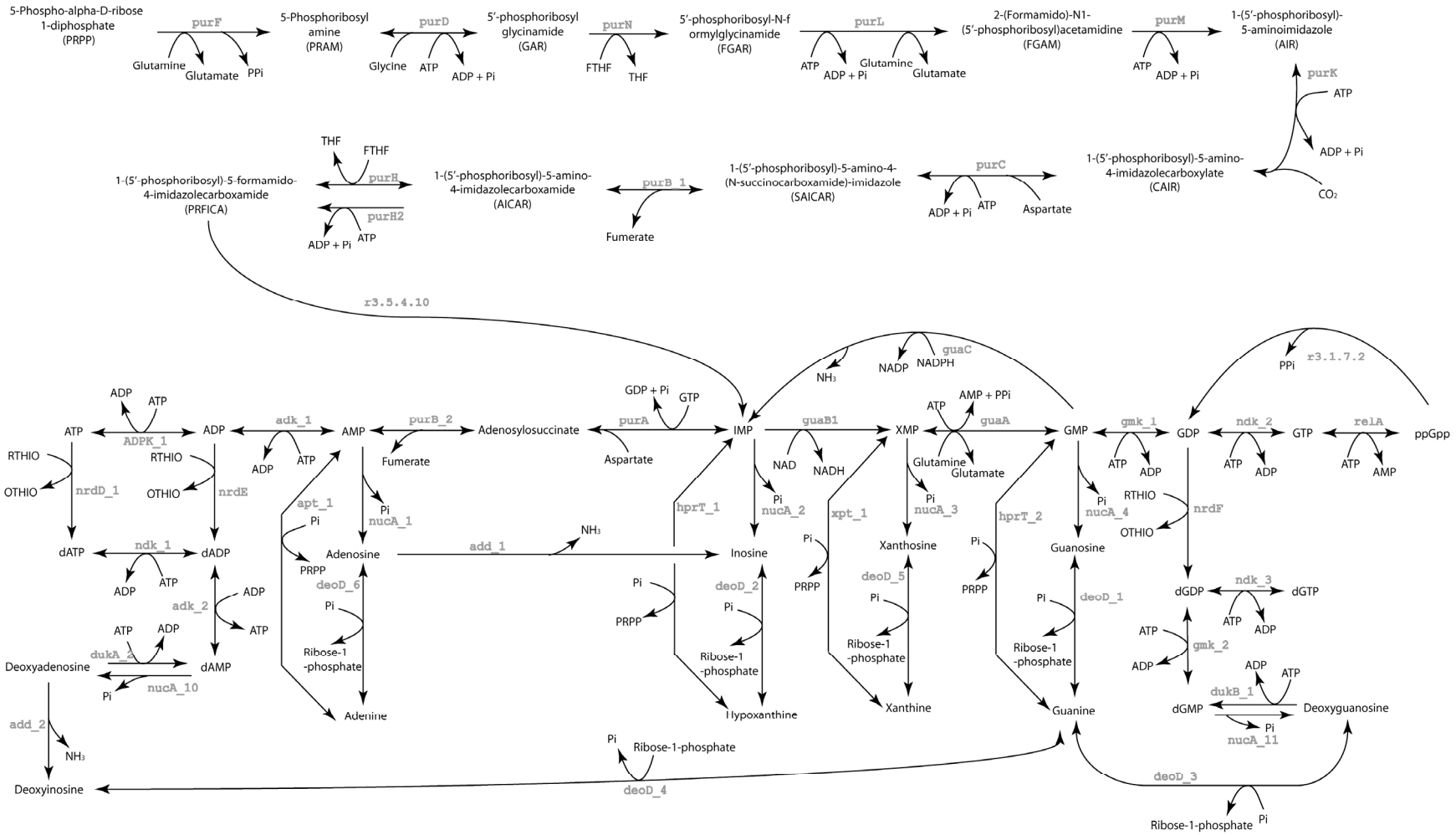

Figure 3.13: The purine metabolic pathways based on annotated genomic data. Gray text indicates tentative gene names.

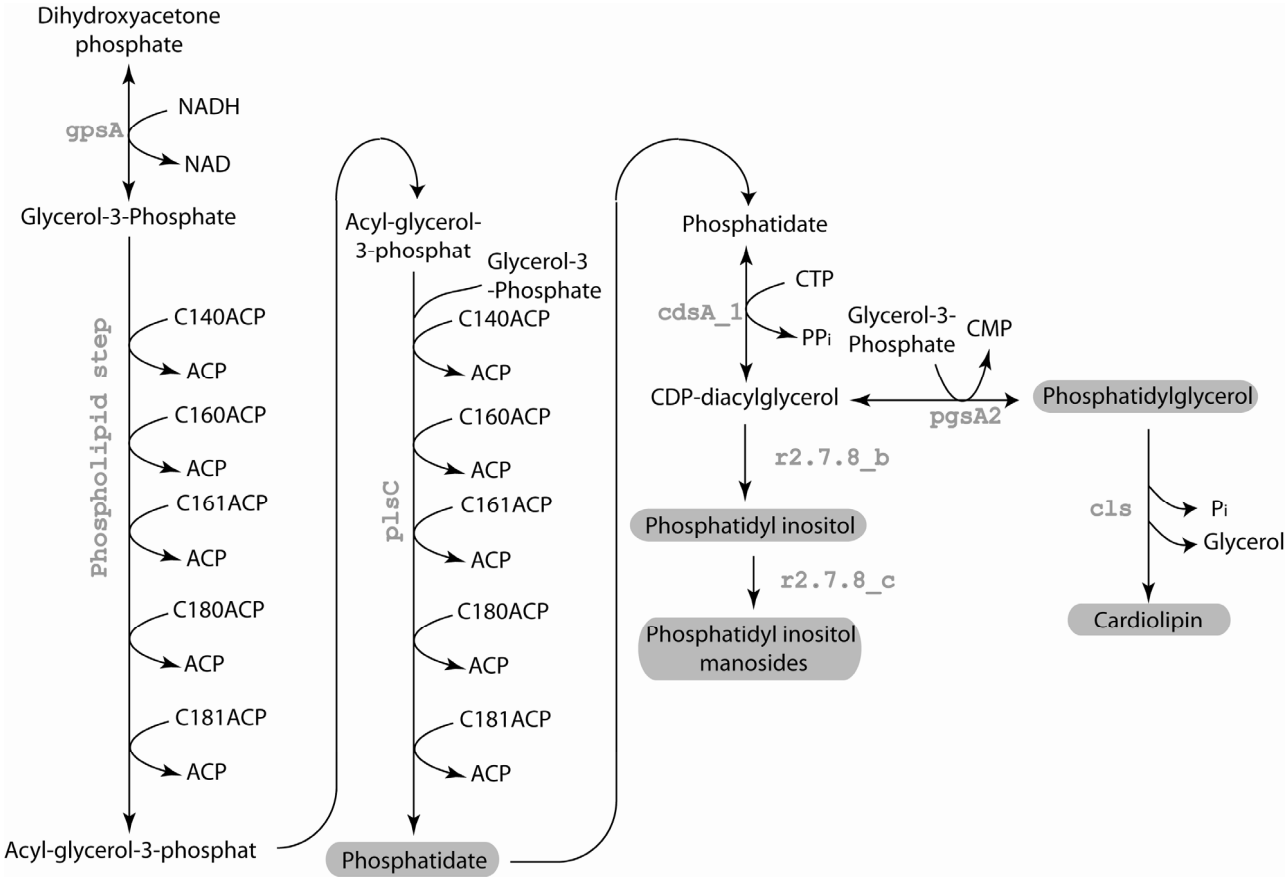

Figure 3.14: The biosynthetic pathways of phospholipids in *C. glutamicum*. Phospholipids in grey ovals are components of the phospholipids fraction in *C. glutamicum* biomass. The ratio of the fatty acids and glycerol-3-phosphate is 1:1. The ratio between fatty acids determines the composition of the phosphatidate fraction, and hence the fatty acid composition of the phospholipids fraction. C140ACP: Myristoyl-[acyl-carrier protein]; C160ACP: Hexadecanoyl-[acyl-carrier protein]; C161ACP: Palmitoyl-[acyl-carrier protein]; C180ACP: Stearoyl-[acyl-carrier protein]; C181: Oleoyl-[acyl-carrier protein]. All fatty acids are in activated form, so no additional energy is needed for biosynthesis.

Cell wall components

The chemical structure of the *C. glutamicum* cell-wall have received some interest due to its role in amino acid export (Eggeling and Sahm, 2001). In addition *C. glutamicum* belongs in the same suborder as the important human pathogens *Corynebacterium diphtheriae* and *Mycobacterium tuberculosis*, which have been studied intensively (Dower *et al.*, 2004). The cell-wall consists of a complex network of the polysaccharide peptidoglycan covalently linked to another complex polysaccharide arabinogalactan, which is further esterified with mycolic acids (Puech *et al.*, 2001). Associated with, but not covalently linked to this fraction a number of lipids are also connected to the cell-wall, the more abundant being phospholipids and trehalose mycolates (Daffé, 2005). The plasma membrane of *C. glutamicum* mainly consists of polar lipids, of which phospholipids are the dominant type. The major building blocks for lipids are fatty acids. Fatty acids are synthesized by fatty acid syntases (FAS), and it is generally believed that *C. glutamicum* (based on results from *Brevibacterium ammoniagenes*) posses two fatty acid syntase I (FAS-I) genes (FAS-IA and FAS-I2) of which one (FAS-IA) is essential for growth (Stuible *et al.*, 1996). The *C. glutamicum* genome does not contain genes encoding for the fatty acid syntase type II system (FAS II) (Daffé, 2005). FAS is a protein complex which is able to synthesize fatty acids in successive additions of two carbon units to an activated form of acetyl-CoA (Stephanopoulos *et al.*, 1998). The carbon units in the fatty acid synthesis are donated from malonyl-CoA which is formed from Ac-CoA via acetyl CoA carboxylase using one ATP (Stryer, 1995b).

Phospholipids biosynthesis

In *C. glutamicum* the major phospholipids constituents are oleic acid (18:1) and palmic acid (16:0) which contribute to more than 90% of the lipid pool of the phospholipids (Collins *et al.*, 1982b; Hoischen and Krämer, 1990). In addition to these fatty acids myristic acid (14:0), pentadecanoic acid (15:0), stearic acid (16:1) and tuberculostearic acid (18:0) are present in minor quantities (Collins *et al.*, 1982b). Based on the annotated genome and experimental data (Hoischen and Krämer, 1990; Nampoothiri *et al.*, 2002),the phospholipids biosynthetic pathways in *C. glutamicum* was reconstructed (Figure 3.14). Phospholipids are synthesized from dihydroxyacetone phosphate via glycerol-3-phosphate which is synthesized by the consumption of NADH. An Acyl-glycerol-3-phosphate is further synthesized by adding fatty acids to glycerol-3-phosphate, and this step is repeated to form phosphatidate. The fatty acids are provided as already activated building blocks – conjugated to acyl carrier protein (ACP). This activation is done during fatty acid biosynthesis. From phosphatidate all other phospholipids are synthesized (Figure 3.14).

Mycolic acids biosynthesis

The majority of the mycolic acid fraction in *C. glutamicum* consists of the 32:2 3OH and 34:1 3OH mycolic acids (Collins *et al.*, 1982a). Other mycolic acids identified are 32:0, 34:0, 36:1 and 36:2 (Jang *et al.*, 1997). In general two types of mycolates are considered to be present in the *C. glutamicum* cell wall: trehalose monocorynemycolate (TMCM) and trehalose decorynemycolate (TDCM) (Daffé, 2005). The “free” mycolic acids are known to form esters with trehalose in order to form mycolates where the mycolic acids are bound within the cell wall. The mycolic acid synthetic pathway is not well characterized, although some of the genes involved have been identified (Brand *et al.*, 2003). Based on structural considerations it has been postulated that mycolic acids are synthesized by condensation and decarboxylation reactions (Daffé, 2005).

Arabinogalactan biosynthesis

Arabinogalactan is a heterogeneous polysaccharide composed mainly of galactosyl residues and arabinofuranosyl residues. *C. glutamicum* cell wall arabinogalactan consists of alternating β(1→5) and β(1→6) linked galactfuranose residues which are polymerized by the high-energy sugar donor UDP-galactofuranosyl to produce a linear galactan domain (Alderwick *et al.*, 2005; Sanders *et al.*, 2001). Three branched arabinan motifs are attached to the C5 position of the β(1→6) linked galactose residue at the 8^{th}, 10^{th} and 12^{th} galactofuranosyl residues of the galactan domain (Alderwick *et al.*, 2005). The arabinan motif consist of a linear β(1→5) arabian core with branching introduced at specific C3 positions along the arabinan polysaccharide (Daffe *et al.*, 1990; Alderwick *et al.*, 2005). Arabinogalactan terminates with β(1→2) linked arabinofuranosyl units in a unique hexa-arabinofuranosyl motif. This is the site where arabinogalactans and mycolic acids are linked together (McNeil *et al.*, 1991). In most mycobacterial species arabinogalactan is covalently attached to peptidoglycan through a phosphodiester linkage via rhamnose and glucosamine (McNeil *et al.*, 1990). This step has not yet been unraveled for *C. glutamicum*; however, it is likely that a similar step occurs in this organism.

Peptidoglycan

Peptidoglycan in *C. glutamicum* is thought to be similar to the most common types present in bacteria, and of same type as found in *Escherichia coli* (Wijayarathua *et al.*, 2001). Peptidoglycan is synthesized from the intermediates, UDP-*N*-acetylmuramate, UDP-*N*-acetyl-D-glucosamine, L-alanine, D-glutamate,, L-glycine, D-alanyl-D-alanine, and meso-2,6-diaminopimelate (Ingraham *et al.*, 1983; Schleifer and Kandler, 1972). In figure 3.15 the reactions and corresponding genes for the biosyntehsis of intermediates used for peptidoglycan in *C. glutamicum* is presented. In addition an overview of the lumped polymerization reaction is shown. The polymerization consists of several reactions that sequentially add the amino acids to the lactyl residue of UDP-*N*-acetylmuramate, followed by addition of UDP-*N*-acetyl-D-glucosamine, forming a peptidoglycan subunit (Ingraham *et al.*, 1983). These subunits are further polymerized, and further linked with peptide bonds by the expense of ATP. During this step an L-alanine molecule is liberated from the chain. Chains of 20-80 subunits are formed (Ingraham *et al.*, 1983).

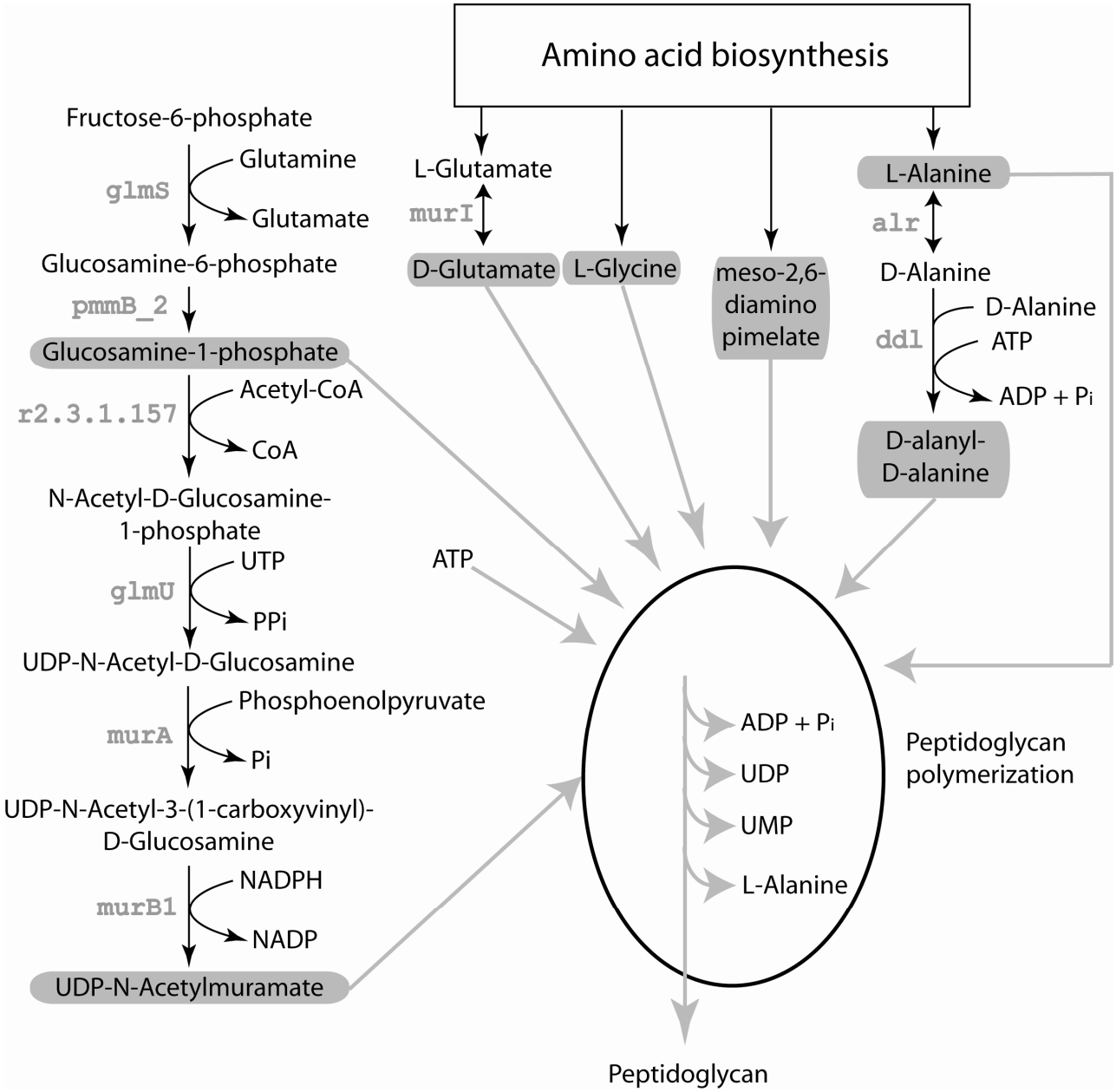

Figure 3.15: The synthetic pathways of intermediates- and the proposed polymerization of peptidoglycan in *C. glutamicum*. Compounds in grey ovals are intermediates which are used for the polymerization of peptidoglycan. Grey arrows indicate polymerization reactions.

References

Abe,S., Takayama,K., and Kinoshita,S. (1967) Taxonomical studies on glutamic acid producing bacteria. Journal of General and Applied Microbiology **13**, 279-301.

Alderwick,L.J., Radmacher,E., Seidel,M., Gande,R., Hitchen,P.G., Morris,H.R., Dell,A., Sahm,H., Eggeling,L., and Besra,G.S. (2005) Deletion of Cg-emb in *Corynebacterianeae* leads to a novel

truncated cell wall arabinogalactan, whereas inactivation of Cg-ubiA results in an arabinan-deficient mutant with a cell wall galactan core. Journal of Biological Chemistry **280**, 32362-32371.

Alifano,P., Fani,R., Lió,P., Lazcano,A., Bazzicalupo,M., Carlomagno,M.S., and Bruni,C.B. (1996) Histidine biosynthetic pathway and genes: Structure, regulation, and evolution. Microbiological Reviews **60**, 44-69.

Ankri,S., Serebrijski,I., Reyes,O., and Leblon,G. (1996) Mutations in the *Corynebacterium glutamicum* proline biosynthetic pathway: a natural bypass of the proA step. Journal of Bacteriology **178**, 4412-4419.

Audette,G.F., Quail,J.W., Hayakawa,K., Bai,C., Chen,R., and Delbaere,L.J.T. (1999) Crystallization and preliminary X-ray diffraction studies of monomeric isocitrate dehydrogenase from *Corynebacterium glutamicum*. Acta Crystallographica Section D **55**, 1584-1585.

Bott,M. and Niebisch,A. (2003) The respiratory chain of *Corynebacterium glutamicum*. Journal of Biotechnology **104**, 129-153.

Brand,S., Niehaus,K., Pühler,A., and Kalinowski,J. (2003) Identification and functional analysis of six mycolyltransferase genes of *Corynebacterium glutamicum* ATCC 13032: the genes *cop1*, *cmt1*, and *cmt2* can replace each other in the synthesis of trehalose dicorynomycolate, a component of the mycolic acid layer of the cell envelope. Archives of Microbiology **180**, 33-44.

Burkovski,A. (2003a) Ammonium assimilation and nitrogen control in *Corynebacterium glutamicum* and its relatives: an example for new regulatory mechanisms in actinomycetes. FEMS Microbiology Reviews **27**, 617-628.

Burkovski,A. (2003b) I do it my way: regulation of ammonium uptake and ammonium assimilation in *Corynebacterium glutamicum*. Archives of Microbiology **179**, 83-88.

Ceredeño-Tárraga,A.M., Efstratiou,A., Dover,L.G., Holden,M.T.G., Pallen,M., Bentley,S.D., Besra,G.S., Churcher,C., James,K.D., De Zoysa,A., Chillingworth,T., Cronin,A., Dowd,L., Feltwell,T., Hamlin,N., Holroyd,S., Jagels,K., Moule,S., Quail,M.A., Rabbinowitsch,E., Rutherford,K.M., Thomsen,N.R., Unwin,L., Whitehead,S., Barrell,B.G., and Parkhill,J. (2003) The complete genome sequence and analysis of *Corynebacterium diphtheriae* NCTC13129. Nucleic Acids Research **31**, 6516-6523.

Claes,W.A., Puhler,A., and Kalinowski,J. (2002) Identification of two *prpDBC* gene clusters in *Corynebacterium glutamicum* and their involvement in propionate degradation via the 2-methylcitrate cycle. Journal of Bacteriology **184**, 2728-2739.

Cocaign-Bousquet,M. and Lindley,N.D. (1995) Pyruvate overflow and carbon flux within the central metabolic pathways of *Corynebacterium glutamicum* during growth on lactate. Enzyme and Microbial Technology **17**, 260-267.

Cocaign-Bousquet,M., Monnet,C., and Lindley,N.D. (1993) Batch kinetics of *Corynebacterium glutamicum* during growth on various carbon substrate mixtures to localise metabolic bottlenecks. Applied Microbiology and Biotechnology **40**, 526-530.

Collins,M.D., Doodfellow,M., and Minnikin,D.E. (1982a) A survey of the structures of mycolic acids in *Corynebacterium glutamicum* and related taxa. Journal of General Microbiology **128**, 129-149.

Collins,M.D., Goodfellow,M., and Minnikin,D.E. (1982b) Fatty acid composition of some mycolic acid-containing coryneform bacteria. Journal of General Microbiology **128**, 2503-2509.

Daffé,M. (2005) The Cell Envelope of Corynebacteria. In Handbook of *Corynebacterium glutamicum* (Edited by Eggeling,L. and Bott,M.) pp. 121-148. CRC Press, Boca Raton.

Daffe,M., Brennan,P.J., and McNeil,M.R. (1990) Predominant structural features of the cell wall arabinogalactan of *Mycobacterium tuberculosis* as revealed through characterization of oligoglycosyl alditol fragments by gas chromatography/mass spectrometry and by 1H and 13C NMR analyses. Journal of Biological Chemistry **265**, 6744-6749.

de Kok,A., Hengeveld,A.F., Martin,A., and Westphal,A.H. (1998) The pyruvate dehydrogenase multi-enzyme complex from Gram-negative bacteria. Biochimica et Biophysica Acta - Protein Structure and Molecular Enzymology **1385**, 353-366.

Dominguez,H., Cocaign-Bousquet,M., and Lindley,N.D. (1997) Simultaneous consumption of glucose and fructose from sugar mixtures during batch growth of *Corynebacterium glutamicum*. Applied Microbiology and Biotechnology **47**, 600-603.

Dominguez,H. and Lindley,N.D. (1996) Complete sucrose metabolism requires fructose phosphotransferase activity in *Corynebacterium glutamicum* to ensure phosphorylation of liberated fructose. Applied and Environmental Microbiology **62**, 3878-3880.

Dominguez,H., Rollin,C., Guyonvarch,A., Guerquin-Kern,J.L., Cocaign-Bousquet,M., and Lindley,N.D. (1998) Carbon-flux distribution in the central metabolic pathways of *Corynebacterium glutamicum* during growth on fructose. European Journal of Biochemistry **254**, 96-102.

Dower,L.G., Ceredeño-Tárraga,A.M., Pallen,M.J., Parkhill,J., and Besra,G.S. (2004) Comparative cell wall core biosynthesis in the mycolated pathogens, *Mycobacterium tuberculosis* and *Corynebacterium diphtheriae*. FEMS Microbiology Reviews **28**, 225-250.

Eggeling,I., Cordes,C., Eggeling,L., and Sahm,H. (1987) Regulation of acetohydroxy acid synthase in *Corynebacterium glutamicum* during fermentation of alfa-ketobutyrate to L-isoleucine. Applied Microbiology and Biotechnology **25**, 346-351.

Eggeling,L. and Sahm,H. (2001) The cell wall barrier of *Corynebacterium glutamicum* and amino acid efflux. Journal of Bioscience and Bioengineering **92**, 201-213.

Eikmanns,B.J. (1992) Identification, sequence analysis, and expression of a *Corynebacterium glutamicum* gene cluster encoding the three glycolytic enzymes glyceraldehyde-3-phosphate dehydrogenase, 3-phosphoglycerate kinase, and triosephosphate isomerase. Journal of Bacteriology **174**, 6076-6086.

Eikmanns,B.J., Follettie,M.T., Griot,M.U., and Sinskey,A.J. (1989) The phosphoenolpyruvate carboxylase gene of *Corynebacterium glutamicum*: Molecular cloning, nucleotide sequence, and expression. Molecular and General Genetics MGG **218**, 330-339.

Eikmanns,B.J., Rittmann,D., and Sahm,H. (1995) Cloning, sequence analysis, expression, and inactivation of the *Corynebacterium glutamicum icd* gene encoding isocitrate dehydrogenase and biochemical characterization of the enzyme. Journal of Bacteriology **177**, 774-782.

Eikmanns,B.J., Thum-Schmitz,N., Eggeling,L., Ludtke,K.U., and Sahm,H. (1994) Nucleotide sequence, expression and transcriptional analysis of the *Corynebacterium glutamicum gltA* gene encoding citrate synthase. Microbiology **140**, 1817-1828.

Fazel,A.M. and Jensen,R.A. (1979a) Aromatic aminotransferases in coryneform bacteria. Journal of Bacteriology **140**, 580-587.

Fazel,A.M. and Jensen,R.A. (1979b) Obligatory biosynthesis of L-tyrosine via the pretyrosine branchlet in coryneform bacteria. Journal of Bacteriology **138**, 805-815.

Follettie,M.T. and Sinskey,A.J. (1986) Molecular cloning and nucleotide sequence of the *Corynebacterium glutamicum pheA* gene. Journal of Bacteriology **167**, 695-702.

Frunzke,J., Engels,V., Hasenbein,S., Gätgens,C., and Bott,M. (2008) Coordinated regulation of gluconate catabolism and glucose uptake in *Corynebacterium glutamicum* by two functionally equivalent transcriptional regulators, *GntR1* and *GntR2*. Molecular Microbiology **67**, 305-322.

Genda,T., Watabe,S., and Ozaki,H. (2006) Purification and characterization of fumarase from *Corynebacterium glutamicum*. Bioscience Biotechnology and Biochemistry **70**, 1102-1109.

Gerstmeier,R., Wendisch,V.F., Schnicke,S., Ruan,H., Farwic,M., Reinscheid,D., and Eikmanns,B.J. (2003) Acetate metabolism and the regulation in *Corynebacterium glutamicum*. Journal of Biotechnology **104**, 99-122.

Gourdon,P., Baucher,M.F., Lindley,N.D., and Guyonvarch,A. (2000) Cloning of the malic enzyme gene from *Corynebacterium glutamicum* and role of the enzyme in lactate metabolism. Applied and Environmental Microbiology **66**, 2981-2987.

Gourdon,P., Raherimandimby,M., Dominguez,H., Cocaign-Bousquet,M., and Lindley,N.D. (2003) Osmotic stress, glucose transport capacity and consequences for glutamate overproduction in *Corynebacterium glutamicum*. Journal of Biotechnology **104**, 77-85.

Guillouet,S. and Engasser,J.M. (1995) Sodium and proline accumulation in *Corynebacterium glutamicum* as a response to an osmotic saline upshock. Applied Microbiology and Biotechnology **43**, 315-320.

Hermann,T. (2003) Industrial production of amino acids by coryneform bacteria. Journal of Biotechnology **104**, 155-172.

Hoischen,C. and Krämer,R. (1990) Membrane alteration is necessary but not sufficient for effective glutamate secretion in *Corynebacterium glutamicum*. Journal of Bacteriology **172**, 3409-3416.

Hwang,B.-J., Yeom,H.-J., Kim,Y., and Lee,H.-S. (2002) *Corynebacterium glutamicum* utilizes both transsulfuration and direct sulfhydrylation pathways for methionine biosynthesis. Journal of Bacteriology **184**, 1277-1286.

Ikeda,M., Okamoto,K., and Katsumata,R. (1998) A transketolase mutant of *Corynebacterium glutamicum.* Applied Microbiology and Biotechnology **50**, 375-378.

Ikeda,M. and Nakagawa,S. (2003) The *Corynebacterium glutamicum* genome: features and impacts on biotechnological processes. Applied Microbiology and Biotechnology **62**, 99-109.

Ingraham,J.L., Maaløe,O., and Niedhardt,F.C. (1983) Growth of the Bacterial Cell. Sinauer Associates, Inc., Sunderland, Massachusetts.

Inui,M., Murakami,S., Okino,S., Kawaguchi,H., Vertés,A.A., and Yukawa,H. (2004) Metabolic analysis of *Corynebacterium glutamicum* during lactate and succinate productions under oxygen deprivation conditions. Journal of Molecular Microbiology and Biotechnology **7**, 182-196.

Ishige,T., Krause,M., Bott,M., Wendisch,V.F., and Sahn,H. (2003) The phosphate starvation stimulon of *Corynebacterium glutamicum* determined by DNA microarray analyses. Journal of Bacteriology **185**, 4519-4529.

Jakoby,M., Tesch,M., Sahn,H., Krämer,R., and Burkovski,A. (1997) Isolation of the *Corynebacterium glutamicum glnA* gene encoding glutamine synthase I. FEMS Microbiology Letters **154**, 81-88.

Jang,K.H., Pierotti,D., Kemp,G.W., Best,G.R., and Britz,M.L. (1997) Mycolic acid composition of *Corynebacterium glutamicum* and its cell surface mutants: effects of growth with glycine and isonicotinic acid hydrazide. Microbiology UK **143**, 3209-3221.

Jetten,M.S., Gubler,M.E., Lee,S.H., and Sinskey,A.J. (1994) Structural and functional analysis of pyruvate kinase from *Corynebacterium glutamicum*. Applied and Environmental Microbiology **60**, 2501-2507.

Jetten,M.S.M. and Sinskey,A.J. (1993) Characterization of phosphoenolpyruvate carboxykinase from *Corynebacterium glutamicum*. FEMS Microbiology Letters **111**, 183-188.

Jetten,M.S.M. and Sinskey,A.J. (1995) Purification and properties of oxaloacetate decarboxylase from *Corynebacterium glutamicum*. Antonie van Leeuwenhoek **67**, 221-227.

Jung,S.-I., Han,M.-S., Kwon,J.-H., Cheon,C.-I., Min,K.-H., and Lee,M.-S. (1998) Cloning of the histidine biosynthetic genes of *Corynebacterium glutamicum*: Organization and sequencing analysis of the *hisA, impA* and *hisF* gene cluster. Biochemical and Biophysical Research Communications **247**, 741-745.

Kalinowski,J., Bathe,B., Bartels,D., Bischoff,N., Bott,M., Burkovski,A., Dusch,N., Eggeling,L., Eikmanns,B.J., and Gaigalat,L. (2003) The complete *Corynebacterium glutamicum* ATCC 13032 genome sequence and its impact on the production of aspartate-derived amino acids and vitamins. Journal of Biotechnology **104**, 5-25.

Kamada,N., Yasuhara,A., and Ikeda,M. (2003) Significance of the non-oxidative route of the pentose phosphate pathway for supplying carbon to the purine-nucleotide pathway in *Corynebacterium ammoniagenes*. Journal of Industrial Microbiology & Biotechnology **30**, 129-132.

Kamada,N., Yasuhara,A., Takano,Y., Nakano,T., and Ikeda,M. (2001) Effect of transketolase modifications on carbon flow to the purine-nucleotide pathway in *Corynebacterium ammoniagenes*. Applied Microbiology and Biotechnology **56**, 710-717.

Kataoka,M., Hashimoto,K.I., Yoshida,M., Nakamatsu,T., Horinouchi,S., and Kawasaki,H. (2006) Gene expression of *Corynebacterium glutamicum* in response to the conditions inducing glutamate overproduction. Letters in Applied Microbiology **42**, 471-476.

Keilhauer,C., Eggeling,L., and Sahm,H. (1993) Isoleucine synthesis in *Corynebacterium glutamicum*: molecular analysis of the *ilvB-ilvN-ilvC* operon. Journal of Bacteriology **175**, 5595-5603.

Kiefer,P., Heinzle,E., Zelder,O., and Wittmann,C. (2004) Comparative metabolic flux analysis of lysine-producing *Corynebacterium glutamicum* cultured on glucose or fructose. Applied and Environmental Microbiology **70**, 229-239.

Kronemeyer,W., Peekhaus,N., Kramer,R., Sahm,H., and Eggeling,L. (1995) Structure of the *gluABCD* cluster encoding the glutamate uptake system of *Corynebacterium glutamicum*. Journal of.Bacteriology **177**, 1152-1158.

Krug,A., Wendisch,V.F., and Bott,M. (2005) Identification of AcnR, a TetR-type repressor of the aconitase gene *acn* in *Corynebacterium glutamicum*. Journal of Biological Chemistry **280**, 585-595.

Kusumoto,K., Sakiyama,M., Sakamoto,J., Noguchi,S., and Sone,N. (2000) Menaquinol oxidase activity and primary structure of cytochrome bd from the amino-acid fermenting bacterium *Corynebacterium glutamicum*. Archives of Microbiology **173**, 390-397.

Lee,H.-S. (2005) Sulfur Metabolism and Its Regulation. In Handbook of *Corynebacterium glutamicum* (Edited by Eggeling,L. and Bott,M.) pp. 351-376. CRC Press, Boca Raton.

Lee,H.-S. and Hwang,B.-J. (2003) Methionine biosynthesis and its regulation in *Corynebacterium glutamicum*: parallel pathways of transsulfuration and direct sulfhydration. Applied Microbiology and Biotechnology **62**, 459-467.

Lee,H.-W., Pan,J.-G., and Lebeault,J.-M. (1998) Enhanced L-lysine production in threonine-limited continuous culture of *Corynebacterium glutamicum* by using gluconate as a secondary carbon source with glucose. Applied Microbiology and Biotechnology **49**, 9-15.

Lee,J.K., Sung,M.H., Yoon,K.H., Yu,J.H., and Oh,T.K. (1993) Cloning and expression of the gene encoding mannose enzyme II of the *Corynebacterium glutamicum* phosphoenolpyruvate-dependent phosphotransferase system in Escherichia coli. Journal of Microbiology and Biotechnology **3**, 1-5.

Liebl,W. (2005) Corynebacterium Taxonomy. In Handbook of *Corynebacterium glutamicum* (Edited by Eggeling,L. and Bott,M.) pp. 9-34. CRC Press, Boca Raton.

Lu,C.-D. (2006) Pathways and regulation of bacterial arginine metabolism and perspectives for obtaining arginine overproducing strains. Applied Microbiology and Biotechnology **70**, 261-272.

Marx,A., de Graaf,A.A., Wiechert,W., Eggeling,L., and Sahm,H. (1996) Determination of the fluxes in the central metabolism of *Corynebacterium glutamicum* by nuclear magnetic resonance spectroscopy combined with metabolite balancing. Biotechnology and Bioengineering **49**, 111-129.

Marx,A., Hans,S., Möckel,B., Bathe,B., and de Graaf,A.A. (2003) Metabolic phenotype of phosphoglucose isomerase mutants of *Corynebacterium glutamicum*. Journal of Biotechnology **104**, 185-197.

McNeil,M., Daffe,M., and Brennan,P.J. (1990) Evidence for the nature of the link between the arabinogalactan and peptidoglycan of mycobacterial cell walls. Journal of Biological Chemistry **265**, 18200-18206.

McNeil,M., Daffe,M., and Brennan,P.J. (1991) Location of the mycolyl ester substituents in the cell walls of mycobacteria. Journal of Biological Chemistry **226**, 13217-13223.

Meier-Wagner,J., Nolden,L., Jakoby,M., Siewe,R., Krämer,R., and Burkovski,A. (2001) Multiplicity of ammonium uptake systems in *Corynebacterium glutamicum*: role of *Amt* and *AmtB*. Microbiology **147**, 135-143.

Miyajima,R., Otsuka,S.-I., and Shiio,I. (1968) Regulation of aspartate family amino acid biosynthesis in *Brevibacterium flavum*. Journal of Biochemistry **63**, 139-148.

Möckel,B., Eggeling,L., and Sahm,H. (1992) Functional and structural analysis of threonine dehydratase from *Corynebacerium glutamicum*. Journal of Bacteriology **174**, 8065-8072.

Molenaar,D., van der Rest,M.E., Drysch,A., and Yucel,R. (2000) Functions of the membrane-associated and cytoplasmic malate dehydrogenases in the citric acid cycle of *Corynebacterium glutamicum.* Journal of Bacteriology. **182**, 6884-6891.

Molenaar,D., van der Rest,M.E., and Petrovic,S. (1998) Biochemical and genetic characterization of the membrane-associated malate dehydrogenase (acceptor) from *Corynebacterium glutamicum*. European Journal of Biochemistry **254**, 395-403.

Moon,M.W., Kim,H.J., Oh,T.K., Shin,C.S., Lee,J.S., Kim,S.J., and Lee,J.K. (2005) Analysis of enzyme II gene mutants for sugar transport and heterologous expression of fructokinase gene in *Corynebacterium glutamicum* ATCC 13032. FEMS Microbiology Letters **244**, 259-266.

Moritz,B., Striegel,K., de Graff,A.A., and Sahm,H. (2000) Kinetic properties of the glucose-6-phosphate and 6-phosphogluconate dehydrogenases from *Corynebacterium glutamicum* and their application for predicting pentose phosphate pathway flux in vivo. European Journal of Biochemistry **267**, 3442-3452.

Mormann,S., Lömker,A., Rückert,C., Gaigalat,L., Tauch,A., Pühler,A., and Kalinowski,J. (2006) Random mutagenesis in *Corynebacterium glutamicum* ATCC 13032 using an IS6100-based transposon vector identified the last unknown gene in the histidine pathway. BMS Genomics **7**, 205.

Nampoothiri,K.M., Hoischen,C., Bathe,B., Möckel,B., Pfefferle,W., Krumbach,K., Sahm,H., and Eggeling,L. (2002) Expression of genes of lipid synthesis and altered lipid composition modulates L-glutamate efflux of *Corynebacterium glutamicum*. Applied Microbiology and Biotechnology 58, 89-96.

Netzer,R., Peters-Wendisch,P., Eggeling,L., and Sahm,H. (2004) Cometabolism of a Nongrowth Substrate: L-Serine Utilization by *Corynebacterium glutamicum*. Applied and Environmental Microbiology **70**, 7148-7155.

Nicholls,D.G. and Ferguson,S.J. (1992) Bioenergetics. Academic Press, London.

Niebisch,A. and Bott,M. (2001) Molecular analysis of the cytochrome bc1-aa3 branch of the *Corynebacterium glutamicum* respiratory chain containing an unusual diheme cytochrome c1. Archives of Microbiology **175**, 282-294.

Niebisch,A. and Bott,M. (2003) Purification of a cytochrome bc1-aa3 supercomplex with quinol oxidase activity from *Corynebacterium glutamicum*. IDENTIFICATION OF A FOURTH SUBUNIT OF CYTOCHROME aa3 OXIDASE AND MUTATIONAL ANALYSIS OF DIHEME CYTOCHROME c1. Journal of Biological Chemistry **278**, 4339-4346.

Nishio,Y., Nakamura,Y., Kawarabayasi,Y., Usada,Y., Kimura,E., Sugimoto,S., Matsui,K., Yamagishi,A., Kikuchi,H., Ikeo,K., and Gojobori,T. (2003) Comparative complete genome sequence analysis of the amino acid replacements responsible for the thermostability of *Corynebacterium efficiens*. Genome Research **13**, 1572-1579.

O'Gara,J.P. and Dunican,L.K. (1995) Mutations in the *trpD* gene of *Corynebacterium glutamicum* confer 5- methyltryptophan resistance by encoding a feedback-resistant *anthranilate* phosphoribosyltransferase. Appl.Environ.Microbiol. **61**, 4477-4479.

Ohnishi,J., Hayashi,M., Mitsuhashi,S., and Ikeda,M. (2003) Efficient 40°C fermentation by a new *Corynebacterium glutamicum* mutant developed by genome breeding . Applied Microbiology and Biotechnology **62**, 69-75.

Omumasaba,C.A., Okai,N., Inui,M., and Yukawa,H. (2004) *Corynebacterium glutamicum* glycaldehyde-3-phosphate dehydrogenase isoforms with opposite, ATP-dependent regulations. Journal of Molecular Microbiology and Biotechnology **8**, 91-103.

Parche,S., Burkovski,A., Sprenger,G.A., Weil,B., Krämer,R., and Titgemeyer,F. (2001) *Corynebacterium glutamicum*: a dissection of the PTS. Journal of Molecular Microbiology and Biotechnology **3**, 423-428.

Park,S.M., Shaw-Reid,C., Sinskey,A.J., and Stephanopoulos,G. (1997) Elucidation of anaplerotic pathways in *Corynebacterium glutamicum* via 13C-NMR spectroscopy and GC-MS. Applied Microbiology and Biotechnology **47**, 430-440.

Park,S.Y., Kim,H.K., Yoo,S.-K., Oh,T.K., and Lee,J.K. (2000) Characterization of *glk*, a gene coding for glucose kinase of *Corynebacterium glutamicum*. FEMS Microbiology Letters **188**, 209-215.

Park,S.-D., Lee,J.-Y., Kim,Y., Kim,J.-H., and Lee,H.-S. (1998) Isolation and analysis of *metA*, a biosynthetic gene encoding homoserine acetyltransferase in *Corynebacterium glutamicum*. Molecules and Cells **8**, 286-294.

Patek,M., Hochmannová,J., Jelínková,M., Nesvera,J., and Eggeling,L. (1998) Analysis of the *leuB* gene from *Corynebacterium glutamicum*. Applied Microbiology and Biotechnology **50**, 42-47.

Patek,M., Krumbach,K., Eggeling,L., and Sahm,H. (1994) Leucine synthesis in *Corynebacterium glutamicum*: enzyme activities, structure of *leuA*, and effect of *leuA* inactivation on lysine synthesis. Applied and Environmental Microbiology **60**, 133-140.

Peters-Wendisch,P., Stoltz,M., Etterich,H., Kennerknecht,N., Sahn,H., and Eggeling,L. (2005) Metabolic engineering of *Corynebacterium glutamicum* for L-serine production. Applied and Environmental Microbiology **71**, 7139-7144.

Peters-Wendisch,P.G., Kreutzer,C., Kalinowski,J., Patek,M., Sahm,H., and Eikmanns,B.J. (1998) Pyruvate carboxylase from *Corynebacterium glutamicum*: characterization, expression and inactivation of the *pyc* gene. Microbiology **144**, 915-927.

Peters-Wendisch,P.G., Netzer,R., Eggeling,L., and Sahm,H. (2002) 3-Phosphoglycerate dehydrogenase from *Corynebacterium glutamicum*: the C-terminal domain is not essential for activity but is required for inhibition by L-serine. Applied Microbiology and Biotechnology **60**, 437-441.

Petersen,S., de Graff,A.A., Eggeling,L., Mollney,M., Wiechert,W., and Sahn,H. (2000) *In vivo* quantification of parallel and bidirectional fluxes in the anaplerosis of *Corynebacterium glutamicum*. Journal of Biological Chemistry **275**, 35932-35941.

Petersen,S., Mack,C., de Graaf,A.A., Riedel,C., Eikmanns,B.J., and Sahm,H. (2001) Metabolic consequences of altered phosphoenolpyruvate carboxykinase activity in *Corynebacterium glutamicum* reveal anaplerotic regulation mechanisms *in vivo*. Metabolic Engineering **3**, 344-361.

Polen,T., Schluesener,D., Poetsch,A., Bott,M., and Wendisch,V.F. (2007) Characterization of citrate utilization in *Corynebacterium glutamicum* by transcriptome and proteome analysis. FEMS Microbiology Letters **273**, 109-119.

Puech,V., Chami,M., Lemassu,A., Laneelle,M.A., Schiffler,B., Gounon,P., Bayan,N., Benz,R., and Daffe,M. (2001) Structure of the cell envelope of corynebacteria: importance of the non-covalently bound lipids in the formation of the cell wall permeability barrier and fracture plane. Microbiology **147**, 1365-1382.

Radmacher,E., Vaitsikova,A., Burger,U., Krumbach,K., Sahm,H., and Eggeling,L. (2002) Linking central metabolism with increased pathway flux: L-Valine accumulation by *Corynebacterium glutamicum*. Applied and Environmental Microbiology **68,** 2246-2250.

Reinscheid,D.J., Eikmanns,B.J., and Sahm,H. (1994) Characterization of the isocitrate lyase gene from *Corynebacterium glutamicum* and biochemical analysis of the enzyme. Journal of Bacteriology **176**, 3474-3483.

Reinscheid,D.J., Schnicke,S., Rittmann,D., Zahnow,U., Sahm,H., and Eikmanns,B.J. (1999) Cloning, sequence analysis, expression and inactivation of the *Corynebacterium glutamicum pta-ack* operon encoding phosphotransacetylase and acetate kinase. Microbiology **145**, 503-513.

Rittmann,D., Schaffer,S., Wendisch,V.F., and Sahn,H. (2003) Fructose-1,6-bisphosphatase from *Corynebacterium glutamicum*: expression and deletion of the *fbp* gene and biochemical characterization of the enzyme. Archives of Microbiology **180**, 285-292.

Rossol,I. and Pühler,A. (2003) The *Corynebacterium glutamicum aecD* gene encodes a C-S lyase with a,b-elimination activity that degrades aminoethylcysteine. Journal of Bacteriology **174**, 2968-2977.

Rückert,C., Pühler,A., and Kalinowski,J. (2003) Genome-wide analysis of the L-methionine biosynthetic pathway in *Corynebacterium glutamicum* by targeted gene deletion and homologous complementation. Journal of Biotechnology **104**, 213-228.

Sahm,H. and Eggeling,L. (1999) D-pantothenate synthesis in *Corynebacterium glutamicum* and use of *panBC* and genes encoding L-valine synthesis for D-pantothenate overproduction. Applied and Environmental Microbiology **65**, 1973-1979.

Sanders,D.A.R., Staines,A.G., McMahon,S.A., McNeil,M.R., Whitfield,C., and Naismith,J.H. (2001) UDP-galactopyranose mutase has a novel structure and mechanism. Nature Structural Biology **8**, 858-863.

Schleifer,K.H. and Kandler,O. (1972) Peptidoglycan types of bacterial cell walls and their taxonomic implications. Bacteriological Reviews **36**, 407-477.

Schreiner,M.E., Fiur,D., Holátko,J., Párèk,M., and Eikmanns,B.J. (2005) E1 Enzyme of the pyruvate dehydrogenase complex in *Corynebacterium glutamicum*: Molecular analysis of the gene and phylogenic aspects. Journal of Bacteriology **187**, 6005-6018.

Schrumpf,B., Schwarzer,A., Kalinowski,J., Pühler,A., Eggeling,L., and Sahn,H. (1991) A functionally split pathway for lysine synthesis in *Corynebacterium glutamicum*. Journal of Bacteriology **173**, 4510-4516.

Schwinde,J.W., Hertz,P.F., Sahm,H., Eikmanns,B.J., and Guyonvarch,A. (2001) Lipoamide dehydrogenase from *Corynebacterium glutamicum*: molecular and physiological analysis of the *lpd* gene and characterization of the enzyme. Microbiology **147**, 2223-2231.

Serebrijski,I., Wojcik,F., Reyes,O., and Leblon,G. (1995) Multicopy suppression by asd gene and osmotic stress-dependent complementation by heterologous *proA* in *proA* mutants. Journal of Bacteriology **177**, 7255-7260.

Shiio,I., Sugimoto,S., and Miyajima,R. (1974) Regulation of 3-deoxy-D-arabino-heptulosonate-7-phosphate synthase in *Brevibacterium flavum*. The Journal of Biochemistry **75**, 987-997.

Siewe,R., Weil,B., Burkovski,A., Eggeling,L., Krämer,R., and Jahns,T. (1998) Urea uptake and urease activity in *Corynebacterium glutamicum*. Archives of Microbiology **169**, 411-416.

Siewe,R., Weil,B., Burkovski,A., Eikmanns,B.J., Eikmanns,M., and Krämer,R. (1996) Functional and genetic characterization of the (methyl)ammonium uptake carrier of *Corynebacterium glutamicum*. The Journal of Biological Chemistry **271**, 5398-5403.

Siewe,R., Weil,B., and Krämer,R. (1995) Glutamine uptake by a sodium-dependent secondary transport system in *Corynebacterium glutamicum*. Archives of Microbiology **164**, 98-103.

Simic,P., Willuhn,J., Sahn,H., and Eggeling,L. (2002) Identification of *glyA* (encoding serine hydroxymethyltransferase) and its use together with the exporter *ThrE* to increase L-threonine accumulation by *Corynebacterium glutamicum*. Applied and Environmental Microbiology **68**, 3321-3327.

Stephanopoulos,G.N., Aristidou,A.A., and Nielsen,J. (1998) Metabolic Engineering - Principles and Methodologies. Academic Press, San Diego, USA.

Stryer,L. (1995a) Biochemistry. W. H. Freeman and Company, New York.

Stryer,L. (1995b) Fatty Acid Metabolism. In Biochemistry (Edited by Stryer,L.) pp. 601-628. W. H. Freeman and Company, New York.

Stuible,H.-P., Wagner,C., Andreou,I., Huter,G., Haselmann,J., and Schweizer,E. (1996) Identification and functional differentiation of two type I fatty acid synthases in *Brevibacterium ammoniagenes*. Journal of Bacteriology **178**, 4787-4793.

Sugimoto,M. and Shiio,I. (1987a) Regulation of glucose-6-phosphate dehydrogenase in *Brevibacterium flavum*. Agricultural and Biological Chemistry **51**, 101-108.

Sugimoto,S. and Shiio,I. (1987b) Regulation of 6-phosphogluconate dehydrogenase in Brevibacterium flavum. Agricultural and Biological Chemistry **51**, 1257-1263.

Sugimoto,M. and Shiio,I. (1989a) Regulation of enzymes for erythose 4-phosphate synthesis in *Brevibacterium flavum*. Agricultural and Biological Chemistry **53**, 2081-2087.

Sugimoto,S. and Shiio,I. (1989b) Fructose metabolism and regulation of 1-phosphofructokinase and 6-phosphofructokinase in *Brevibacterium flavum*. Agricultural and Biological Chemistry **53**, 1261-1268.

Sugimoto,S.-I. and Shiio,I. (1977) Enzymes of the tryptophan synthetic pathway in *Brevibacterium flavum*. The Journal of Biochemistry **81**, 823-833.

Tauch,A., Kaiser,O., Hain,T., Goesmann,A., Weisshaar,B., Albersmeier,A., Bekel,T., Bischoff,N., Brune,I., Chakraborty,T., Kalinowski,J., Meyer,F., Rupp,O., Schneiker,S., Viehoever,P., and Pühler,A. (2005) Complete genome sequence and analysis of the multiresistant nosocomial pathogen *Corynebacterium jeikeium* K411, a lipid-requiring bacterium of the human skin flora. Journal of Bacteriology **187**, 4671-4682.

Usuda,Y., Tujimoto,N., Abe,C., Asakura,Y., Kimura,E., Kawahara,Y., Kurahashi,O., and Matsui,H. (1996) Molecular cloning of the *Corynebacterium glutamicum* ('*Brevibacterium lactofermentum*' AJ12036) *odhA* gene encoding a novel type of 2-oxoglutarate dehydrogenase. Microbiology-Uk **142**, 3347-3354.

Utagawa,T. (2004) Production of arginine by fermentation. The Journal of Nutrition **134**, 2854S-2857S.

Vallino,J.J. and Stephanopoulos,G. (1993) Metabolic flux distribution in *Corynebacterium glutamicum* during growth and lysine overproduction. Biotechnology and Bioengineering **41**, 633-646.

Vallino,J.J. and Stephanopoulos,G. (1994) Carbon flux distributions at the glucose 6-phosphate branch point in *Corynebacterium glutamicum* during lysine overproduction. Biotechnology Progress **10**, 327-334.

von der Osten,C.H., Barbas,C.H., Wong,C.F., and Sinskey,A.J. (1989) Molecular cloning, nucleotide sequence and fine-structural analysis of the *Corynebacterium glutamicum fda* gene: structural comparison of *C. glutamicum* fructose-1,6-biphosphate aldolase to class I and class II aldolases. Molecular Microbiology **3**, 1625-1637.

Wada,M., Awano,N., Haisa,K., Takagi,H., and Nakamori,S. (2002) Purification, characterization and identification of cysteine desulfhydrase of *Corynebacterium glutamicum*, and its relationship to cysteine production. FEMS Microbiology Letters **217**, 103-107.

Wada,M., Awano,N., Yamazawa,H., Takagi,H., and Nakamori,S. (2004) Purification and characterization of O-acetylserine sulfhydrylase of *Corynebacterium glutamicum*. Bioscience Biotechnology and Biochemistry **68**, 1581-1583.

Wendisch,V.F., de Graaf,A.A., Sahm,H., and Eikmanns,B.J. (2000) Quantitative determination of metabolic fluxes during coutilization of two carbon sources: Comparative analyses with *Corynebacterium glutamicum* during growth on acetate and/or glucose. Journal of Bacteriology **182**, 3088-3096.

Wendisch,V.F., Spies,M., Reinscheid,D., Schnicke,S., Sahn,H., and Eikmanns,B.J. (2004) Regulation of acetate metabolism in *Corynebacterium glutamicum*: transcriptional control of the isocitrate lyase and malate synthase genes. Archives of Microbiology **168**, 262-269.

Wijayarathua,C.D., Wachi,M., and Nagai,K. (2001) Isolation of *ftsI* and *murE* genes involved in peptidoglycan synthesis from *Corynebacterium glutamicum*. Applied Microbiology and Biotechnology **55**, 466-470.

Willis,L.B., Lessard,P.A., and Sinskey,A.J. (2005) Synthesis of L-Threonine and Branched-Chain Amino Acids. In Handbook of *Corynebacterium Glutamicum* (Edited by Eggeling,L. and Bott,M.) pp. 511-531. CRC Press, Boca Raton.

Yukawa,H., Omumasaba,A., Nonaka,H., Kós,P., Okai,N., Suzuki,N., Suda,M., Tsuge,Y., Watanabe,J., Ikeda,Y., Vertes,A.A., and Inui,M. (2007) Comparative analysis of the *Corynebacterium glutamicum* group and complete genome sequence of strain R. Microbiology **153**, 1042-1058.

Zhao,Y. and Lin,Y.-H. (2002) Distribution of ATP and reducing equivalents in *Corynebacterium glutamicum* during amino acid resolution. Process Biochemistry **37**, 1455-1461.

Chapter 4

4. In Silico Genome-Scale Reconstruction and Validation of the *Corynebacterium glutamicum* Metabolic Network

(Paper A)

Kjeld Raunkjær Kjeldsen[1,2], Jens Nielsen[2,3]

[1]Center for Microbial Biotechnology, DTU Biosys, Technical University of Denmark, DK-2800 Lyngby, Denmark; [2]Agro&Ferm A/S, Limfjordsvej 4, DK-6715 Esbjerg N, Denmark. [3]Corresponding author; telephone: (+45) 45252696; Fax: (+45) 45884148; E-mail: jn@biocentrum.dtu.dk

This manuscript have been accepted for publication in "Biotechnology and Bioengineering"

Abstract

A genome-scale metabolic model of the Gram-positive bacteria *Corynebacterium glutamicum* ATCC 13032 was constructed comprising 446 reactions and 411 metabolites, based on the annotated genome and available biochemical information. The network was analyzed using constraint based methods. The model was extensively validated against published flux data, and flux distribution values were found to correlate well between simulations and experiments. The split pathway of the lysine synthesis pathway of *C. glutamicum* was investigated, and it was found that the direct dehydrogenase variant gave a higher lysine yield than the alternative succinyl pathway at high lysine production rates. The NADPH demand of the network was not found to be critical for lysine production until lysine yields exceeded 55% (mmol lysine · (mmol glucose)$^{-1}$). The model was validated during growth on the organic acids acetate and lactate. Comparable flux values between *in silico* model and experimental values were seen, although some differences in the phenotypic behavior between the model and the experimental data were observed.
Keywords: *Corynebacterium glutamicum*; Genome scale metabolic model; L-lysine production

Introduction

The Gram-positive bacterium *Corynebacterium glutamicum* is used for the industrial production of different amino acids, of which L-lysine and L-glutamate are produced in the largest quantities with annual production levels of 800,000 ton and 1,300,000 ton respectively. Due to its commercial importance, this organism has received at lot of attention, and significant resources have been invested in the development of efficient producer strains. Various approaches have been pursued in order to improve product yield and productivity. Mutagenesis and screening have been used with success, but with the development of molecular biological methods metabolic engineering has been applied extensively also (Cremer et al., 1991; Eggeling et al., 1998). Furthermore, fluxomics (Wittmann and Heinzle, 2002), metabolomics (Strelkov et al., 2004) or a combination of methods (Krömer et al., 2004) have been used to characterize engineered strains. These studies, often where different parts of the cell have been studied separately, have given a lot of insight into *C. glutamicum*. However, with the development of high-throughput technologies it is believed that a more holistic understanding of the whole system is essential to help extracting knowledge from these data (Palsson, 2000), consequently allowing a better identification of targets improving yields and productivity. The final goal in this respect is to develop an *in silico* model combining kinetic information about specific reactions. Due to the complexity of biology and the lack of kinetic information, such a model has not yet been constructed for *C. glutamicum* or any other organism.

The first step towards a complete model of an organism is a genome-scale metabolic model where the annotated genome is used in combination with available experimental data to create a list of reactions that then forms the basis for a stoichiometric model. This type of models have already been constructed for a number of species such as *Saccharomyces cerevisiae* (Förster et al., 2003), *Escherichia coli* (Reed et al., 2003), *Lactococcus lactis* (Oliveira et al., 2005), *Staphylococcus aurerus* (Heinemann et al., 2005), *Streptomyces coelicolor* (Borodina et al., 2005), *Helicobacter pylori K* (Schilling et al., 2002), *Haemophilus influenzae* (Schilling and Palsson, 2000), *Methanosarcina barkeri* (Feist et al., 2006) and *Lactobacillus plantarum* (Teusink et al., 2006). Besides from a convenient overview of the organism and its capabilities, stoichiometric models can in some cases be used to predict phenotypic behavior during different environmental and genetic conditions (Edwards and Palsson, 2000; Edwards et al., 2001; Oliveira et al., 2005), and can directly be used to test biological hypotheses (Patil et al., 2004). Stoichiometric genome-scale

models can be combined with data from high-throughput techniques such as transcriptomics (Covert et al., 2004; Åkesson et al., 2004) or fluxomics (Herrgård et al., 2006) and combining this with constraint-based methods (Price et al., 2003) the prediction power of the models can be improved.

In this paper we present the first step towards a systematic biological model of *C. glutamicum*. A genome-scale metabolic model of the organism is constructed from the annotated genome of the wild type strain ATCC 13032, available literature and own experimental observations. The model is validated against data found in literature under different conditions such as different biomass production burdens and growth on different carbon sources.

Materials and Methods

The interconnectivity of metabolites in a network of biological reactions is given by reaction equations defining the stoichiometric conversion of substrates into products for each reaction (Schilling et al., 1999). Reactions are enzymatic reactions converting a substrate into a product, or transport reactions moving metabolites between different parts of the system, intracellular, extracellular or between different compartments. Active reactions in the biological system are fluxes serving to dissipate or generate metabolites. Following the law of conservation of mass, a balance describing the reaction rate of a particular metabolite through a particular reaction can be written as (Stephanopoulos et al., 1998):

(eq. 1) $$0 = r_{met} = S \cdot v$$

The stoichiometric matrix **S** is an *m x n* matrix where *m* is the number of metabolites and *n* is the number of reactions or fluxes taking place within the metabolic network. The vector **v** refers to the reaction rate of each individual reaction or flux in the metabolic network. Metabolic models usually also include constraints, which will lead to the definition of a solution space in which the solution to the network equation must lie (Price et al., 2003). Constraints in a model are dealt with by introducing constraint equations to the metabolic network, which can assign a direction of a given reaction (reversibility or irreversibility) according to known thermodynamic constraints. These equations are typically of the form $\alpha_i \leq v_i \leq \beta_i$, where α_i and β_i are the feasible lower and upper limit of the reaction rate v_i, respectively. In practice the upper and lower limits are set to arbitrarily high values when a reaction is reversible without any regulation, whereas α_i is set to zero when a reaction is irreversible. Constraint reactions can also be used to set a maximum flux through a given reaction based on biochemical information.

The above described equation system is usually underdetermined due to the fact that the number of unknown fluxes exceeds the number of metabolites in the network, leading to a number of possible solutions, and hence, no unique solution (Bonarius et al., 1997). To cope with this linear programming/optimization can be used to maximize (or minimize) for a certain metabolite objective (e.g. growth or product formation) and seeking its maximal (or minimal) value within the stoichiometrically defined domain. This procedure is often referred to as flux-balance analysis (Palsson, 2006). In the present paper flux-balance analysis is carried out using linear optimization, where the objective functions used are optimizing for either growth or lysine production. Flux-balance analysis was performed using the in-house software BioOptv4.9 employing LINDO API for linear optimization. BioOptv4.9 is available by contacting the corresponding author.

Construction of genome-scale metabolic model

Genome scale metabolic models can be constructed using data from different sources. In this work the model was constructed in three steps: (i) construction of a crude model consisting of mass balances for catabolic reactions leading to the formation of metabolites; (ii) defining the reactions involved in polymer and biomass synthesis, and energy requirements; (iii) complete the metabolic network by adding missing reactions, and to revise the reactions added in the first step with respect to physiochemical conditions (reversibility of reactions).

Table 4.1: Metabolites considered being required for biomass in *C. glutamicum.*

Protein (0.52 protein g/g DCW)	mmol/g protein
Alanine	1.268
Arginine	0.361
Aspartate	0.368
Aspargine	0.368
Cysteine	0.084
Glutamate	1.044
Glutamine	0.650
Glycine	0.671
Histidine	0.128
Isoleucine	0.359
Leucine	0.669
Lysine	0.355
Methionine	0.144
Phenylalanine	0.244
Proline	0.303
Serine	0.467
Threonine	0.519
Tryptophan	0.052
Tyrosine	0.148
Valine	0.520
ATP (polymerization energy)	38.44
DNA (0.01 g DNA/g DCW)	mmol/g DNA
dAMP	0.748
dCMP	0.871
dTMP	0.748
dGMP	0.871
ATP (polymerization energy)	4.44

RNA (0.05 g RNA/g DCW)	mmol/g RNA
AMP	0.69
GMP	1.01
CMP	0.70
UMP	0.70
ATP (polymerization energy)	1.24
Lipids (0.13 g Lipids/g DCW)	
Mycolic acids (0,102 g Mycolic acids/ g DCW)	mmol/g mycolic acids
Trehalose monocyrynomycolate	0.061
Trehalose dicyrynomycolate	0.043
Free Mycolic Acids	1.875
Phospholids (0.028 g phospholipids/g DCW)	mmol/g phospholipids
Phosphatic acid	0.033
Phosphatidylglycerol	1.133
Cardiolipin	0.007
Phosphatidyllinositol	0.042
Phosphatidyllinositol mannoside	0.065
Cell Wall Carbohydrates (0.19 g Cell Wall Carbohydrate/g DCW)	
Peptidoglycan (0.095 g peptidoglycan/g DCW)	mmol/g peptidoglycan
N-acetylmuramic acid	1.026
N-acetylglucosamine	1.026
L-alanine	1.026
Diaminopimelinic acid	1.026
D-glutamate	1.026
D-alanine	2.052
ATP (polymerization energy)	5.129
Arabinogalactan (0.095 g Arabinogalactan/g DCW)	mmol/g arabinogalactan
Arabinose	4.650
Galactose	0.498

First step was carried out based on the published annotated genome (Kalinowski et al., 2003). The KEGG database (http://www.genome.ad.jp/kegg/) and the BioCyc database (http://www.biocyc.com/) were used in this process, because these databases present annotation of each gene linked to its function. In addition, these databases give a graphical overview of the metabolism of the organism. Data for step two was found in literature from different sources, as shown in the supplementary material (Appendix I). Maintenance requirements for the model was determined changing the ATP demand (ATP used for maintenance and assembling of

macromolecules) for maximal biomass yield on substrate (Y_{sx}) fitted experimental values. The third step was done by reviewing biochemical literature for *C. glutamicum* or by using own unpublished observations.
The complete model including a list of references used for the re-construction is available as supplementary files (Appendix I).

Biomass synthesis equations

For genome scale metabolic models the equations defining the biomass synthesis in a genome-scale model are important. The biomass-equation consists of reactions converting single molecules into macromolecules, which are building blocks of the biomass. For each macromolecule an equation was formulated based on literature, and energy consumption associated with the assembling reactions was also included (see supplementary material – Appendix I). The representative averaged biomass composition of a *C. glutamicum* strain can be seen in table 4.1. Since no data on energy requirements for polymerization of macromolecules in *C. glutamicum* could be found, these values were approximated using values for *E. coli* (Ingraham et al., 1983). The macromolecule components were lumped in a final biomass assembly reaction based on their weight fraction of the biomass. In our model we included protein, DNA, RNA and cell-wall components as macromolecules. The macromolecular composition of biomass was taken from Cocaign-Bousquet et al., (1996) whereas composition of each macromolecule was taken from different references (see supplementary material – Appendix II). This same biomass composition was used for all our simulations.

Macromolecular composition

Data for the amino acid composition of the protein fraction in *C. glutamicum* was taken from Cocaign-Bousquet et al., (1996). The composition of the DNA was calculated based on G+C-content of the genomic sequence of *C. glutamicum* ATCC 13032 (Kalinowski et al., 2003). It was assumed that RNA consisted of 5% mRNA, 75% rRNA and 20% tRNA (molar). The nucleotide composition of mRNA was taken as for genomic DNA. The nucleotide composition of rRNA was calculated from the sequences of 16S, 23S and 5S ribosomal RNA units. And finally tRNA composition was found from sequences of leucine and glycine transporting RNAs. Sequences were downloaded from GenBank (http://www.ncbi.nlm.nih.gov).

The chemical structure of the *C. glutamicum* cell-wall has been intensively studied and consists of a complex network of the polysaccharide peptidoglycan covalently linked to another complex polysaccharide arabinogalactan, which is further esterified with mycolic acids (Puerch et al., 2001). Associated with, but not covalently linked to this fraction a number of lipids are also connected to the cell-wall, the more abundant being phospholipids and trehalose mycolates (Daffé, 2005). For simplification the cell-wall components mentioned above have been divided into individual lumped reactions which are part of the biomass equation based on their fraction.
The plasma membrane of *C. glutamicum* mainly consists of polar lipids, of which phospholipids are the dominant type. In *C. glutamicum* the major phospholipids constituents are oleic acid (18:1) and palmic acid (16:0), which contribute to more than 90% of the lipid pool of the phospholipids (Collins et al., 1982b; Hoischen and Krämer, 1990). In addition to these fatty acids, myristic acid (14:0), pentadecanoic acid (15:0), stearic acid (16:1) and tuberculostearic acid (18:0) are present in

minor quantities (Collins et al., 1982b). Based on the published data of *C. glutamicum* a lumped reaction with molar ratios of each individual phospholipid was made.

The stoichiometric equation formation of peptidoglycan was described by a lumped reaction. The molar composition was estimated based on data from different sources (Daffé, 2005; Keedie and Cure, 1978). Also the arabinogalactan fraction was described by a lumped reaction due to its complexity. Data used was taken from (Puerch et al., 2001).
The mycolic acid synthetic pathway is not well characterized, although some of the genes involved have been identified (Brand et al., 2003). Based on structural considerations it has been postulated that mycolic acids are synthesised by a condensation and decarboxylation reactions (Daffé, 2005). The "free" mycolic acids are known to form esters with trehalose in order to form mycolates were the mycolic acids are bound within the cell wall. The majority of the mycolic acid fraction consists of the 32:2 3OH and 34:1 3OH mycolic acids (Collins et al., 1982a). Other mycylic acids identified are 32:0, 34:0, 36:1 and 36:2 (Jang et al., 1997). In general two types of mycolates are considered to be present in the *C. glutamicum* cell wall: trehalose monocorynemycolate (TMCM) and trehalose decorynemycolate (TDCM) (Daffé, 2005), both of which was included in the model. Data from Daffé (2005) was used to make a lumped reaction for the mycolic acid fraction of the cell.

Energy requirements for growth and maintenance

In addition to the stoichiometry of each individual macromolecule and the overall biomass assembling reaction, the stoichiometry of the growth and non-growth associated energy connected to biomass is important in a metabolic model. In our model we used the value of 29.2 mmol ATP · $(g\ biomass)^{-1}$ for growth associated ATP demand as estimated by Cocaign-Bousquet et al. (1996) based on experimentally determined macromolecule composition of *C. glutamicum* and known anabolic pathways. ATP demand for growth associated maintenance reactions was found by fitting the biomass yield to experimental value of 0.61 g biomass· $(g\ glucose)^{-1}$ found by Cocaign-Bousquet et al. (1996). ATP requirements for growth were kept constant for biomass synthesis for all simulations, as generally done in flux-balance analysis simulations.

Simulation methods

As mentioned above, linear optimizations were conducted using the BioOptv4.9 software. Split points in the network solutions were checked to see if the results were unique, or if other optima were possible. Results presented in this paper were unique, unless else is mentioned. The NADPH generating reaction catalyzed by malic enzyme (EC 1.1.1.40) and the reaction decarboxylating oxaloacetate catalysed by oxaloacetate decarboxylase (EC 4.1.1.13) were constrained to zero when glucose was used as carbon source based on biochemical evidence (Petersen et al., 2000).

Results & Discussion

Reconstruction of the Corynebacterium glutamicum metabolic network:

We constructed a genome scale model of the *C. glutamicum* metabolic network (for statistics see table 4.2). The constructed metabolic network consisted of 446 reactions, all of which were unique (iso-enzymes were removed), which represent 15% of the protein encoding genes identified in *C.*

glutamicum (Kalinowski et al., 2003). 411 metabolites were involved in the metabolic network of which 55 were involved in transport reactions, and had an internal equivalent (Table 4.2).

Energy requirements for biomass formation

Macromolecule composition of biomass was taken from Cocaign-Bousquet et al. (1996). ATP demand for biomass assembly was set to 29 mmol · (g biomass)$^{-1}$ (Cocaign-Bousquet et al., 1996), and ATP demand for maintenance was adjusted so the maximum biomass yield (g biomass · (g glucose)$^{-1}$) was 0.61 (Cocaign-Bousquet et al., 1996). The ATP demand for maintenance was found to be 19 mmol · (g biomass)$^{-1}$, which is higher than values earlier reported in literature (1.8-9.2 mmol ATP (g biomass)$^{-1}$) (de Graaf, 2000; Verela et al., 2004). The high ATP demand for maintenance may be due to an underestimated growth associated ATP demand. Another reason may be that the composition of the respiratory chain affects the P/O-ratio and hence the ATP yield (Bott and Niebisch, 2003). When maximizing for growth the *in silico* model uses the most efficient oxidative phosphorylation, which may not be the case in reality.

Table 4.2: Statistics for the genome scale model

Total Genes in *C. glutamicum* (ORFs)	**3002**
Reactions in genome scale model	**446**
Biochemical evidence	213
Clear function (functional annotation derived from probable homologues)	209
Tentative function (functional annotation derived from tentative homologues)	22
Putative function (added reactions to complete network)	2
Active reactions during growth on glucose	**199**
Metabolites in genome scale model	**411**
Internal metabolites	356
External metabolites (metabolites involved in transport reactions)	55

Model validation

Simulations for model validation were carried out according to what is described in the section "simulation details". Simulations were done by maximizing for lysine production and constraining biomass production.

Pentose phosphate pathway (PPP) fluxes

The genome-scale metabolic model was validated against published data on metabolic flux distributions during various growth- and lysine production regimes, and with different strains. The publications used for this comparison were Krömer et al. (2004); Wittmann and Heinzle (2001); Wittmann and Heinzle (2002) and Vallino & Stephanopoulos (1993). The data-sets Krömer et al. (2004), Wittmann and Heinzle (2001) and Wittmann and Heinzle (2002) were all based on batch cultivations where flux distributions were determined using ^{13}C-labelled glucose, whereas Vallino & Stephanopoulos (1993) used bioreaction network analysis for estimation of flux distributions.

The individual datasets for the three first references were selected to give the same lysine yields (18%) and three different stains were represented (ATCC 13287, ATCC 21253 and ATCC 21526, respectively). The fourth data-set from Vallino and Stephanopoulos (1993) was selected to have a data point at a higher lysine yield (30%). All the flux data are from balanced growth conditions, and details on how the fluxes were found are given in the original papers. *In silico* simulations were carried out yielding lysine conversion yields in the range of the values found in the published data, in this case being 18% (mmol lysine · (mmol glucose)$^{-1}$) and 30%, respectively. In all the experiments used to validate the model the biomass yields were lower than the *in silico* model (in same order as above: 0.38; 0.33; 0.26 and 0.27 g biomass · (g glucose)$^{-1}$)) which could partly be explained by the fact that by-products in all cases were produced, which were not the case for simulations. Moreover, stoichiometric parameters such as the P/O ratio and ATP yields and maintenance requirements may change due to different strain backgrounds and growth conditions. Although all three references of Krömer et al. (2004), Wittmann and Heinzle (2001) and Wittmann and Heinzle (2002) showed lysine yields of 18%, some variation in fluxes from reference to reference were seen (Figure 4.1; 3 first fluxes from the top). At the level of glucose-6-phosphate where this compound is converted either towards the pentose phosphate pathway (PPP) or the glycolysis a 12% absolute difference was seen (59% to 71% towards PPP) between the fluxes in the experiments. The *in silico* model predicted a 61% flux towards PPP at this split, which correlated well with two of the experiments (Figure 4.1) (Krömer et al., 2004; Wittmann and Heinzle, 2002), whereas the flux was higher (71%) for the data of Wittmann and Heinzle (2001) (Figure 4.1). For the three experiments the tricarboxyic acid (TCA)-flux ranged from 46% to 68% whereas the model simulated value was 51% (Figure 4.1).

When simulations were carried out fitting the data of Vallino and Stephanoupoulos (1993) (Figure 4.1), a higher flux through the PPP was seen for the model (84%) than it was the case for literature values (69%). Instead Vallino and Stephanopoulos (1993) saw a higher flux through the TCA (46%) when compared to the *in silico* model (36%). Instead the anaplerotic flux from pyruvate/phosphoenolpyruvate into oxaloacetate was higher for the model (48%) than for the data of Vallino and Stephanopoulos (1993) (41%). Although differences were seen between the published data and the *in silico* model, fluxes were all in the same range, and coherence between experimental data and model data could be recognized.

Data from Vallino and Stephanoupoulos (1993) was taken at early exponential phase, just as lysine synthesis had initiated after the depletion of threonine, and with a high growth rate. Looking at data from the same reference for late exponential phase, the difference between model predictions and observed values were bigger (data not shown), even though lysine yields were only marginally changed. The PPP-flux decreased to 41% and the TCA-flux increased to 70% (Vallino and Stephanopoulos, 1993). The change in fluxes was thought to be due to a decrease in growth rate, which were followed by ATP excess (Vallino and Stephanopoulos, 1993). The excess ATP needed to be consumed i.e. through futile cycles, which lead to a redirection of carbon from the PPP towards the TCA cycle due to biological regulatory issues. Such changes in metabolism due to biochemical regulation can not be predicted by the model, since it doesn't take biological and biochemical regulations into account.

Glycolysis fluxes

Model flux values through the glycolysis were in general consistent with observed experimental values. A higher drain of carbon from glycolysis was seen in data from Krömer et al. (2004) when compared to model values and other experimental values. This can partly be explained by by-

product formation, where significant amounts of extra-cellular glycerol and dehydroxyacetone phosphate were observed (Krömer et al., 2004).

Relationship between PPP- and TCA-fluxes during lysine production

It is known that the relationship between the TCA and the PPP is important for lysine production since a high reaction rate of the PPP is necessary to support NADPH generation when lysine synthesis is high. A tendency for this correlation can be seen from experimental data from literature when TCA- and PPP-fluxes at different lysine yields are compared (Figure 4.3; symbols), a correlation which have also been suggested by Kelle et al. (2005). Such a correlation is also predicted by the model (Figure 4.3; lines). In general the TCA-flux was higher for the experimental values when compared to the model, and the PPP-fluxes for the experimental data presented here were in most cases lower than values for the corresponding *in silico* simulations. The reason for the generally lower TCA-fluxes for the *in silico* model when compared to experimental data was the higher anaplerotic netflux, which from a stoichiometric point of view is optimal for lysine production. The *in silico* model will per definition chose this pathway which may not be the case in reality, where biological regulation will affect the operation of the biological network.

A bend of both the TCA-flux and the PPP-flux curves were seen for the *in silico* flux data when lysine yield exceeded 55% (Figure 4.3). At this point a flattening of the curves was observed (the TCA-flux decreased at a lower rate and the PPP-flux increased at a lower rate). This metabolic change is discussed further in the next section. Some of the differences in flux distributions between the experiments mentioned above can probably be explained by different strain backgrounds, and different cultivation conditions.

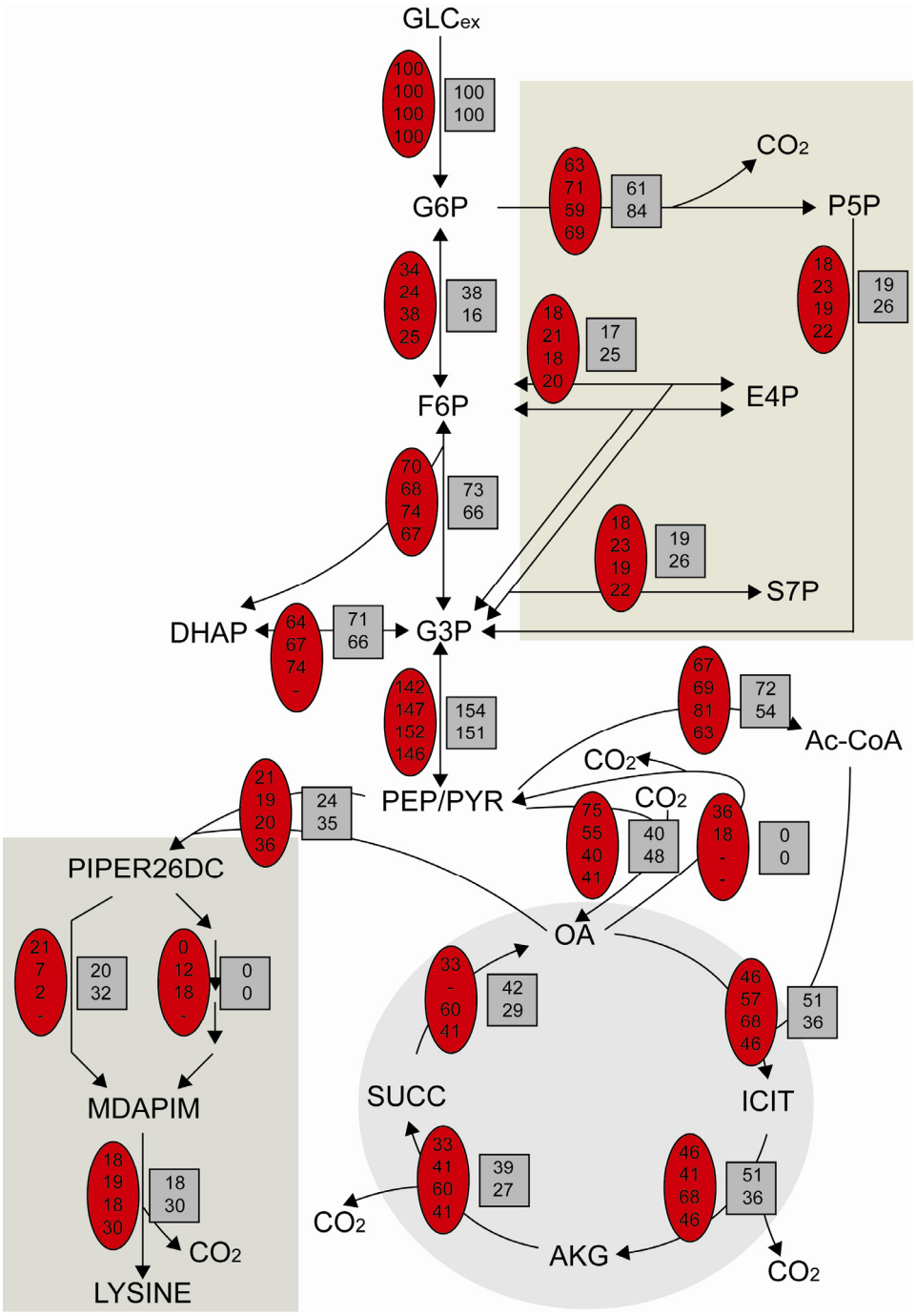

Figure 4.1: Flux distribution values for genome-scale model simulations (shown in grey boxes) and literature values (shown in red ovals) found by metabolic flux analysis. Flux values are expressed as molar percentage of the specific uptake of glucose. When no flux was available from the data the symbol (-) was used. Y_{sx} values for the model simulations was constrained to 0.48 and 0.40 (g biomass · (g glucose)$^{-1}$), from top and down. Literature values were taken from (from top and down): Krömer et al. (2004); Wittmann and Heinzle (2001); Wittmann and Heinzle (2002) and Vallino and Stephanopoulos (1993). Abbreviations: GLC_{ex}: extracellular glucose; G6P: glucose-6-phosphate; F6P: fructose-6-phosphate; P5P: pentose-5-phosphate; E4P: erythose-4-phosphate; S7P: sedoheptulose-7-phosphate; DHAP: dihydroxyacetone phosphate; G3P: glyceraldehyde phosphate; PEP: phosphoenolpyruvate; PYR: pyruvate; Ac-CoA: acetyl CoA; ICIT: isocitrate; AKG: α-ketogluterate; SUCC: succinate; OA: oxaloacetate; PIPER26DC: L-piperidine 2,6-dicarboxylate; MDAPIM: meso-2,6-diaminopimelate.

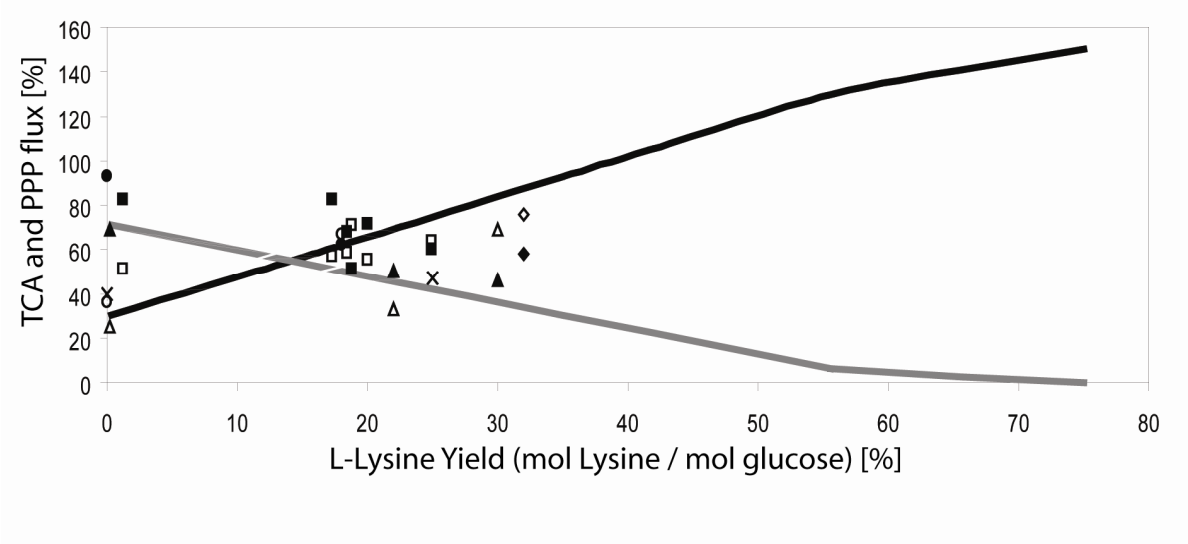

Figure 4.3: Flux through the TCA cycle and the Pentose phosphate pathway (PPP) at different lysine conversion yields. Black line: PPP flux for *in silico* organism; Grey line TCA flux for *in silico* organism. Open symbols are PPP fluxes and filled symbols are TCA fluxes from experimental metabolic flux analysis from different references. Squares: Wittmann and Heinzle (2002); diamonds: Marx et al. (1999); Triangles: Vallino et al. (1993); Circles: Marx et al. (1997); Crosses: PPP data from Sonntag et al (1995).

Maximizing for lysine production

Simulations for lysine production were done by maximizing for lysine production as the objective function, and constraining biomass production at different levels (see text for details). Simulations were carried out according to what is described in the section "simulation details".

Negative effect of ATP excess on lysine production

The maximum lysine yields were found constraining the biomass yields at different levels using the genome-scale model (Figure 4.4A and 4.5A). The model predicted a maximum lysine yield of 75% when no biomass was produced (Figure 4.4A and 4.5A), which is the maximum theoretical value for this organism (Stephanopoulos and Vallino, 1991). As biomass synthesis increased towards the maximum, lysine yields decreased (Figure 4.4A and 4.5A). The decrease observed was not linear as a bend of the curve was observed when the lysine yield was around 55%, and Y_{sx}-values were 20%, corresponding to a decreasing Y_{xp}-value: less lysine was produced per cell unit (Figure 4.4A). Also when plotting the TCA- and PPP-flux data versus the lysine yield, a bend is observed at a yield of 55% (Figure 4.3). This shift in the central metabolism was investigated, and it was found that the change was due to a change in ATP availability, where the regime was changed from an ATP limiting condition to an ATP excess condition. During the synthesis of lysine in *C. glutamicum*, a net ATP-production is seen. ATP is consumed for biomass related reactions, however when the ATP produced during lysine production exceeds the ATP demand for biomass synthesis, ATP is in

excess. The way the model copes with this, is to burn ATP in a number of futile cycles, of which an example can be recognized in figure 4.5A, bottom flux, where a futile cycle between the C_3-pool (pyruvate) and the C_4-pool (oxaloacetate) can be recognized with the net reaction of ATP → AMP + Pi + Pi. This change from ATP limitation to ATP excess changes the regime and hence can explain the changes observed in figure 4.5A and figure 4.3.

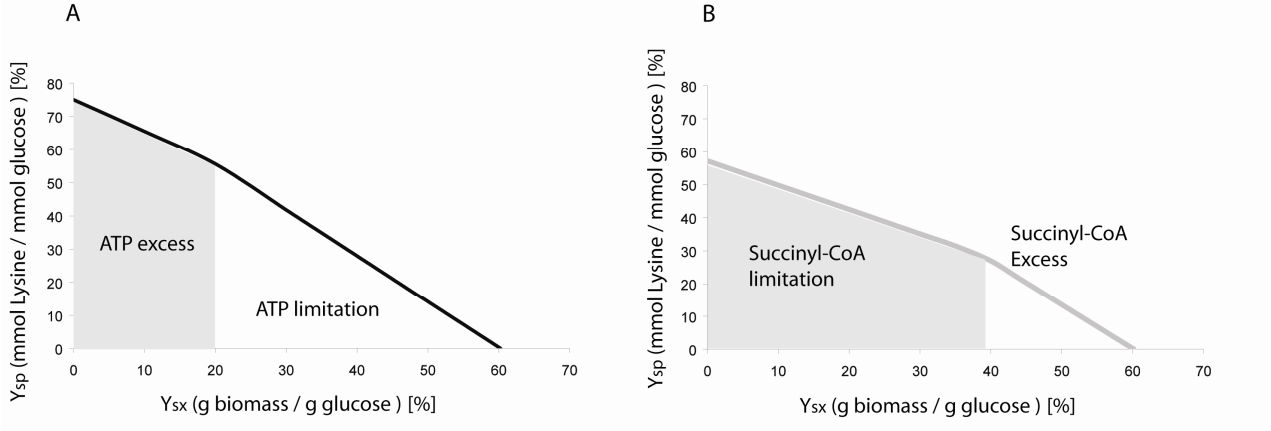

Figure 4.4: Simulation results for *in silico* model when maximizing for lysine production and constraining biomass production. Results presented as lysine yield (Y_{sp}) as a function of the biomass yield (Y_{sx}) both expressed as percentage. **A)** *In silico* model with dehydrogenase branch 100%. **B)** *In silico* model with dehydrogenase branch constrained to zero.

Split in the lysine synthetic pathway and its effect on lysine yield

In the lysine synthesis pathway of *C. glutamicum* two pathways are possible. Either the direct dehydrogenase variant (*ddh*), or the succinylase variant which involves four reactions (Schrumpf et al., 1991). When using the genome-scale model for maximizing for lysine production the dehydrogenase variant is always preferred. This is due to the fact that the succinylase variant consumes the intermediate succinyl-CoA, which is an intermediate of the TCA cycle, requiring this to be active during lysine synthesis, which is not the case when the dehydrogenase variant is used. The exclusive use of the dehydrogenase variant is however far from reality based on experimental data, which shows that both variants most often are used at different ratios. Experiments have shown that the ratio between the two variants varies between a ratio higher than 2:3 for the succinylase variant with values ranging from 67-68% (Sonntag et al., 1993) to 72-89% (Wittmann and Heinzle, 2002), and with the dehydrogenase variant being the dominant pathway with values of 63% (Wittmann and Heinzle, 2001) using this pathway. The flux ratio between the two variants was even shown to change through a fermentation starting with a 72% flux through the dehydrogenase variant, decreasing to around zero at the end of the fermentation (Sonntag et al., 1993). This difference in the ratio of these two pathways was also seen for the experiments selected for the

validation (Figure 4.1). Either the dehydrogenase variant was used alone (Figure 4.1; top), or a combination of the dehydrogenase variant and the succinyl variant with different ratios was seen (Figure 4.1; 2nd and 3rd value from the top). As mentioned earlier a significant difference was seen between the TCA-fluxes for the experiments shown in figure 4.1. In addition it can be seen that for the first three experiments (Krömer et al., (2004); Wittmann and Heinzle, (2001); Wittmann and Heinzle, (2002)), the flux through the TCA cycle and the route which was used through the lysine pathway (dehydrogenase variant or succinylase variant) correlated, so when a high flux through the succinylase variant was seen, a higher TCA-flux could be observed. This observation may explain some of the differences seen between the TCA-fluxes and the anaplerotic netfluxes (Figure 4.2). Based on these observations it was considered relevant to make simulations constraining the dehydrogenase variant to zero, in order to investigate the effect of this pathway on lysine yields.

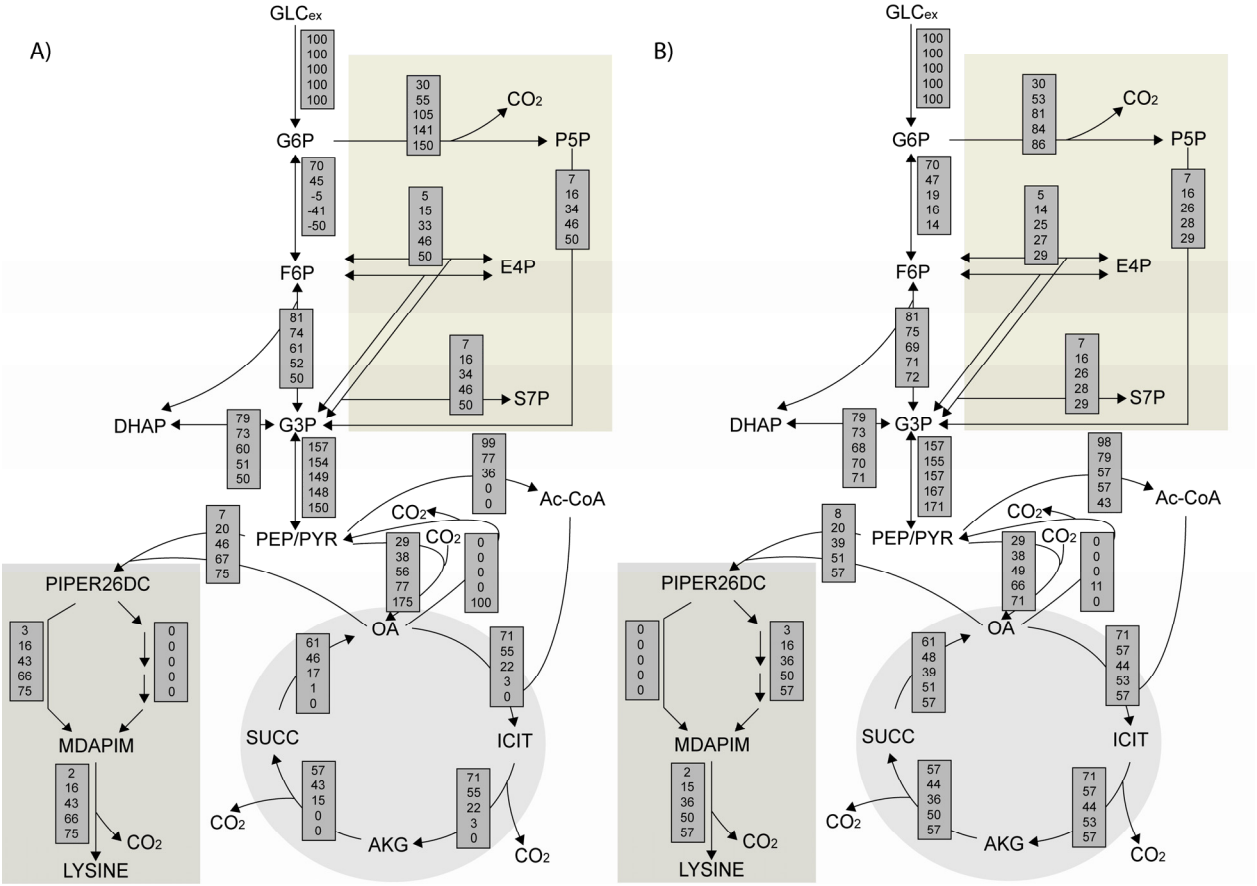

Figure 4.5: Flux distribution values (shown in grey boxes) for *in silico* simulations maximizing for lysine production constraining biomass production at different levels. Fluxes expressed as molar percentage of specific glucose uptake. Biomass yield (Y_{sx}) constrained to (from top and down) 0.60, 0.50, 0.30, 0.10 and 0.0 (g biomass · (glucose)$^{-1}$. **A)** Direct dehydrogenase variant of lysine synthesis pathway used. **B)** Succinylase variant of lysine synthesis pathway used. Abbreviations see figure 1.

From these simulations it was seen that the maximum lysine yield dropped to 57%, when no biomass was produced (Figure 4.5B). The simulation results showed that as the carbon demand for biomass production was increased, the difference in lysine yields decreased, and at Y_{sx} values higher than 40% (g biomass · (g glucose)$^{-1}$) the maximum theoretical lysine yields were only marginally different, with the dehydrogenase variant being the most efficient pathway (Figure 4.4A and 4.4B). At high growth rate the TCA activity required for biomass synthesis was sufficient to

produce succinyl-CoA for lysine production via the succinyl branch. The succinylase variant of the lysine synthetic pathway is competing for succinylase-CoA with the TCA reaction succinyl-CoA synthease converting succinyl-CoA to succinate with the formation of an ATP. The marginally higher lysine yield for the dehydrogenase variant during high biomass formation could be explained by the missing ATP from the succinyl-CoA synthease reaction. Furthermore, it was seen that the decrease in the maximum lysine yield was due to the requirement for a higher activity of the TCA to support lysine synthesis with succinyl-CoA (Figure 4.5). As a consequence more CO_2 was produced and carbon was lost. For simulations where the biomass formation was constrained to zero, the flux through the PPP was significantly lower (86%) for the *ddh*-negative strain (Figure 4.5B), when compared to simulations where the dehydrogenase variant was used (150%) (Figure 4.5A), and for the latter a cycling of the PPP was seen. The loss in carbon is due to the fact that the PPP is more efficient in NADPH generation (2 NADPH per CO_2) than the TCA cycle (1 NADPH per CO_2). If the efficiency of NADPH generation for the PPP was set to 1 mole of NADPH per CO_2, the maximum lysine yield was found to be 57% as it was the case for the *ddh*-negative *in silico* strain (data not shown), indicating that the difference seen on the maximum yield between the two strains could be explained entirely by the increased activity of the TCA cycle. For the *ddh*-negative *in silico* strain a bend of the curve was seen (Figure 4.4B; grey line), as it was observed for simulations using the dehydrogenase branch, although the bend was seen earlier. The explanation for this bend was however different. In the case of the *ddh*-negative strain it was due to a limitation of succinyl-CoA, and not related to ATP excess as it was the case where the dehydrogenase variant was exclusively used. Based on these results, the *ddh*-gene looks like a promising target for overexpression by metabolic engineering. *ddh* has already been investigated as a potential bottleneck in lysine production. The results have been inconsistent since both positive effects (Schrumpf et al., 1991) (2-5-fold decrease in lysine accumulation when *ddh* was knocked out) and negative effects (Eggeling et al., 1998) (10-30% decrease by up-regulation of *ddh*) on lysine production by altering the flux through this pathway have been seen. For the latter no growth rate was reported for the *ddh*-up-regulated strain. However, for the parental strain a specific growth rate of 0.27 hr^{-1} was reported. If it is assumed that the *ddh*-up-regulated strain had the same specific growth rate it is possible that TCA activity was sufficient to support the succinylase variant with succinyl-CoA, hence abolishing the potential positive effect of the genetic manipulation. Based on the reported simulations and the experimental work done so far on this target it would be interesting to investigate this pathway more intensively, since there is - from a theoretical point of view - a large potential for improving lysine production, at least when we are getting closer to the theoretical maximum for this organism.

NADPH or NADH dependent Glutamate Dehydrogenase

The simulation experiments comparing two different glutamate dehydrogenases were carried out according to what is described in the section “simulation details”, except that the NADPH-dependent glutamate dehydrogenase (*gdh*) was replaced with a NADH-dependent glutamate dehydrogenase in some cases. The objective function used was maximization for lysine production and biomass was constrained to different levels as described in the text.

Marginal improvement in lysine production, but significant redistribution of central carbon metabolis, as an effect of NADH-dependent glutamate dehydrogenase.

For the synthesis of one mole of lysine four molecules of NADPH is consumed. For this reason the NADPH supply in *C. glutamicum* has received a lot of attention. Marx et al. (1999) addressed this challenge by replacing the NADPH-dependent glutamate dehydrogenase (*gdh*) with an NADH-dependent *gdh*. However, this change in the metabolism of the organism did not result in improved lysine production. Instead significant redistribution of the central metabolism was observed, consequently leading to increased biomass production and lower lysine yield (Marx et al., 1999). The study made by Marx et al. (1999) was used as a case study for the genome-scale model.
Simulation experiments were carried out replacing the NADPH-dependent *gdh*-reaction with an NADH-dependent *gdh*-reaction, and the results were compared to "wild type" simulations with a NADPH-dependent *gdh*-reaction. Simulation data was further compared to experimental data.

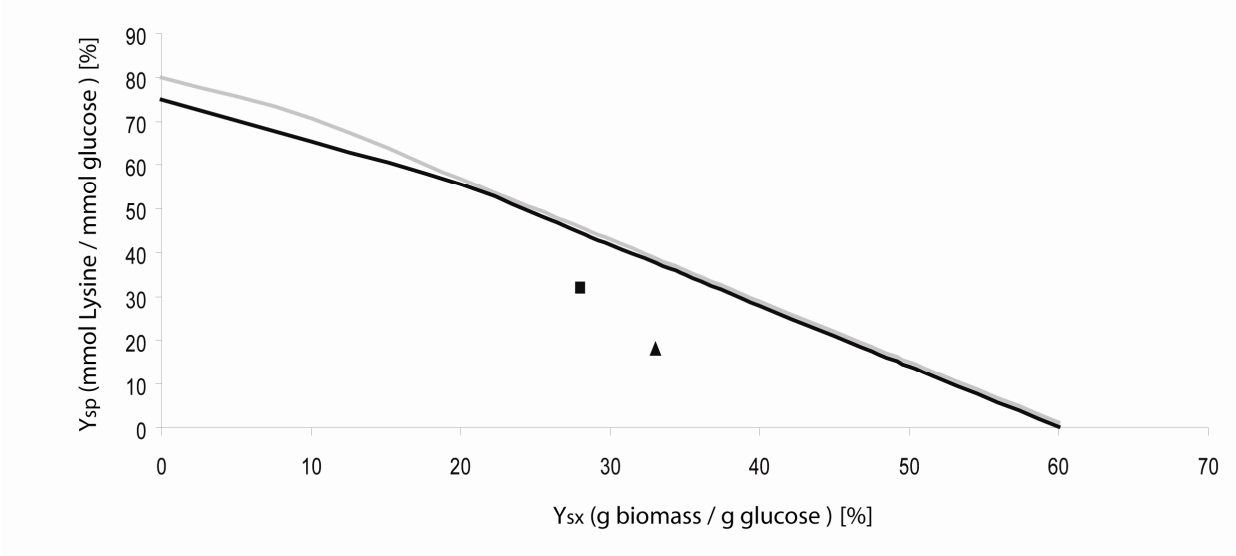

Figure 4.6: Simulation results maximizing for lysine production constraining biomass formation at different levels. Results shown are *in silico* strains (Black line: NADPH dependent glutamate dehydrogenase (*gdh*); Grey line: NADH dependent *gdh*) and experimental data from Marx et al. (1999) (square: NADPH-dependent *gdh*; Triangle: NADH-dependent *gdh*).

Simulation experiment data showed general higher lysine production with the NADH-dependent *gdh*. However, the effect was only marginal when the biomass yield exceeded Y_{sx}-values of about 0.15 g biomass · (g glucose)$^{-1}$ consumed (Figure 4.6), which is typically the case in real fermentations. The maximum theoretical yield was increased to 80% (Figure 4.6). As it was seen in the work of Marx et al. (1999), the model predicted a higher lysine yield (45%: Figure 4.7A) for the *in silico* strain carrying the NADPH dependent *gdh*-reaction, than for the strain substituted with the NADH- dependent *gdh*-gene (39%: Figure 4.7B) when the biomass formation was constrained at the same values as reported in the experiments (0.28 and 0.33 g biomass · (g glucose)$^{-1}$ for the NADPH-dependent strain and NADH-dependent strain respectively). However, the difference was lower than it was seen in the experimental work (30% for the NADPH-dependent strain and 18% for the NADH-dependent strain).

To eliminate the effect of the different biomass formation that was seen in the experimental work, simulations were carried out constraining the biomass at the same rate (0.30 g biomass · (g glucose)$^{-1}$ consumed). The result gave a higher lysine yield (43%) for the NADH dependent strain when compared to the NADPH dependent strain (42%). This marginal increase

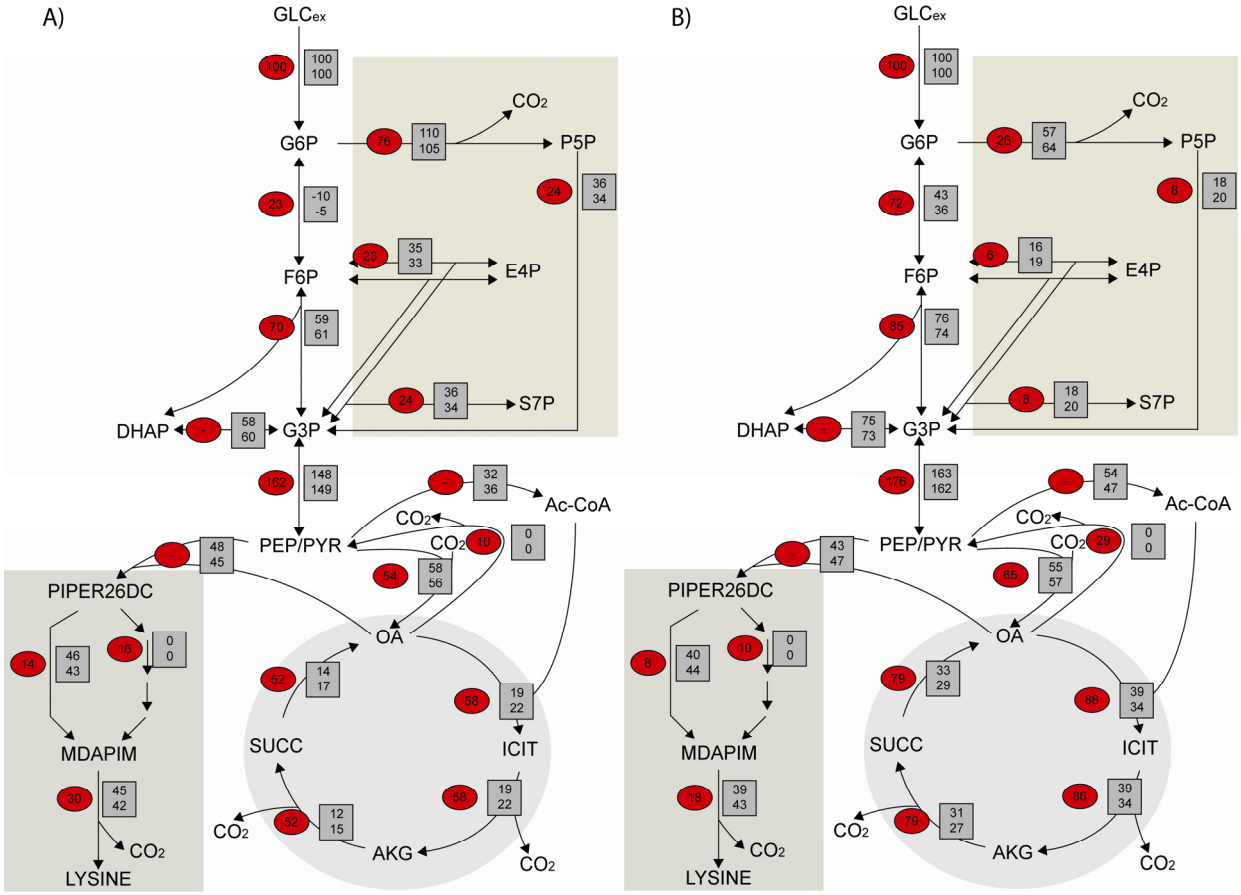

Figure 4.7: Flux distribution values for genome-scale model simulations (shown in grey boxes) and literature values from Marx et al. (1999) found by metabolic flux analysis (shown in red ovals). All fluxes are expressed as molar percentage of specific glucose uptake. Upper simulation value biomass production (Y_{sx}) constrained as experimental value (0.28 g biomass · (glucose)$^{-1}$ for 7A) and 0.33 g biomass · (glucose)$^{-1}$ for **7B**)). Lower simulation value Y_{sx} constained to 0.30 g biomass · (glucose)$^{-1}$ for both 7A) and 7B. **7A)** Flux distribution values for experimental strain or *in silico* strain with NADPH dependent Glutamate dehydrogenase (GDH). **7B)** Flux distribution values for experimental strain or *in silico* strain with NADH dependent GDH. Abbreviations as for figure 1.

was due to a small increase in Y_{sx} for the NADH-dependent strain compared to the NADPH-dependent *gdh*-strain, resulting in more carbon being available for lysine synthesis. The simulation data showed a decreased NADPH generation for the *in silico* strain containing the NADH-dependent *gdh* when compared to the NADPH-dependent strain (161% and 222%, respectively). As expected the moles of NADPH consumed per mole of lysine produced was lowered significantly for the NADH-dependent strain. The minimum theoretical requirement for NADPH was lowered from 4.0 to 3.0 (NADPH per lysine) in the NADH-dependent *gdh* strain (without any biomass production) when compared to the strain with a NADPH-dependent *gdh* (data not shown). Simulations using the same biomass production burdens (0.30 g biomass · g glucose^{-1} consumed) also showed a lower demand for NADPH. The strain with a NADH dependent *gdh* used 3.8 moles of NADPH per mole of lysine produced, whereas the strain with the NADPH-dependent *gdh* used

5.6 moles of NADPH per mole of lysine. The experimental data from Marx et al. (1999) showed a higher NADPH demand per mole of lysine produced (7.7 moles per lysine and 6.6 moles per lysine for the NADH-dependent strain and NADPH-dependent strain, respectively). These higher values were due to the relatively low lysine yields as compared to simulations, and the lower NADPH demand for the NADPH-dependent strain can be explained by the lower flux of metabolites towards biomass formation as compared to the NADH-dependent strain.

In conclusion a significant redistribution of the central metabolism of the *in silico* organism is observed as an effect of the substitution of the NADPH-dependent *gnd* with a NADH-dependent *gnd*. Although the model is unable to predict the precise change in phenotypic behavior (Increased growth and absolute change in carbon flux distributions), the simulation results are surprisingly consistent with the results of Marx et al. (1999). In addition the model predicts a higher lysine production with the NADH-dependent *gdh* strain. However, the improvement is only marginal when the biomass yield exceeds 15% of glucose consumption and an improvement on lysine yield is only seen when this is already high (Y_{sp}> 55%) (Figure 4.6). That NADPH is not limiting on lysine production, and that the central carbon metabolism is able to adjust to NADPH requirements of the cell is now generally accepted based on experimental studies on the regulation of the PPP (Moritz et al., 2000; Vallino and Stephanopoulos, 1994). It would however be interesting to see if this is also the case when lysine yields approaches the theoretical maximum, and some recent results have in fact indicated that this is the case, as it was seen by Becker et al. (2005) where genetic manipulations leading to an increased PPP-flux resulted in increased lysine production.

Growth of *C. glutamicum* on lactate and acetate

Simulations for growth on lactate and acetic acid were conducted by maximizing for growth as the objective function. Simulations were carried out according to what is described in the section "simulation details", except no constraints were made on the two reactions catalyzed by malic enzyme and oxaloacetate decarboxylase. In some cases constraints were made on individual reactions, which are described in the text.

C. glutamicum is able to grow on various substrates including a number of organic acids such as lactate (Cocaign-Bousquet and Lindley, 1995) and acetate (Wendisch et al., 2000). Simulations were carried out using acetate and lactate as carbon source, and the results were compared to results found in literature.

Lactate as carbon source

Simulations maximizing for growth was carried out when lactate was used as a carbon source (Figure 4.8). As expected the *in silico* organism could utilize lactate as a carbon source. The maximum biomass yield on substrate was 0.54 g biomass · (g lactate)$^{-1}$, which was lower than when glucose was used as a substrate (0.61 g biomass · (g glucose)$^{-1}$). The difference was due to the lower efficiency in ATP- and NADPH synthesis, when the gluconogenetic pathways were included in the model. Experimental data for a carbon limited chemostat showed a biomass yield of 0.36 g biomass · (g lactate)$^{-1}$ (D = 0.17 hr^{-1}) whereas the yield increased as dilution rate was increased (Cocaign-Bousquet and Lindley, 1995). It needs to be emphasized that in the biomass yield calculations made by Cocaign-Bousquet and Lindley (1995) the pyruvate produced as a byproduct was subtracted from the substrate carbon, so the biomass yield on lactate including pyruvate production in reality was lower. For a dilution rate of 0.28 hr^{-1} the biomass yield was 0.42 g biomass · (g lactate)$^{-1}$ (0.3 g biomass · (g lactate)$^{-1}$ when pyruvate production was taken into account). At this dilution rate the

chemostat was not carbon limited, and an overflow of pyruvate was seen resulting in excretion of this compound. At the organisms maximum growth rate (μ = 0.35 hr^{-1}) a biomass yield of 0.61 g biomass · (g lactate)$^{-1}$ (0.4 g biomass · (g lactate)$^{-1}$ when pyruvate production was included) was seen, and the efflux of pyruvate was further increased. When comparing experimental data with simulation data, it was seen that the model data (Figure 4.8; grey boxes) was comparable to the data for the carbon-limited chemostat with μ = 0.17 hr^{-1} (Figure 4.8; red ovals 1st flux from the top), whereas for data for the maximum growth rate (μ = 0.35 hr^{-1}), fluxes around phosphoenolpyruvate, pyruvate, oxaloacetate and malate were significantly different (Figure 4.8; red ovals 2nd flux from top). In addition to this an efflux of pyruvate (21% of lactate uptake), and a reduced flux through the TCA was observed (Cocaign-Bousquet and Lindley, 1995). Looking more into details of the experimental data at high growth rates, and hence high substrate uptake rates, growth rate

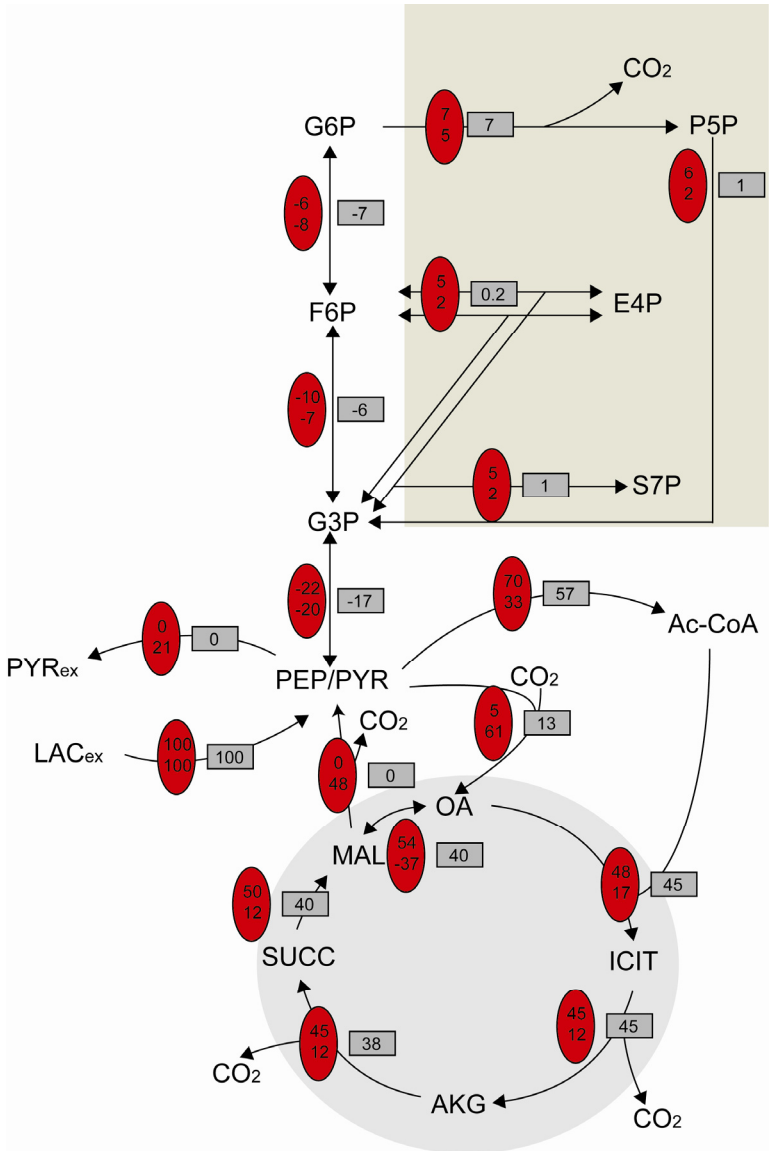

Figure 4.8: Metabolic flux distribution of *C. glutamicum* growing on lactate and maximizing for growth. All fluxes are expressed as molar percentage of the specific uptake rate of lactate. Numbers in red ovals are taken from Cocaign-Bousquet and Lindsley (1995). Upper flux μ = 0.17 hr^{-1}; lower flux μ = 0.35 hr^{-1}. Numbers in grey boxes are results from simulations with *in silico* organism. LAC_{ex}: extracellular lactate; PYR_{ex}: extracellular pyruvate. Other abbreviations see figure 1.

limitations within the central metabolism were observed (Cocaign-Bousquet and Lindley, 1995). During these conditions some enzymes became rate limiting, and the organism found alternative pathways which could not be predicted by the model.

One major difference between the model and the experimental data was the operation of an alternative NADPH supply by a cyclic operation of pyruvate carboxylase, coupled to a reversed flux through malate dehydrogenase, converting oxaloacetate to malate, and then back to pyruvate using malic enzyme. The net result of this cycling was the generation of a NADPH using an ATP and a NADH. This behavior was not predicted by the *in silico* model. However, when

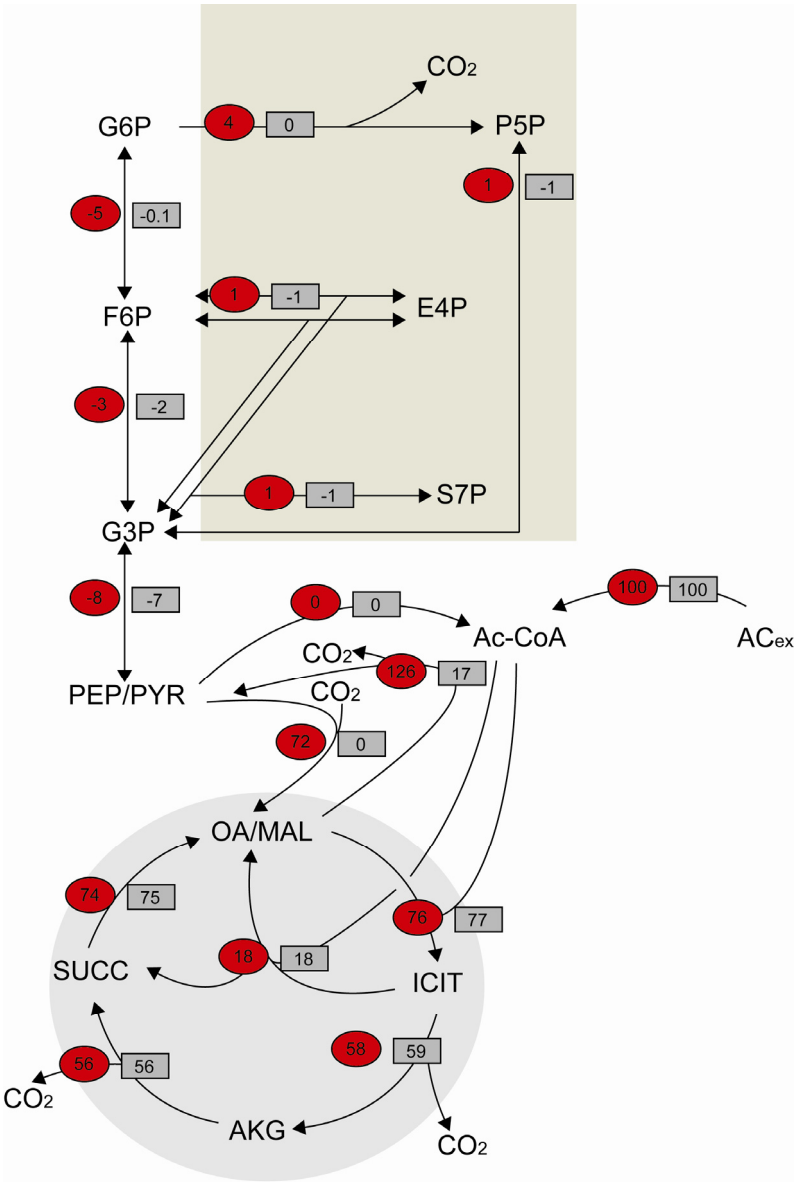

Figure 4.9: Metabolic flux distribution of *C. glutamicum* growing on acetate and maximizing for growth. All fluxes are expressed as molar percentage of the specific uptake rate of acetate. Numbers in red ovals are taken from Wendisch et al. (2000). Numbers in grey boxes are results from model simulations. AC_{ex}: extracellular acetate. Other abbreviations see figure 1.

simulations were carried out constraining the flow of pyruvate limiting the flow towards Ac-CoA as it was seen in the data of Cocaign-Bousquet and Lindley (1995), the same flux patterns could be recognized (data not shown). The maximum biomass yield was decreased to 0.52 g biomass · (g lactate)$^{-1}$ under these conditions. The model could not predict the behavior observed in the

experiment, because this flux distribution is not the most stoichiometrically efficient for the *in silico* organism. However, *in silico* model predictions were close to the results obtained in the work of Cocaign-Bousquet and Lindley (1995) when no rate limitations were seen.

Acetate as carbon source

Maximization for growth was simulated during growth on either acetate as single carbon source (Figure 4.9), or during simultaneous acetate and glucose consumption (data not shown). The maximum biomass yield on acetate (0.48 g biomass · (g acetate)$^{-1}$) was found to be lower than on glucose (0.61 g biomass · (g glucose)$^{-1}$), and the glyoxylate shunt was observed to be active. Both observations were consistent with experimental data (Wendisch et al., 2000), although biomass yields for the experimental data was lower being 0.24 g biomass · (g acetate)$^{-1}$ and 0.34 g biomass · (g glucose)$^{-1}$ for acetate and glucose respectively.

It was observed that no growth was possible for the *in silico* organism when the glyoxylate shunt was shut down (data not shown), which was also observed by Wendisch et al. (2000). During optimal growth the model predicted a flux through the glyoxylate cycle corresponding to 25% of the substrate uptake (Figure 4.9). This flux was 18% for the experimental data of Wendisch et al. (2000). Further investigation of the glyoxylate shunt branch point showed, that when the carbon flux through the glyoxylate shunt was constrained to 18% of the acetate uptake, the biomass yield was lowered to 0.35 g biomass · (g acetate)$^{-1}$ (data not shown). When the carbon flux through the glyoxylate shunt was increased by constraining this flux, a decrease in the biomass yield was seen (data not shown), indicating that the carbon flux predicted by the model is truly a maximum for the *in silico* organism.

The model predicted that the flux through the PPP was entirely omitted, and NADPH needed for biomass was solely generated by the isocitrate dehydrogenase reaction, whereas the data of Wendisch et al. (2000) showed a low flux (4%) through the PPP. When PPP-flux was constrained to 4% simultaneously with the glyoxylate shunt constrain above, the biomass yield further decreased to 0.33 g biomass · (g acetate)$^{-1}$. The TCA-flux was higher for the experimental data as it was the case for the model.

Simulations for co-metabolism of acetate and glucose were carried out (data not shown). Wendisch et al. (2000) found that the glyoxylate cycle was active during co-metabolism of these two substrates, which was a surprise since this was not seen for *E. coli* cells grown under the same conditions (Walsh and Koshland, 1985), and since this pathway is not essential when glucose is present. The model predicted the same behavior when substrate uptake was constrained at the same levels (data not shown). However, when the glyoxylate cycle was removed from the model the growth yield of the organism was not altered (data not shown), which in practice means that from a stoichiometric point of view it is insignificant which route is used under the given conditions. The preferred use of the glyoxylate route in Wendisch et al. (2000) is probably due to acetate specific induction, which earlier has been seen for *C. glutamicum* during these conditions (Gerstmeier et al., 2003). Anaplerotic fluxes were higher for the experimental data than for the model, and a significant cycling between C3 and C4 was seen (Figure 4.9) resulting in an anaplerotic netflux of 54% towards the pyruvate/phosphoenolpyruvate pool which was higher than for the model (17%) (Figure 4.9).

Conclusions

A validated metabolic network of *C. glutamicum* ATCC 13032 was constructed, and by using flux-balance analysis the *in silico* model was able to predict metabolic fluxes during lysine production and growth under various conditions, which were consistent with experimental values. This work also showed that genome scale metabolic model simulations needs to be combined with data from other sources, i.e. flux data or transciptomic data, in order to improve the prediction power of the model. The model was able to predict potential targets for metabolic engineering for improving lysine production in *C. glutamicum*, and hence serves as a useful tool for future directing of metabolic engineering strategies resulting in improved lysine production. The model also serves as an extensive compendium on *C. glutamicum* metabolism, and it is our hope that by combining the model with datasets from high throughput experimental techniques such as transcriptomics, fluxomics and metabolomics, the prediction power of the model can be further improved.

Acknowledgments

Ana Paula Oliveira is acknowledged for help and guidance during model construction and for introducing the Biooptv4.9 software.

References

Åkesson M, Förster J, Nielsen J. 2004. Integration of gene expression data into genome-scale metabolic models. Metabolic Engineering 6:285-293.

Becker J, Klopprogge C, Zelder O, Heinzle E, Wittmann C. 2005. Amplified expression of fructose 1,6-bisphosphatase in *Corynebacterium glutamicum* increases *in vivo* flux through the pentose phosphate pathway and lysine production on different carbon sources. Applied and Environmental Microbiology 71:8587-8596.

Bonarius HPJ, Schmid G, Tramper J. 1997. Flux analysis of underdetermined metabolic networks: the quest for the missing constraints. Trends in Biotechnology 15:308-314.

Borodina I, Krabben P, Nielsen J. 2005. Genome-scale analysis of *Streptomyces coelicolor* A3(2) metabolism. Genome Research 15:820-829.

Bott M, Niebisch A. 2003. The respiratory chain of *Corynebacterium glutamicum*. Journal of Biotechnology 104:129-153.

Brand S, Niehaus K, Pühler A, Kalinowski J. 2003. Identification and functional analysis of six mycolyltransferase genes of *Corynebacterium glutamicum* ATCC 13032: the genes *cop1*, *cmt1*, and *cmt2* can replace each other in the synthesis of trehalose dicorynomycolate, a component of the mycolic acid layer of the cell envelope. Archives of Microbiology 180:33-44.

Cocaign-Bousquet M, Guyonvarch A, Lindley ND. 1996. Growth rate-dependent modulation of carbon flux through central metabolism and the kinetic consequences for glucose-limited chemostat cultures of *Corynebacterium glutamicum*. Applied and Environmental Microbiology 62:429-436.

Cocaign-Bousquet M, Lindley ND. 1995. Pyruvate overflow and carbon flux within the central metabolic pathways of *Corynebacterium glutamicum* during growth on lactate. Enzyme and Microbial Technology 17:260-267.

Collins MD, Doodfellow M, Minnikin DE. 1982a. A survey of the structures of mycolic acids in *Corynebacterium glutamicum* and related taxa. Journal of General Microbiology 128:129-149.

Collins MD, Goodfellow M, Minnikin DE. 1982b. Fatty acid composition of some mycolic acid-containing coryneform bacteria. Journal of General Microbiology 128:2503-2509.

Covert MW, Knight EM, Reed JL, Herrgard MJ, Palsson BØ. 2004. Integrated high-throughput and computational data elucidates bacterial networks. Nature 429:92-96.

Cremer J, Eggeling L, Sahm H. 1991. Control of the lysine biosynthesis sequence in *Corynebacterium glutamicum* as analysed by overexpression of the individual corresponding genes. Applied and Environmental Microbiology. 57:1746-1752.

Daffé M. 2005. The Cell Envelope of Corynebacteria. In: Eggeling L, Bott M, editors. Handbook of *Corynebacterium glutamicum.* Boca Raton: CRC Press. p 121-148.

de Graaf AA. 2000. Metabolic flux analysis of *Corynebacterium glutamicum*. In: Schügerl K, Bellgard KH, editors. Bioreaction Engineering: modelling and control. Berlin: Springer Verlag. p 506-555.

Edwards JS, Ibarra RU, Palsson BØ. 2001. *In silico* predictions of *Escherichia coli* metabolic capabilities are consistent with experimental data. Nature Biotechnology 19:125-130.

Edwards JS, Palsson BØ. 2000. The *Escherichia coli* MG1655 *in silico* metabolic genotype: Its definition, characteristics, and capabilities. PNAS 97:5528-5533.

Eggeling L, Oberle S, Sahm H. 1998. Improved L-lysine yield with *Corynebacterium glutamicum*: use of *dapA* resulting in increased flux combined with growth limitation. Applied Microbiology and Biotechnology 49:24-30.

Feist AM, Scholten JCM, Palsson BØ, Brockman FJ, Ideker T. 2006. Modelling methanogenesis with a genome-scale metabolic reconstruction of *Methanosarcina barkeri*. Molecular Systems Biology 2:1-14.

Förster J, Famili I, Fu P, Palsson BØ, Nielsen J. 2003. Genome-scale reconstruction of the *Saccharomyces cerevisiae* metabolic network. Genome Research 13:244-253.

Gerstmeier R, Wendisch VF, Schnicke S, Ruan H, Farwic M, Reinscheid D, Eikmanns BJ. 2003. Acetate metabolism and the regulation in *Corynebacterium glutamicum*. Journal of Biotechnology 104:99-122.

Heinemann M, Kümmel A, Ruinatscha R, Panke S. 2005. *In silico* genome-scale reconstruction and validation of the *Staphylococcus aureus* metabolic network. Biotechnology and Bioengineering 92: 850-864.

Herrgård MJ, Fong SS, and Palsson BØ. 2006. Identification of Genome-scale metabolic network models using experimentally measured flux profiles. PLoS Computationel Biology 2:676-686.

Hoischen C, Krämer R. 1990. Membrane alteration is necessary but not sufficient for effective glutamate secretion in *Corynebacterium glutamicum*. Journal of Bacteriology 172:3409-3416.

Ingraham JL, Maaløe O, Niedhardt FC. 1983. Growth of the Bacterial Cell. Sunderland, Massachusetts: Sinauer Associates, Inc. 435 p.

Jang KH, Pierotti D, Kemp GW, Best GR, Britz ML. 1997. Mycolic acid composition of *Corynebacterium glutamicum* and its cell surface mutants: effects of growth with gycine and isonicotinic acid hydrazide. Microbiology UK 143:3209-3221.

Kalinowski J, Bathe B, Bartels D, Bischoff N, Bott M, Burkovski A, Dusch N, Eggeling L, Eikmanns BJ, Gaigalat L. 2003. The complete *Corynebacterium glutamicum* ATCC 13032 genome sequence and its impact on the production of -aspartate-derived amino acids and vitamins. Journal of Biotechnology 104:5-25.

Keddie RM, Cure GL. 1978. Cell-wall Compsition of Coryneform Bacteria. In: Bousfield IJ, Calley AG, editors. Coryneform Bacteria. London: Academic Press. p 47-84.

Kelle R, Hermann T, Bathe B. 2005. L-Lysine Production. In: Eggeling L, Bott, M, editors. Handbook of *Corynebacterium glutamicum*. Boca Raton: CRC Press. p 465-488.

Krömer JO, Sorgenfrei O, Klopprogge K, Heinzle E, Wittmann C. 2004. In-depth profiling of lysine-producing *Corynebacterium glutamicum* by combined analysis of the transcriptome, metabolome, and fluxome. Journal of bacteriology 186:1769-1784.

Marx A, de Graaf AA, Wiechert W, Eggeling L, Sahm H. 1996. Determination of the fluxes in the central metabolism of *Corynebacterium glutamicum* by nuclear magnetic resonance spectroscopy combined with metabolite balancing. Biotechnology and Bioengineering 49:111-129.

Marx A, Striegel K, de Graaf AA, Sahm H, Eggeling L. 1997. Response of the central metabolism of *Corynebacterium glutamicum* to different flux burdens. Biotechnology and Bioengineering 56:168-180.

Marx A, Eikmanns BJ, Sahm H, de Graaf AA, Eggeling L. 1999. Response of the central metabolism in *Corynebacterium glutamicum* to the use of an NADH-dependent glutamate dehydrogenase. Metabolic Engineering 1:35-48.

Moritz B, Striegel K, de Graff AA, Sahm H. 2000. Kinetic properties of the glucose-6-phosphate and 6-phosphogluconate dehydrogenases from *Corynebacterium glutamicum* and their application for predicting pentose phosphate pathway flux in vivo. European Journal of Biochemistry 267:3442-3452.

Oliveira AP, Nielsen J. Förster J. 2005. Modelling *Lactococcus lactis* using a genome-scale flux model. BMC Microbiology 5:39.

Palsson BØ. 2000. The challenges of *in silico* biology. Nature Biotechnology 18:1147-1150.

Palsson BØ. 2006 Systems Biology: Properties of Reconstructed Networks. New York: Cambrigde University Press. 322 p.

Patil KR, Åkesson M, Nielsen J. (2004). Use of genome-scale microbial models for metabolic engineering. Current Opinion in Biotechnology 15:64-69.

Petersen S, de Graff AA, Eggeling L, Mollney M, Wiechert W, Sahn H. 2000. *In vivo* quantification of parallel and bidirectional fluxes in the anaplerosis of *Corynebacterium glutamicum*. Journal of Biological Chemistry 275:35932-35941.

Price ND, Papin JA, Schilling CH, Palsson BØ. 2003. Genome-scale microbial *in silico* models: the constrain-based approach. Trends in Biotechnology 21:162-169.

Puech V, Chami M, Lemassu A, Laneelle MA, Schiffler B, Gounon P, Bayan N, Benz R, Daffé M. 2001. Structure of the cell envelope of corynebacteria: importance of the non-covalently bound lipids in the formation of the cell wall permeability barrier and fracture plane. Microbiology 147:1365-1382.

Reed JR, Vo TD, Schilling CH, Palsson BØ. 2003. An expanded genome-scale model of *Escherichia coli* K-12 (iJR904 GSM/GPR). Genome Research 4:R54.

Schilling CH, Covert MW, Famili I, Church GM, Edwards JS, Palsson BØ. 2002. Genome-scale metabolic model of *Helicobacter pylori* 26695. Journal of Bacteriology 184:4582-4593.

Schilling CH, Palsson,BØ. 2000. Assessment of the metabolic capabilities of *Haemophilus influenzae* Rd through a genome-scale pathway analysis. Journal of Theoretical Biology 203:249-283.

Schilling CH, Schuster S, Palsson BØ, Heinrich R. 1999. Metabolic pathway analysis: basic concepts and scientific applications in the post-genomic era. Biotechnology Progress 15:296-303.

Schrumpf B, Schwarzer A, Kalinowski J, Pühler A, Eggeling L, Sahn H. 1991. A functionally split pathway for lysine synthesis in *Corynebacterium glutamicum*. Journal of Bacteriology 173:4510-4516.

Sonntag K, Eggeling L, de Graaf AA, and Sahm H. 1993. Flux partitioning in the split pathway of lysine synthesis in *Corynebacterium glutamicum*. Quantification by 13C- and 1H-NMR spectroscopy. European Journal of Biochemistry 213:1325-1331.

Sonntag K, Schwinde JW, de Graaf AA, Marx A, Eikmanns BJ, Wiechert W, Sahm H. 1995. 13C NMR studies of the fluxes in the central metabolism of *Corynebacterium glutamicum* during growth and overproduction of amino acids in batch cultures. Applied Microbiology and Biotechnology 44:489-495.

Stephanopoulos G, Vallino JJ. 1991. Network rigidity and metabolic engineering in metabolite overproduction. Science 252:1675-1681.

Stephanopoulos G, Aristidou AA, Nielsen J. 1998. Metabolic Engineering - Principles and Methodologies. California, San Diego: Academic Press. 725 p.

Strelkov S, Elstermann M, Schomburg D. 2004. Comprehensive analysis of metabolites in *Corynebacterium glutamicum* by gas chromatography/mass spectromety. Journal of Biological Chemistry 385:853-861.

Teusink B, Wiersma A, Molenaar D, Francke C, de Vos WM, Siezen RJ, Smid EJ. 2006. Analysis of growth of *Lactobacillus plantarum* WCFS1 on a complex medium using a genome-scale model. Journal of Biological Chemistry 281:40041-40048.

Vallino JJ, Stephanopoulos G. 1993. Metabolic flux distribution in *Corynebacterium glutamicum* during growth and lysine overproduction. Biotechnology and Bioengineering 41:633-646.

Vallino JJ, Stephanopoulos G. 1994. Carbon flux distributions at the glucose 6-phosphate branch point in *Corynebacterium glutamicum* during lysine overproduction. Biotechnology Progress 10:327-334.

Varela CA, Baez ME, Agosin E. 2004. Osmotic stress response: Quantification of cell maintenance and metabolic fluxes in a lysine-overproducing strain of *Corynebacterium glutamicum*. Applied and Environmental Microbiology 70:4222-4229.

Walsh K, Koshland DE. 1985. Branch point control by the phosphorylation state of isocitrate dehydrogenase. Journal of Biological Chemistry 260:8430-8437.

Wendisch VF, de Graaf AA, Sahm H, Eikmanns BJ. 2000. Quantitative determination of metabolic fluxes during co-utilization of two carbon sources: comparative analyses with *Corynebacterium glutamicum* during growth on acetate and/or glucose. Journal of Bacteriology 182:3088-3096.

Wittmann C, Heinzle E. 2001. Application of MALDI-TOF MS to lysine-producing *Corynebacterium glutamicum*: A novel approach for metabolic flux analysis. European Journal of Biochemistry 268:2441-2455.

Wittmann C, Heinzle E. 2002. Genealogy profiling through strain improvement by using metabolic network analysis: metabolic flux genealogy of several generations of lysine-producing *Corynebacteria*. Applied and Environmental Microbiology 68:5843-5859.

Chapter 5

5. Comparative analysis of eight metabolic engineering strategies implemented in an L-lysine producing *Corynebacterium glutamicum* production strain

(Paper B)

Kjeld Raunkjær Kjeldsen[1,2], Jens Nielsen[2,3,4]

[1]Center for Microbial Biotechnology, DTU Biosys, Technical University of Denmark, DK-2800 Lyngby, Denmark; [2]Agro&Ferm A/S, Limfjordsvej 4, DK-6715 Esbjerg N, Denmark.
[3] Current address: Department of Chemical and Biological Engineering, Chalmers University of Technology, SE-412 95 Gothenburg, Sweden
[4] Corresponding author; telephone: (+45) 45252696; Fax: (+45) 45884148; E-mail: nielsenj@chalmers.se

This manuscript have been submitted for publication in "Metabolic Engineering"

Abstract

Eight different metabolic engineering strategies were evaluated for their ability to improve the production of lysine in an industrially relevant *Corynebacterium glutamicum* production strain. The eight stains constructed for this work were evaluated in fed-batch fermentations under conditions simulating industrial scale fermentation. Over-expression of the two NADPH generating genes present in the pentose phosphate pathway, *zwf* and *gnd*, both resulted in increased lysine yields of 5% and 6%, respectively, indicating that the co-factor NADPH was limiting for lysine synthesis in this stain. Over-expression of the genes *lysC* and *pyc* both showed negative effects on overall lysine yield with yields of 83% and 89% of the control strain, respectively. No significant effects on overall lysine yields were seen for over-expression of four genes located in the lysine synthesis pathway, *dapA*, *dapC*, *dapF* and *lysE.*
Keywords: Corynebacterium glutamicum; lysine; central carbon metabolism; fed-batch fermentation

Introduction

Corynebacterium glutamicum is a gram-positive bacterium widely used in the production of amino acids. The amino acid produced in the largest quantity by this bacterium is L-lysine of which the annual production today is about 1,100,000 ton L-lysine,HCl with an expected increase in demand of 10% per year. For many years production strains have been improved by many rounds of undirected mutagenesis followed by screening for increased productivity and yield. However, since the arise of readily available genetic manipulation tools and the publication of the genome of the *C. glutamicum* ATCC 13032 type strain (Ikeda and Nakagawa, 2003; Kalinowski et al., 2003) considerable efforts have been made to use metabolic engineering in improving lysine yields and productivity. A number of succesful examples of metabolic engineering have been presented (Cremer et al., 1990; Cremer et al., 1991; Eggeling et al., 1998; Hartmann et al., 2003; Koffas et al., 2002; Koffas et al, 2003). Due to large commercial interest in lysine and the use of *C. glutamicum* as a model organism for studying the central metabolism in actinomycetes this organism has been intensively investigated. This has led to a quite unique accumulation of experimental information and a list of potential bottlenecks towards the synthesis of lysine. However, strains used in metabolic engineering studies have in many cases been strains with relatively low lysine production compared to commercial production strains. In this study we investigate various previously reported metabolic engineering strategies on the commercially relevant production strain *C. glutamicum* KK-11, and evaluated the effect of these strategies under relevant production conditions.

Based on earlier findings eight different genes were selected for metabolic engineering. In all cases the genes were up-regulated. The targets for metabolic engineering were selected so different parts of the metabolism were engineered (Figure 5.1). Our primary focus was to study the effect of engineering the central carbon metabolism and the first committed step towards lysine production, but we also included metabolic engineering targets in the lysine pathway. It is known that *C. glutamicum* has a high demand for NADPH for the overproduction of lysine (Moritz et al., 2000; Marx et al., 1999) and a relationship between a high flux through the NADPH generating pentose phosphate pathway (PPP) and a high lysine production has been identified (Kiefer et al., 2004; Wittmann and Heinzle, 2002). Based on this the two genes, *gnd* and *zwf*, responsible for the NADPH generating reactions in this pathway were selected for up-regulation. Pyruvate carboxylase (*pyc*) has been found to be the main anaplerotic pathway for lysine biosynthesis (Park et al., 1997; Peters-Wendisch et al., 1998; Petersen et al., 2000), and increasing

the product of this reaction, oxaloacetate, may increase lysine production. Our last primary target was the aspartate kinase (*lysC*), which is the reaction and gene in the lysine pathway that has been given most attention in metabolic engineering studies due to its importance in regulation of flux towards lysine-, methionine and threonine synthesis. In the wild type strain this reaction is feed back inhibited by lysine and threonine, making this reaction a key step in regulation of the synthesis of lysine (Kelle et al., 2005). In all known *C. glutamicum* strains overproducing lysine the *lysC*-gene is known to have mutations causing feed back resistance. Over-expression of *lysC* has shown positive effects on lysine production (Cremer et al., 1991; Eggeling et al., 1998).

In addition to the four key targets another four targets downstream *lysC* were selected

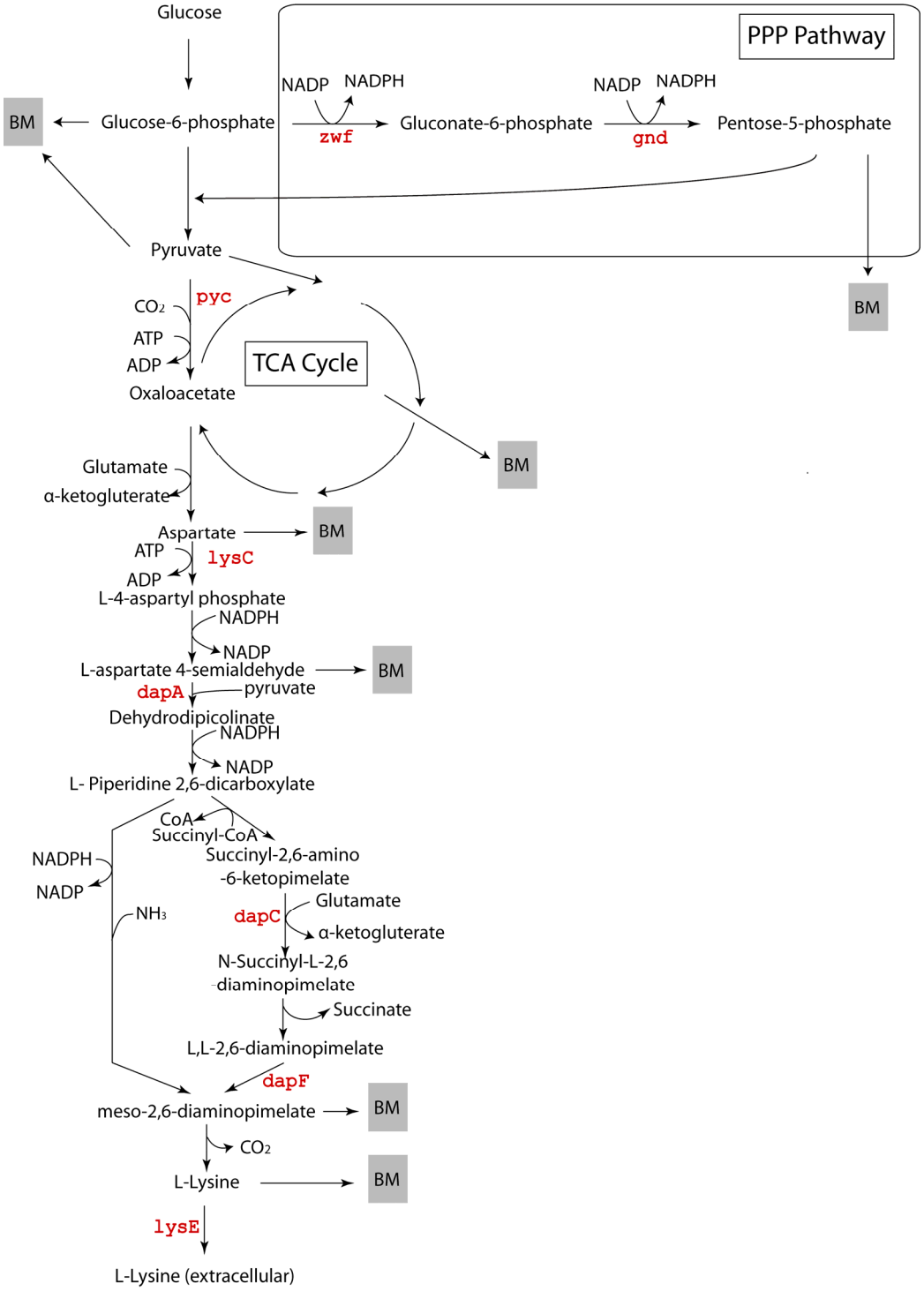

Figure 5.1: Overview of the L-lysine metabolism in *C. glutamicum*. Genes up-regulated in this study is marked in red. BM: biomass.

for metabolic engineering. Dihydrodipicolate synthase (*dapA*) is another enzyme in the lysine synthetic pathway which has received attention due to its presence at the split between lysine and homoserine. Up-regulation of this gene has in some cases led to an increase in lysine production (Cremer et al., 1991; Eggeling et al., 1998). Succinyl-amino-ketopimelate transaminase (*dapC*) and diaminopimelate epimerase (*dapF*), two reactions part of the succinylase branch of the lysine pathway, have both been shown as rate limiting in the synthesis of lysine since up-regulation of each of these genes gave a positive effect on lysine production (Hartmann et al., 2003). The efflux of lysine from the cytosol of the bacterium is carried out by the transport protein lysine permerase (*LysE*) (Vrljic et al., 1996). This exporter is tightly controlled in the wild type strain making this an obvious candidate for optimization of lysine production.

Materials and methods

Bacterial strains and plasmids

The lysine producing strain used in this study was the industrial strain *C. glutamicum* KK-11. This strain is derived from multiple rounds of mutagenesis and screening from the *C. glutamicum* wild-type strain ATCC 13032. KK-11 is prototrophic for all amino acids. Electrocompetent *C. glutamicum* KK-11 cells were produced following the method of Eggeling and Reyes (2005). Electro competent *Escherichia coli* DB10B and chemically competent Mach1™-T1^{R} *E. coli* cells (Invitrogen) were used for initial molecular work. The *E.coli – C. glutamicum* shuttle vector pEC-XK99E (Tauch et al., 2003) was used for over-expression of individual genes.

Medium
All chemicals used were purchased from either Sigma-Aldrich or VWR International. For cultivation of *E. coli* Luria-Bertani (LB) medium (Bertani, 1951) was prepared and added 5 g/L glucose after sterilization. Solid plates were prepared adding 1.5% agar before sterilization. When needed, kanamycin was added after cooling of the sterilized medium. Medium for pre-cultures of *C. glutamicum* was prepared with brain heart infusion (BHI) broth, and 5 g/L glucose. Glucose and BHI broth were sterilized separately (121°C for 15 minutes) and aseptically poured together when cooled. When needed kanamycin and Isopropyl β-D-1-thiogalactopyranoside (IPTG) were added by sterile filtration. Solid plates were prepared by adding 1.5% agar to the BHI broth before sterilization. Fermentation medium (FM-1) for fed-batch lysine fermentations was prepared containing (pr kg of medium): 4.36 g corn steep liquor (CSL) (dry weight), 40 g glucose, 2.5 g $(NH_4)_2SO_4$, 15.7 g H_3PO_4, 0.60 g citric acid, 0.90 g KH_2PO_4, 1.20 g K_2HPO_4, 0.63 g $MgSO_4$, 1.13 g Na_2HPO_4, 20 mg $FeSO_4 \cdot 7\ H_2O$, 20 mg $ZnSO_4 \cdot H_2O$, 2.20 mg $CuSO_4 \cdot 5\ H_2O$. Medium was sterilized at 121°C for 30 minutes. After sterilization and cooling to 30°C vitamins (4.6 mg thiamine, 1.3 mg biotin, 11.3 mg calciumpantothenate and 5.7 mg nicotinic acid), 25 mg kanamycin and 0.23 g IPTG was added by sterile filtration. Feed medium (FM-2) was prepared containing (pr kg of medium): 400 g glucose, 4.5 g citric acid, 28.3 g KH_2PO_4, 4.0 g $MgSO_4$, 4.67 g Na_2HPO_4, 60 g $(NH_4)_2SO_4$, 100 mg $FeSO_4 \cdot 7\ H_2O$, 10 mg $ZnSO_4 \cdot H_2O$, 10 mg $CuSO_4 \cdot 5\ H_2O$, 10 mg $NiCl_2 \cdot 6$ H2O 18.3 mg $CoCl_2$, 10 mg $(NH_4)_6Mo_7O_{24} \cdot 4\ H_2O$, 10 mg $MnSO_4 \cdot H_2O$. Glucose was sterilized separately (121°C for 30 minutes) and the rest was sterilized together (121°C for 30 minutes). After cooling the two parts were aseptically poured together and vitamins (4.6 mg thiamine, 1.3 mg biotin, 11.3 mg calciumpantothenate and 5.7 mg nicotinic acid), 25 mg kanamycin and 0.23 g IPTG was added by sterile filtration. Shake flask medium (SFM-1) for enzymatic assays was prepared contained (pr kg of medium): 18 g glucose, 2.5 g CSL (dry weight), 0.45 g H_3PO_4, 0.61 g citric acid, 1.2 g KH_2PO_4,

1.0 g K_2SO_4, 0.7 g $MgSO_4$, 1.2 g Na_2HPO_4, 92.4 g MOPS sodium salt, 23.8 mg $FeSO_4 \cdot 7\ H_2O$, 15.9 mg $ZnSO_4 \cdot H_2O$, 2.3 mg $CuSO_4 \cdot 5\ H_2O$. After serilization (121°C for 15 minutes) 10 g $(NH_4)_2SO_4$, 4.87 mg thiamine, 11.9 mg calciumpantothenate, 6.0 mg nicotinic acid, 1.3 mg biotin, 0.23 g IPTG and 25 mg kanamycin was added by sterile filtration.

Table 5.1: Strains constructed for this work

Strain	Host	Plasmid	Inserted gene	Over-expressed Enzyme
KK11-control	KK11	pEC-XK99E	-	-
KK11-zwf	KK11	pEC-XK99E	zwf	Glucose-6-phosphate dehydrogenase
KK11-gnd	KK11	pEC-XK99E	gnd	6-phosphogluconate dehydrogenase
KK11-pyc	KK11	pEC-XK99E	pyc	Pyruvate carboxylase
KK11-lysC	KK11	pEC-XK99E	lysC	Aspartate kinase
KK11-dapA	KK11	pEC-XK99E	dapA	Dihydrodipicolate synthase
KK11-dapC	KK11	pEC-XK99E	dapC	Succinyl-amino-ketopimelate transaminase
KK11-dapF	KK11	pEC-XK99E	dapF	Diaminopimelate epimerase
KK11-lysE	KK11	pEC-XK99E	lysE	Lysine permerase

Construction of plasmids and C. glutamicum strains

Standard protocols were used for the construction and analysis of plasmid DNA. Purification of chromosomal DNA from *C. glutamicum* was performed by the following method: 5 mL of overnight culture (BHI broth) was harvested by centrifugation. Supernatant was carefully removed and discharged using a pipette. Pellet was washed dissolving the pellet in TE-buffer (pH 7.6) followed by centrifugation (13,000 g). Supernatant was carefully removed. Pellet was dissolved in 1 ml TE-buffer (pH 7.6) containing 15 mg/mL lysozyme followed by incubation for 180 minutes at 37°C. 3 ml TE-buffer (pH 8.2) containing 400 mM NaCl, 220 µL 10% SDS and 3 mg proteinase K was added, and tubes were incubated for 300 minutes at 50°C. After ended incubation 1 mL saturated NaCl solution (approximately 6 M) was added. Solution was vortexed for 2 minutes before it was centrifuged for 15 minutes at 13,000 g. Supernatant was carefully transferred to a clean Eppendorf tube and DNA was precipitated adding 0.5 mL 3 M sodium acetate (pH 5.2) and 16.5 mL 96% ethanol, incubated at -20°C for 30 minutes followed by 30 minutes of centrifugation at maximum speed. Supernatant was carefully removed and discarded pellet was air-dried before it was dissolved in 200 µL TE-buffer (pH 7.6). For each of the 8 genes selected for this study (Table 5.1) a PCR was carried out containing: 1x High Fidelity PCR Buffer (Invitrogen), 10 mM dNTP, 2 mM $MgSO_4$, 0.2 µM of each primer (Table 5.2), 1 µL chromosomal DNA from *C. glutamicum* KK-11, 1 unit Platinum® *Taq* High Fidelity polymerase (invitrogen), autoclaved distilled water to 50 µL. PCR was carried out using the following conditions: 95°C 2 min; 95°C 30 s, 64°C 30 s, 68°C 4 minutes for 5 cycles; 95°C 30 s, 60°C 30 s, 68°C 4 min for 5 cycles; 95°C 30 s, 56°C 30 s, 68°C 4 min for 10 cycles; 95°C 30 s, 52°C 30 s, 68°C 4 min for 10 cycles; 68°C 10 min. The blunt end PCR products were added T-overhangs adding one unit of *Taq* polymerase (Invitrogen) directly into the PCR-tube and incubating for 10 minutes at 72°C. PCR fragments were ligated into a TOPO® vector using TOPO pCR®2.1-TOPO® Kit (Invitrogen) and the vector was introduced into chemically competent Mach1™-$T1^R$ *E. coli* cells (Invitrogen). Two independent positive colonies were selected and grown in LB medium and plasmid DNA was purified using JETstar (Genomed).

Plasmid DNA was shipped to sequencing (MWG Biotech, Germany). That no mutations had occurred during PCR was confirmed by analyzing two independent clones. PCR fragments were cut out and purified using the GFX PCR DNA and Gel Band Purification kit (Amersham Biosciences) and ligated into the plasmid pEC-XK99E using T4 DNA ligase (Invitrogen). Transformation was carried out using 15 µL electro competent *E. coli* DB10B (Invitrogen) which was transferred to an icecold 0.2 mm cuvette. 10 µL pEC-XK99E ligation-mix was added to the cells and the mix was incubated at ice for 5 minutes before electroporation (25 µF, 200Ω, 2500V). Immediately after electroporation the cuvette was placed on ice and 0.5 mL LB medium was added. Cells were incubated at 37°C for 60 minutes before cells were plated on LB plates with 50 mg/L kanamycin and incubated over night at 37°C. Presence of gene-products in plasmids was confirmed by PCR using the following method: Cell material from a colony was transferred to a PCR tube before a reaction mix was added containing 1 x PCR buffer, 2.5 mM $MgCl_2$, 0.2 mM dNTP, 0.5 µM of each primer, 2.5 U *Taq* Polymerase (Invitrogen) and autoclaved water to a final volume of 100 µl. PCR was carried out using the following conditions: 94°C 5 min; 94°C 30 s, 55°C 30 s, 72°C 30 s for 25 cycles; 72°C 10 min for 1 cycle. Plasmid DNA purification was conducted on transformants incubated over night (37°C, 200 rpm) in LB medium with 50 mg/L kanamycin. GFX Micro Plasmid Prep Kit (GE Healthcare) was used for the purification. The purified plasmids were introduced to *C. glutamicum* using the following method. 150 µL elektrocompetent *C. glutamicum* (Eggeling and Reyes, 2005) was added 10 µL purified pEC-XK99E from *E. coli* and the protocol from Eggeling and Ryes (2005) was followed. After electroporation cells were plated on BHI agar containing 91 g/L sorbitol and 15 mg/L kanamycin. Plates were incubated at 30 °C until visible colonies were seen. Presence of gene-products in the vector was confirmed by PCR as described earlier.

Table 5.2: Primer sequences designed for amplification of genes from strain KK11, and added nucleotides at the 5'-end for convenient restriction sites. Underlined nucleotides are introduced restriction sites.

Primer	Sequence
EcoRI-*lysC*-F	5'-gaattcgtggccctggtcgtacagaaat -3'
SmaI-*lysC*-R	3'-cccgggttagcgtccggtgcctgcataa-5'
EcoRI-*dapC*-F	5'-gaattcatgacctctcgcaccccgcttg-3'
SmaI-*dapC*-R	3'-cccgggttagctcaggcgagaaacaaag-5'
EcoRI-*dapA*-F	5'-gaattcatgagcacaggtttaacagcta-3'
SmaI-*dapA*-R	3'-cccgggttatagaactccagctttttc-5'
EcoRI-*gnd*-F	5'-gaattcatgccgtcaagtacgatcaata-3'
SmaI-*gnd*-R	3'-cccgggttaagcttcaacctcggagcgg-5'
EcoRI-*lysE*-F	5'-gaattcatggaaatcttcattacaggtc-3'
SmaI-*lysE*-R	3'-cccgggctaacccatcaacatcagtttg-5'
MfeI-*dapF*-F	5'-caattggtgaatttgaccatccccttg-3'
SmaI-*dapF*-R	3'-cccgggttagatctgcacctcaccgagt-5'
MfeI-*zwf*-F	5'-caattggtgagcacaaacacgacccccct-3'
SmaI-*zwf*-R	3'-cccgggttatggcctgcgccaggtgtga-5'
MfeI-*pyc*-F	5'-caattggtgtcgactcacacatcttcaa-3'
EcoRV-*pyc*-R	3'-gatatcttaggaaacgacgacgatcaag-5'

L-Lysine production in 7 L fermentor

Fermentations were carried out with 2.0 kg medium as initial amount; the temperature was kept at 30°C. During the batch phase agitation was controlled at 800 rpm. The Fed-batch phase was initiated when all glucose in the batch medium was consumed. Agitation and aeration was controlled so dissolved oxygen was kept > 20% throughout the whole fermentation. pH was controlled at 7.0 by NH_4OH (25%) addition. The sugar feeding rate was kept constant and the glucose concentrations never exceeded 5 g/kg. Weight of the fermenter, sugar feed and NH_4OH were monitored online.

Sampling and sample processing

Medium samples were periodically taken for measurement of sugar, lysine and optical density. Samples were taken with intervals ranging from 4-6 hours. Sample amount was 20-30 g. Lysine, glucose and biomass removed from the bioreactor was taken into account in the yield calculations. Biomass concentration was determined by measuring OD_{620} assuming $OD_{620} \cdot 3.9^{-1}$ g biomass (dry cell weight) $\cdot$ kg^{-1}. Culture samples were centrifuged and separated in supernatant and biomass samples and stored at -20°C until further analysis.

Glucose

The glucose concentrations in the supernatant were measured by HPLC. Separation of sugars was achieved using a CarboPac PA 1 column 4 × 50 mm (Dionex Corporation, USA) as precolumn followed by a CarboPac PA 1 column 40 × 250 mm (Dionex , USA) with 160 mM NaOH as mobile phase. Detection and quantification was performed with an amperometric impulse-detector (Electrochemical detector ED 50 Dionex, Germany).

Lysine

Samples for amino acid analysis were first processed by extraction of 1 g supernatant in 10 mL 0.1 M HCl for 5 minutes while stirred by a magnetic stirrer. The sample was then added 5 mL 5-sulfosalicylic acid (6% w/v) and stirred for another 5 minutes before centrifugation at 4000 g in 10 minutes. An appropriate amount of the supernatant was transferred to a container where pH was adjusted to 2.20 ± 0.02 with 1 M NaOH. The sample was transferred to a 25 mL volumetric flask which was filled using sodium citrate loading buffer (0.20 M, pH 2.20) (Biochrom Ltd., Cambrigde Science Park, England). The sample was filtrated through a 0.22-µm pore size filter, diluted if necessary and loaded on a Biochrom 30 (Biochrom, Ltd., Cambrigde Science Park, England). Amino acids were separated using a pH gradient on a Oxidised Hydrolysate Column (Biochrom, Ltd., Cambrigde Science Park, England) and detection was carried out by a postcolumn derivatized with ninhydrin reagent followed by measuring absorbance at 440 (proline) or 570 nm (all other amino acids).

Enzyme assays

The activity of the enzymes glucose-6-phosphate dehydrogenase, 6-phosphogluconate dehydrogenase, pyruvate carboxylase and aspartate kinase was determined on cell extracts of homogenized cells. Cells were grown in 100 mL medium (SFM-1) in a 500 mL baffled shake-flask (30°C, 200 rpm) and harvested at the late exponential phase (~OD_{620} = 20) by centrifugation. Cells were washed twice with Tris-HCl buffer (pH and concentration depending on the assay). Cells were resuspended in 5 mL Tris-HCl buffer and transferred to a DT-20 Ultra Turrax tube, and the sample was homogenized on an IKA Ultra Turrax Tube Drive (IKA-Werke, Staufen, Germany) for 5

minutes. The sample was centrifuged for 10 minutes at maximum speed and the supernatant was transferred to a clean tube and immediately cooled on ice. The homogenized cell extract was used for enzyme assays. Protein concentrations were determined using the method of Bradford (1976). Glucose-6-phosphate dehydrogenase and 6-phosphogluconate dehydrogenase was assayed using a method based on Sugimoto and Shiio (1987). A mixture was prepared containing 50 mM Tris/HCl (pH 7.5), 1 mM $NADP^+$, 10 mM $MgCl_2$ and crude cell extract. Reaction was initiated by the addition of 4 mM glucose 6-phosphate or 1 mM 6-phosphogluconate to a final volume of 0.5 mL. Enzyme activity was measured by continuously measuring the increase in absorbance at 340 nm while incubating at 30°C. Pyruvate carboxylase was assayed by a method based on Payne and Moris (1969). A mixture was prepared containing 90 mM Tris-HCl (pH 8.0), 50 mM $NaHCO_3$, 5 mM $MgCl_2$, 0.10 mM Acetyl CoA, 0.25 mM DTNB, 5 U citrate synthase, 5 mM ATP, 5 mM pyruvate and crude cell extract to a final volume of 1 mL. Assays were incubated at 30°C and activity was measured by continuously measuring the increase in absorbance at 412 nm. Aspartate kinase was assayed based on the method from Black and Wright (1954). Reaction mixtures were prepared with 180 mM Tris-HCl (pH 7.5), 10 mM $MgSO_4 \cdot 6\ H_2O$, 5 mM L-aspartic acid, 10 mM ATP (adjusted to pH 7.0 with NaOH), 160 mM $NH_2OH \cdot HCl$ (neutralized with NaOH) and crude cell extract to a final volume of 500 µL was mixed and incubated at 60°C. The reaction was stopped by the addition of 500 µL 5% (w/v) $FeCl_3$-solution. Enzyme activity was measured as the change in absorbance at 540 nm.

Calculations and Statistics

Lysine yields (g lysine · (g glucose)$^{-1}$) and biomass yields (g biomass · (g glucose)$^{-1}$) were calculated as an average for the whole fermentation (overall yield), and for 2 different phases of the fed-batch phase of the fermentation (phase 1 and phase 2). Glucose, lysine and biomass removed by sampling were taken into account which was also the case for evaporation. Yields for the two fed-batch phases was determined from the slope of the curve when plotting glucose consumed vs. lysine produced or glucose consumed vs. cell dry weight produced for the whole phase. All yields were normalized to the accumulated yield of the control fermentation. Data were analyzed using students T-test, and effects was considered significant when $P \leq 0.05$.

Results and discussion

Enzyme activities of key enzymes for engineered strains

In order to evaluate whether over-expression resulted in higher enzyme activities for our four primary targets, enzyme activities for the two NADPH generating enzymes in the PPP (*zwf* and *gnd*), the oxaloacetate generating step from pyruvate (*pyc*) and the first step in the lysine synthetic pathway (*lysC*) were measured by enzymatic assays. From this data it could be seen that in all cases enzyme activities were increased when the genes were overexpressed (Figure 5.2). Differences were observed for the effect of the metabolic engineering strategy on the increase in enzyme activities. For 6-phosphogluconate dehydrogenase and aspartate kinase an increase higher than 4 fold was observed, whereas glucose-6-phosphate dehydrogenase activity and pyruvate carboxylase activity only increased 1.6 and 1.7 fold, respectively. A decrease in enzyme activity was observed for the two PPP enzymes (*zwf* and *gnd*) when the opposite gene was upregulated.

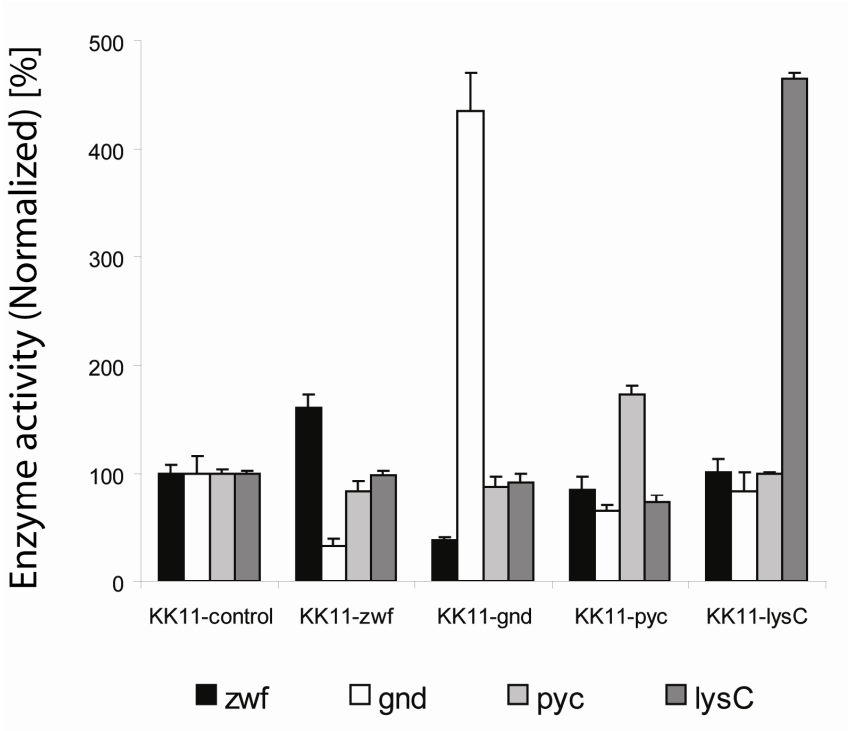

Figure 5.2: Enzyme activities relative to protein in cell extract. Values normalized to KK11-control strain. Data represent mean values from three determinations.

Table 5.3: Lysine yields for constructed strains. Yields normalized to Y_{sp}-total for the control-strain. Numbers in bold are significant different from control strain (P > 0.05)

Over-expressed gene		Y_{sp} (Phase 1)	Y_{sp} (Phase 2)	Y_{sp} (Overall)
		[%]	[%]	[%]
Control	(n = 4)	90 ± 7	111 ± 5	100 ± 2
zwf	(n = 2)	95 ± 1	**120** ± 1	**105** ± 1
gnd	(n = 2)	**105** ± 2	**128** ± 4	**106** ± 0
pyc	(n = 2)	90 ± 2	**95** ± 2	**89** ± 2
lysC	(n = 2)	**59** ± 5	**102** ± 1	**83** ± 4
dapA	(n = 2)	90 ± 8	109 ± 0	97 ± 3
dapC	(n = 2)	84 ± 11	111 ± 2	102 ± 6
dapF	(n = 2)	**105** ± 0	109 ± 2	102 ± 1
lysE	(n = 2)	93 ± 4	112 ± 6	102 ± 1

Characterization of fed-batch fermentations

For each constructed strain two independent fed-batch fermentations were carried out, and for the control strain carrying an empty plasmid (KK11-control), four independent fermentations were conducted. Fermentations were designed to resemble real industrial fermentation conditions. In all cases fermentations were run for more than 65 hours, and the lysine titer exceeded 60 g/kg and the biomass concentrations exceeded 25 g DCW/kg. Fermentation profiles for a KK11-control- and a KK11-gnd fermentation are presented in figure 5.3 (the lysine concentrations are normalized to 100 for the control strain and data for the engineered strain is related to this). The fermentations were carried out with a batch phase until the initial glucose concentration was depleted (batch phase), and after this the fed-batch phase was initiated. The fed-batch phase was divided into two different phases (phase 1 and phase 2) based on biomass growth, where growth was seen in phase 1 and only limited growth was seen in phase 2.

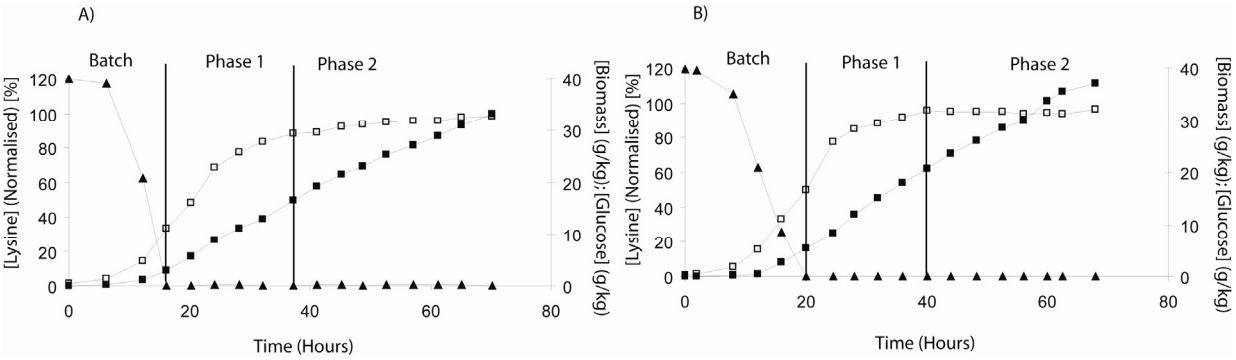

Figure 5.3: Examples of fermentation profiles for this study. A) KK11-control B) KK11-gnd. The division between the different phases of the fermentation is indicated. Triangles: glucose concentration; White squares: biomass concentration; Filled squares: lysine titer normalized to KK11-control-data.

Influence of genetic manipulations on lysine yield

The different genetically manipulated strains were compared concerning lysine yield (Table 5.3). As expected the control strain showed a lower lysine yield in phase 1 of the fermentations (90% of the overall yield) and a higher yield in phase 2 with a yield of 111% of the overall yield. The two strains with up-regulated PPP-genes, KK11-zwf and KK11-gnd, both showed a positive effect on the genetic manipulations responding with a 5% and 6% increase in overall lysine yield, respectively, when compared to the total yield of the KK11-control strain. For the two phases of the fed-batch phase KK11-zwf showed a significantly higher yield in phase 2 (8% higher). Becker et al. (2007) also observed an increase in the lysine yield upon up-regulation of the *zwf*-gene, but they observed improvements of 33%-38% depending on the strategy used. However, the reference strain used by Becker et al. (2007) had a much lower productivity compared to the stain used in our study, and an improvement in this range would therefore be difficult to achieve by a single change in KK11. The strain KK11-gnd was producing lysine at significantly higher yields than the control strain in both phase 1 and phase 2 (16% higher and 15% higher respectively). The up-regulation of this gene has earlier been reported in patent literature (Duncan et al., 2004), but to our knowledge this is the first time the up-regulation of this gene have been evaluated intensively. However, Ohnishi et al. (2005) identified this enzyme as important in the regulation of the PPP-flux, and they found that a mutation in 6-phosphogluconate dehydrogenase (Ser→361→Phe) lead to an 8% increase in PPP-flux, which resulted in improved lysine production. The positive effect on up-

regulation of both *zwf* and *gnd* was unexpected since it could be expected that only one of the enzymes was limiting the flux through the PPP.

Table 5.4: Biomass yields for constructed strains. Yields normalized to Y_{sx}-total for the control-strain. Numbers in bold are significant different from control strain (P > 0.05)

Over-expressed gene		Y_{sx} (Phase 1)	Y_{sx} (Phase 2)	Y_{sx} (Overall)
		[%]	[%]	[%]
Control	(n = 4)	159 ± 37	60 ± 6	100 ± 5
zwf	(n = 2)	168 ± 29	**30** ± 1	100 ± 7
gnd	(n = 2)	**97** ± 11	55 ± 0	101 ± 9
pyc	(n = 2)	173 ± 14	**49** ± 1	98 ± 14
lysC	(n = 2)	178 ± 39	51 ± 12	106 ± 1
dapA	(n = 2)	185 ± 30	**46** ± 1	94 ± 0
dapC	(n = 2)	230 ± 60	65 ± 16	112 ± 22
dapF	(n = 2)	169 ± 50	50 ± 5	96 ± 2
lysE	(n = 2)	144 ± 59	57 ± 1	94 ± 2

However, it is likely that the changes in metabolite concentrations due to one genetic manipulation can cause a flux-change due to transcriptional regulation or allosteric regulation of the enzymes. Such an effect has earlier been seen for the genes *lysC* and *dapA* in a lysine producing *C. glutamicum* strain, where up-regulation of each of these genes resulted in a similar increase in lysine flux (Cremer et al., 1991; Eggeling et al., 1998). The strain KK11-pyc showed a negative effect on lysine yield with a decrease to 89% of the yield of the KK11-control on strain. Lysine yields for the KK11-pyc strain in phase 1 was not significantly different from the control strain, but in phase 2, a decrease of 14 % was seen. The same effect was reported by Koffas et al. (2002) where the up-regulation of this gene in the strain *C. glutamicum* ATCC 21253 resulted in a lower lysine yield. In the same study up-regulation of the same gene in another strain (*C. glutamicum* ATCC 21799) had, however, no effect on the final lysine yield, which again shows that the effect on lysine production by engineering of the central carbon metabolism can be very strain dependent. For KK11-lysC there was also observed a negative effect on the total lysine yield (83% of KK11-control). For the two phases KK11-lysC had a significantly lower lysine yield in both phase 1 and phase 2, i.e. 36% and 9% for phase 1 and phase 2, respectively. The *lysC* gene-product has earlier been identified as a limitation for lysine production (Hua et al., 2000; Jetten et al., 1995), and our observed decrease in lysine yield did therefore not match our expectations. Up-regulation of the lysC-geneproduct aspartate kinase has earlier been connected with growth restrictions in defined minimal media (Koffas et al., 2003), which was also observed for KK11-lysC (Data not shown). However, during growth in complex media no difference between this strain and KK11-control could be seen (data not shown). The negative effect observed by us may therefore be due to other issues such as kinetics or different regulation in our reference strain.

For the strains KK11-dapA, KK11-dapC, KK11-dapF and KK11-lysE no significant changes in overall lysine yield was seen as a result of the genetic manipulations. For *dapA* similar results was found by Hua et al. (2000), while Cremer et al. (1988), Cremer et al. (1991) and Eggeling et al. (1998) saw an increase in lysine production up-regulating this gene. Based on the results in the present study the *dapA* gene-product dihydrodipicolinate syntase was not limiting for

lysine production in KK11. KK11-dapF showed an increase in lysine yield in phase 1 of 16%, while no positive effect was seen for phase 2. The positive effect in phase 1 could be confirmed by the data of Hartmann et al. (2003). Here a positive effect of up-regulation of *dapF* in a shake-flask experiment was seen (13% higher lysine titer). That no effect was seen in phase 2 can be connected to the lower biomass production in this part of the fermentation (Ysx = 169 for phase 1 and 50 for phase 2). When the carbon flux towards growth is decreased drain from the TCA cycle necessary to support biomass is lowered. During this phase it can be expected that the TCA flux is lowered, as seen for simulations with an *in silico* model of *C. glutamicum* (Kjeldsen & Nielsen, 2008), and the availability of succinyl-CoA, an intermediate in both the TCA cycle and in the succinylase branch of the lysine synthesis pathway, is decreased. In this case another reaction in the lysine pathway becomes limiting and the effect of overexpression of *dapF* is abolished. For the *dapC* gene Hartmann et al. (2003) saw a positive effect on lysine production on up-regulation of this gene in a lysine producing strain. Such an effect was not seen in KK11 on up-regulation of *dapC*, which is also part of the succinylase branch suggesting that this step is not limiting in the succinylase branch in KK11. No effect was seen on lysine yields on up-regulating *lysE* indicating that the lysine export capacity of KK11 is sufficient under the conditions in this study.

Influence of genetic manipulations on biomass yield

The biomass yield for KK11-control showed a higher yield for phase 1 (159%) than for phase 2 (60%) when compared to the biomass yield for the whole fermentation (Table 5.4). This was a general observation for all the strains except for KK11-gnd, for which the biomass yield in phase 1 and the total biomass yield were similar. For the biomass yield for the whole fermentation no significant differences were seen between the strains in which enzymes had been up-regulated and the reference strain KK11-control. For the two phases of the fermentation a lower biomass yield was seen for KK11-gnd in phase 1 (39% lower than KK11-control). In phase 2 the biomass yields of the strains KK11-zwf, KK11-pyc and KK11-dapA were significant lower than the KK11-control strain (59%, 18% and 23% lower, respectively). The low biomass yield in phase 1 for strain KK11-gnd could indicate a higher flux towards PPP, limiting growth due to a lower TCA flux. This same effect was not seen in phase 1 when *zwf* was up-regulated, but instead it was observed in phase 2 where the biomass yield was lower compared to KK11-control. A similar effect was observed by Becker et al. (2007) when *zwf* was up-regulated. An up-regulation of *dapA* has earlier been seen to decrease the flux towards biomass due to a decreased flux towards threonine and methionine (Eggeling et al., 1998). A decrease in biomass yield in the later phase of the fermentation could be recognized in the present study when *dapA* was up-regulated. This decrease was not followed by an significant increase in lysine yield. An increased level of the *pyc* gene-product pyruvate carboxylase has in some cases shown higher biomass levels (Koffas et al., 2002; Koffas et al., 2003). This was not the case when *pyc* was up-regulated in KK11-control. Instead a decrease was seen in the later phase of the fermentation. No effect on biomass yield was seen for KK11-lysE.

Correlation between biomass yield and lysine yield

A clear correlation between the biomass yield and the lysine yield was seen for the data of all the fermentations (Figure 5.4). It could be recognized that the biomass yield was decreasing when the lysine yield was increasing, which indicates that carbon was redirected from biomass synthesis to lysine production. A similar correlation was predicted by simulations of a genome scale metabolic model (Kjeldsen and Nielsen, 2008), and interestingly the slope of the linear regression of the data of the present work is almost the same as that predicted by the genome scale model simulations.

Experimental data fitted best to the simulations where the succinylase variant of the lysine synthetic pathway was used, which could indicate that this pathway is the dominant one in KK11. In the present study the two different fed-batch phases of the fermentation (Phase 1 and Phase 2) were clearly separated. Data for phase 1 had a higher variation than data from phase 2. Especially the

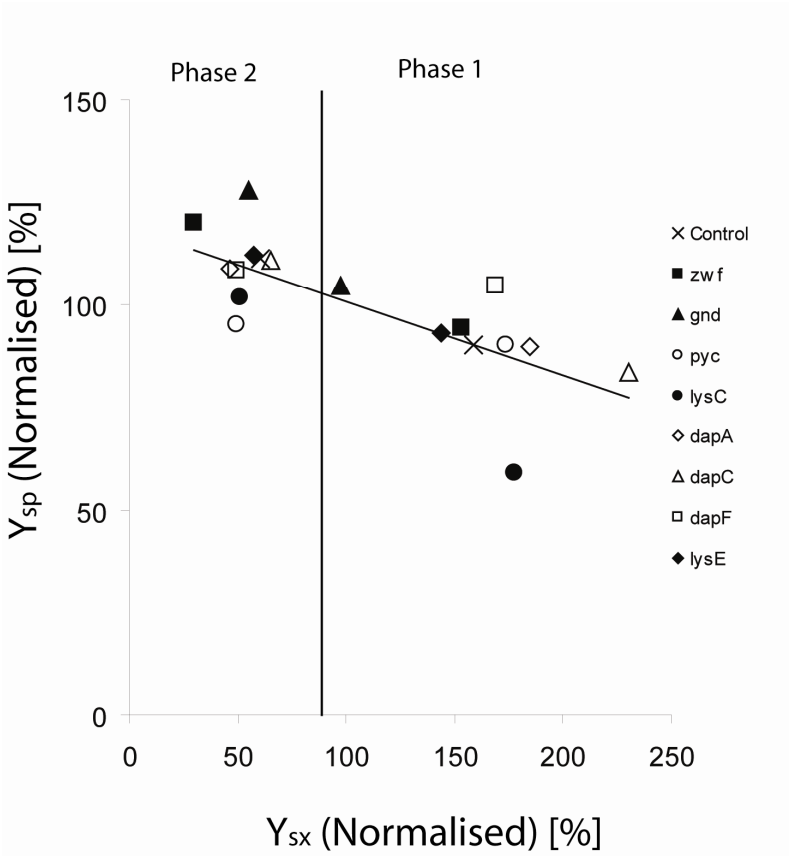

Figure 5.4: Normalized biomass yields plotted against normalized lysine yields. The division between the two phases is indicated by a vertical line. The linear regression is made based on all yield data from table 3 and table 4

biomass yields varied more in phase 1, but in most cases the biomass yield correlated well with the lysine yield indicating that differences in lysine yields in most cases were growth related. As discussed earlier KK11-lysC showed a significant lower lysine yield in phase 1, and the data for this strain is also quite clearly an outlier on the plot in this phase, indicating that the low lysine yield was not entirely due to increased biomass formation. Data for KK11-dapF is also an outlier from the regression line, but data for this strain are placed above the regression line indicating better carbon utilization in this part of the fermentation for this mutant. The significant increased lysine yield of KK11-gnd on the other hand showed a quite clear correlation to biomass yield. Phase 2 is from an industrial point the most interesting part since this is the longest part of the fermentation process, and also here the largest part of the carbon source is used. Data for KK11-pyc and KK11-lysC were both below the regression line, confirming that neither of the metabolic engineering strategies used in the construction of these strains were good. As discussed earlier up-regulating both NADPH generating steps in the PPP (*gnd* and *zwf*) resulted in significant higher lysine yields which strongly indicates that this part of the metabolism is in fact limiting for lysine production in KK11. For KK11-zwf the improved lysine yield was correlated with a lower biomass yield, whereas this was not the case for KK11-gnd.

In conclusion we find that even though metabolic engineering strategies are reported to be successful for improving lysine production, many of these strategies can not be transferred directly to industrial strains. However, through comparative analysis of several different strategies our results points to that supply of the co-factor NADPH may in fact be a limitation for high-producing strains, which probably mainly are derived based on mutations in the lysine pathway.

Acknowledgments

The authors thank PhD Flemming Jørgensen and PhD Peter Ravn (Bioneer A/S) for contributing to the metabolic engineering work. We also want to thank PhD Henrik Pedersen (AgroFerm A/S) for his contribution to the work.

References

Bertani,G., 1951. Studies on lysogenesis - I. The mode of phage liberation by lysogenic *Escherichia coli*. J. Bacteriol. 62, 293-300.

Becker,J., Klopprogge,C., Herold,A., Zelder,O., Bolten,C.J., Wittmann,C., 2007. Metabolic flux engineering of L-lysine production in *Corynebacterium glutamicum* - over expression and modification of G6P dehydrogenase. J. Biotechnol. 132, 99-109.

Black,S. and Wright,N.G., 1954. β-Aspartate kinase and β-aspartylphosphate. J.Biol.Chem. 213, 27-38.

Bradford, M. M., 1976. A rapid and sensitive method for the quantification of microgram quantities of protein utilizing the principle of protein-dye binding. Anal. Biochem. 72, 245-248.

Cremer,J., Treptow,C., and Eggeling,L., 1988. Regulation of enzymes of lysine biosynthesis in *Corynebacterium glutamicum*. J. Gen. Microbiol. 134, 3221-3229.

Cremer,J., Eggeling,L., Sahm,H. 1990. Cloning the *dapA dapB* cluster of the lysine-secreting bacterium *Corynebacterium glutamicum*. Mol. Genet. Genomics. (Historical Archive) 220, 478-480.

Cremer,J., Eggeling,L., Sahm,H., 1991. Control of the lysine biosynthesis sequence in *Corynebacterium glutamicum* as analysed by overexpression of the individual corresponding genes. Appl. Environ. Microbiol. 57, 1746-1752.

Duncan,L.K., McCormack,A., Stapleton,C., Burke,K., Mockel,B., 2004. Process for the preparation of L-amino acids using a gene encoding 6-phosphogluconate dehydrogenase. US Patent Application 0063181 A1.

Eggeling,L. and Reyes,O., 2005. Experiments. In: Eggeling,L., Bott,M. (Ed.), Handbook of *Corynebacterium glutamicum*. CRC Press, Boca Raton, pp. 535-562.

Eggeling,L., Oberle,S., Sahm,H., 1998. Improved L-lysine yield with *Corynebacterium glutamicum*: use of *dapA* resulting in increased flux combined with growth limitation. Appl. Microbiol. Biotechnol. 49, 24-30.

Hartmann,M., Tauch,A., Eggeling,L., Bathe,B., Mockel,B., Puhler,A., Kalinowski,J., 2003. Identification and characterization of the last two unknown genes, *dapC* and *dapF*, in the succinylase branch of the -lysine biosynthesis of *Corynebacterium glutamicum*. J. Biotechnol. 104, 199-211.

Hua,Q., Yang,C., Shimizu,K., 2000. Metabolic control analysis for lysine synthesis using *Corynebacterium glutamicum* and experimental verification. J. Biosci. Bioeng. 90, 184-192.

Jetten,M.S.M., Follettie,M.T., Sinskey,A.J., 1995. Effect of different levels of aspartokinase on the lysine production by *Corynebacterium glutamicum*. Appl. Microbiol.Biotechnol. 43, 76-82.

Kalinowski,J., Bathe,B., Bartels,D., Bischoff,N., Bott,M., Burkovski,A., Dusch,N., Eggeling,L., Eikmanns,B.J., Gaigalat,L., 2003. The complete *Corynebacterium glutamicum* ATCC 13032 genome sequence and its impact on the production of aspartate-derived amino acids and vitamins. J. Biotechnol. 104, 5-25.

Ikeda,M. and Nakagawa,S., 2003. The *Corynebacterium glutamicum* genome: features and impacts on biotechnological processes. Appl. Microbiol. Biotechnol. 62, 99-109.

Kelle,R., Hermann,T., Bathe,B., 2005. L-Lysine production. In: Eggeling,L., Bott,M. (Ed.), Handbook of *Corynebacterium glutamicum*. CRC Press, Boca Raton, pp. 465-488.

Kiefer,P., Heinzle,E., Zelder,O., Wittmann,C., 2004. Comparative metabolic flux analysis of lysine-producing *Corynebacterium glutamicum* cultured on glucose or fructose. Appl. Environ. Microbiol. 70, 229-239.

Kjeldsen,K.R. and Nielsen,J., 2008. *In silico* genome-scale reconstruction and validation of the *Corynebacterium glutamicum* metabolic network. Biotechnol. Bioeng. In Press.

Koffas,M.A.G., Jung,G.Y., Aon,J.C., Stephanopoulos,G., 2002. Effect of pyruvate carboxylase overexpression on the physiology of *Corynebacterium glutamicum*. Appl. Environ. Microbiol. 68, 5422-5428.

Koffas,M.A.G., Jung,G.Y., Stephanopoulos,G., 2003. Engineering metabolism and product formation in *Corynebacterium glutamicum* by coordinated gene overexpression. Metab. Eng. 5, 32-41.

Marx,A., Eikmanns,B.J., Sahm,H., de Graaf,A.A., Eggeling,L., 1999. Response of the central metabolism in *Corynebacterium glutamicum* to the use of an NADH-dependent glutamate dehydrogenase. Metab. Eng. 1, 35-48.

Moritz,B., Striegel,K., de Graff,A.A., Sahm,H., 2000. Kinetic properties of the glucose-6-phosphate and 6-phosphogluconate dehydrogenases from *Corynebacterium glutamicum* and their application for predicting pentose phosphate pathway flux in vivo. Eur. J. Biochem. 267, 3442-3452.

Ohnishi,J., Kakahira,R., Mitsuhashi,S., Kakita,S., and Ikeda,M., 2005. A novel *gnd* mutation leading to increased L-lysine production in *Corynebacterium glutamicum*. FEMS Microbiol. Lett. 242, 265-274.

Park,S.M., Shaw-Reid,C., Sinskey,A.J., Stephanopoulos,G., 1997. Elucidation of anaplerotic pathways in *Corynebacterium glutamicum* via 13C-NMR spectroscopy and GC-MS. Appl. Microbiol. Biotechnol. 47, 430-440.

Payne,J. and Morris,J.G., 1969. Pyruvate carboxylase in *Rhodopseudomonas spheroides*. J. Gen. Microbiol. 59, 97-101.

Peters-Wendisch,P.G., Kreutzer,C., Kalinowski,J., Patek,M., Sahm,H., Eikmanns,B.J., 1998. Pyruvate carboxylase from *Corynebacterium glutamicum*: characterization, expression and inactivation of the *pyc* gene. Microbiology 144, 915-927.

Petersen,S., de Graff,A.A., Eggeling,L., Mollney,M., Wiechert,W., Sahn,H., 2000. In vivo quantification of parallel and bidirectional fluxes in the anaplerosis of *Corynebacterium glutamicum*. J. Biol. Chem. 275, 35932-35941.

Sugimoto,S., Shiio,I., 1987. Regulation of 6-phosphogluconate dehydrogenase in *Brevibacterium flavum*. Agric. Biol. Chem. 51, 1257-1263.

Tauch,A., Pühler,A., Kalinowski,J., Thierbach,G., 2003. Plasmids in *Corynebacterium glutamicum* and their molecular classification by comparative genomics. J. Biotechnol. 104, 27-40.

Vrljic,M., Sahm,H., Eggeling,L., 1996. A new type of transporter with a new type of cellular function: L-lysine export from *Corynebacterium glutamicum*. Mol. Microbiol. 22, 815-826.

Wittmann,C., Heinzle,E., 2002. Genealogy profiling through strain improvement by using metabolic network analysis: metabolic flux genealogy of several generations of lysine-producing Corynebacteria. Appl. Environ. Microbiol. 68, 5843-5859.

Chapter 6

6. Metabolic network analysis of *Corynebacterium glutamicum* during L-lysine production in CSL based complex medium using ^{13}C-labeled glucose

Paper C

Kjeld Kjeldsen[1,2], Anna Lantz[1], Jette Thykaer[1], Henrik Pedersen[2] and Jens Nielsen[1,3,4]

[1]Center for Microbial Biotechnology, DTU Biosys, Technical University of Denmark, DK-2800 Lyngby, Denmark
[2]Agro&Ferm A/S, Limfjordsvej 4, DK-6715 Esbjerg N, Denmark.
[3] Current address: Department of Chemical and Biological Engineering, Chalmers University of Technology, SE-412 95 Gothenburg, Sweden
[4] Corresponding author; telephone: (+45) 45252696; Fax: (+45) 45884148; E-mail: nielsenj@chalmers.se

Abstract

Two L-lysine producing strains of *Corynebacterium glutamicum*, a high producing strain KK-11 and a low producing strain ATCC 21253, were compared during growth and lysine production during fed-batch fermentaions using a complex medium. Using [U-$^{13}C_6$]glucose the uptake of nine different amino acids present in the complex medium was estimated during batch fermentation. Alanine, isoleucine, leucine, phenylanaline, proline, threonine and valine were taken up by both strains, although the ratio between *de novo* synthesis and uptake was different for the two strains. Glycine and serine were not taken up by any of the strains. Estimations of flux distributions in the batch- and fed-batch phase were carried out using [1-^{13}C]glucose. A comparison of the two strains was made both in the batch phase and in the fed-batch phase of the fermentations. In the batch phase the pentose phosphate pathway and the anaplerotic netflux was higher in the high producing strain, whereas the TCA flux was lower. Finally, a significant ATP-consuming futile cycle involving anaplerotic reactions was identified in the low producing strain. The data from the production phase of the fed-batch fermentation showed an increased flux through the pentose phosphate pathway for both strains.

Introduction

Amino acid production by the gram positive bacteria *Corynebacterium glutamicum* is one of the major processes in industrial biotechnology. The amino acid produced in the largest quantity by this bacterium is L-lysine of which the annual production today is about 1,100,000 ton L-lysine,HCl with an expected increase in demand of 8% per year. Optimization of cultivation strategies and producer strains has led to increased yields and productivities. Much of this improvement has been achieved by random mutagenesis strategies followed by intensive screening programs. Recent years more direct methods have been applied using metabolic engineering. In order to improve the performance of a production organism by metabolic engineering a detailed knowledge of intracellular fluxes in the central metabolism may be useful for predicting strategies for direct modifications of the organism by genetic engineering. Metabolic network analysis combining metabolite balancing and ^{13}C-labeling patterns (Christensen and Nielsen, 1999b) can be used as a tool in this respect.

Throughout the last decade the metabolic network of *C. glutamicum* has been thoroughly investigated using methods based on ^{13}C-labeled substrates (Kiefer *et al.*, 2004; Krömer *et al.*, 2004; Marx *et al.*, 1996; Petersen *et al.*, 2000; Wittmann and Heinzle, 2002). This has led to a unique knowledge about the central metabolism of this organism under various conditions.

In commercial production of lysine a complex medium containing various carbon sources such as corn steep liquor (CSL), is normally used, and the metabolic fluxes in this type of media may be different from the fluxes in a defined minimal medium. However, conducting metabolic network analysis using ^{13}C-labeled substrate in complex media is challenging since uptake of non-labeled substrate influences both the metabolite balancing and the labeling patterns of the biomass components. Therefore sophisticated methods need to be used in order to deal with these challenges. Amino acids from the macromolecular pool of the biomass protein are often chosen for analysis in metabolic network analysis using ^{13}C-labeled substrates (Christensen and Nielsen, 1999a; Christiansen *et al.*, 2002; Marx *et al.*, 1996). The labeling patterns of the amino acids reflect the labeling of the intermediates in the central carbon metabolism and thereby the fluxes of the

metabolic network. In order to make an accurate metabolic network analysis it is therefore required to know the precise amino acid uptake to be able to take the contribution of unmarked carbon into account when the flux model is made.
Labeling patterns of amino acids have been determined from continuous cultures in steady state (Christensen and Nielsen, 2000; Marx *et al.*, 1996) or in the exponential growth phase of batch cultures (Pedersen *et al.*, 2000), which also represents a physiological steady state. However, since the batch phase of commercial lysine production only represents a part of the fermentation, it is of great interest to be able to determine the metabolic fluxes in the fed-batch phase following the batch phase. However, when a metabolic shift occurs during a batch or fed-batch fermentation the labeling patterns of the amino acids do not reflect the *in vivo* fluxes at a given time. However, they give an integral value of the metabolic fluxes, which allow us to identify fluxes affected by the physiological change based on the tendencies seen in the labeling patterns of the biomass. This can be used to elucidate metabolic changes in the central metabolism during non balanced growth.
In this study metabolic network analysis on two lysine producing *C. glutamicum* strains grown in complex media containing CSL was conducted. Amino acid uptake was determined in a parallel study where 32%[U-$^{13}C_6$]glucose was used as carbon source.

Materials and Methods

Strains
Two L-lysine producing strains of *Corynebacterium glutamicum* was used in this study. Both strains were obtained by sequential random mutagenesis by UV radiation and by the use of chemical mutagens. The strain ATCC 21253 was obtained from the American Type Culture Collection (Manassas, Va.), whereas the strain KK-11 was kindly donated by Agro&Ferm A/S.

Propagation
A frozen culture of *C. glutamicum* was used to inoculate agar plates containing (per litre distilled water): 37 g brain heart broth (Merck), 15 g agar, 5 g glucose. The plates were inoculated for 36 hr at 30 °C, and a single colony was used to inoculate a 500 mL baffled Erlenmeyer flask containing 100 mL media containing (per kg distilled water): 5 g glucose, 2.4 g corn step liquor (49% DW), 5.2 g H_3PO_4 (85 % (wt/wt)), 0.075 g Na_2-EDTA, 1.2 g KH_2PO_4, 1 g K_2SO_4, 0.7 g $MgSO_4$, 1.2 g $NaHPO_4$, 92.4 g 3-morpholinopropanesulforic acid (MOPS) sodium salt, 0.15 g threonine, 0.10 g leucine, 0.04 g methionine, 12.4 mg $FeSO_4 \cdot 7\ H_2O$, 8.26 mg $ZnSO_4 \cdot H_2O$, 1.21 mg $CuSO_4 \cdot 5\ H_2O$ and 26 mg citric acid. After sterilization (121 °C, 20 minutes) and vitamins and ammonium sulphate was added by sterile filtration so the concentration was (per kg distilled water): 4.87 mg thiamine, HCl, 11.92 mg calcium pantothenate, 6.03 mg nicotinic acid, 1.32 mg D-biotin and 10 g $(NH_4)_2SO_4$. Cultures were inoculated and incubated in a rotary shaker at 30 °C and 250 rpm for 48 hours before they were used to make freeze stocks by mixing 667 µL 50 % (w/v) glycerol with 1000 µL culture and transferred to a -80 °C freezer where they were stored until used as inoculum for the tracer experiment.

Batch medium
A batch medium was prepared containing (per kg distilled water): 2.4 g corn step liquor (49% DW), 5.2 g H_3PO_4 (85 % (m/m)), 0.075 g Na_2-EDTA, 1.2 g KH_2PO_4, 1 g K_2SO_4, 0.7 g $MgSO_4$, 1.2 g $NaHPO_4$, 0.15 g threonine, 0.10 g leucine, 0.04 g methionine, 12.4 mg $FeSO_4 \cdot 7\ H_2O$, 8.26 mg $ZnSO_4 \cdot H_2O$, 1.21 mg $CuSO_4 \cdot 5\ H_2O$ and 26 mg citric acid, 4.87 mg thiamine, HCl, 11.92 mg

calcium pantothenate and 6.03 mg nicotinic acid. The vitamins were sterile filtrated into the medium together with $(NH_4)_2SO_4$ and glucose after the rest of the components had been sterilized (121 °C, 20 minutes) and the medium had been cooled to 30 °C. For batch cultivations the initial glucose concentrations were 17 $g \cdot L^{-1}$ and $(NH_4)_2SO_4$ concentrations were 10 $g \cdot L^{-1}$. The glucose used was either 99% [1-^{13}C] (Omicron Biochemicals, Inc.) or a mixture of 32% [U-$^{13}C_6$] (Isotech, Inc.) and 68% naturally labeled glucose. For fed-batch operations a feed-medium was prepared containing (per kg distilled water): 17 g glucose 99% [1-^{13}C] and 10 g $(NH_4)_2SO_4$. The two components was sterilized separately and mixed after cooling.

Bioreactors and cultivation conditions
The cultivations were carried out in a small scale bioreactor with a working volume of 250 ml designed and made in house. Cultivations were carried out at 30 °C and pH was kept constant at 7.0 using 5 % (v/v) NH_4OH. Bioreactor was aerated with 2 VVM and agitated with 700 rpm to ensure aerobic conditions. Feed medium, NH_4OH and fermenter were all placed on balances and the changes in weight was monitored online.

Biomass measurements
Dry cell weight (DCW) content of the medium was determined by OD_{620} measurements followed by a calculation using a preciously determined OD_{620}:DCW-ratio. The OD_{620}:DCW-ratio was obtained in fermentations identical to the fermentations used for ^{13}C flux analysis. At specified time points samples taken and OD_{620} was measured. In addition samples were centrifuged and washed twice with distilled water followed by drying at 105 °C until constant weight. A OD_{620}:DCW-ratio was determined using data from 6 independent fermentations.

Sampling procedure
Samples were immediately put on ice and centrifuged. Pellet and a supernatant were separated, and the supernatant was filtrated through a 0.22-µm pore size filter before both parts were stored at -20°C until further analysis.

Amino acids analysis
Samples for amino acid analysis were first processed by extraction of 1 g sample in 10 mL 0.1 M HCl for 5 minutes while stirred by a magnetic stirrer. The sample was then added 5 mL 5-sulfosalicylic acid (6% w/v) and stirred for another 5 minutes before centrifugation at 4000 g in 10 minutes. An appropriate amount of the supernatant was transferred to a container where pH was adjusted to 2.20 ± 0.02 with 1 M NAOH. The sample was transferred to a 25 mL volumetric flask which was filled using sodium citrate loading buffer (0.20 M, pH 2.20) (Biochrom Ltd., Cambrigde Science Park, England). The sample was filtrated through a 0.22-µm pore size filter, diluted if necessary and loaded on a Biochrom 30 (Biochrom, Ltd., Cambrigde Science Park, England). Amino acids were separated using a pH gradient on a Oxidised Hydrolysate Column (Biochrom, Ltd., Cambrigde Science Park, England) and detection was carried out by a postcolumn derivatized with ninhydrin reagent followed by measuring absorbance at 440 (proline) or 570 nm (all other amino acids).

Glucose measurement
Separation of sugars was achieved using a CarboPac PA 1 column 4 × 50 mm (Dionex Corporation, USA) as precolumn followed by a CarboPac PA 1 column 40 × 250 mm (Dionex , USA) with 160 mM NaOH as mobile phase. Detection and quantification was performed with an amperometric impulse-detector (Electrochemical detector ED 50 Dionex, Germany).

Organic acids measurement
The concentration of organic acids in the supernatant was determined by HPLC. A Dionex ICS-1000 ion chromatography system with a IonPac ICE-AS6 (250 × 9 mm) column (Dionex, USA) together with an anionic micromembrane suppressor AMMS ICE (Dionex, USA) were used for detection of organic acids. The eluent used was 0.4 mM heptaflurobutyric acid and 12 mM tetrabutylamonium hydroxide was used as reagent. The operation conditions used were as follows: sample volume 20 µL; system backpressure 800 psi; background conductance 14~16 µS; effluent flow rate 1 mL/min and reactant flow rate 1 mL/min. Samples were measured for the presence of lactate, acetate, malate and succinate.

Analysis of the ^{13}C-labeling patterns
The labeling patterns of the amino acids incorporated into the biomass were analyzed by GC-MS, and the labeling patterns of the central metabolites were subsequently deduced from the knowledge of the biochemical relationship between precursors and amino acids (Christensen and Nielsen, 1999a; Marx *et al.*, 1996). The biomass used for analysis was harvested by centrifugation and washed twice with 50 mM Na_2HPO_4 buffer containing 0.9% (w/w) NaCl, pH adjusted to 7.0 with HCl. Approximately 15 mg biomass (dry) was hydrolyzed using 600 µL 6 M HCl at 105°C for 16 h. After hydrolyzation the sample was centrifuged and the supernatant was transferred into vials and dried at 105°C. The dried sample was dissolved in 1 mL dH_2O, and the sample was extracted by solid phase extraction adding the entire sample to a Dowex cation exchange column containing 100 mg dowex exchange resin (50W x 8 – 400) dissolved in 50% (w/w) glycerol. The sample was slowly allowed to pass through the resin allowing the resin to dry out. After this the resin was washed with 1 mL 50% ethanol followed by 200 µL 1 M NaOH. The sample was extracted by adding 1 mL extract solution (33.3% ethanol (v/v), 6.7% pyridine and 60% (v/v) of a solution containing 1% NaOH (wt/v) in saline (0.9% NaCl (wt/v)). The amino acid extract was divided into two and used for derivatization by ethylchloroformate or (*N,N*)-dimethylformamide dimethylacetal.

Ethylchloroformate (ECF) derivatization
The amino acid extract was added 50 µL ECF. After the formation of carbon dioxide had ceased the derivatives was extracted adding 200 µL propyl acetate and mixing followed by adding 50 µL 1 M HCl. The oraganic phase was collected for GC-MS analysis.

(N,N)-dimethylformamide dimethylacetal (DMFDMA) derivatization
The amino acid extract was added 200 µL 1 M HCl and dried at 105°C. The dried sample was added 200 µL DMFDMA and 200 µL acetonnitril and vortexed. The samples was derivatized at 100°C for 20 min, and the sample was transferred to -20°C for 10 min. Sample was used for GC-MS analysis.

GC-MS parameters
GC-MS analysis was done on an Agilent (palo Alto, CA, USA) HP 6890 gas chromatograph coupled to a HP 5973 quadruple mass selective detector in positive electron impact ionization (EI^+) using an electron energy of 70 eV. The GC was equipped with a 4.0 mm i.d. Siltek gooseneck splitless deactivated liner (Restek, Bellefonte, PA, USA), and a Supelco (Bellefonte, PA, US) SLB-5 MS column, 15 m, 0.25 mm i.d., 0.25 µm film. Helium of a purity of 99.999% was used as carrier gas at a constant linear gas velocity 35 cm/ s. Transfer line temperature was 280ºC, quadruple temperature 150ºC and MS source 200ºC. The GC-MS system was controlled from Agilent MSD Chemstation v. D.01.02.16.

For ECF derivatives the following method was used: The oven temperature was initially held at 75°C for one min. Hereafter the temperature was raised with a gradient of 40°C min^{-1} until 165°C. Then 4°C until 190°C and 40°C upto 240°C. At the end, temperature was increased to 260°C with a gradient of 4°C min^{-1} and held constant for 4 minutes. The flow through the column was held constant at 1.3 mL He min^{-1}. Temperature of the inlet, 200°C. Interface temperature, 280°C.Quadrupole temperature, 105°C.

DMFDMA derivatives was measured using the following method: The oven temperature was initially held at 60°C for one min. Hereafter the temperature was raised with a gradient of 20°C min^{-1} until 130°C. Then 4°C until 150°C and 40°C upto 260°C and held constant for 4.25 minutes. The flow through the column was held constant at 1 mL He min^{-1}. Temperature of the inlet, 230°C. Interface temperature, 270°C.Quadrupole temperature, 105°C.
For all the above methods, samples of 1 µL were injected in the splitless (30 sec, split 1:20) mode at 200ºC using hot needle.

In the mass spectrometer, the derivatives were ionized and subsequently fragmented, and the mass distribution of each individual fragment was measured (Christensen and Nielsen, 1999a). From the abundance of the measured peaks in the mass spectrum, the summed fractional labelling (SFL) of each fragment was calculated using (eq. 1), where m_i is the abundance of the (m+i)-mass isotopomer and n is the total number of carbon atoms in the fragment. The calculated SFL was corrected for the occurrence of naturally labeling from other atoms (Wittmann and Heinzle, 1999).

$$SFL = \frac{\sum_{i=0}^{n} i \cdot m_i}{\sum_{j=0}^{n} m_j} \cdot 100\% \qquad (1)$$

The calculated SFLs were used to analyze the metabolic network.

Amino acid uptake
The amino acid uptake from the complex medium was measured using the concept of reciprocal labeling (Christensen, 2001). Here the 32%[U-$^{13}C_6$]glucose and 68% naturally labeled glucose was used as substrate. The fraction of amino acids taken up from the complex medium could be calculated from eq. 2.

$$Uptake(\%) = \frac{32.75 - \frac{SFL}{n}}{32.75 - 1.11} \cdot 100\% \qquad (2)$$

Here *n* is the number of carbon atoms in the fragment measured. The labeling from naturally labeled sugar is 1.11%, so the labeling of a carbon atom completely synthesized *de novo* from glucose is 32.75%.

Table 6.1: Medium and yield coefficients for cultivations in this study

Strain	Phase	Substrate	μ (h^{-1})	Y_{sp} (g g^{-1})	Y_{sx} (g g^{-1})
ATCC 21253	Batch	[1-^{13}C]glucose	0.51	0	0.51
ATCC 21253	Fed-Batch	[1-^{13}C]glucose	0	0.24	0.04
ATCC 21253	Batch	[U-$^{13}C_6$]glucose	0.50	0	0.50
KK-11	Batch	[1-^{13}C]glucose	0.28	0.21	0.31
KK-11	Fed-Batch	[1-^{13}C]glucose	0.03	0.37	0.21
KK-11	Batch	[U-$^{13}C_6$]glucose	0.28	0.21	0.31

Estimation of metabolic fluxes

The flux distribution of the metabolic network was estimated from metabolite and ^{13}C balancing (Christensen and Nielsen, 1999a; Marx *et al.*, 1996). The inputs to the model included biomass yield (see table 6.1), lysine yield (see table 6.1), biomass composition (Wittmann and de Graaf, 2005), and the labeling patterns of amino acids not taken up from the medium (see table 6.2). The complete metabolic network is given in figure 6.1.

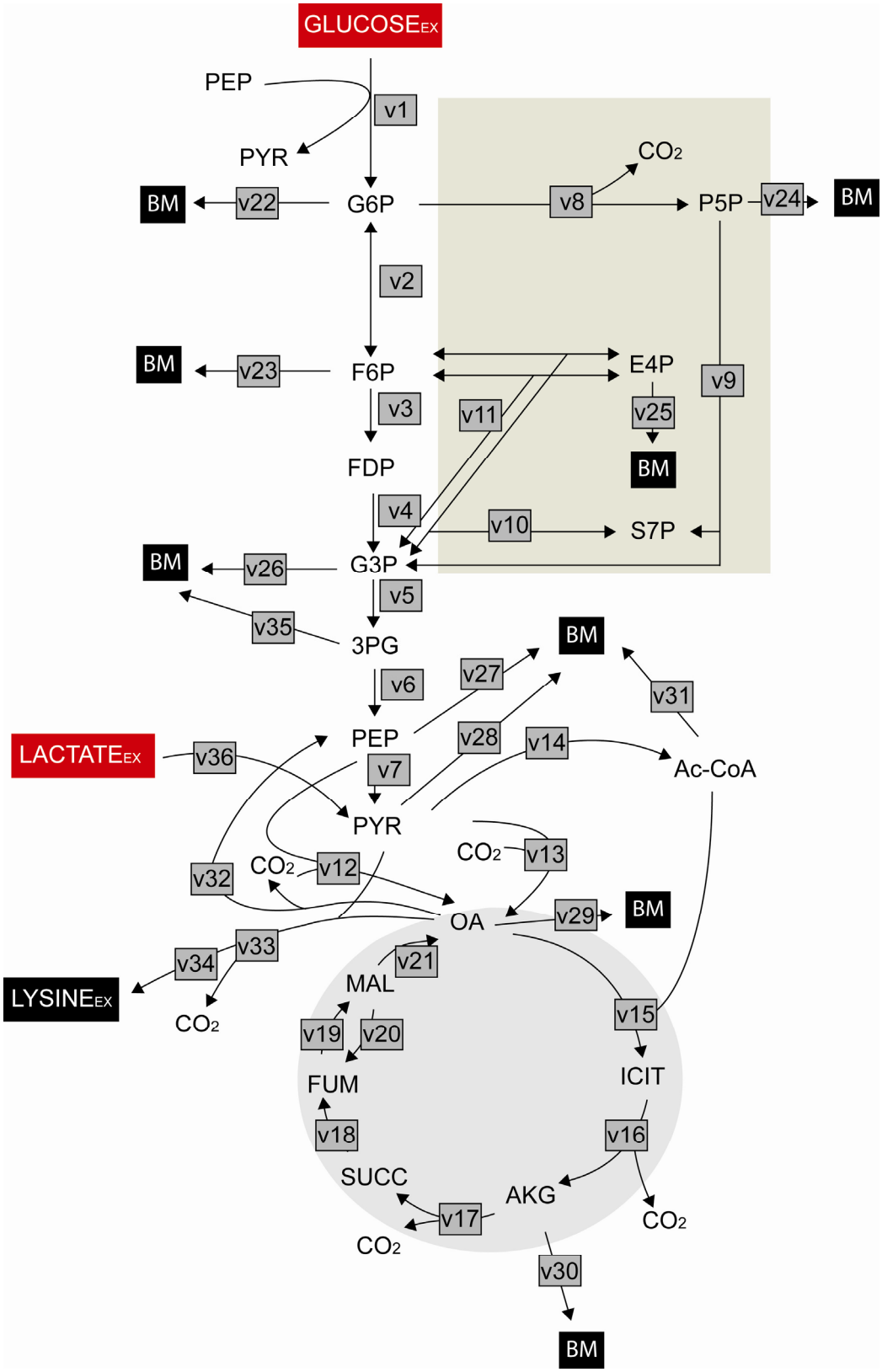

Figure 6.1: Metabolic network of *C. glutamicum*, including uptake of lactic acid and excretion of lysine. Abbreviations: $GLUCOSE_{EX}$: external glucose; G6P: glucose-6-phosphate; F6P: fructose-6-phosphate; P5P: pentose-5-phosphate; E4P: erythose-4-phosphate; S7P: sedoheptulose-7-phosphate; FDP: fructose-1,6-bisphosphate;G3P: glyceraldehyde phosphate; 3PG: 3-phosphoglycerate; PEP: phosphoenolpyruvate; PYR: pyruvate; Ac-CoA: acetyl CoA; ICIT: isocitrate; AKG: α-ketogluterate; SUCC: succinate; FUM: fumerate; MAL: malate; OA: oxaloacetate; $LYSINE_{EX}$: external lysine; $LACTATE_{EX}$: external lactic acid; BM: biomass drain.

Table 6.2: Percentage of amino acids taken up from the medium and amino acids available in medium of total amino acids in biomass during exponential growth in complex medium

Amino acid	Ion cluster and derivatives	ATCC 21253		KK-11	KK-11
		Uptake (%)	Available in medium (%)*	Uptake (%)	Available in medium (%)*
Alanine	ECF: Ala 116; DMFDMA: Ala 99, Ala 158	7.2 ± 3.2	32	7.7 ± 1.5	20
Aspartate	ECF: Asp 188; DMFDMA: Asp 115, Asp 216	2.6 ± 1.6	0	0.1 ± 1.1	0
Glutamate	DMFDMA: Glu 143, Glu 230	2.5 ± 1.5	1	0.8 ± 1.6	0
Glycine	ECF: Gly 175; DMFDMA: Gly 144, Gly 85	0	6	1.8 ± 2.5	6
Isoleucine	ECF: Ile 158	64.6	11	27.8	7
Leucine	ECF: Leu 158	100	94	41.4	58
Lysine	ECF: Lys 156	2.8	1	0	1
Phenylalanine	ECF: Phe 192; DMFDMA: Phe 143	12.2 ± 23	21	13.0 ± 17	13
Proline	ECF: Pro 142	24.4	46	14.8	28
Serine	ECF: Ser 132	0	8	0	5
Threonine	ECF: Thr 146, Thr 175	94.9 ± 6.8	201	31.7 ± 3.8	124
Valine	ECF: Val 144; DMFDMA: Val 127, Val 143, Val 186	18.0 ± 1.0	15	6.1 ± 1.3	9

*: Available amino acid in medium = ((mg amino acid available in the medium)·(mg amino acid incorporated in biomass)$^{-1}$)·100%

Results

Cultivation of C. glutamicum ATCC 21253 and KK-11

The cultivation profiles of lysine fermentation with *C. glutamicum* ATCC 21253 and *C. glutamicum* KK-11 is displayed in figure 6.2 and growth rates and yield coefficients are shown in table 6.1. The fermentations were divided into two phases: A batch phase with high growth and low lysine production, and a fed-batch phase with low growth and high lysine production. The two phases are separated by a black line (Figure 6.2). Growth for both strains was exponential in the first part of the fermentation, and for KK-11 exponential growth was seen for the entire batch phase with a growth rate of 0.28 hr^{-1}. For ATCC 21253 two distinct growth phases were observed in the batch phase, where a maximum growth (μ = 0.51 hr^{-1}) was seen from start to around 10 hours. After this a significant decrease in growth was seen as the growth rate in this period was 0.08 hr^{-1}. The change in growth correlated with the depletion of leucine, methionine and threonine from the medium (data not shown). The continuing growth after the depletion of these essential amino acids can be explained by the use of endogenous threonine and methionine for growth (Vallino and Stephanopoulos, 1993). For KK-11 the biomass concentration decreased slowly from 4.8 g DCW · kg^{-1} to 2.5 g DCW · kg^{-1} during the fed-batch phase due to dilution. When the data were corrected for dilution, a specific growth rate of 0.03 hr^{-1} was observed. For ATCC 21253 the biomass concentration was lowered from 5.8 g DCW · kg^{-1} to 2.5 g DCW · kg^{-1} in the fed-batch phase, which approximately corresponded to the dilution, and hence there was no significant growth in this period. In this period leucine, threonine and methionine was depleted which could explain the low growth in this phase. Lysine excretion was seen for the whole fermentation for the KK-11-cultivation, and the final lysine,HCl titer reached 4.3 g · kg^{-1}, which corresponded to a lysine yield of 0.31 g lysine, HCl · g $glucose^{-1}$. For the ATCC 21253-cultivation lysine excretion was first initiated when leucine was depleted from the medium after 10 hours. Lysine excretion was

increased when the fed-batch phase was started, and the final lysine,HCl titer reached 2.5 g · kg^{-1} corresponding to a lysine yield of 0.16 g lysine, HCl · g $glucose^{-1}$ at the end of the fermentation. No significant byproduct formation was observed during the cultivations, and lactic acid present in the batch medium (0.4 g · kg^{-1}) was depleted during the exponential phase for both strains (data not shown).

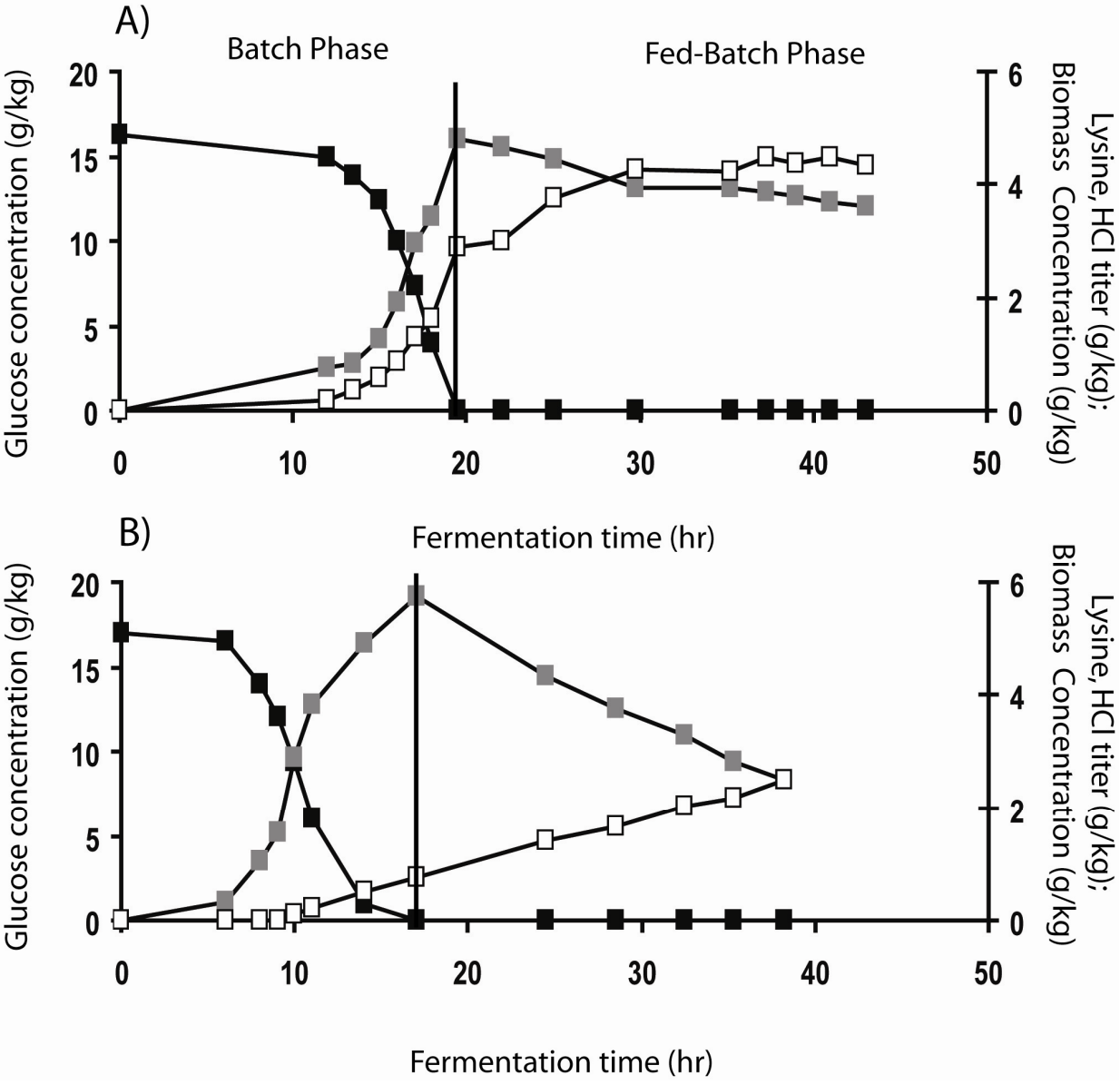

Figure 6.2: Fermentation profile for fed-batch cultivations with the high producing strain *C. glutamicum* KK-11 (A) and the low producing strain *C. glutamicum* ATCC 21253. Black squares: Glucose concentration (g/kg); Grey squares: Biomass concentration (g DCW/kg); White squares: lysine,HCl concentration (g/kg).

Amino acid uptake in complex medium

Amino acids taken up from the medium during the batch phase were identified in cultivations using 32%[U-$^{13}C_6$]glucose and 68% naturally labeled glucose was as substrate. From the calculated

labeling patterns (eq. 1) the uptake of twelve amino acids could be calculated using eq. 2, and the results are shown in table 6.2. To account for the differences in availability of the different amino acids it was calculated how much of each individual amino acid was taken up normalized to the availability of the amino acid (Table 6.2).Most amino acids present in significant amounts were taken up by both strains although it was seen that the different amino acids were taken up at different ratios. The three amino acids aspartate, lysine and glutamate were not taken up by any of the strains. This was expected since these amino acids were not present in significant amounts in the medium (Table 6.2). Glycine and serine were both present in small amounts in the medium, but no uptake of these amino acids was seen. The uptake of valine and phenylalanine corresponded with the available amino acids in the medium for both stains, indicating that these amino acids were fully utilized. For the two amino acids alanine and proline, only part of the proteinoic amino acid pool originated from the complex medium, 20% and 35% of alanine and 52% and 53% of proline originated from the medium for ATCC 21253 and KK-11, respectively. One possible explanation could be that both amino acids can serve as nitrogen donors for *C. glutamicum* (Burkovski, 2005) i.e. the amino acids can be metabolized via a transaminase reactions yielding ammonia and pyruvate or α-ketogluterate. If this was the case we would expect to see changes in the labeling patterns of pyruvate and α-ketogluterate due to the contribution of unmarked carbon from the breakdown products. Such changes could not be recognized from the data since glutamate (originated from α-ketogluterate) and lysine (originated from pyruvate) were completely synthesized from ^{13}C-glucose. For ATCC 21253 all proteinoic leucine and threonine was taken up from the medium, which was expected since these amino acids are essential for this strain. For the same strain isoleucine uptake was 587% of the available isoleucine in the medium. This very high uptake of isoleucine in this strain could be explained by the fact that isoleucine in *C. glutamicum* is synthesized from threonine by the incorporation of a pyruvate molecule (Möckel *et al.*, 1992). This way most proteinoic isoleucine originated from unlabelled threonine and labeled pyruvate originating from the ^{13}C-labeled glucose. The high producing strain KK-11 partly synthesized (68%) and partly took up (32%) threonine, although this amino acid was present in high amounts in the medium. This was also the case for leucine and isoleucine where 41% of the leucine pool of the biomass was taken up from the medium. For isoleucine a significant amount originated from unlabeled threonine, however the majority of the proteinoic isoleucine was synthesized *de novo* from glucose.

Table 6.3: Summed fractional labelling of biomass components in batch culture of ATCC 21253 and KK-11 grown on [1-^{13}C]glucose in CSL based complex medium.

		ATCC 21253		KK-11	
Ion Cluster	Precursor	Measured SFL	Estimated SFL	Measured SFL	Estimated SFL
Lysine 156	OAA{2,3,4}; PYR{2,3}	83.4	85.5	73.6	74.7
Aspartate 188	OAA{2,3,4}	51.3	52.7	45.3	48.7
Aspartate 216	OAA{1,2,3,4}	58.7	61.7	55.3	56.0
Aspartate 115	OAA{2}	11.1	10.9	11.5	11.2
Glycine 144	G3P{1,2}	4.4	4.7	4.4	4.4
Glycine 175	G3P{2}	5.3	4.7	-	-
Glycine 85	G3P{2}	-	-	1.8	1.7
Serine 132	G3P{2,3}	34.5	34.3	28.4	27.9
Glutamate 230	AKG{1,2,3,4,5}	85.1	85.5	76.6	74.7
Glutamate 143	AKG{1,2}	42	41.8	40.2	37

Flux distribution during exponential growth in complex medium

The metabolic network applied contains the glycolysis, the pentose phosphate pathway and the TCA cycle. The anaploresis is represented by pyruvate carboxylase, phosphoenolpyruvate carboxylase and phosphoenolpyruvate carboxykinase. In addition to these anaplerotic reactions malic enzyme and oxaloacetate decarbyxylase have also been reported in *C. glutamicum*, however based on biochemical evidence the activity of these reactions during growth on glucose are low or absent (Petersen *et al.*, 2000) why these reactions were not included in the network. The metabolic flux distributions in the batch phase of fermentations using 99% [1-C^{13}]glucose in complex medium were estimated from SFLs of fragments of aspartate, glutamate, lysine, serine and glycine (Table 6.3). These amino acids were not taken up in significant amounts by any of the strains used in this study, and therefore they were synthesized *de novo* from the labeled glucose. The lactic acid contribution from the CSL was also included in the model. Lactic acid is entering the central metabolism of *C. glutamicum* as pyruvate, and an irreversible flux from lactic acid to pyruvate was therefore included into the model taking the contribution of unlabelled pyruvate into account. That all SFLs were based on samples in isotopic steady state was ensured by analyzing three independent samples in the exponential phase. For all SFL-data used for the flux estimation deviations were found to be lower than 0.5% (absolute)(data not shown) indicating the presence of an isotopic steady state. The estimated flux distributions are given in figure 6.3. All fluxes are given relative to 100 mol of glucose taken up. The standard deviation for the SFLs was set to 0.05 in the model, and most estimations were within the range of this standard deviation. The estimated SFLs from the glycine ioncluster were in some cases not within the standard deviation. These values were low why an experimental error can not be excluded. The sensitivity of these values were tested and it was concluded that flux distributions only were changed marginally (1-2% absolute) when the SFLs were changed ±10% (Data not shown). Estimated and measured SFLs for the glutamate 143 and aspartate 188 ion clusters were also found to differ for KK-11 cultivations. Sensitivity test showed that ±10% (relative) of these fragments did not change the flux distributions significantly (data not shown).

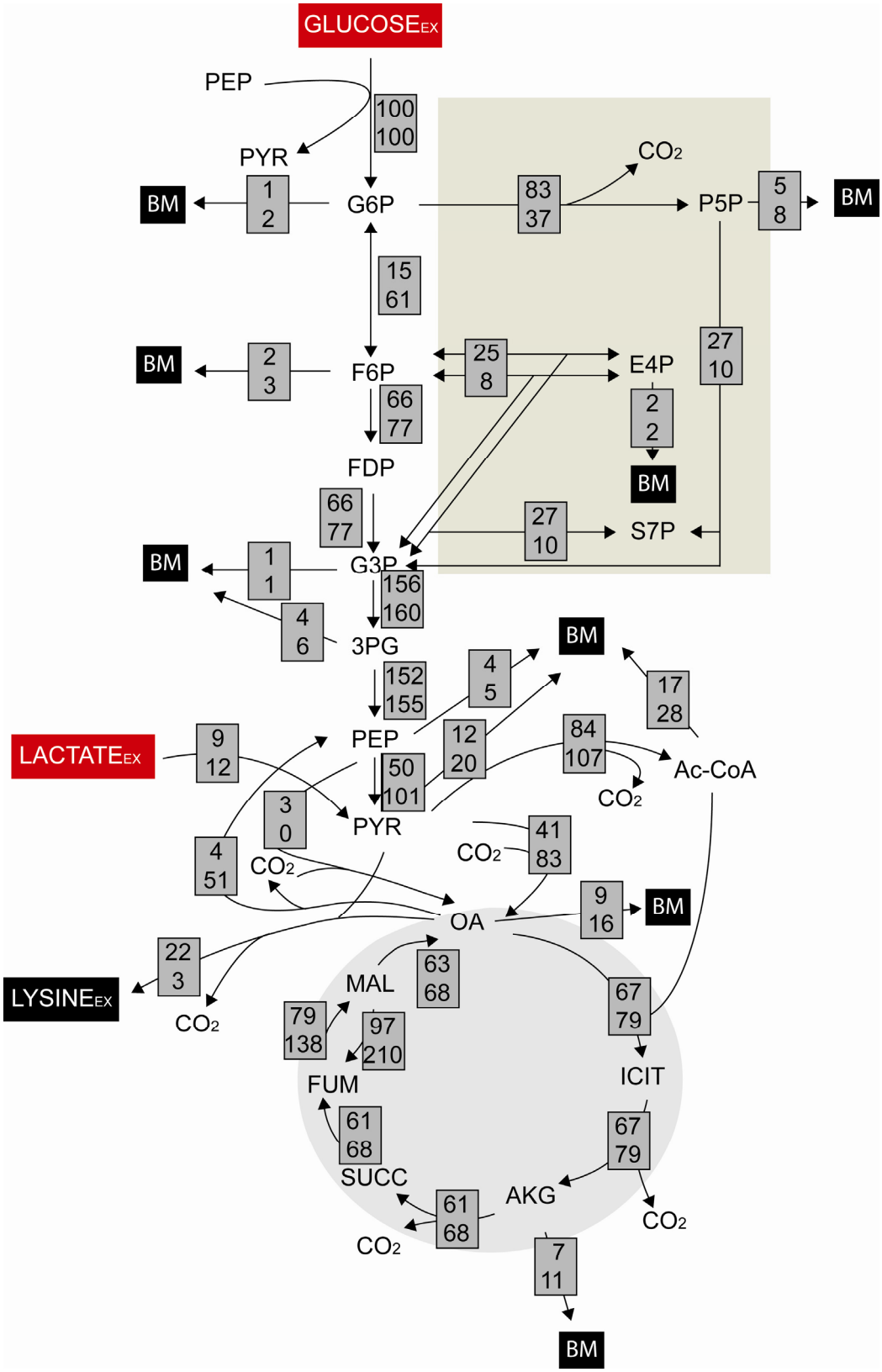

Figure 6.3: Carbon flux distributions in the central part of *C. glutamicum* KK-11 and *C. glutamicum* ATCC 21253 (displayed in that order from top to bottom) during low lysine production and high specific growth of the batch phase. Results are estimated from the best fit to experimental data for combined metabolite balancing and isotope balancing using metabolite data in table 1 SFL-data in table 3, and biomass requirement data from Witmann and de Graff (2005). Flux estimations are normalised to glucose uptake (1.10 mmol glucose · g DCW^{-1} and 0.66 1.10 mmol glucose · g DCW^{-1}). For abbreviations see figure 6.1.

Fluxes at the glucose-6-phosphate node into glycolysis and pentose phosphate pathway
As shown in figure 6.3 a significant difference in flux distribution around the glucose-6-phosphate node was seen between the two *C. glutamicum* strains KK-11 and ATCC 21253. For the high producing strain KK-11 the flux through the pentose phosphate pathway was 83% and the glycolytic flux was 15%. The pentose phosphate pathway flux reported here is significantly higher than what is generally reported in literature. Wittmann and Heinzle (2002) reported pentose phosphate fluxes between 57% and 64% for various lysine producing strains, and Wittmann and Heinzle (2001) reported a pentose phosphate flux of 71% for ATCC 21253 in the lysine producing phase. The higher pentose phosphate pathway flux reported here may be explained by lack of, or reduced control of, the pentose phosphate pathway flux in this highly mutagenized strain. In the wild type the activity of both NADPH generating enzymes glucose-6-phosphate dehydrogenase and 6-phosphogluconate dehydrogenase are inhibited by NADPH (Moritz *et al.*, 2000). Mutations reducing this inhibition resulting in a increased flux through the pentose phosphate pathway have earlier been identified for both glucose-6-phosphate dehydrogenase (Becker *et al.*, 2007) and 6-phosphogluconate dehydrogenase (Ohnishi *et al.*, 2005). For ATCC 21253 the pentose phosphate pathway flux was 37% and the flux through the glycolysis was 61%. ATCC 21253 have been studied earlier and pentose phosphate pathway fluxes have been observed to be 56% (Wittmann and Heinzle, 2002) and 71% (Wittmann and Heinzle, 2001a) under lysine production. In the present study samples were taken just before the lysine production phase had initiated and when growth rate was at maximum, and the lysine yield was therefore low compared to the studies mentioned above. Using the same technique as applied here pentose phosphate pathway fluxes of 40% and 36% have been reported in the *C. glutamicum* wild type strain ATCC 13032 (Sonntag *et al.*, 1995) and the non-excreting strain *C. glutamicum* LE4 strain (Marx *et al.*, 1997) corresponding well with the values found here. In both strains the carbon flux into the pentose phosphate pathway was much higher than the anabolic demands of the pentose phosphate pathway intermediates erythose-4-phosphate and ribose-5-phosphate. Most of the carbon was therefore redirected back into the glycolytic pathway at the level of fructose-6-phosphate and glycaldehyde-3-phosphate. Although a significant difference was observed at the upper level of the glycolysis it was seen that at the lower part of the glycolysis between 3-phosphoglycerate and phosphoenolpyruvate the two strains revealed very similar fluxes with 152% and 155% for KK-11 and ATCC 21253, respectively.

Fluxes around the pyruvate node
As pyruvate is one of the key metabolites in *C. glutamicum* the fluxes around this compound is important when analyzing the metabolic network. Pyruvate connects glycolysis, the TCA cycle, anaplerosis, anabolic reactions and lysine synthesis. The pyruvate yielding fluxes included in this model were lactate uptake (v36 – figure 6.1) and the two phosphoenolpyruvate converting reactions pyruvate kinase (v7 – figure 6.1) and the PTS glucose uptake system (v1). The major difference between the two strains was a significant higher flux from phosphoenolpyruvate to pyruvate, 101% for the ATCC 21253 strain compared to 50% for KK-11, mediated by the pyruvate kinase flux. The higher flux was connected to an ATP-consuming futile cycle, where pyruvate was converted to oxaloacetate (83%) and oxaloacetate was further converted to phosphoenolpyruvate (51%) corresponding to the difference seen for pyruvate kinase flux. Such a futile cycle have been reported for numerous lysine producing and non-producing strains (Krömer *et al.*, 2004; Marx *et al.*, 1996; Wittmann and Heinzle, 2001a; Wittmann and Heinzle, 2001b). Surprisingly the flux of this cycle was much lower for the high producing strain, where only a decarboxylating flux of 4% was observed. As a result the anaplerotic netflux for KK-11 was higher (41+3-4 = 40%) than it was the case for ATCC 21253 (83+0-51 = 32%). It is generally accepted that there is a correlation between a high anaplerotic netflux and a high lysine production (Kjeldsen and Nielsen, 2008), a correlation

which is also seen when these two strains are compared. For both strains the major carboxylating reaction was pyruvate carboxylase (v13 – figure 6.1) contributing to more than 90% of the carboxylation for KK-11 and 100% for ATCC 21253. This is in agreement with earlier findings for this organism (Petersen *et al.*, 2000).

TCA cycle
The low producing strain ATCC 21253 exhibited a flux of 79% entering the TCA cycle, whereas the high producing strain KK-11 showed a significant lower value of 67% (figure 6.3). The reduced growth for the high producing strain KK-11 compared to the low producing strain is reflected in the lower TCA flux, thus adapting to the lower anabolic- and ATP-demand. Instead a higher oxaloacetate demand for lysine synthesis mediated a higher anaplerotic netflux.

NADPH balancing
From the obtained information on the metabolic flux distribution a balance for NADPH formation and consumption can be set up. As previously shown there are three major NADPH generating reactions in *C. glutamicum* during cultivation on glucose: glucose-6-phosphate dehydrogenase (Sugimoto and Shiio, 1987a), 6-phosphogluconate dehydrogenase (Sugimoto and Shiio, 1987b) and isocitrate dehydrogenase (Eikmanns *et al.*, 1995). This leads to a NADPH formation of 83 + 83 + 67 = 233% for the high producing strain KK-11, and 37 + 37 + 79 = 153% for the low producing stain ATCC 21253. NADPH is required for growth and for lysine production. With a demand of 16.429 mmol NADPH · (g biomass)$^{-1}$ (Wittmann and de Graaf, 2005) and biomass yields of 54.3 g · (mol glucose)$^{-1}$ and 90.5 g · (mol glucose)$^{-1}$ for KK-11 and ATCC 21253, respectively and with a demand of four NADPH for one molecule of lysine the NADPH demand for KK-11 is 176% and for ATCC 21253 it is 156%. This leads to a NADPH excess of 57% for the high producing strain KK-11. Similar findings have been reported in other lysine producing strains (Krömer *et al.*, 2004; Wittmann and Heinzle, 2001a; Wittmann and Heinzle, 2002). For ATCC 21253 the NADPH balance almost closed with a deficit of only 3%.

Flux estimation during fed-batch fermentation
The labeling patterns of the proteinoic amino acids of the biomass are used for flux estimations. Since the labeling patters of the protein pool changes relatively slowly compared to physiological responses of the cells, an error occurs when making flux estimations on non-steady state cultures with non-constant physiological behavior. However, the labeling patterns of the proteinoic amino acids formed after a metabolic shift due to changes in physiological behavior will be reflected in the labeling patterns of the combined pools of “old” and “new” protein. Using the generally applied method for flux estimations as used earlier for the batch cultivations, samples taken at different parts of the fed-batch phase were analyzed. As samples taken in the fed-batch phase are not steady state samples, the *in vivo* fluxes estimated do not represent the real fluxes, but they do point to trends in changes in the metabolism. Flux estimations using this strategy have earlier been termed “integrated fluxes” (Jonsbu *et al.*, 2001).

Integrated fluxes through the central carbon metabolism
Three integrated fluxes related to central carbon metabolism were analyzed to see the effect of the change from high specific growth and low lysine production to low specific growth and high lysine production as seen in table 6.1. The fluxes evaluated were the pentose phosphate pathway, the anaplerotic netflux, and the flux through the TCA cycle (Figure 6.4A and Figure 6.4B). For the fluxes presented here a smooth development in the fluxes was generally observed indicating that the metabolic changes due to the physiological change were constant. For the high producing strain

KK-11 a 1.1-fold increase in the pentose phosphate pathway flux was seen so the integrated flux was 91% at the last part of the fed-batch phase (Figure 6.2A). For the low producing strain ATCC 21253, a 1.4 increase in the pentose phosphate pathway flux was seen as a consequence of the physiological change of the culture so an integrated flux of 51% was seen at the end of the fed-batch phase (Figure 6.4B). The TCA cycle flux for KK-11 was decreased 1.2-fold so the flux at the end of the fed-batch phase was 72%, and the anaplerotic netflux increased 1.1-fold. For ATCC 21253 the TCA flux increased 1.2 fold and the anaplerotic netflux decreased 1.3 fold. The increase in the pentose phosphate pathway flux as a consequence of the change in physiological state of the culture seen for both strains was thought to be a consequence of the decreased growth rate lowering the requirement for ATP and precursors for biomass synthesis. Earlier work on profiling lysine fermentations has shown results which are inconsistent with our findings. Batch-cultures of ATCC 21253 was analyzed throughout a fermentation by metabolite balancing (Vallino and Stephanopoulos, 1993), and fluxes were found to fluctuate throughout the fermentation, so the pentose phosphate pathway flux increased from 25% when no lysine was produced to 69% when the lysine production phase had just initiated and then dropped to 40% at the later lysine production phase. In another study batch cultures of *C. glutamicum* ATCC 13237 was analyzed by metabolite balancing and isotopomer modeling throughout a lysine fermentation (Krömer *et al.*, 2004). They found that the pentose phosphate pathway flux decreased from 72% to 52% when the fermentation changed from high growth and no lysine production to low specific growth and lysine production. Further, they found that the TCA cycle flux decreased from 70% to 53%, and from 69% to 46% and

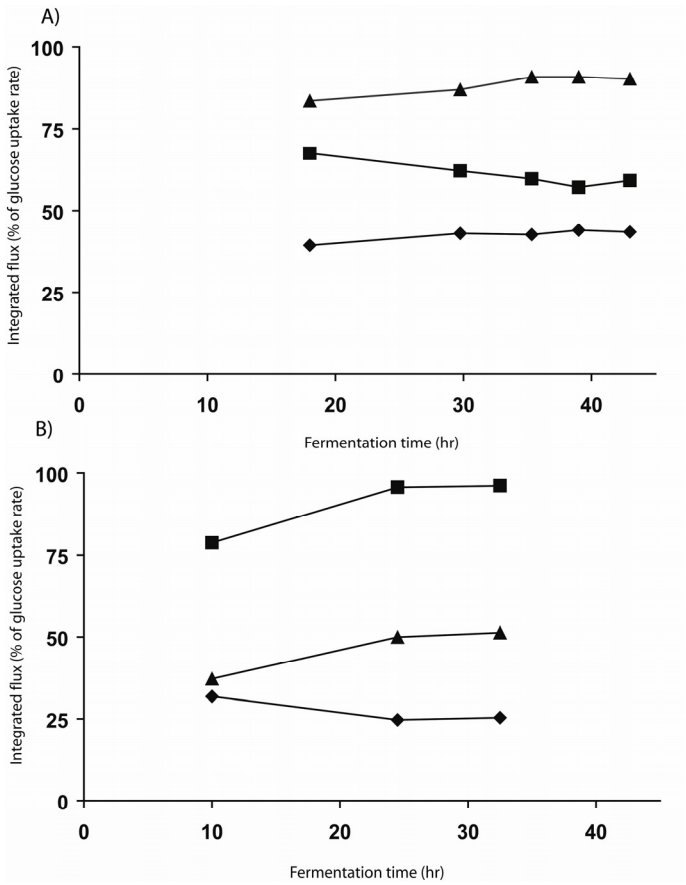

Figure 6.4: Integrated fluxes through the central carbon metabolism of two *C. glutamicum* strains. A) *C. glutamicum* KK-11. B) *C. glutamicum* ATCC 21253. Squares: Pentose phosphate pathway flux; Triangles: TCA flux; Diamonds: Anaplerotic netflux.

back to 70% in the study of Vallino and Stephanopoulos (1993). The major differences between the data of Krömer et al. (2004) and Vallino and Stephanopoulos (1993) and the data presented in this paper are the different fermentation strategies applied, and the use of complex medium. In this paper carbon limited fed-batch is applied to avoid the production of byproducts often seen under batch cultivations, which is expected to change the *in vivo* flux distribution. In addition to this the use of complex medium is likely to affect the metabolic fluxes. Both factors may explain the differences seen between earlier published data and the data in this paper. Another explanation for the inconsistence between data presented here and earlier findings could be that the data presented here are integrated fluxes, and is therefore an average of the whole fermentation and not a snapshot of the present in vivo fluxes at a given time as seen for the data of Vallino and Stephanopoulos (1993) and Krömer et al. (2004). When comparing the two strains KK-11 and ATCC 21253 the development in the TCA flux and anaplerotic netflux were found to be different. For KK-11 the development was expected since an increase in lysine production is generally known to decrease TCA cycle flux and increase the anaplerotic netflux (Kjeldsen and Nielsen, 2008). However, for ATCC 21253 this was not the case under these conditions. Previously a rigid regulation of the carbon flux at the oxaloacetate node in a lysine producing ATCC 21253 strain in continuous culture was observed, demanding a higher TCA flux under conditions where oxaloacetate demand was increased (Kiss and Stephanopoulos, 1991). The oxaloacetate demand was in fact increased 1.1-fold through for the cultivations in this study. Later work on batch cultures of ATCC 21253 and related strains did not show a rigid oxaloacetate node (Wittmann and Heinzle, 2002). However, as pointed out by Wittmann and Heinzle (2002) the metabolic regulation in *C. glutamicum* might be different under the conditions of reduced growth in batch cultures compared to that of continuous culture. And this may also be the case when compared to data from fed-batch cultures. When evaluating the significant differences between the integrated fluxes of the two strains compared in this study, it needs to be taken into account that it seems possible that different mutations affecting metabolic regulation have been introduced to the two strains during random mutagenesis.

Conclusion

Two strains of *C. glutamicum*, a low producing strain ATCC 21253 and a high producing strain KK-11, were evaluated under batch and fed-batch lysine production in complex medium. The flux distribution values found for the low producing strain were in some cases inconsistent with what have been reported earlier for this strain in batch cultivations in defined medium. This emphasizes the importance of developing methods for *in vivo* flux estimation to be able to understand industrial processes. We were able to identify changes in the central metabolism as a result of the change in physiological state mediated by the change from batch to fed-batch fermentation, changing the culture from high growth-low lysine excretion to low growth-high lysine excretion. Methods for *in vivo* flux estimations in unbalanced systems such as fed-batch or repeated fed-batch systems are needed in order to fully understand these systems. The method presented here can be used to identify tendencies in such systems. The results presented here for an industrial production strain illustrates that significant differences can be seen between industrial production strains and low producing strains.

References

Becker,J., Klopprogge,C., Herold,A., Zelder,O., Bolten,C.J., and Wittmann,C. (2007) Metabolic flux engineering of L-lysine production in *Corynebacterium glutamicum* - over expression and modification of G6P dehydrogenase. Journal of Biotechnology **132**, 99-109.

Burkovski,A. (2005) Nitrogen Metabolim and Its Regulation. In Handbook of *Corynebacterium glutamicum* (Edited by Eggeling,L. and Bott,M.) pp. 333-350. CRC Press, Boca Raton.

Christensen,B. (2001) Metabolic Network Analysis: Principles, Methodologies and Applications. PhD-Thesis - BioCentrum-DTU, Technical University of Denmark, Lyngby.

Christensen,B. and Nielsen,J. (1999a) Isotopomer analysis using GC-MS. Metabolic Engineering **1**, 282-290.

Christensen,B. and Nielsen,J. (1999b) Metabolic network analysis. A powerfull tool in metabolic engineering. Advances in Biochemical Engineering **66**, 209-231.

Christensen,B. and Nielsen,J. (2000) Metabolic network analysis of *Penicillum chrysogenum* using 13C-labelled glucose. Biotechnology and Bioengineering **68**, 652-659.

Christiansen,T., Christiansen,B., and Nielsen,J. (2002) Metabolic network analysis of *Bacillus clausii* on minimal and semirich medium using 13C-labeled glucose. Metabolic Engineering **4**, 159-169.

Eikmanns,B.J., Rittmann,D., and Sahm,H. (1995) Cloning, sequence analysis, expression, and inactivation of the *Corynebacterium glutamicum icd* gene encoding isocitrate dehydrogenase and biochemical characterization of the enzyme. Journal of Bacteriology **177**, 774-782.

Jonsbu,E., Christensen,B., and Nielsen,J. (2001) Changes of *in vivo* fluxes through central metabolic pathways during production of nystatin by *Streptomyces noursei* in batch culture. Applied Microbiology and Biotechnology **56**, 93-100.

Kiefer,P., Heinzle,E., Zelder,O., and Wittmann,C. (2004) Comparative metabolic flux analysis of lysine-producing *Corynebacterium glutamicum* cultured on glucose or fructose. Applied and Environmental Microbiology **70**, 229-239.

Kiss,R.D. and Stephanopoulos,G. (1991) Metabolic characterization of a L-lysine producing strain by continuous culture. Biotechnology and Bioengineering **39**, 565-574.

Kjeldsen,K.R. and Nielsen,J. (2008) *In silico* genome-scale reconstruction and validation of the *Corynebacterium glutamicum* metabolic network. Biotechnology and Bioengineering In Press.

Krömer,J.O., Sorgenfrei,O., Klopprogge,K., Heinzle,E., and Wittmann,C. (2004) In-depth profiling of lysine-producing *Corynebacterium glutamicum* by combined analysis of the transcriptome, metabolome, and fluxome. Journal of Bacteriology **186**, 1769-1784.

Marx,A., de Graaf,A.A., Wiechert,W., Eggeling,L., and Sahm,H. (1996) Determination of the fluxes in the central metabolism of *Corynebacterium glutamicum* by nuclear magnetic resonance spectroscopy combined with metabolite balancing. Biotechnology and Bioengineering **49**, 111-129.
Marx,A., Striegel,K., de Graaf,A.A., Sahm,H., and Eggeling,L. (1997) Response of the central metabolism of *Corynebacterium glutamicum* to different flux burdens. Biotechnology and Bioengineering **56**, 168-180.

Möckel,B., Eggeling,L., and Sahm,H. (1992) Functional and structural analysis of threonine dehydratase from *Corynebacerium glutamicum*. Journal of Bacteriology **174**, 8065-8072.

Moritz,B., Striegel,K., de Graff,A.A., and Sahm,H. (2000) Kinetic properties of the glucose-6-phosphate and 6-phosphogluconate dehydrogenases from *Corynebacterium glutamicum* and their application for predicting pentose phosphate pathway flux in vivo. European Journal of Biochemistry **267**, 3442-3452.

Ohnishi,J., Kakahira,R., Mitsuhashi,S., Kakita,S., and Ikeda,M. (2005) A novel *gnd* mutation leading to increased L-lysine production in *Corynebacterium glutamicum*. FEMS Microbiology Letters **242**, 265-274.

Pedersen,H., Christensen,B., Hjort,C., and Nielsen,J. (2000) Construction and characterization of an oxalic acid non-producing strain of *Aspergillus niger*. Metabolic Engineering **2**, 34-41.

Petersen,S., de Graff,A.A., Eggeling,L., Mollney,M., Wiechert,W., and Sahn,H. (2000) *In vivo* quantification of parallel and bidirectional fluxes in the anaplerosis of *Corynebacterium glutamicum*. Journal of Biological Chemestry **275**, 35932-35941.

Sonntag,K., Schwinde,J.W., de Graaf,A.A., Marx,A., Eikmanns,B.J., Wiechert,W., and Sahm,H. (1995) 13C NMR studies of the fluxes in the central metabolism of *Corynebacterium glutamicum* during growth and overproduction of aminoacids in batch cultures. Applied Microbiology and Biotechnology **44**, 489-495.

Sugimoto,M. and Shiio,I. (1987a) Regulation of glucose-6-phosphate dehydrogenase in *Brevibacterium flavum*. Agricultural and Biological Chemistry **51**, 101-108.

Sugimoto,S. and Shiio,I. (1987b) Regulation of 6-phosphogluconate dehydrogenase in *Brevibacterium flavum*. Agricultural and Biological Chemistry **51**, 1257-1263.

Vallino,J.J. and Stephanopoulos,G. (1993) Metabolic flux distribution in *Corynebacterium glutamicum* during growth and lysine overproduction. Biotechnology and Bioengineering **41**, 633-646.

Wittmann,C. and de Graaf,A.A. (2005) Metabolic flux analysis in *Corynebacterium glutamicum*. In Handbook of *Corynebacterium glutamicum* (Edited by Eggeling,L. and Bott,M.) pp. 277-304. CRC Press, Boca Raton.

Wittmann,C. and Heinzle,E. (1999) Mass spectrometry for metabolic flux analysis. Biotechnology and Bioengineering **62**, 739-750.

Wittmann,C. and Heinzle,E. (2001a) Application of MALDI-TOF MS to lysine-producing *Corynebacterium glutamicum*: A novel approach for metabolic flux analysis. European Journal of Biochemestry **268**, 2441-2455.
Wittmann,C. and Heinzle,E. (2001b) Modeling and experimental design for metabolic flux analysis of lysine-producing *Corynebacteria* by mass spectrometry. Metabolic Engineering **3**, 173-191.

Wittmann,C. and Heinzle,E. (2002) Genealogy profiling through strain improvement by using metabolic network analysis: metabolic flux genealogy of several generations of lysine-producing *Corynebacteria*. Applied and Environmental Microbiology **68**, 5843-5859.

Chapter 7

Conclusion and discussion

In the present PhD project various strategies have been applied in order to pursue the overall goal of improving an industrial L-lysine producing *Corynebacterium glutamicum* strain. The experimental part of the project can be divided into three separate parts all of which are described below.

Reconstruction and analysis of C. glutamicum metabolic network

A mathematical model of the metabolic network of *C. glutamicum* based on genomic information, and based on the wealth of biochemical information which is available for this organism due to its long history as a commercial relevant organism was constructed and validated against earlier published data. The *in silico* model constructed in this study is described in detail in chapter 4, and was made based on the annotated genome of the wild type strain of *C. glutamicum* (ATCC 13032) and published biochemical information on *C. glutamicum*. The model was validated against data from a series of well recognized scientific papers, and the model predictions were found to fit well with experimental data. The model was used to analyze the metabolic network during lysine production, and based on this a number of biological hypotheses were suggested to improve lysine production in *C. glutamicum*. The first prediction made by the model was that a high ATP production under high lysine production resulted in a limitation in lysine production. This was the case at high lysine yield (>55%) and low growth. When ATP was in excess under these conditions the model had to handle this excess energy burning up excess ATP in futile cycles suboptimal for lysine synthesis. Secondly, the model predicted a limitation in lysine production when the succinylase branch of the lysine synthetic pathway was preferred over the dehydrogenase branch. The result was a decrease in maximal theoretical lysine yield from 0.75 mmol lysine · (mmol glucose)$^{-1}$ to 0.57 mmol lysine · (mmol glucose)$^{-1}$ due to a relatively higher activity of the TCA cycle because of the involvement of the TCA intermediate Succinyl-CoA. The higher TCA cycle activity was suboptimal for lysine production because of a loss of carbon due to CO_2 –production. Thirdly, the model predicted a correlation between a high pentose phosphate pathway flux and high lysine production. This correlated well with earlier published data, and increasing the flux through the pentose phosphate pathway by metabolic engineering was chosen as a metabolic engineering strategy. The fourth prediction made from the analysis of the *in silico* model was the correlation between increasing anaplerotic netflux and increasing lysine production. This correlation could also be confirmed from a large number of scientific papers, why this strategy also was chosen for metabolic engineering.

The *in silico* model constructed and presented in this thesis is made from data from various sources based on data from different strains including both lysine producing and non-producing strains. To improve the prediction power of the model and to fit the predictions to a specific strain (i.e. a highly mutagenized production strain) the model needs to be adjusted and improved with data from the specific strain. The data in this respect could be *in vivo* flux data or transkriptomic data made under production relevant conditions. It is believed that by implementing this type of data from the high producing strain used in this study the prediction power will be improved, when the metabolic network is analyzed and when biological hypotheses are tested *in silico*. In this study *in vivo* flux

estimations on the high producing strain was conducted, but, these data were not implemented in the model presented in this thesis as they were first obtained at the end of the PhD study.

Comparison of various metabolic engineering strategies in a high producing C. glutamicum strain

Various metabolic engineering strategies were tested in a high producing *C. glutamicum* strain as described in chapter 5. Based on the findings in the metabolic network reconstruction and based on results reported in literature three parts of the metabolism were selected for metabolic engineering. As predicted by the *in silico* model the pentose phosphate pathway was selected to increase the NADPH formation. The two NADPH generating enzymes glucose-6-phosphate dehydrogenase (*zwf*) and 6-phosphogluconate dehydrogenase (*gnd*) was up-regulated, and both modifications were seen to have a positive effect on lysine yield of 5% and 6%, respectively, indicating that NADPH was in fact limiting under high lysine producing conditions. The enzyme pyruvate carboxylase (*pyc*) was also selected for up-regulations to increase the anaplerotic netflux which is believed to be beneficial for lysine production based on findings in literature and predictions by the *in silico* model. This modification resulted in a decrease in lysine production and did not fit our initial expectations. Five enzymes in the lysine synthetic pathway were selected for up-regulation based on results found in literature. The enzymes were aspartate kinase (*lysC*), dihydrodipicolate syntase (*dapA*), succinylaminoketopimelate transaminase (*dapC*), diaminopimelate epimerase (*dapF*) and lysine permerase (*lysE*). Only the strain with an up-regulated aspartate kinase activity showed a significant effect on the overall lysine yield, and this effect was negative. In this study it was seen that although metabolic engineering strategies had earlier been shown to be beneficial for lysine production in *C. glutamicum* strains, many of these strategies could not be transferred directly to a high producing industrial strain.

In vivo flux estimations under industrial relevant conditions

Estimations of *in vivo* fluxes under growth and lysine production in complex medium and during batch and fed-batch fermentation were conducted. These results are presented in detail in chapter 6. For the industrial strain, *C. glutamicum* KK-11, a higher flux through the pentose phosphate pathway was seen compared to earlier published data. This high flux may be explained by the fact that this highly mutagenized strain can be expected to have mutations not present in low producing strains. In addition to this the role of the complex medium components can affect metabolic fluxes. In addition to flux estimations during balanced growth present in the batch phase of the fermentation, the method was employed on samples from the fed-batch phase of the fermentation. These results were used to identify metabolic changes when the physiological state of the cells was changed. The tendencies identified employing this method was an increase in the pentose phosphate pathway flux, a decrease in the TCA flux, and a increase in the anaplerotic net flux. Another *C. glutamicum* strain, ATCC 21253, earlier used in flux estimation studies was also included in the flux estimation study. This strain was found to have lower pentose phosphate pathway fluxes compared with the industrial strain. And during the change from batch to fed-batch fermentation the tendencies were different than what was seen for the industrial strain. The pentose phosphate pathway flux was increased as seen for the industrial strain, but TCA flux was increased and anaplerotic netflux decreased. These differences are discussed more in detail in chapter 6.

The idea of making metabolic flux estimations under production relevant conditions is quite appealing seen from an industrial point of view, because this will give a true picture of what is

going on in the industry scale fermentation. On the other hand it is not trivial at all to get reliable flux estimation results due to a number of practical challenges. First of all industrial fermentations are typically carried out in complex medium containing complex components such as corn steep liquor, molasses, protein hydrolysates etc. Many of these components will affect the results of the measurements making the basis of the flux estimation, and this needs to be taken into account. In the present study some of these challenges were met by excluding data which were affected by the complex components. However, this limits the number of inputs to the flux model which may affect the accuracy of the flux estimations. Another problem is the fact that flux balance estimations are made during balanced growth which is seen during exponential growth. However, for an industrial scale lysine production process the exponential growth phase is only a small part of the fermentation, and measurements in this phase does not represent the production phase which is the most interesting part from an industrial point of view. In this study the effects of the physiological changes made when the fermentation was changed from batch to fed-batch was analyzed by looking at the integrated fluxes which gave a clear indication on these changes based on the tendencies seen in the development in flux distributions. This approach of course has some limitations since the results reflect an average of the "old" biomass produced before the physiological change and the "new" biomass. The results can therefore not be used to identify the absolute fluxes at a given time-point. Even though there have recently been developed concepts and methods for flux quantification during dynamic growth conditions through measurements of labeling patterns in intracellular metabolites, this is still quite complex due to the turn over of both protein and transaminase reaction involving amino acids and keto-acids.

The *in vivo* flux distribution estimations found for the industrial production strain can be used to improve the *C. glutamicum in silico* metabolic model presented in this study to fit the industrial production strain used in this study.

Industrial relevance of project

In this industrial PhD-project a number of industrial relevant problems have been addressed. The main purpose of the project was to improve a *C. glutamicum* industrial production strain. To pursue this goal the above mentioned methods were applied. Each of these methods has earlier been applied on *C. glutamicum* or other organism. In this study the three methods has been unified to form a strategy for strain improvement (Figure 7.1). Using the constructed *in silico* metabolic model biological hypotheses can be tested and predictions can be used to propose metabolic engineering strategies. These strategies can be tested using metabolic engineering followed by an evaluation of the effects on lysine production of the metabolic engineering strategies making fermentations, simulating production scale fermentation conditions. In addition to this the development of a method for estimating *in vivo* metabolic fluxes under production-like conditions gives a direct measure for the effect of the introduced modification on the metabolic flux distribution, and these results can be used to improve the *in silico* model. As seen in figure 7.1 all three parts are connected and it is the idea that by continuing this process the metabolic model will be improved, the predictions will be improved and at the end an improved production strain will be the result.

Another challenge which has been addressed is the use of complex medium, which is generally applied in industry scale fermentations. As mentioned above a number of problems can be identified using complex based medium. In this study metabolic flux estimations were conducted in complex medium, and this represents a major new contribution to the field of flux analysis of lysine producing strains.

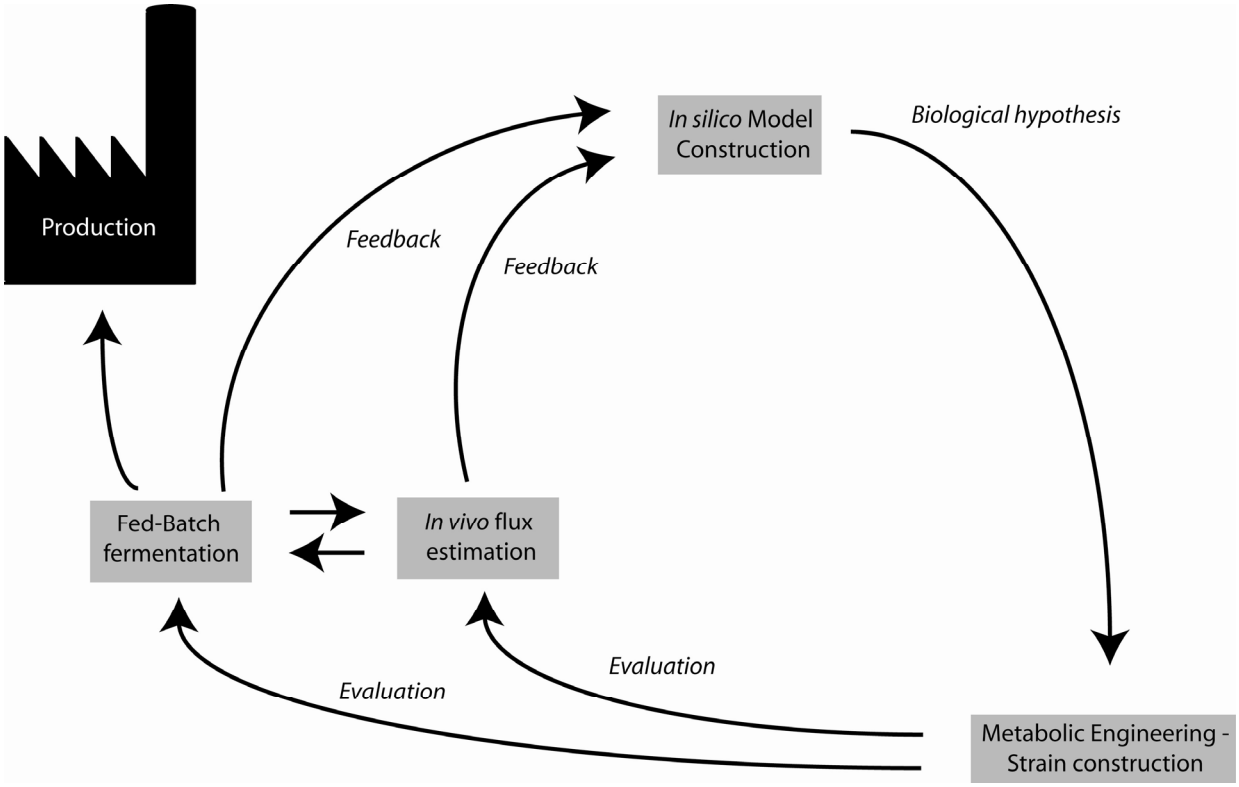

Figure 7.1: Strategy for continuous production strain improvement

Furthermore, in this study the organism used in most experiments was an industrial relevant production strain with yields and productivities significantly higher than what is generally reported in literature. The use of an organism with these characteristics makes the results much more interesting from an industrial point of view. In particular it is interesting to note that many of the different metabolic engineering strategies that have shown to be successful for laboratory strains are found not to have a positive effect on an industrial strain, which points to that industrial strains are already highly optimized and that it is therefore not always possible to transfer metabolic engineering strategies from laboratory strains to industrial strains.

Appendix I

Reaction list for genome-scale reconstruction of *Corynebacterium glutamicum* metabolic network

Appendix I: Reaction list for genome-scale reconstruction of *C. glutamicum*

ORF	EC Number	Gene name	Reactions	Reference(s)
		-REACTIONS		
		# 1. SUBSTRATES UTILISATION		
		# 1.1 CARBON SOURCES		
		#Glycerol		
Q8NLP9	2.7.1.30	glpK	ATP + GL <-> ADP + GL3P	
		#Ethanol		
Q8NLX9	1.1.1.1	adhA	ACAL + NADH <-> ETH + NAD	
Q8NLZ0	1.2.1.3	dhaS_1	ACAL + NAD -> NADH + AC	
		#Glycerate		
Q8NNV1	2.7.1.31	glxK	ATP + GLYR <-> ADP + 3PG	
		#N-acetyl-D-glucosamine-6-phosphate		
	3.1.2.5	r3.1.2.5	NAGA6P -> GA6P + AC	
		# C5 compounds		
		# L-arabinose, D-arabitol, D-lyxose, D-ribose, D-xylose, L-lyxose, L-xylitol,		
Q8NN81	2.7.1.15	rbsK1	ATP + RIB <-> ADP + R5P	
		Putative-ARA	R5P + UTP -> UDPARA + PI	
Q6M8P0	2.7.1.17	xylB	ATP + XYL -> ADP + X5P	
		# Hexoses		
		#Fructose		
Q8NTZ3	2.7.1.4	iolC	FRU + ATP -> F6P + ADP	
		#Glucose		
Q6M788	5.4.2.2	pmmB	G1P <-> G6P	
		#Mannose		
Q8NSC8	5.3.1.8	manA	MAN6P <-> F6P	
Q8NSD0	5.4.2.8	pmmA	MAN6P <-> MAN1P	
Q6M738	2.7.7.22	rmlA2	GTP + MAN1P <-> PPI + GDPMAN	
		#Galactose		
Q8NNH0	2.7.1.6	r2.7.1.6	ATP + GLAC <-> GAL1P + ADP	
	5.1.3.2	galE	UDPG <-> UDPGAL	
	2.7.7.9	galU1	UTP + G1P <-> PPI + UDPG	
		# D-gluconate		
Q8NLD4	2.7.1.12	gntK	ATP + GLUC <-> ADP + D6PGC	
		# Disaccharides		
		# sucrose		
Q8NMD5	3.2.1.26	scrB	SUC6P -> FRU + G6P	Yokota & Lindley (2005)
		# celobiose		
		#Trehalose		
		treY	POLYGLC <-> MLTTRE	Tzvetkov et al (2003)
		treZ	MLTTRE <-> TRE	Tzvetkov et al (2003)
		otsA	G6P + UDPG <-> UDP + TRE6P	Tzvetkov et al (2003)
		otsB	TRE6P <-> TRE+ PI	Tzvetkov et al (2003)
		treS	MLT <-> TRE	Tzvetkov et al (2003)
		# organic acids		
		# acetate		
P77845	2.7.2.1	ackA	ATP + AC -> ADP + ACETYLP	Reinsheid et al (1999)
P77844	2.3.1.8	pta	COA + ACETYLP <-> ACCOA + PI	Reinsheid et al (1999)
		# propionate		
		prpDBC	PROPIONATE + OA -> PYR + SUCC	Claes et al (2002)
		# fumerate		
Q6M7L9	1.2.1.2	fdhF	FOR + NAD -> CO2 + NADH	
		# lactate		
		# Amino acids		
		#Alanine		

		D-Ala_degrade	DALA + FAD -> FADH2 + PYR + NH3	
Q8NT35	2.6.1.19	bALA_degrade	bALA + AKG -> GLU + MALONATES	
Q8NSX1	1.2.1.27	msmA	MALONATES + COA + NAD -> CO2 + ACCOA + NADH	
		#Aspargine		
Q8NNP5	3.5.1.1	asp	ASN -> ASP + NH3	
		#Serine		
Q8NQ09	4.3.1.17	sdaA	SER -> PYR + NH3	
		# Glutamate family (glutamate, glutamine, arginine, proline)		
		# glutamate		
Q8NT35	2.6.1.19	gabT	GABA + AKG <-> SUCCSAL + GLU	
		gabD2	SUCCAL + NADP <-> NADPH + GLU	
		# 1.2 SULPHATE METABOLISM		
	2.7.7.4	cysND	SLF + ATP + GTP <-> APS + PPI + GDP + PI	Lee (2005)
Q8NLX1				
Q6M242	1.8.4.8	cysH_1	APS + RTHIO -> OTHIO + H2SO3 + AMP	Lee (2005)
		cysI	H2SO3 + 3 NADPH <-> H2S + 3 NADP	Lee (2005)
		cysC	APS + ATP <-> ADP + PAPS + PI	Lee (2005)
Q8NLX0	1.8.4.8	cysH_2	PAPS + RTHIO -> OTHIO + H2SO3 + PAP	Lee (2005)
		#added model in order to balance PAP		
		unk_34	PAP -> AMP + PI	Added reaction
		# 1.3 NITROGEN METABOLISM		
	3.5.1.5	ureA	UREA -> CO2 + 2 NH3	Siewe et al (1998); Beckers et al (2004)
Q9RHM6				
		NH3/NH4-eq.	NH3 <-> NH4	Added reaction
		# 1.4 PHOSPHOROUS METABOLISM		
		Pyrophosphate	PPI <-> PI + PI	Added reaction - Artificial for balancing
		# 2. CARBOHYDRATE METABOLISM		
		# 2.1 GLYCOLYSIS/GLUCONEOGENESIS		
		#Reactions prior EMP		
Q8NS31	5.3.1.9	pgi	G6P <-> F6P	Marx et al (2003)
Q8NR14	2.7.1.11	pfkA	ATP + F6P <-> ADP + FDP	Sugimoto et al (1989)
Q8NP81	2.7.1.11	pfkB	ATP + F1P -> ADP + FDP	Sugimoto et al (1989)
Q6M4B1	2.7.1.2	glk	ATP + GLC -> ADP + G6P	Park et al (2000)
	3.1.3.11	fbp	FDP -> F6P + PI	Rittmann et al (2003)
		#Glycolysis		
	4.1.2.13	fda	FDP <-> DHAP + G3P	von der Osten et al (1989)
P19537				
P19583	5.3.1.1	tpiA	G3P <-> DHAP	Eikmanns (1992)
	1.2.1.12	gapA	G3P + PI + NAD <-> NADH + 13PDG	Eikmanns (1992); Bathe et al (1996)
Q01651				
		##gapB more active when AC is used as carbon source (Eggeling and Bott (2005, pp 224), gapB reversibel acording to literature. However, NADPH generation if not constrained to be ireversibel		
		#gapB	G3P + PI + NADP <-> NADPH + 13PDG	
Q6M6L3	1.2.1.12	gapB	NADPH + 13PDG -> G3P + PI + NADP	Eikmanns (1992)
Q01655	2.7.2.3	pgk	ADP + 13PDG <-> ATP + 3PG	Eikmanns (1992)
Q8NTA5	5.4.2.1	pgm	3PG <-> 2PG	Yokota & Lindley (2005)
Q8NRS1	4.2.1.11	eno	2PG <-> PEP	Yokota & Lindley (2005)
	2.7.1.40	pyk	PEP + ADP -> PYR + ATP	Jetten et al (1994); Netzer et al (2004)
Q46078				
Q8NSW3	2.7.9.2	pps	ATP + PYR -> AMP + PEP + PI	Jetten et al (1994b)
		# 2.2 CITRATE CYCLE (TCA CYCLE)		
		#TCA Cycle		
Q8NNF6	1.2.4.1	aceE	PYR + LIPO -> ACLIPO + CO2	kalinowski et al (2003)
		##aceF not found so far		
	2.3.1.12	aceF	ACLIPO + COA -> ACCOA + DLIPO	
Q8NSI4	1.8.1.4	lpd	DLIPO + NAD -> LIPO + NADH	Schwinde et at (2001)
P42457	2.3.3.1	gltA	ACCOA + OA -> CIT + COA	Eikmanns et al (1994)
Q8NQ98	4.2.1.3	acn	CIT <-> ICIT	Krug et al (2005)
P50216	1.1.1.42	icd	ICIT + NADP -> AKG + CO2 + NADPH	Eikmanns et al (1995)
P96746	1.2.4.2	odhA	AKG + LIPO -> SDLIPO + CO2	Usuda et al (1996)
Q8NNJ2	2.3.1.61	sucB	SDLIPO + COA -> DLIPO + SUCCOA	Zhao & Lin (2002)
	6.2.1.5	sucD	ADP + PI + SUCCOA -> ATP + SUCC + COA	Zhao & Lin (2002)
Q8NMK8				
Q8NMK7	1.3.5.1	sdhCAB	SUCC + MK -> FUM + MKH2	Bott & Niebisch (2003)
		#sdhA_1	SUCC + FAD -> FUM + FADH2	
		#sdhA_2	FUM + FADH2 -> SUCC + FAD	

Q8NRN8	4.2.1.2	fumC	FUM <-> MAL	Zhao & Lin (2002)
		##Precence of mdh2 is uncertain		
Q8NSK9	1.1.1.82	mdh2	MAL + NADP -> OA + NADPH	
		##reversibel iaccording to literature. However a cycle with mqo is made so menaquinol electrontransport		
Q8NN33	1.1.1.37	mdh	MAL + NAD -> NADH + OA	Molenaar et al (2000)
		#Glycosylate shunt		
P42449	4.1.3.1	aceA	ICIT <-> SUCC + GLX	Reinsheid et al (1994)
	4.1.3.2	aceB	ACCOA + GLX -> MAL + COA	Reinsheid et al (1994b)
		#Anaplerotic reactions		
P12880	4.1.1.31	ppc	PEP + CO2 -> PI + OA	Eikmanns et al (1989)
	6.4.1.1	pyc	ATP + PYR + CO2 -> ADP + PI + OA	Peters-Wendisch et al
O54587				(1998)
		##pckG mainly glucogenic enzyme		
	4.1.1.32	##pckG	GTP + OA <-> GDP + PEP + CO2	Riedel et al (2001)
Q9AEM1	4.1.1.32	pckG	GTP + OA -> GDP + PEP + CO2	Riedel et al (2001)
		##mez mainly glucogenic enzyme		
	1.1.1.40	##mez	MAL + NADP <-> CO2 + NADPH + PYR	Vallino & Stephanoupoulos (1993)
	1.1.1.40	mez	MAL + NAD <-> CO2 + NADPH + PYR	Vallino &
Q8NLD5				Stephanoupoulos (1993)
	4.1.1.3	Odx	OA -> PYR + CO2	Jetten & Sinskey (1995)
		# 2.3 PENTOSE PHOSPHATE PATHWAY		
Q6M517	1.1.1.49	zwf&opcA	G6P + NADP -> 6PG + NADPH	Moritz et al (2000)
Q8NQI2	1.1.1.44	gnd	6PG + NADP -> Ru5P + CO2 + NADPH	Moritz et al (2000)
Q8NQ49	5.1.3.1	rpe	Ru5P <-> X5P	Yokata & Lindley (2005)
Q8NMZ0	5.3.1.26	rpi	Ru5P <-> R5P	Yokata & Lindley (2005)
Q6M519	2.2.1.1	tkt_1	R5P + X5P <-> G3P + S7P	Yokata & Lindley (2005)
Q8NQ64	2.2.1.2	tal	G3P + S7P <-> E4P + F6P	Yokata & Lindley (2005)
Q8NQ65	2.2.1.1	tkt_2	E4P + X5P <-> F6P + G3P	Yokata & Lindley (2005)
		#3.Respiratory Energy Metabolism		
Q79VG1	1.6.99.3	ndh	NADH + MK -> MKH2 + NAD	Bott & Niebisch (2003)
Q6M7Z1	1.3.5.1	sdhCAB	SUCC + MK -> FUM + MKH2	Bott & Niebisch (2003)
	1.1.99.16	mqo	MAL + MK -> OA + MKH2	Bott & Niebisch (2003);
O69282				Molenaar et al (2000)
Q8NMG5	1.2.2.2	poxB	PYR + MK -> AC + CO2 + MKH2	Bott & Niebisch (2003)
Q8NRY8	1.1.1.28	dld2	LAC + MK -> PYR + MKH2	Bott & Niebisch (2003)
Q8NLN0	1.1.1.27	lldD	LLAC + MK -> PYR + MKH2	Bott & Niebisch (2003)
Q6M4X2	1.1.99.5	glpD	GL3P + MK -> DHAP + MKH2	Bott & Niebisch (2003)
Q8NU48	1.5.1.12	putA	PRO + MK -> P5C + MKH2	Bott & Niebisch (2003)
		#Electron transfer from Menaquinol to Oxygen		
		#(1H+/e-); Eggeling and Bott (2005) pp 325		
		cyto-bd-complex	MKH2 + 0.5 O2 + 2 H_PO -> MK + 2 H_POxt	Bott & Niebisch (2003)
		#(3H+/e-); Eggeling and Bott (2005) pp 325		
		bc1-aa3-complex	MKH2 + 0.5 O2 + 6 H_PO -> MK + 6 H_POxt	Bott & Niebisch (2003)
		#3.3 Electron tranfer from Menaquinol to Nitrate		
		narGHIJ	NO3 + MKH+ 2 H_PO -> NO2 + MK + 2 H_POxt	Bott & Niebisch (2003)
		#3.4 F1F0.ATP Syntase		
		## Maximal P/O ratio can be set by changing the amount of protons consumed per one ATP synthesis, here P/O ratio is 6/3=2		
		## (observed values for Protons/ATP is between 3-4 → P/O = 1.5-2 (Bott & Niebisch (2003))		
		ATPase-complex	ADP + PI + 4 H_POxt -> ATP + 4 H_PO	Bott & Niebisch (2003)
		#3.4 Hydrogenperoxide		
Q6M8A6	1.11.1.6	katA	2 H2O2 -> O2	
		#3.2 Heme Biosynthesis and cytocrome c Maturation		
		NCgl0233+NCgl1244	GLU + ATP -> AMP + GLUTAMYLTRNA	Bott & Niebisch (2003)
		hemA	GLUTAMYLTRNA + NADPH -> NADP + GSA	Bott & Niebisch (2003)
		hemL	GSA -> 5AL	Bott & Niebisch (2003)
		hemB	2 5AL <-> PORIII	Bott & Niebisch (2003)
		hemC	4 PORIII -> 4 NH3 + HYDROXYMEBI	Bott & Niebisch (2003)
		hemD	HYDROXYMEBI -> UROPORIII	Bott & Niebisch (2003)
		hemE	UROPORIII -> 4 CO2 + COPPIII	Bott & Niebisch (2003)
		hemN	COPPIII -> 2 CO2 + PROIX	Bott & Niebisch (2003)
		hemG	PROIX -> PROPORIX	Bott & Niebisch (2003)
		hemH	PROPORIX -> PROTOHEMEIX	Bott & Niebisch (2003)
		Heme c	PROTOHEMEIX <-> HEMEC	Bott & Niebisch (2003)

		ctaB	PROTOHEMEIX <-> HEMEO	Bott & Niebisch (2003)
		ctaA	HEMEO <-> HEMEA	Bott & Niebisch (2003)
		#3.3 Menaquinone Biosynthesis		
		menF	CHOR -> ICHOR	Bott & Niebisch (2003)
		menD	ICHOR + AKG -> PYR + CO2 + SHCHC	Bott & Niebisch (2003)
		menC	SHCHC -> OSB	Bott & Niebisch (2003)
		menE	ATP + OSB + COA -> AMP + PPI + OSBCOA	Bott & Niebisch (2003)
		menB	OSBCOA -> COA + DHN	Bott & Niebisch (2003)
		menA	DHN -> CO2 + DMK	Bott & Niebisch (2003)
		menG	DMK + SAM -> SAH + MK	Bott & Niebisch (2003)
		# 4. BIOMASS BIOSYNTHESIS		
		# 4.1 AMINO ACID BIOSYNTHESIS		
		# Glutamate family (glutamate, glutamine, arginine, proline)		
		# Glutamate/glutamine biosynthesis		
Q79VE3	6.3.1.2	glnA	ATP + GLU + NH3 -> ADP + PI + GLN	Jacoby et al (1997)
Q8NTW7	1.4.1.13	gltBD	GLN + AKG + NADPH -> 2 GLU + NADP	Burkowski (2003)
P31026	1.4.1.4	gdh	AKG + NH3 + NADPH -> GLU + NADP	Burkowski (2003)
		# Proline synthesis		
P46546	2.7.2.11	proB	GLU + ATP -> ADP + GLUP	Ankri et al (1996)
Q8NU48	1.5.1.12	putA1	P5C + NAD -> GLU + NADH	
	1.2.1.41	proA	GLUP + NADPH -> NADP + PI + GLUGSAL	Serebrijski et al (1995)
P45638				
	Spontaneous	rGLUGSAL	GLUGSAL <-> P5C	Serebrijski et al (1995)
Q6M511	4.3.1.12	ocd	ORN -> PRO + NH3	Serebrijski et al (1995)
Q6M511	2.6.1.13	r2.6.1.13	ORN + AKG -> GLU + P5C	Serebrijski et al (1995)
P46540	1.5.1.2	proC	P5C + NADPH -> PRO + NADP	Serebrijski et al (1995)
		# Arginine synthesis		
	2.3.1.1	argR	GLU + ACCOA <-> NAGLU + COA	Serebrijski et al (1995)
Q59281	2.7.2.8	argB	ATP + NAGLU <-> ADP + NAGLUP	
	1.2.1.38	argC	NAGLUP + NADPH <-> NAGLUS + NADP +	
Q59279			PI	
Q59282	2.6.1.11	argD	NAGLUS + GLU <-> NAORN + AKG	
Q59280	2.3.1.35	argJ	NAORN + GLU -> ORN + NAGLU	
Q59283	2.1.3.3	argF	CAP + ORN -> PI + CITR	
	6.3.5.5	carA	2 ATP + GLN + CO2 -> 2 ADP + PI + GLU +	
P58893			CAP	
O85176	6.3.4.5	argG	ATP + CITR + ASP -> AMP + PPI + NAS	
O88101	4.3.2.1	argH	NAS -> FUM + ARG	
		# The branched chain amino acids (isoleucine, valine, leucine)		
		# Valine biosynthesis (ilv-genes shared between VAL and ILE pathway!!)		
P42463	2.2.1.6	ilvBN_val	2 PYR -> ACLAC + CO2	Radmacher et al (2002)
Q57179	1.1.1.86	ilvC_val	ACLAC + NADPH -> DHMVA + NADP	Radmacher et al (2002)
Q8NQZ9	4.2.1.9	ilvD_val	DHMVA -> OIVAL	Radmacher et al (2002)
Q79VE5	2.6.1.42	ilvE_val	OIVAL + GLU -> VAL + AKG	Radmacher et al (2002)
		# Isoleucine biosynthesis		
Q04513	4.3.1.19	ilvA_ile	THR -> OBUT + NH3	Möckel et al (1992)
	2.2.1.6	ilvBN_ile	OBUT + PYR -> ABUT + CO2	Keilhauer et al (1993);
P42463				Leyval et al (2003)
	1.1.1.86	ilvC_ile	ABUT + NADPH -> DHMV + NADP	Keilhauer et al (1993);
Q57179				Leyval et al (2003)
	4.2.1.9	ilvD_ile	DHMV -> OMVAL	Keilhauer et al (1993);
Q8NQZ9				Leyval et al (2003)
Q79VE5	2.6.1.42	ilvE_ile	OMVAL + GLU -> ILE + AKG	Leyval et al (2003)
		# leucine biosynthesis		
P42455	2.3.3.13	leuA	OIVAL + ACCOA -> IPPMAL + COA	Paték et al (1998)
P58946	4.2.1.33	leuCD	IPPMAL -> CBHCAP	Willis et al (2005)
	1.1.1.85	leuBP	CBHCAP + NAD -> 2OMOP + NADH + CO2	Paték et al (1998)
P94631				
Q79VE5	2.6.1.42	ilvE	2OMOP + GLU -> LEU + AKG	Groeger & Sahn (1987)
		# The aspartate family (aspartate, asparagine, threonine, lysine, methionine)		
		# Aspartate biosynthesis		
Q6M8B5	2.6.1.1	aspB	OA + GLU -> ASP + AKG	Cremer et al (1991)
Q59200	4.3.1.1	aspA	ASP -> FUM + NH3	
		# Asparagine biosynthesis		
	6.3.5.4	ltsA	ATP + ASP + GLN -> AMP + PPI + ASN +	
Q8NNK1			GLU	
	6.3.1.1	NCgl2116	ATP + ASP + NH3 -> PPI + AMP + ASN	
		# Threonine biosynthesis		

P08499	1.1.1.3	hom	ASPSA + NADPH -> HSER + NADP	Reinsheid et al (1991)
P07128	2.7.1.39	thrB	ATP + HSER -> ADP + PHSER	Miyajima et al (1968)
P23669	4.2.3.1	thrC	PHSER -> THR + PI	Malumbres et al (1994)
		# Lysine biosynthesis		
P26512	2.7.2.4	lysC	ATP + ASP -> ADP + AP	Cremer et al (1991)
P26511	1.2.1.11	asd	AP + NADPH + H -> ASPSA + PI + NADP	Cremer et al (1991)
P19808	4.2.1.52	dapA	ASPSA + PYR -> DEHYDRODIPICOLINAT	Cremer et al (1991)
	1.3.1.26	dapB	DEHYDRODIPICOLINATE + NADPH ->	Cremer et al (1990)
P40110			PIPER26DC + NADP	
	2.3.1.26	dapD	PIPER26DC + SUCCOA -> SDAAKP + COA	Cremer et al (1990)
Q6M8B5	2.6.1.1	dapC	SDAAKP + GLU -> SDAPIM + AKG	Cremer et al (1991)
Q59284	3.5.1.18	dapE	SDAPIM -> SUCC + DAPIM	Wehrmann et al (1995)
Q8NP73	5.1.1.7	dapF	DAPIM -> MDAPIM	Cremer et al (1991)
	1.4.1.16	ddh	PIPER26DC + NH3 + NADPH -> MDAPIM +	Schrumpf et al (1991)
P04964			NADP	
P09890	4.1.1.20	lysA	MDAPIM -> LYS + CO2	Cremer et al (1991)
		# Methionine biosynthesis		
O68640	2.3.1.31	metX	ACCOA + HSER -> COA + OAHSER	Park et al (1998)
Q79VI4	2.5.1.49	metY	OAHSER + H2S -> HCYS + AC	Hwang et al (2002)
	2.5.1.48	metB	OAHSER + CYS -> LLCT + AC	Lee & Hwang (2003);
Q79VD9				Rückert et al (2003)
	4.4.1.8	metC	LLCT -> PYR + NH3 + HCYS	Lee & Hwang (2003);
Q93QC6				Rückert et al (2003)
Q93PM7	2.1.2.1	glyA	SER + THF <-> GLY + METHF	Simic et al (2002)
	1.7.99.5	metF	METHF + NADPH -> MTHF + NADP	Lee & Hwang (2003);
Q8NNM2				Rückert et al (2003)
	2.1.1.13	metH	MTHF + HCYS <-> MET + THF	Lee & Hwang (2003);
Q6M580				Rückert et al (2003)
	2.5.1.6	metK	ATP + MET -> PPI + SAM	Lee & Hwang (2003);
Q9K5E4				Rückert et al (2003)
	3.3.1.1	ahcY	SAH <-> HCYS + ADENOSINE	Lee & Hwang (2003);
Q8NSC4				Rückert et al (2003)
		# The pyruvate family (alanine)		
	2.6.1.66	NCgl0388	VAL + PYR -> ALA + OIVAL	
Q8RSU9	5.1.1.1	alr	ALA <-> DALA	
		# The serine family (serine, glycine, cysteine)		
		# Serine biosynthesis		
	1.1.1.95	serA	3PG + NAD -> NADH + PHP	Peters-Wendisch et al
Q8NQY7				(2002)
	2.6.1.52	serC	PHP + GLU -> AKG + 3PSER	Peters-Wendisch et al
Q8NS51				(2005)
	3.1.3.3	serB	3PSER -> PI + SER	Peters-Wendisch et al
Q6M2V2				(2005)
		# Glycine biosynthesis		
		##See glyA in methionine synthesis		
		# Cysteine biosynthesis		
Q6M2R8	2.3.1.30	cysE	ACCOA + SER -> COA + OASER	Wada et al (2002)
Q6M2R9	2.5.1.47	cysKM	OASER + H2S -> AC + CYS	Wada et al (2004)
		# The histidine family		
		# Histidine biosynthesis		
Q9Z472	2.4.2.17	hisG	PRPP + ATP -> PPI + PRBATP	Alifano et al (1996)
Q9Z471	3.6.1.31	hisI_1	PRBATP -> PPI + PRBAMP	Alifano et al (1996)
Q8NNT9	3.5.4.19	hisI_2	PRBAMP -> PRFP	Alifano et al (1996)
O68602	5.3.1.16	hisA	PRFP -> PRLP	Jung et al (1998)
Q9Z472	2.4.2.17	hisFH	PRLP + GLN -> GLU + AICAR + DIMGP	Jung et al (1998)
Q9KJU3	4.2.1.19	hisB_1	DIMGP <-> IMACP	Alifano et al (1996)
Q9KJU4	2.6.1.9	hisC	IMACP + GLU <-> HISOLP + AKG	Alifano et al (1996)
	3.1.3.15	hisB_2	HISOLP -> PI + HISOL	Alifano et al (1996)
Q8NNT5	1.1.1.23	hisD	HISOL + 2 NAD -> HIS + 2 NADH	Alifano et al (1996)
		# The aromatic family		
		# The shikimate pathway		
P35170	2.5.1.54	aroG	PEP + E4P -> 3DDAH7P + PI	Linn et al (2001)
Q9X5D2	4.2.3.4	aroB	3DDAH7P -> DQT + PI	Ideka (2005)
O52377	4.2.1.10	aroQ	DQT -> DHSK	Ideka (2005)
Q9X5C9	1.1.1.25	aroE	DHSK + NADPH -> SME + NADP	Ideka (2005)
Q9X5D1	2.7.1.71	aroK	ATP + SME -> ADP + SME3P	Ideka (2005)
Q9Z470	2.5.1.19	aroA	PEP + SME3P -> 5EPS3P + PI	Ideka (2005)
Q9X5D0	4.2.3.5	aroC	5EPS3P -> CHOR + PI	Ideka (2005)
		# Tryptophan biosynthesis		

P06557	4.1.3.27	trpE&trpG	CHOR + GLN -> AN + PYR + GLU	Sugimoto & Shiio (1977)
P06559	2.4.2.18	trpD	AN + PRPP -> NPRAN + PPI	Sugimoto & Shiio (1977)
P06560	4.1.1.48	trpC	NPRAN -> CPAD5P	Sugimoto & Shiio (1977)
P06562	4.2.1.20	trpA&trpB	SER + CPAD5P -> TRP + G3P + CO2	Sugimoto & Shiio (1977)
		# Tyrosine and phenylalanine biosynthesis		
	5.4.99.5	csm	CHOR -> PHEN	Ideka (2005)
Q6M8C9	1.3.1.12	tyrA	PHEN + NAD -> NADH + PRETYR + CO2	Fazel & Jensen (1979)
	2.6.1.57	r2.6.1.57	PRETYR + GLU -> AKG + TYR	Fazel & Jensen (1979)
	4.2.1.51	pheA	PHEN -> PHPYR + CO2	Follettie & Sinskey (1986)
P10341				
	2.6.1.5	NCgl0215&NCgl2020	PHPYR + GLU -> PHE + AKG	Fazel & Jensen (1979)
		# 4.2 NUCLEOTIDE BIOSYNTHESIS		
		#PURINE		
Q8NRU9	2.7.6.1	prs	ATP + R5P -> AMP + PRPP	
Q8NMI9	2.4.2.14	purF	PRPP + GLN -> PPI + GLU + PRAM	
Q8NMH3	6.3.4.13	purD	ATP + PRAM + GLY <-> ADP + PI + GAR	
Q6M6S8	2.1.2.2	purN	GAR + FTHF <-> THF + FGAR	
	6.3.5.3	purL	ATP + FGAR + GLN <-> ADP + PI + FGAM +	
Q8NMI5			GLU	
Q8NMJ0	6.3.3.1	purM	FGAM + ATP -> ADP + PI + AIR	
Q6M768	4.1.1.21	purK	AIR + CO2 + ATP <-> CAIR + ADP + PI	
	6.3.2.6	purC	CAIR + ATP + ASP <-> ADP + PI + SAICAR	
Q8NMH6				
Q8NMH5	4.3.2.2	purB_1	SAICAR <-> FUM + AICAR	
Q8NS21	2.1.2.3	purH	AICAR + FTHF <-> THF + PRFICA	
Q8NS21	3.5.4.10	r3.5.4.10	PRFICA <-> IMP	
Q8NM16	6.3.4.4	purA	GTP + IMP + ASP <-> GDP + PI + ASUC	
Q8NMH5	4.3.2.2	purB_2	ASUC <-> FUM + AMP	
Q8NM99	1.1.1.205	guaB1	IMP + NAD -> XMP + NADH	
	6.3.5.2	guaA	ATP + XMP + GLN <-> AMP + PPI + GMP +	
Q8NSR1			GLU	
		#PYRINE		
Q8NM11	2.4.2.10	pyrE_1	OROA + PRPP -> PPI + OMP	
	6.3.5.5	NCgl1547&NCgl1548	CO2 + 2 ATP + GLN -> GLU + CAP + 2 ADP	
P58893			+ PI	
Q8NQ38	2.1.3.2	pyrB	CAP + ASP -> CAASP + PI	
Q8NQ39	3.5.2.3	pyrC	CAASP -> DOROA	
Q8NQC0	1.3.3.1	pyrD	DOROA + O2 -> OROA + H2O2	
Q8NQ40	4.1.1.23	pyrF	OMP -> UMP + CO2	
	6.3.5.3	pyrG_2	ATP + UTP + GLN -> GLU + ADP + PI + CTP	
Q8NMI5				
		#pyrE_2	DOROA + NAD -> OROA + NADH	
Q8NS38	2.1.1.45	thyA	METTHF + DUMP -> DTMP + DHF	
	2.1.1.148	thyX	METHF + DUMP + FADH2 <-> FAD + DUMP +	
P40111			THF	
Q8NQL7	6.3.4.2	pyrG_1	ATP + UTP + NH3 -> ADP + PI + CTP	
Q8NLT9	3.5.4.13	dcd_1	CTP -> UTP + NH3	
Q8NLT9	3.5.4.13	dcd_2	DCTP -> DUTP + NH3	
		#Nucleotide Salvage Pathways		
P49973	2.7.4.3	adk_1	ATP + AMP <-> ADP + ADP	
P49973	2.7.4.3	adk_2	ATP + DAMP <-> ADP + DADP	
Q8NQK7	2.7.4.14	cmk_1	ATP + UMP <-> ADP + UDP	
Q8NQK7	2.7.4.14	cmk_2	ATP + CMP <-> ADP + CDP	
Q8NQK7	2.7.4.14	cmk_3	ATP + DCMP <-> ADP + DCDP	
Q8NSC3	2.7.4.9	tmk	DTMP + ATP <-> ADP + DTDP	
Q8NSC3	2.7.4.9	umk	DUMP + ATP -> ADP + DUDP	
Q8NN43	2.7.4.6	ndk_4	ATP + ADP <-> ATP + ADP	
Q8NN43	2.7.4.6	ndk_10	ATP + UDP <-> UTP + ADP	
Q8NN43	2.7.4.6	ndk_11	ATP + CDP <-> CTP + ADP	
Q8NN43	2.7.4.6	ndk_2	ATP + GDP <-> ADP + GTP	
Q8NN43	2.7.4.6	ndk_3	ATP + DGDP <-> ADP + DGTP	
Q8NN43	2.7.4.6	ndk_12	ATP + DTDP <-> ADP + DTTP	
Q8NN43	2.7.4.6	ndk_1	ATP + DADP <-> ADP + DATP	
Q8NN43	2.7.4.6	ndk_4	ATP + DUDP <-> ADP + DUTP	
Q8NN43	2.7.4.6	ndk_5	ATP + DCDP <-> ADP + DCTP	
Q8NQ42	2.7.4.8	gmk_1	ATP + GMP <-> ADP + GDP	
Q8NQ42	2.7.4.8	gmk_2	ATP + DGMP <-> ADP + DGDP	
	2.7.4.22	r2.7.4.22	ATP + UMP <-> ADP + UDP	
Q8NL59	1.8.1.9	trxB	OTHIO + NADPH -> NADP + RTHIO	
Q6M2U5	1.17.4.1	nrdF_10	CDP + RTHIO -> DCDP + OTHIO	

Q79VD6	1.17.4.1	nrdF_4	UDP + RTHIO -> DUDP + OTHIO	
Q6M2U5	1.17.4.1	nrdD_1	ATP + RTHIO -> DATP + OTHIO	
Q79VD6	1.17.4.1	nrdD_2	GTP + RTHIO -> DGTP + OTHIO	
Q8NUB7	3.1.3.5	nucA_1	AMP -> ADENOSINE + PI	
Q8NUB7	3.1.3.5	nucA_2	IMP -> INOSINE + PI	
Q8NUB7	3.1.3.5	nucA_3	XMP -> XANTHOSINE + PI	
Q8NUB7	3.1.3.5	nucA_4	GMP -> GUANOSINE + PI	
Q8NUB7	3.1.3.5	nucA_5	CMP -> CYTIDINE + PI	
Q8NUB7	3.1.3.5	nucA_6	UMP -> URIDINE + PI	
Q8NUB7	3.1.3.5	nucA_7	DTMP -> THYMIDINE + PI	
Q8NUB7	3.1.3.5	nucA_8	DUMP -> DEOXYURIDINE + PI	
Q8NUB7	3.1.3.5	nucA_9	DCMP -> DEOXYCYTIDINE + PI	
Q8NUB7	3.1.3.5	nucA_10	DAMP -> DEOXYADENOSINE + PI	
Q8NUB7	3.1.3.5	nucA_11	DGMP -> DEOXYGUANOSINE + PI	
Q8NLV1	3.2.2.1	r3.2.2.1_1	ADENOSINE -> ADENINE + RIB	
Q8NQR2	3.2.2.1	r3.2.2.1_2	INOSINE -> HXAN + RIB	
Q8NLV1	3.2.2.1	r3.2.2.1_3	XANTHOSINE -> XHANTHINE + RIB	
Q8NQR2	3.2.2.1	r3.2.2.1_4	GUANOSINE -> GUANINE + RIB	
Q6M2E9	2.4.2.8	r2.4.2.8_1	HXAN + PRPP -> XMP + PPI	
Q6M2E9	2.4.2.8	r2.4.2.8_2	GUANINE + PRPP -> GMP + PPI	
Q6M2E9	2.4.2.8	r2.4.2.8_3	ADENINE + PRPP -> AMP + PPI	
O87330	2.4.2.7	r2.4.2.7_1	ADENINE + PRPP -> AMP + PPI	
O87330	2.4.2.7	r2.4.2.7_2	GUANINE + PRPP -> GMP + PPI	
	3.1.5.1	r3.1.5.1	DGTP -> DEOXYGUANOSINE + PI + PI + PI	
Q6M8C7	3.5.4.1	r3.5.4.1	CYTOSINE -> URA + NH3	
Q6M8Q7	3.2.2.4	amn	AMP -> R5P + ADENINE	
Q8NPA9	3.6.1.23	dut	DUTP -> DUMP + PPI	
P59011	2.4.2.9	pyrR	URA + PRPP <-> UMP + PPI	
Q8NTH9	3.6.1.45	ushA	UDPG -> UMP + G6P	Wendisch & Bott (2005)
		# 4.3 LIPIDS BIOSYNTHESIS		
		# Fatty acids biosynthesis (Path I)		
	6.4.1.2	accDA	ATP + ACCOA + CO2 <-> ADP + PI +	
Q6M6V5			MALCOA	
Q6M2X6	2.3.1.85	fas-IB_1	MALCOA + ACP -> MALACP + COA	
Q6M6V0	2.3.1.85	fas-IA_1	ACCOA + ACP -> ACACP + COA	
	2.3.1.85; 1	FASC140	ACACP + 6 MALACP + 12 NADPH -> 12	
			NADP + C140ACP + 6 CO2 + 6 ACP	
	2.3.1.85; 1	FASC150	ACACP + 6.5 MALACP + 13 NADPH -> 13	
			NADP + C150ACP + 6.5 CO2 + 6.5 ACP	
	2.3.1.85; 1	FASC160	ACACP + 7 MALACP + 14 NADPH -> 14	
			NADP + C160ACP + 7 CO2 + 7 ACP	
	2.3.1.85; 1	FASC161	ACACP + 7 MALACP + 13 NADPH -> 13	
			NADP + C161ACP + 7 CO2 + 7 ACP	
	2.3.1.85; 1	FASC180	ACACP + 8 MALACP + 16 NADPH -> 16	
			NADP + C180ACP + 8 CO2 + 8 ACP	
	2.3.1.85; 1	FASC181	ACACP + 8 MALACP + 15 NADPH -> 15	
			NADP + C181ACP + 8 CO2 + 8 ACP	
		# Fatty acids biosynthesis (Path II) (no encoding genes for this system) (Eggeling and Bott, (2005) pp 134)		
		#Mycolic acid Biosynthesis		
	6.2.1.3	fas-IA_MA	0.071 C140ACP + 0.332 C150ACP + 0.408	
			C160ACP + 0.189 C161ACP -> ACP +	
Q6M1Y6			FREEMYCOLICACID	
	2.3.1.122	cmt	FREEMYCOLICACID + TRE + ATP <-> TMCM	Brand et al (2003)
Q8NTG4			+ ADP	
	2.3.1.122	cmt_3	TMCM + TRE + ATP <-> TDCM + ADP	Daffé (2005); Brand et al
Q6M6M6				(2003)
		# Phospholipids biosynthesis		
		gpsA	DHAP + NADH <-> GL3P + NAD	Nampoothiri et al (2002)
		# synthesis of phosphatidylglycerol (80% of all phospholidids (Eggeling and Bott. 2005)		
		Phospholipid-step	GL3P + 0.004 C140ACP + 0.438 C160ACP +	Hoischen & Krämer
			0.004 C161ACP + 0.010 C180ACP + 0.544	(1990)
			C181ACP -> AGL3P + ACP	
		plsC	AGL3P + 0.004 C140ACP + 0.438 C160ACP	Hoischen & Krämer
			+ 0.004 C161ACP + 0.01 C180ACP + 0.544	(1990)
			C181ACP -> PA + ACP	
		cdsA_1	PA + CTP <-> CDPDG + PPI	Nampoothiri et al (2002)
		cdsB	CDPDG + SER <-> CMP + PS	Nampoothiri et al (2002)

		pgsA2	CDPDG + GL3P <-> CMP + PG	Nampoothiri et al (2002)
		#synthesis of cardiolipin		
		r2.7.8.a	PG -> PI + CL + GL	Nampoothiri et al (2002)
		#synthesis of phosphatidyl inositol		
		r2.7.8.b	CDPDG -> PIT	Nampoothiri et al (2002)
		#synthesis of phosphatidyl inositol mannosides		
		r2.7.8.c	PIT -> PIM	Nampoothiri et al (2002)
		# synthesis of phosphatidylethanolamine		
		cdsA	CTP + PA <-> PPI + CDPDG	Nampoothiri et al (2002)
		# 4.4 PEPTIDOGLYCAN PRECURSORS BIOSYNTHESIS		
		# D-glutamate synthesis		
	5.1.1.3	murI	DGLUTAMATE <-> GLU	Ingraham et al (1983);
Q9XDZ7				Daffé (2005)
		# D-alanyl-D-alanine synthesis		
	6.3.4.2	ddl	ATP + 2 DALA <-> ADP + PI + ALAALA	Ingraham et al (1983);
Q8NQL7				Daffé (2005)
		# NAG and NAM biosynthesis		
	2.6.1.16	glmS	GLN + F6P -> GLU + GA6P	Ingraham et al (1983);
Q8NND3				Daffé (2005)
	3.5.99.6	pmmB_1	GA6P -> F6P + NH3	Ingraham et al (1983);
Q8NMD4				Daffé (2005)
	5.4.2.2	pmmB_2	GA6P -> GA1P	Ingraham et al (1983);
Q6M788				Daffé (2005)
	2.3.1.57	r2.3.1.157	ACCOA + GA1P -> NAGA1P + COA	Ingraham et al (1983); Daffé (2005)
	2.7.7.23	glmU	UTP + NAGA1P -> UDPNAG + PPI	Ingraham et al (1983);
Q8NRU8				Daffé (2005)
	2.5.1.7	murA	UDPNAG + PEP -> UDPNACVG + PI	Ingraham et al (1983);
Q8NML5				Daffé (2005)
	1.1.1.158	murB	UDPNACVG + NADPH -> UDPNAM + NADP	Ingraham et al (1983);
Q8NTF4				Daffé (2005)
		# 4.5 COFACTORS BIOSYNTHESIS		
		# Nicotinamide nucleotides (NAD+, NADP+) biosynthesis		
	3.5.1.19	r3.5.1.19	NAM -> NIC + NH3	
	2.4.2.11	r2.4.2.11	NIC + ATP + PRPP -> NACN + ADP + PI + PPI	Added reaction
Q8NN57	2.7.7.18	r2.7.7.18	NACN + ATP -> PPI + NAAD	
Q8NMN7	6.3.1.5	nadE	ATP + NAAD + NH3 -> AMP + PPI + NAD	
	6.3.5.1	r6.3.5.1	ATP + NAAD + GLN -> AMP + PPI + NAD + GLU	
Q8NQM1	2.7.1.23	ppnK	NAD + ATP <-> NADP + ADP	
		# Riboflavin (vitamin B2), FMN and FAD biosynthesis		
Q8NQ52	3.5.4.25	ribA	GTP -> D6RP5P + FOR + PPI	
Q8NQ50	3.5.4.26	ribG	D6RP5P -> A6RP5P + NH3	
	1.1.1.193	NCgl1535	A6RP5P + NADPH -> A6RP5P2 + NADP	
Q8NQ53	2.5.1.9	ribH	A6RP5P2 -> A6RP5P + PI	
Q8NQ51	2.5.1.9	rib_1	R5P -> FOR + DHB4P	
Q8NQ53	2.5.1.9	rib_2	A6RP5P + DHB4P -> O2 + PI + D8RL	
Q8NQ51	2.5.1.9	rib_3	D8RL -> A6RP5P + RIBFLAV	
Q8NP47	2.7.1.26	ribF	ATP + RIBFLAV -> ADP + FMN	
	2.7.7.2	rib_4	ATP + FMN -> FAD + PPI	
		# Coenzyme-A biosynthesis		
Q8NRQ2	2.7.1.33	coaA	ATP + PNTO -> ADP + 4PPNTO	
	6.3.2.5;4.1	coaD	4PPNTO + CYS + ATP -> PPI + DPCOA + CO2 + AMP	Added reaction
P58897	2.7.1.24	coaE	DPCOA + ATP -> ADP + COA + PI	
Q8NMS4	2.7.8.7	acpS	COA -> PAP + ACP	
		# Folate biosynthesis		
Q8NM84	3.5.4.16	folE	GTP -> FOR + AHTD	
Q6M3H3	3.1.3.1	phoD	AHTD -> DHP + 3 PI	
Q8NMV7	3.1.3.1	phoB	AHTD -> DHP + 3 PI	
Q8NM86	4.1.2.25	folX	DHP -> AHHMP	
	2.7.6.3	folK	AHHMP + ATP -> AMP + AHHMD	
	6.3.5.8	r6.3.5.8	CHOR + GLN -> GLU + PYR + 4A4DOCHOR	
	4.1.3.38	r4.1.3.58	4A4DOCHOR -> PABA	
P11744	2.5.1.15	sulI	PABA + AHHMD -> PPI + DHPT	
	6.3.2.12	folC	ATP + DHPT + GLU -> DHF + ADP + PI	
Q8NS39	1.5.1.3	folA	DHF + NADPH -> NADP + THF	
Q8NS39	1.5.1.3	fol_1	FOL + NADPH <-> DHF + NADP	

	3.5.4.9	folD_1	METTHF <-> FTHF	
Q8NSM0	1.5.1.5	folD_2	METHF + NADP <-> METTHF + NADPH	
	1.5.1.20	r1.5.1.20	METHF + NADPH -> MTHF + NADP	
	2.3.2.17	fol_2	THF + ATP + GLU <-> ADP + PI + THFG	
Q8NTC5	3.5.1.10	r3.5.1.10	FTHF -> THF + FOR	
		# Biotin biosynthesis		
		##Lack of bioF (Eggeling and Bott (2005, p 46)		
		#bio_F	ALA -> KAPA	
P46395	2.6.1.62	bioA	KAPA + SAM -> DAPA + SAH	
	6.3.3.3	bioD	DAPA + ATP + CO2 <-> DTBIOTIN + ADP +	
P46397			PI	
P46396	2.8.1.6	bioB	DTBIOTIN + SLF <-> BIOTIN	
		# Pantotheate Synthesis		
Q9X712	2.1.2.11	panB	OIVAL + METHF -> AKP + THF	Sahn & Eggeling (1999)
1.1.1.169	1.1.1.169	panE	AKP + NADPH -> PANT + NADP	Sahn & Eggeling (1999)
Q9X4N0	4.1.1.11	panD	ASP -> bALA + CO2	Sahn & Eggeling (1999)
	6.3.2.1	panC	ATP + PANT + bALA -> AMP + PPI + PNTO	Sahn & Eggeling (1999)
Q9X713				
		# 4.6 MACROMOLECULES BIOSYNTHESIS (mmoles used for the synthesis of 1 g of macromolecule, exc		
		# The energy for polymerisation of building blocks into macromolecules is included in the reactions. For		
		#Protein is in mmol of amino acids for protein to 1 g DW Biomass		
		PROTEIN_Ass	0.666 ALA + 0.190 ARG + 0.194 ASN + 0.194 ASP + 0.044 CYS + 0.342 GLN + 0.548 GLU + 0.353 GLY + 0.067 HIS + 0.189 ILE + 0.351 LEU + 0.187 LYS + 0.076 MET + 0.128 PHE + 0.159 PRO + 0.245 SER + 0.273 THR + 0.028 TRP + 0.078 TYR + 0.273 VAL + 19.7 ATP -> 19.7 ADP + 19.7 PI + PROTEIN	
		DNA_Ass	0.748 DAMP + 0.871 DCMP + 0.748 DTMP + 0.871 DGMP + 4.44 ATP -> 4.44 ADP + 4.44 PI + 3.238 PPI + DNA	
		RNA_Ass	0.69 ATP + 1.01 GTP + 0.70 CTP + 0.70 UTP + 1.24 ATP -> 1.24 ADP + 1.24 PI + RNA + 3.10 PPI	
		ARABINOGALACTAN_Ass	0.498 UDPGAL + 4.650 UDPARA -> 5.148 UDP + ARABINOGALACTAN	
		PEPTIDOGLYCAN_Ass	1.106 UDPNAM + 1.106 UDPNAG + 1.106 ALA + 1.106 MDAPIM + 1.106 DGLUTAMATE + 1.106 GLY + 2.052 ALAALA + 4.426 ATP -> PEPTIDOGLYCAN + 4.426 ADP + 4.426 PI + 1.106 UDP + 1.106 UMP + 1.126 ALA	
		FREEMYCOLICACID_Ass	0.007 C140ACP + 0.014 C150ACP + 0.437 C160ACP + 0.012 C161ACP + 0.009 C180ACP + 0.521 C181ACP -> ACP + FREEMYCOLICACID	
		MYCOLICACID_Ass	0.061 TMCM + 0.043 TDCM + 1.875 FREEMYCOLICACID -> MYCOLICACID	
		PHOSPHOLIPID_Ass	0.033 PA + 1.133 PG + 0.007 CL + 0.042 PIT + 0.065 PIM -> PHOSPHOLIPID	
		biomass_ass	PROTEIN + 0.010 DNA + 0.05 RNA + 0.028 PHOSPHOLIPID + 0.095 PEPTIDOGLYCAN + 0.095 ARABINOGALACTAN + 0.102 MYCOLICACID + 29.2 ATP + 18.5 ATP -> BIOMASS + 29.2 ADP + 29.2 PI + 18.5 ADP + 18.5 PI	Cougain & Bouchet (1996)
		# 6. MAINTENANCE		

		#maintenance	ATP -> ADP + PI	
		# 7. TRANSPORT REACTIONS		
		# 7.1 FREE DIFFUSSION		
		UREA_diffusion	UREAxt <-> UREA	Siewe et al (1998); Beckers et al (2004)
		CO2_diffusion	CO2xt <-> CO2	
		NO3_diffusion	NO3xt <-> NO3	
		SLF_diffusion	SLFxt <-> SLF	
		O2_diffusion	O2xt <-> O2	
		THR_diffusion	THRxt <-> THR	Palmieri et al (1996)
		PHE_diffusion	PHExt <-> PHE	Burkowski & Krämer (2002)
		TYR_diffusion	TYRxt <-> TYR	Burkowski & Krämer (2002)
		ILE_diffusion	ILExt <-> ILE	Burkowski & Krämer (2002)
		NH3_diffusion	NH3xt <-> NH3	Siewe et al (1998)
		# 7.2 PEP-dependent Transporters		
Q8NP80	2.7.1.69	FRU_in_PEP	FRUxt + PEP -> PYR + F6P	Yokota & Lindley (2005)
Q45298	2.7.1.69	GLC_in_PEP	GLCxt + PEP -> PYR + G6P	Yokota & Lindley (2005)
Q46072	2.7.1.69	MAN_in_PEP	MANxt + PEP -> PYR + MAN6P	Yokota & Lindley (2005)
Q8NMD6	2.7.1.69	SUC_in_PEP	SUCxt + PEP -> PYR + SUC6P	Yokota & Lindley (2005)
Q6M488	2.7.1.69	TRE_in_PEP	TRExt + PEP -> PYR + TRE6P	Yokota & Lindley (2005)
		# 7.3 ATP-driven Transporters		
Q8NMK1	3.6.3.27	pstB_ATP	ATP + PIxt -> ADP + PI + PI	
		GLU_ATP	GLUxt + ATP -> GLU + ADP + PI	Kronenmeyer et al (1995)
		RIB_ATP	RIBxt + ATP -> RIB + ADP + PI	
		XYL_ATP	XYLxt + ATP -> XYL + ADP + PI	
		URA_ATP	URAxt + ATP -> URA + ADP + PI	
		BET_ATP	BETxt + ATP -> BET + ADP + PI	
		amt_ATP	NH4xt + ATP -> NH4 + ADP + PI	Burkowski & Krämer (2002)
		SLF_ATP	SLFxt + ATP -> SLF + ADP + PI	
	3.6.3.17	GLC_in	GLCxt + ATP -> GLC + ADP + PI	
		THR_ATP	THR + ATP -> THRxt + ADP + PI	
		aroP1_ATP	TRPxt + ATP -> TRP + ADP + PI	Burkowski & Krämer (2002)
		aroP2_ATP	TYRxt + ATP -> TYR + ADP + PI	Burkowski & Krämer (2002)
		aroP3_ATP	PHExt + ATP -> PHE + ADP + PI	Burkowski & Krämer (2002)
		MET_ATP	METxt + ATP -> MET + ADP + PI	Burkowski & Krämer (2002)
		ILE_ATP	ILE + ATP -> ILExt + ADP + PI	Burkowski & Krämer (2002)
		ORN_ATP	ORNxt + AT <-> ORN + ADP + PI	Burkowski & Krämer (2002)
		UREA_ATP	UREAxt + ATP -> UREA + ADP + PI	Beckers et al (2004)
		# 7.4 PROTON-LINKED ACTIVE TRANSPORT		
		Proton_ATP	H_transport_xt + ADP + PI <-> H_transport + ATP	
		CIT_H	CITxt + H_transport_xt -> CIT + H_transport	
		Phosphate_H	PIxt + H_transport_xt -> PI + H_transport	Wendisch & Bott (2005)
		ARG_H	ARG + H_transport -> ARGxt + H_transport_xt	
		LysE	LYS + 2 H_transport_xt -> LYSxt + 2 H_transport	
		NO3_H	NO3xt + H_transport_transport_xt -> NO3 + H	
		GLU_H	GLUxt + H_transport_xt -> GLU + H_transport	
		GLUC_H	GLUCxt + H_transport_xt -> GLUC + H_transport	
		GABA_H	GABAxt + H_transport_xt -> GABA + H_transport	
		UREA_H	UREAxt + H_transport_xt <-> UREA + H_transport	Siewe et al (1998)

AC_H	Acxt + H_transport_xt <-> AC + H_transport	Ebbighausen et al (1991)
# 7.6 OTHER TRANSPORT		
# Sodium associated transport		
Na-transporter	Na + H_transport_xt <-> Naxt + H_transport	
# Symport		
ILE_S	ILExt + Naxt -> ILE + Na	Ebbighausen et al (1989b)
VAL_S	VALxt + Naxt -> VAL + Na	Ebbighausen et al (1989b)
LEU_S	LEUxt + Naxt -> LEU + Na	Ebbighausen et al (1989b)
ALA_S	ALAxt + Naxt -> Na + ALA	
PRO_S	PROxt + Naxt <-> Na + PRO	
nptA_S	PIxt + Naxt -> Na + PI	Wendisch & Bott (2005)
SER_S	SER + Na -> SERxt + Naxt	Somic et al (2001)
GLU_S	GLUxt + Naxt -> GLU + Na	
THR_S	THR + Na -> THRxt + Naxt	Palmieri et al (1996)
# Antiport		
GLN_S	GLNxt + Na <-> Naxt + GLN	Siewe et al (1995)
#Transporters of unknown Mechanisms		
NAM_in	NAMxt -> NAM	
Nitrate_in	NO3xt -> NO3	
Nitrite_in	NO2xt -> NO2	
Met_out	MET -> METxt	
PANT_in	PANTxt -> PANT	
BIOTIN_in	BIOTINxt -> BIOTIN	
Lys_in1	LYSxt + ALA -> LYS + ALAxt	Burkowski & Krämer (2002)
Lys_in2	LYSxt + VAL -> LYS + VALxt	Burkowski & Krämer (2002)
Lys_in3	LYSxt + LEU -> LYS + LEUxt	Burkowski & Krämer (2002)
VAL_in	VALxt -> VAL	Ebbighausen et al (1989b)
ILE_in	ILExt -> ILE	Ebbighausen et al (1989b)
LEU_in	LEUxt -> LEU	Ebbighausen et al (1989b)
#Putative transportsystems		
GL_in_out	GLxt <-> GL	
ETH_in_out	ETHxt <-> ETH	
#AC_in_out	ACxt + H_transport_xt <-> AC + H_transport	
#LLAC_in_out	LLACxt + H_transport_xt <-> LLAC + H_transport	
LLAC_in_out	LLACxt <-> LLAC	
AC_in_out	ACxt <-> AC	
GLAC_in_out	GLACxt <-> GLAC	
T3_in_out	T3xt <-> T3	
GLYR_in_out	GLYRxt <-> GLYR	
Propionate_in_out	PROPIONATExt + H_transport_xt <-> PROPIONATE + H_transport	
Formate_in_out	FORxt + H_transport_xt <-> FOR + H_transport	
LAC_in_out	LACxt + H_transport_xt <-> LAC + H_transport	
ASN_in_out	ASNxt <-> ASN	
ASP_in_out	ASPxt <-> ASP	
GLY_in_out	GLYxt <-> GLY	
CYS_in_out	CYSxt <-> CYS	
HIS_in_out	HISxt <-> HIS	
PPI_in_out	PPIxt <-> PPI	
PYR_transport	PYRxt <-> PYR	
FRU_out	FRU -> FRUxt	

Appendix I: List of metabolites for genome-scale model

Abbreviation	Metabolite
13PDG	3-Phospho-D-glyceroyl phosphate
2OMOP	2-oxo-4-methyl-3-carboxypentenanoate
2PG	2-Phospho-D-glycerate
3DDAH7P	3-deoxy-D-arabino-heptonate 7-phosphate
3PG	3-Phospho-D-glycerate
3PSER	3-Phosphoserine
4A4DOCHOR	4-Amino-4-deoxychorismate
4PPNTO	D-4'-Phosphopantothenate
5AL	5-aminolevulinate
5EPS3P	5-enolpyruvylshikimate 3-phosphate
6PG	6-Phosphogluconate
A6RP5P	5-Amino-6-(5'-phosphoribosylamino)uracil
A6RP5P2	5-Amino-6-(5'-phosphoribitylamino)uracil
ABUT	2-Aceto-2-hydroxybutanoate
AC	Acetate
ACACP	Acyl-[acyl-carrier protein]
ACAL	Acetaldehyde
ACCOA	Acetyl Co-A
ACETYLP	Acetyl-P
ACLAC	2-Acetolactate
ACLIPO	S-acetyldihydrolipoamide
ACP	Acyl-carrier protein
ADENINE	Adenine
ADENOSINE	Adenosine
ADP	ADP
AGL3P	Acyl-sn-glycerol 3-phosphate
AHHMD	2-Amino-7,8-dihydro-4-hydroxy-6-(diphosphooxymethyl)pteridine
AHHMP	2-Amino-4-hydroxy-6-hydroxymethyl-7,8-dihydropteridine
AHTD	2-Amino-4-hydroxy-6-(erythro-1,2,3-trihydroxypropyl)-dihydropteridine triphosphate
AICAR	1-(5'-Phosphoribosyl)-5-amino-4-imidazolecarboxamide
AIR	Aminoimidazole ribotide: (1-(5-phosphoribosyl)-5-aminoimidazole)
AKG	2-Oxoglutarate
AKP	2-Dehydropantoate
ALA	L-Alanine
ALAALA	D-alanyl-D-alanine
AMP	AMP
AN	Anthranilate
AP	L-4-aspartyl phosphate
APS	Adenylylsulfate
ARABINOGALACTAN	Arabinogalactan (cell wall component)
ARG	L-Arginine
ASN	L-Asparagine
ASP	L-Aspartate
ASPSA	L-Aspartate 4-semialdehyde
ASUC	N6-(1,2-Dicarboxyethyl)-AMP; Adenosylosuccinate
ATP	ATP
bALA	beta-Alanine
BET	Betaine
BIOMASS	Biomass
BIOTIN	biotin
C140ACP	Myristoyl-[acyl-carrier protein]

C150ACP	Pentadecanoyl-[acyl-carrier protein]
C160ACP	Hexadecanoyl-[acyl-carrier protein]
C161ACP	Palmitoyl-[acyl-carrier protein]
C180ACP	Stearoyl-[acyl-carrier protein]
C181ACP	Oleoyl-[acyl-carrier protein]
CAIR	1-(5-Phospho-D-ribosyl)-5-amino-4-imidazolecarboxylate
CAP	Carbamoyl phosphate
CBHCAP	3-Isopropylmalate
CDP	CDP
CDPDG	CDP-diacylglycerol
CHOR	Chorismate
CIT	Citrate
CITR	L-Citrulline
CL	Cardiolipin (biomass component)
CMP	CMP
CO2	CO2
COA	CoA
COPPIII	Coproporphyrinogen III
CPAD5P	1-(2-Carboxyphenylamino)-1-deoxy-D-ribulose 5-phosphate
CTP	CTP
CYS	L-Cysteine
CYTIDINE	Cytidine
CYTOSINE	Cytosine
CAASP	N-Carbamoyl-L-aspartate
D6PGC	6-Phospho-D-gluconate
D6RP5P	2,5-Diamino-6-hydroxy-4-(5'-phosphoribosylamino)-pyrimidine
D8RL	6,7-Dimethyl-8-(1-D-ribityl)lumazine
DADP	dADP
DALA	D-alanine
DAMP	dAMP
DAPA	7,8-aminopelargonic acid
DAPIM	L,L-2,6-Diaminopimelate
DATP	dATP
DCDP	dCDP
DCMP	dCMP
DCTP	dCTP
DEHYDRODIPICOLINAT	Dehydrodipicolinate
DEOADENOSINE	Deoxyadenosine
DEOXYCYTIDINE	Deoxycytidine
DEOXYGUANOSINE	Deoxyguanosine
DEOXYURIDINE	Deoxyuridine
DGDP	dGDP
DGDP	dGDP
DGLUTAMATE	D-Glutamate
DGMP	dGMP
DGTP	dGTP
DHAP	Glycerone phosphate
DHB4P	3,4-dihydroxy-2-butanone-4-P
DHF	Dihydrofolate
DHMV	2,3-dihydroxy-3-methylvalerate
DHMVA	(R)-2,3-dihydroxy-3-methylbutanoate
DHN	1,4-dihydroxy-2-naphthoate
DHP	2-Amino-4-hydroxy-6-(D-erythro-1,2,3-trihydroxypropyl)-7,8-dihydropteridine
DHPT	Dihydropteroate
DHSK	3-Dehydroshikimate
DIMGP	D-erythro-1-(Imidazol-4-yl)glycerol 3-phosphate
DLIPO	Dihydrolipoamide
DMK	2-Demethylmenaquinone

DNA	DNA (biomass component)
DOROA	(S)-Dihydroorotate
DPCOA	Dephospho-CoA
DQT	3-Dehydroquinate
DTBIOTIN	Dethiobiotin
DTDP	dTDP
DTMP	dTMP
DTTP	dTTP
DUDP	dUDP
DUMP	dUMP
DUTP	dUTP
E4P	D-Erythrose 4-phosphate
ETH	Ethanol
F1P	D-Fructose 1-phosphate
F6P	beta-D-Fructose 6-phosphate
FAD	FAD
FADH2	FADH2
FDP	beta-D-Fructose 1,6-bisphosphate
FGAM	2-(Formamido)-N1-(5'-phosphoribosyl)acetamidine
FGAR	5'-Phosphoribosyl-N-formylglycinamide
FMN	FMN
FOL	Folate
FOR	Formate
FREEMYCOLICACID	Free Mycolic acids and Mycolic acids bonded to Arabinogalactan
FRU	D-Fructose
FTHF	10-Formyltetrahydrofolate
FUM	Fumarate
G1P	D-Glucose 1-phosphate
G3P	D-Glyceraldehyde 3-phosphate
G6P	alpha-D-Glucose 6-phosphate
GA1P	D-Glucosamine 1-phosphate
GA6P	D-Glucosamine 6-phosphate
GABA	4-Aminobutanoate
GAL1P	D-Galactose 1-phosphate
GAR	5'-Phosphoribosylglycinamide
GDP	GDP
GDPMAN	GDPmannose
GL	Glycerol
GL3P	sn-Glycerol-3-phosphate
GLAC	D-Galactose
GLC	alpha-D-Glucose
GLN	L-Glutamine
GLU	L-Glutamate
GLUC	D-Gluconate
GLUGSAL	L-Glutamate 5-semialdehyde
GLUP	alpha-D-Glutamyl phosphate
GLUTAMYLTRNA	GLUTAMYLTRNA
GLX	Glyoxylate
GLY	Glycine
GLYR	(R)-glycerate
GMP	GMP
GSA	Glutamate-1-semialdehyd
GTP	GTP
GUANINE	Guanine
GUANOSINE	Guanosine
H_PO	Protons assosiated with electron transport chain
H_transport	Protons assosiated with transport reactions over the membrane
H2O2	H2O2

H2S	Hydrogen sulfide
H2SO3	Sulfite
HCYS	Homocysteine
HEMEA	Heme a
HEMEC	Heme c
HEMEO	Heme o
HIS	L-Histidine
HISOL	L-Histidinol
HISOLP	L-Histidinol phosphate
HSER	L-Homoserine
HXAN	Hypoxhantine
HYDROXYMEBI	hydroxymethylbilane
ICHOR	Isochorismate
ICIT	Isocitrate
ILE	L-Isoleucine
IMACP	3-(Imidazol-4-yl)-2-oxopropyl phosphate
IMP	IMP
INOSINE	Inosine
IPPMAL	2-Isopropylmalate
KAPA	7-keto-8-aminopelargonic acid
LAC	(R)-Lactate, D-Lactate
LEU	L-Leucine
LIPO	Lipoamide
LLAC	(S)-Lactate, L-Lactate
LLCT	L-Cystathionine
LYS	L-Lysine
MAL	Malate
MALACP	Malonyl-[acyl-carrier protein]
MALCOA	Malonyl-CoA
MALONATES	Malonate semialdehyde
MAN	Mannose
MAN1P	alpha-D-Mannose 1-phosphate
MAN6P	D-Mannose 6-phosphate
MDAPIM	meso-2,6-Diaminopimelate
MET	L-Methionine
METHF	5,10-Methenylenetetrahydrofolate
METTHF	5,10-Methenyltetrahydrofolate
Mg	Magnesium
MK	menaquinone
MKH2	menaquinol
MLT	Maltose
MLTTRE	Maltooligosyl trehalose
MTHF	5-Methyltetrahydrofolate
MYCOLICACID	Mycolic acid
Na	Sodium (assoiated in transport reactions)
NACN	Nicotinate D-ribonucleotide
NAD	NAD+
NADH	NADH
NADP	NADP+
NADPH	NADPH
NAGA1P	N-Acetyl-D-glucosamine 1-phosphate
NAGA6P	N-Acyl-D-glucosamine 6-phosphate
NAGLU	N-Acetyl-L-glutamate
NAGLUP	N-Acetyl-L-glutamate 5-phosphate
NAGLUS	N-Acetyl-L-glutamate 5-semialdehyde
NAM	Nicotinamide
NAORN	N2-Acetyl-L-ornithine
NAS	(Nomega-L-arginino)succinate

NH3	NH3
NH4	NH4
Ni	Nickel
NIC	Nicotinate
NIC	Nicotinate
NO2	nitrite
NO3	nitrate
NPRAN	N-(5-Phospho-D-ribosyl)anthranilate
NAAD	Deamido-NAD+
O2	Oxygen
OA	Oxaloacetate
OAHSER	O-Acetyl-L-homoserine
OASER	O-Acetyl-L-serine
OBUT	2-Oxobutanoate
OIVAL	(R)-2-Oxoisovalerate
OMP	Orotidine 5'-phosphate
OMVAL	3-Methyl-2-oxobutanoate
ORN	L-Ornithine
OROA	Orotate
OSB	O-succinylbenzoate
OSBCOA	O-succinylbenzoate-CoA
OTHIO	Oxidized thioredoxin
P5C	(S)-1-Pyrroline-5-carboxylate
PA	Phosphatidate
PABA	4-Aminobenzoate
PANT	(R)-Pantoate
PAP	Adenosine 3',5'-bisphosphate
PAPS	3'-Phosphoadenylylsulfate
PEP	Phosphoenolpyruvate
PEPTIDOGLYCAN	Peptidoglycan (biomass component)
PG	Phosphatidylglycerol
PHE	L-Phenylalanine
PHEN	Prephenate
PHOSPHOLIPID	Phospholipids (biomass component)
PHP	3-Phosphonooxypyruvate
PHPYR	Phenylpyruvate
PHSER	O-Phospho-L-homoserine
PI	Orthophosphate
PIM	Phosphatidyl inositol mannosides
PIPER26DC	L(delta-1)-Piperideine-2,6-dicarboxylate
PIT	Phosphatidyl inositol
PNTO	(R)-Pantothenate
POLYGLC	Glucose Polymers
PORIII	Porphobilinogen III
PPI	Pyrophosphate
PRAM	5-Phosphoribosylamine
PRBAMP	N1-(5-Phospho-D-ribosyl)-AMP
PRBATP	N1-(5-Phospho-D-ribosyl)-ATP
PRETYR	Pretyrosine
PRFICA	1-(5'-Phosphoribosyl)-5-formamido-4-imidazolecarboxamide
PRFP	5-(5-Phospho-D-ribosylaminoformimino)-1-(5-phosphoribosyl)-imidazole-4-carboxamide
PRLP	N-(5'-Phospho-D-1'-ribulosylformimino)-5-amino-1-(5"-phospho-D-ribosyl)-4-imidazolecarboxamide
PRO	L-Proline
PROIX	Protoporphyringen IX
PROPIONATE	Propionate
PROPORIX	Protopotphyrin IX

PROTEIN	Proteins (biomass component)
PROTOHEMEIX	Protoheme IX
PRPP	5-Phospho-alpha-D-ribose 1-diphosphate
PS	Phosphatidylserine
PYR	Pyruvate
R1P	D-Ribose 1-phosphate
R5P	D-Ribose 5-phosphate
RIB	D-Ribose
RIBFLAV	Riboflavin
RNA	RNA (biomass component)
RTHIO	Reduced thioredoxin
Ru5P	Ribulose-5-phosphate
S7P	Sedoheptulose 7-phosphate
SAH	S-Adenosyl-L-homocysteine
SAICAR	1-(5'-Phosphoribosyl)-5-amino-4-(N-succinocarboxamide)-imidazole
SAM	S-Adenosyl-L-methionine
SDAPIM	N-Succinyl-L-2,6-diaminopimelate
SDLIPO	S-Succinyldihydrolipoamide
SDAAKP	Succinyl-2,6-amino-6-ketopimelate
SER	L-Serine
SHCHC	2-succinyl-6-hydroxy-2,4-cyclohexadiene-1-carboxylate
SLF	Sulfate
SMALL MOLECULES	Small molecules pool (biomass component)
SME	Shikimate
SME3P	Shikimate 3-phosphate
SUC	Sucrose
SUC6P	Sucrose 6-phosphate
SUCC	Succinate
SUCCOA	Succinyl-CoA
SUCCSAL	Succinate semialdehyde
T3	D-Glyceraldehyde
TDCM	Trehalose Decorynemycolate
THF	Tetrahydrofolate
THFG	Tetrahydrofolyl-[Glu](n)
THR	L-Threonine
THYMIDINE	Thymidine
TMCM	Trehalose Monocorynemycolate
TRE	alpha,alpha-Trehalose
TRE6P	alpha,alpha'-Trehalose 6-phosphate
TRP	L-Tryptophan
TYR	L-Tyrosine
UDP	UDP
UDPARA	UDP-L-Arabinose
UDPG	UDPglucose
UDPGAL	UDP-D-galactose
UDPNACVG	UDP-N-acetyl-3-(1-carboxyvinyl)-D-glucosamine
UDPNAG	UDP-N-acetyl-D-glucosamine
UDPNAM	UDP-N-acetylmuramate
UMP	UMP
URA	Uracil
UREA	Urea
URIDINE	Uridine
UROPORIII	Uroporphyrinogen III
UTP	UTP
VAL	L-Valine
X5P	D-Xylulose-5-phosphate
XANTHOSINE	Xanthosine
XHANTHINE	Xhanthine

XMP	Xanthosine 5'-phosphate
XYL	D-Xylose

Appendix I: Reference list for genome-scale model construction

Alifano,P., Fani,R., Lió,P., Lazcano,A., Bazzicalupo,M., Carlomagno,M.S., and Bruni,C.B. (1996) Histidine biosynthetic pathway and genes: Structure, regulation, and evolution. *Microbiological Reviews* **60,** 44-69.

Ankri,S., Serebrijski,I., Reyes,O., and Leblon,G. (1996) Mutations in the Corynebacterium glutamicum proline biosynthetic pathway: a natural bypass of th proA step. *J.Bacteriol.* **178,** 4412-4419.

Bathe,B., Kalinowski,J., and Pühler,A. (1996) A physical and genetic map of the *Corynebacterium glutamicum* ATCC 13032 chromosome. *Molecular Genetics and Genomics* **252,** 255-265.

Beckers,G., Bendt,A.K., Krämer,R., and Burkovski,A. (2004) Molecular identification of the urea uptake system and transciptional analysis of urea transporter- and urea-encoding genes in *Corynebacterium glutamicum* . *Journal of*

Bott,M. and Niebisch,A. (2003) The respiratory chain of *Corynebacterium glutamicum* . *Journal of Biotechnology* **104,**

Brand,S., Niehaus,K., Pühler,A., and Kalinowski,J. (2003) Identification and functional analysis of six mycolyltransferase genes of *Corynebacterium glutamicum* ATCC 13032: the genes *cop1* , *cmt1* , and *cmt2* can replace each other in the synthesis of trehalose dicorynomycolate, a component of the mycolic acid layer of the cell envelope. *Archives of*

Burkovski,A. (2003) I do it my way: regulation of ammonium uptake and ammonium assimilation in *Corynebacterium glutamicum* . *Archives of Microbiology* **179,** 83-88.

Burkovski,A. and Krämer,R. (2002) Bacterial amino acid transport proteins: occurrence, functions, and significance for biotechnological applications. *Applied Microbiology and Biotechnology* **58,** 265-274.

Claes,W.A., Puhler,A., and Kalinowski,J. (2002) Identification of two *prpDBC* gene clusters in *Corynebacterium glutamicum* and their involvement in propionate degradation via the 2-methylcitrate cycle. *J.Bacteriol.* **184,** 2728-2739.

Cocaign-Bousquet,M., Guyonvarch,A., and Lindley,N.D. (1996) Growth rate-dependent modulation of carbon flux through central metabolism and the kinetic consequences for glucose-limited chemostat cultures of *Corynebacterium*

Cremer,J., Eggeling,L., and Sahm,H. (1990) Cloning the *dapA dapB* cluster of the lysine-secreting bacterium *Corynebacterium glutamicum* . *Molecular Genetics and Genomics (Historical Archive)* **220,** 478-480.

Cremer,J., Eggeling,L., and Sahm,H. (1991) Control of the lysine biosynthesis sequence in *Corynebacterium glutamicum* as analysed by overexpression of the individual corresponding genes. *Appl.Environ.Microbiol.* **57,** 1746-1752.

Daffé,M. (2005) The Cell Envelope of Corynebacteria. In *Handbook of Corynebacterium glutamicum* (Edited by Eggeling,L. and Bott,M.) Pp. 121-148. CRC Press, Boca Raton.

Ebbighausen,H., Weil,B., and Krämer,R. (1989) Transport of branched-chain amino acids in *Corynebacterium glutamicum* . *Archives of Microbiology* **151,** 238-244.

Ebbighausen,H., Weil,B., and Krämer,R. (1991) Carrier-mediated acetate uptake in *Corynebacterium glutamicum* . *Archives of Microbiology* **155,** 505-510.

Eikmanns,B.J. (1992) Identification, sequence analysis, and expression of a *Corynebacterium glutamicum* gene cluster encoding the three glycolytic enzymes glyceraldehyde-3-phosphate dehydrogenase, 3-phosphoglycerate kinase, and

Eikmanns,B.J., Follettie,M.T., Griot,M.U., and Sinskey,A.J. (1989) The phosphoenolpyruvate carboxylase gene of *Corynebacterium glutamicum* : Molecular cloning, nucleotide sequence, and expression. *Molecular and General Genetics*

Eikmanns,B.J., Rittmann,D., and Sahm,H. (1995) Cloning, sequence analysis, expression, and inactivation of the Corynebacterium glutamicum icd gene encoding isocitrate dehydrogenase and biochemical characterization of the

Eikmanns,B.J., Thum-Schmitz,N., Eggeling,L., Ludtke,K.U., and Sahm,H. (1994) Nucleotide sequence, expression and transcriptional analysis of the *Corynebacterium glutamicum gltA* gene encoding citrate synthase. *Microbiology* **140,** 1817-

Fazel,A.M. and Jensen,R.A. (1979a) Aromatic aminotransferases in coryneform bacteria. *Journal of Bacteriology* **140,**

Fazel,A.M. and Jensen,R.A. (1979b) Obligatory biosynthesis of L-tyrosine via the pretyrosine branchlet in coryneform bacteria. *Journal of Bacteriology* **138,** 805-815.

Follettie,M.T. and Sinskey,A.J. (1986) Molecular cloning and nucleotide sequence of the *Corynebacterium glutamicum pheA* gene. *Journal of Bacteriology* **167,** 695-702.

Groeger,U. and Sahn,H. (1987) Microbial production of L-leucine from alpha-ketoisocaproate by *Corynebacterium glutamicum* . *Appl.Environ.Microbiol.* **25,** 352-356.

Hoischen,C. and Krämer,R. (1990) Membrane alteration is necessary but not sufficient for effective glutamate secretion in *Corynebacterium glutamicum* . *Journal of Bacteriology* **172,** 3409-3416.

Hwang,B.-J., Yeom,H.-J., Kim,Y., and Lee,H.-S. (2002) *Corynebacterium glutamicum* utilizes both transsulfuration and direct sulfhydrylation pathways for methionine biosynthesis. *Journal of Bacteriology* **184,** 1277-1286.

Ikeda,M. (2005) L-Tryptophan Production. In *Handbook of Corynebacterium glutamicum* (Edited by Eggeling,L. and Bott,M.) Pp. 489-510. CRC Press, Boca Raton.

Ingraham,J.L., Maaløe,O., and Niedhardt,F.C. (1983) *Growth of the Bacterial Cell* . Sinauer Associates, Inc., Sunderland,

Jakoby,M., Tesch,M., Sahn,H., Krämer,R., and Burkowski,A. (1997) Isolation of the *Corynebacterium glutamicum glnA* gene encoding glutamine syntase I. *FEMS Microbiology Letters* **154,** 81-88.

Jetten,M.S., Gubler,M.E., Lee,S.H., and Sinskey,A.J. (1994a) Structural and functional analysis of pyruvate kinase from Corynebacterium glutamicum. *Appl.Environ.Microbiol.* **60,** 2501-2507.

Jetten,M.S.M. and Anthony,J.S. (1995) Purification and properties of oxaloacetate decarboxylase from *Corynebacterium glutamicum* . *Antonie van Leeuwenhoek* **67,** 221-227.

Jetten,M.S.M., Pitoc,G.A., Follettie,M.T., and Sinskey,A.J. (1994b) Regulation of phospho(enol)-pyruvate- and oxaloacetate-converting enzymes in Corynebacterium glutamicum. *Applied Microbiology and Biotechnology* **41,**

Jung,S.-I., Han,M.-S., Kwon,J.-H., Cheon,C.-I., Min,K.-H., and Lee,M.-S. (1998) Cloning of the histidine biosynthetic genes of *Corynebacterium glutamicum* : Orgenization and sequencing analysis of the *hisA, impA* and *hisF* gene cluster. *Biochemical and Biophysical Research Communications* **247,** 741-745.

Kalinowski,J., Bathe,B., Bartels,D., Bischoff,N., Bott,M., Burkovski,A., Dusch,N., Eggeling,L., Eikmanns,B.J., and Gaigalat,L. (2003) The complete Corynebacterium glutamicum ATCC 13032 genome sequence and its impact on the production of -aspartate-derived amino acids and vitamins. *Journal of Biotechnology* **104,** 5-25.

Keilhauer,C., Eggeling,L., and Sahm,H. (1993) Isoleucine synthesis in Corynebacterium glutamicum: molecular analysis of the ilvB-ilvN-ilvC operon. *J.Bacteriol.* **175,** 5595-5603.

Kronemeyer,W., Peekhaus,N., Kramer,R., Sahm,H., and Eggeling,L. (1995) Structure of the gluABCD cluster encoding the glutamate uptake system of Corynebacterium glutamicum. *J.Bacteriol.* **177,** 1152-1158.

Krug,A., Wendisch,V.F., and Bott,M. (2005) Identification of AcnR, a TetR-type repressor of the aconitase gene *acn* in *Corynebacterium glutamicum* . *J.Biol.Chem.* **280,** 585-595.

Lee,H.-S. (2005) Sulfur Metabolism and Its Regulation. In *Handbook of Corynebacterium glutamicum* (Edited by Eggeling,L. and Bott,M.) Pp. 351-376. CRC Press, Boca Raton.

Lee,H.-S. and Hwang,B.-J. (2003) Methionine biosynthesis and its regulation in *Corynebacterium glutamicum* : parallel pathways of transsulfuration and direct sulfhydration. *Applied Microbiology and Biotechnology* **62,** 459-467.

Leyval,D., Uy,D., Delaunay,S., Goergen,J.L., and Engasser,J.M. (2003) Characterisation of the enzyme activities involved in the valine biosynthetic pathway in a valine-producing strain of *Corynebacterium glutamicum* . *Journal of*

Lin,L.L., Liao,H.F., Chien,H.R., and Hsu,W.H. (2001) Identification of essential cysteine residues in 3-Deoxy-d-Arabino-Heptulosonate-7-Phosphate Synthase from *Corynebacterium glutamicum* . *Current Microbiology* **42,** 426-431.

Malumbres,M., Mateos,L.M., Lumbreras,M.A., Guerrero,C., and Martin,J.F. (1994) Analysis and expression of the *thrC* gene of Brevibacterium lactofermentum and characterization of the encoded threonine synthase. *Appl.Environ.Microbiol.*

Marx,A., Hans,S., Möckel,B., Bathe,B., and de Graaf,A.A. (2003) Metabolic phenotype of phosphoglucose isomerase mutants of *Corynebacterium glutamicum* . *Journal of Biotechnology* **104,** 185-197.

Miyajima,R., Otsuka,S.-I., and Shiio,I. (1968) Regulation of aspartate family amino acid biosynthesis in *Brevibacterium flavum* . 1. Inhibition by amino acids of the enzymes in threonine biosynthesis. *Journal of Biochemistry* **63,** 139-148.

Möckel,B., Eggeling,L., and Sahm,H. (1992) Functional and structural analysis of threonine dehydratase from *Corynebacerium glutamicum* . *Journal of Bacteriology* **174,** 8065-8072.

Molenaar,D., van der Rest,M.E., Drysch,A., and Yucel,R. (2000) Functions of the membrane-associated and cytoplasmic malate dehydrogenases in the citric acid cycle of *Corynebacterium glutamicum* . *J.Bacteriol.* **182,** 6884-6891.

Moritz,B., Striegel,K., de Graff,A.A., and Sahm,H. (2000) Kinetic properties of the glucose-6-phosphate and 6-phosphogluconate dehydrogenases from *Corynebacterium glutamicum* and their application for predicting pentose phosphate pathway flux *in vivo* . *European Journal of Biochemistry* **267,** 3442-3452.

Nampoothiri,K.M., Hoischen,C., Bathe,B., Möckel,B., Pfefferle,W., Krumbach,K., Sahm,H., and Eggeling,L. (2002) Expression of genes of lipid synthesis and altered lipid composition modulates L-glutamate efflux of *Corynebacterium*

Netzer,R., Peters-Wendisch,P., Eggeling,L., and Sahm,H. (2004) Cometabolism of a Nongrowth Substrate: L-Serine Utilization by *Corynebacterium glutamicum* . *Appl.Environ.Microbiol.* **70,** 7148-7155.

Palmieri,L., Berns,D., Krämer,R., and Eikmanns,M. (1996) Threonine diffusion and threonine transport in *Corynebacterium glutamicum* and their role in threoninge production. *Archives of Microbiology* **165,** 48-54.

Park,S.Y., Kim,H.K., Yoo,S.-K., Oh,T.K., and Lee,J.K. (2000) Characterization of *glk* , a gene coding for glucose kinase of *Corynebacterium glutamicum* . *FEMS Microbiology Letters* **188,** 209-215.

Park,S.-D., Lee,J.-Y., Kim,Y., Kim,J.-H., and Lee,H.-S. (1998) Isolation and analysis of metA, a biosynthetic gene encoding homoserine acetyltransferase in *Corynebacterium glutamicum* . *Molecules and Cells* **8,** 286-294.

Pátèk,M., Hochmannová,J., Jelínková,M., Nesvera,J., and Eggeling,L. (1998) Analysis of the *leuB* gene from *Corynebacterium glutamicum* . *Applied Microbiology and Biotechnology* **50,** 42-47.

Peters-Wendisch,P., Stoltz,M., Etterich,H., Kennerknecht,N., Sahn,H., and Eggeling,L. (2005) Metabolic Engineering of *Corynebacterium glutamicum* for L-serine production. *Appl.Environ.Microbiol.* **71,** 7139-7144.

Peters-Wendisch,P.G., Kreutzer,C., Kalinowski,J., Patek,M., Sahm,H., and Eikmanns,B.J. (1998) Pyruvate carboxylase from *Corynebacterium glutamicum* : characterization, expression and inactivation of the *pyc* gene. *Microbiology* **144,**

Peters-Wendisch,P.G., Netzer,R., Eggeling,L., and Sahm,H. (2002) 3-Phosphoglycerate dehydrogenase from *Corynebacterium glutamicum* : the C-terminal domain is not essential for activity but is required for inhibition by L-

Radmacher,E., Vaitsikova,A., Burger,U., Krumbach,K., Sahm,H., and Eggeling,L. (2002) Linking Central Metabolism with Increased Pathway Flux: L-Valine Accumulation by *Corynebacterium glutamicum* . *Appl.Environ.Microbiol.* **68,**

Reinscheid,D., Eikmanns,B.J., and Sahn,H. (1994a) Malate synthase from Corynebacterium glutamicum: sequence analysis of the gene and biochemical characterization of the enzyme. *Microbiology* **140,** 3099-3108.

Reinscheid,D.J., Eikmanns,B.J., and Sahm,H. (1994b) Characterization of the isocitrate lyase gene from Corynebacterium glutamicum and biochemical analysis of the enzyme. *J.Bacteriol.* **176,** 3474-3483.

Reinscheid,D.J., Eikmanns,B.J., and Sahn,H. (1991) Analysis of a *Corynebacterium glutamicum hom* gene coding for a feed-back reistant homoserine dehydrogenase. *Journal of Bacteriology* **173,** 3228-3230.

Reinscheid,D.J., Schnicke,S., Rittmann,D., Zahnow,U., Sahm,H., and Eikmanns,B.J. (1999) Cloning, sequence analysis, expression and inactivation of the Corynebacterium glutamicum pta-ack operon encoding phosphotransacetylase and

Riedel,C., Rittmann,D., Dangel,P., Möckel,B., Sahn,H., and Eikmanns,B.J. (2001) Characterization, expression, and inactivation of the phosphoenolpyruvate carboxykinase gene from *Corynebacterium glutamicum* and significance of the enzyme for growth and amino acid production. *Journal of Molecular Microbiology and Biotechnology* **3,** 573-583.

Rittmann,D., Schaffer,S., Wendisch,V.F., and Sahn,H. (2003) Fructose-1,6-bisphosphatase from *Corynebacterium glutamicum* : expression and deletion of the *fbp* gene and biochemical characterization of the enzyme. *Archives of*

Rückert,C., Pühler,A., and Kalinowski,J. (2003) Genome-wide analysis of the L-methionine biosynthetic pathway in Corynebacterium glutamicum by targeted gene deletion and homologous complementation. *Journal of Biotechnology*

Sahm,H. and Eggeling,L. (1999) D-pantothenate synthesis in *Corynebacterium glutamicum* and use of *panBC* and genes encoding L-valine synthesis for D-pantothenate overproduction. *Appl.Environ.Microbiol.* **65,** 1973-1979.

Schrumpf,B., Schwarzer,A., Kalinowski,J., Pühler,A., Eggeling,L., and Sahn,H. (1991) A functionally split pathway for lysine synthesis in *Corynebacterium glutamicum* . *Journal of Bacteriology* **173,** 4510-4516.

Schwinde,J.W., Hertz,P.F., Sahm,H., Eikmanns,B.J., and Guyonvarch,A. (2001) Lipoamide dehydrogenase from *Corynebacterium glutamicum* : molecular and physiological analysis of the *lpd* gene and characterization of the enzyme.

Serebrijski,I., Wojcik,F., Reyes,O., and Leblon,G. (1995) Multicopy suppression by asd gene and osmotic stress-dependent complementation by heterologous proA in proA mutants. *J.Bacteriol.* **177,** 7255-7260.

Siewe,R., Weil,B., Burkovski,A., Eggeling,L., Krämer,R., and Jahns,T. (1998) Urea uptake and urease activity in *Corynebacterium glutamicum* . *Archives of Microbiology* **169,** 411-416.

Siewe,R., Weil,B., and Krämer,R. (1995) Glutamine uptake by a sodium-dependent secondary transport system in *Corynebacterium glutamicum* . *Archives of Microbiology* **164,** 98-103.

Simic,P., Sahm,H., and Eggeling,L. (2001) L-threonine export: use of peptides to identify a new translocator from *Corynebacterium glutamicum* . *Journal of Bacteriology* **183,** 5317-5324.

Simic,P., Willuhn,J., Sahn,H., and Eggeling,L. (2002) Identification of *glyA* (encoding serine hydroxymethyltransferase) and its use together with the exporter ThrE to increase L-threonine accumulation by *Corynebacterium glutamicum* .

Sugimoto,S. and Shiio,I. (1989) Fructose metabolism and regulation of 1-phosphofructokinase and 6-phosphofructokinase in *Brevibacterium flavum* . *Agricultural and Biological Chemistry* **53,** 1261-1268.

Sugimoto,S.-I. and Shiio,I. (1977) Enzymes of the tryptophan synthetic pathway in *Brevibacterium flavum* . *The Journal*

Tzvetkov,M., Klopprogge,C., Zelder,O., and Liebl,W. (2003) Genetic dissection of trehalose biosynthesis in *Corynebacterium glutamicum* : inactivation of trehalose production leads to impaired growth and an altered cell wall lipid

Usuda,Y., Tujimoto,N., Abe,C., Asakura,Y., Kimura,E., Kawahara,Y., Kurahashi,O., and Matsui,H. (1996) Molecular cloning of the *Corynebacterium glutamicum* ('Brevibacterium lactofermentum' AJ12036) *odhA* gene encoding a novel type of 2-oxoglutarate dehydrogenase. *Microbiology-Uk* **142,** 3347-3354.

Vallino,J.J. and Stephanopoulos,G. (1993) Metabolic flux distribution in *Corynebacterium glutamicum* during growth and lysine overproduction. *Biotechnology and Bioengineering* **41,** 633-646.

von der Osten,C.H., Barbas,C.H., Wong,C.F., and Sinskey,A.J. (1989) Molecular cloning, nucleotide sequence and fine-structural analysis of the *Corynebacterium glutamicum fda* gene: structural comparison of *C. glutamicum* fructose-1,6-biphosphate aldolase to class I and class II aldolases. *Molecular Microbiology* **3,** 1625-1637.

Wada,M., Awano,N., Haisa,K., Takagi,H., and Nakamori,S. (2002) Purification, characterization and identification of cysteine desulfhydrase of *Corynebacterium glutamicum* , and its relationship to cysteine production. *FEMS Microbiology*

Wada,M., Awano,N., Yamazawa,H., Takagi,H., and Nakamori,S. (2004) Purification and characterization of *O* -acetylserine sulfhydrylase of *Corynebacterium glutamicum* . *Bioscience Biotechnology and Biochemistry* **68,** 1581-1583.

Wehrmann,A., Morakkabati,S., Kramer,R., Sahm,H., and Eggeling,L. (1995) Functional analysis of sequences adjacent to dapE of Corynebacterium glutamicum reveals the presence of aroP, which encodes the aromatic amino acid transporter.

Willis,L.B., Lessard,P.A., and Sinskey,A.J. (2005) Synthesis of L-Threonine and Branched-Chain Amino Acids. In *Handbook of Corynebacterium Glutamicum* (Edited by Eggeling,L. and Bott,M.) Pp. 511-531. CRC Press, Boca Raton.

Yokota,A. and Lindley,N.D. (2005) Central Metabolism: Sugar Uptake and Conversion. In *Handbook of Corynebacterium glutamicum* (Edited by Eggeling,L. and Bott,M.) Pp. 215-240. CRC Press, Boca Raton.

Zhao,Y. and Lin,Y.H. (2002) Flux distribution and partitioning in *Corynebacterium glutamicum* grown at different specific growth rates. *Process Biochemistry* **37,** 775-785.

Appendix II

Biomass compostition of *Corynebacterium glutamicum* used for genome-scale reconstruction

Table 1. Macromolecular composition:
An overall cellular composition of *Corynebacterium glutamium* was found in Cocaign-Bousquet *et al.* (1996).

Component	g·g^{-1} DCW	Reference	Comments	Organism	Conditions
Protoplast	**0.580**				
Protein	0.520	Cocaign-Bousquet *et al* (1996)		*C. glutamicum* ATCC 17965	Batch; Exponential phase
DNA	0.010	Cocaign-Bousquet *et al* (1996)		*C. glutamicum* ATCC 17965	Batch; Exponential phase
RNA	0.050	Cocaign-Bousquet *et al* (1996)		*C. glutamicum* ATCC 17965	Batch; Exponential phase
Lipids	**0.130**	Cocaign-Bousquet *et al* (1996)		*C. glutamicum* ATCC 17965	Batch; Exponential phase
Mycolic acids	0.102	Eggeling and Bott (2005) pp 125, Purch *et al* (2001)	Rest after Phospholipids were substracted from lipid fraction - Literature values 7.5-8%	C. glutamicum CGL2005 + CGL2022	Exponential Phase
Phospholipids	0.028	Hoichen & Cremer (1990)	Estimated from data of Hoichen & Cremer (1990) using an average molecular weight of 895 g/mol calculated in lipid-section	*C. glutamicum* ATCC 13032	Early glutamate production phase
Cell wall Carbohydrates	**0.190**	Cocaign-Bousquet *et al* (1996)		*C. glutamicum* ATCC 17965	Batch; Exponential phase
Peptidoglycan	0.095	Keddie and Cure (1978); Integram *et al.* (1983)	50 % of cell wall carbohydrates (estimation)	*C. glutamicum* ATCC 13032	
Arabinogalactan	0.095		50 % of cell wall carbohydrates (estimation)	*C. glutamicum* ATCC 13032	
Ash	**0.100**	Cocaign-Bousquet *et al* (1996)		*C. glutamicum* ATCC 17965	Batch; Exponential phase
SUM	1.000				

Biomass biosynthesis equation for synthesis of 1 g biomass:
PROTEIN + 0.010 DNA + 0.05 RNA + 0.028 PHOSPHOLIPID + 0.095 PEPTIDOGLYCAN + 0.095 ARABINOGALACTAN + 0.102 MYCOLICACID + 29.2 ATP + 18.5 ATP -> BIOMASS + 29.2 ADP + 29.2 PI + 18.5 ADP + 18.5 PI

Table 2.1. Averaged protein composition:
Average amino acids composition determined for *C. glutamicum* MH 20-22B (Continuous culture) (Marx *et al* . (1996)) and *C. glutamicum* ATCC 17965 (Cocaign-Bousquet *et al.* (1996)). The pool of intracellular glutamate and glutamine was also included in the protein fraction. Energy requirement for polymerisation was taken as for *E. coli* (Neidhardt *et al.* (1987).

Amino acid	µmol/g DW	MW	MW[a] substracted water	mg/g DCW	mg/g protein	µmol/g protein
Alanine	666	89.09	71.09	47.31	96.0	1268
Arginine	190	175.21	157.21	29.79	60.5	361
Asx (asp + asn)	387	132.6	114.6	44.29	89.9	736
Cysteine	44	121.15	103.15	4.54	9.2	84
Glutamate	423	147.13	129.13	54.62	110.9	806
Glutamine	317	146.2	128.15	40.56	82.3	603
Glutamate-intra	125	147.13	129.13	16.14	32.8	238
Glutamine-intra	25	146.2	128.15	3.14	6.4	47
Glycine	353	75.07	57.07	20.12	40.8	671
Histidine	67	156.16	138.16	9.26	18.8	128
Isoleucine	189	131.17	113.17	21.33	43.3	359
Leucine	351	131.17	113.17	39.72	80.6	669
Lysine	187	146.19	128.19	23.91	48.5	355
Methionine	76	149.21	131.21	9.91	20.1	144
Phenylalanine	128	165.19	147.19	18.84	38.2	244
Proline	159	115.13	97.13	15.44	31.3	303
Serine	245	105.09	87.09	21.34	43.3	467
Threonine	273	119.12	101.12	27.56	55.9	519
Tryptophan	28	204.23	186.23	5.12	10.4	52
Tyrosine	78	181.19	163.19	12.65	25.7	148
Valine	273	117.14	99.14	27.07	54.9	520
				492.65	1000.0	
Energy requirement for polymerisation						19.71

[a] water is substracted from MW to account for water excretion during peptide bond formation

Table 2.2 Protein composition (Marx *et al* . (1996):
The amino acids composition determined for *C. glutamicum* MH 20-22B *(Continuous culture)* is taken from Marx et al. (1996) Energy requirement for polymerisation was taken as for *E. coli (*Neidhardt *et al.* (1987).

Amino acid	µmol/g DW	MW	MW[a] substracted water	mg/g DCW	mg/g protein	mmol/g protein
Alanine	606	89.09	71.09	43.08	83.7	1143
Arginine	189	175.21	157.21	29.71	57.8	357
Asx (asp + asn)	399	132.6	114.6	45.73	88.9	753
Cysteine	87	121.15	103.15	8.97	17.4	164
Glutamate	360	147.13	129.13	46.49	90.4	679
Glutamine	147	146.2	128.15	18.84	36.6	277
Glutamate-intra	250	147.13	129.13	32.28	62.8	472
Glutamine-intra	49	146.2	128.15	6.28	12.2	92
Glycine	361	75.07	57.07	20.60	40.0	681
Histidine	71	156.16	138.16	9.81	19.1	134
Isoleucine	202	131.17	113.17	22.86	44.4	381
Leucine	440	131.17	113.17	49.79	96.8	830
Lysine	202	146.19	128.19	25.89	50.3	381
Methionine	146	149.21	131.21	19.16	37.2	275
Phenylalanine	133	165.19	147.19	19.58	38.1	251
Proline	170	115.13	97.13	16.51	32.1	321
Serine	225	105.09	87.09	19.60	38.1	425
Threonine	275	119.12	101.12	27.81	54.1	519
Tryptophan	54	204.23	186.23	10.06	19.5	102

Tyrosine	81	181.19	163.19	13.22	25.7	153
Valine	284	117.14	99.14	28.16	54.7	536
				514.42	1000.0	
Energy requirement for polymerisation						**20.37**

[a] water is substracted from MW to account for water excretion during peptide bond formation

Table 2.3 Protein composition (Cocaign-Bousquet *et al* . (1996):
The amino acids composition determined for *C. glutamicum* ATCC 17965 is taken from (Cocaign-Bousquet et al. (1996)) Energy requirement for polymerisation was taken as for *E. coli* (Neidhardt *et al* . (1987).

Amino acid	**µmol/g DW**	**MW**	**MW[a] substracted water**	**mg/g DCW**	**mg/g protein**	**mmol/g protein**
Alanine	725	89.09	71.09	51.54	109.5	1394
Arginine	190	175.21	157.21	29.87	63.4	365
Asx (asp + asn)	374	132.6	114.6	42.86	91.0	719
Cysteine	1	121.15	103.15	0.10	0.2	2
Glutamate	486	147.13	129.13	62.76	133.3	935
Glutamine	486	146.2	128.15	62.28	132.3	935
Glutamate-intra	0	147.13	129.13	0.00	0.0	0
Glutamine-intra	0	146.2	128.15	0.00	0.0	0
Glycine	344	75.07	57.07	19.63	41.7	662
Histidine	63	156.16	138.16	8.70	18.5	121
Isoleucine	175	131.17	113.17	19.80	42.1	337
Leucine	262	131.17	113.17	29.65	63.0	504
Lysine	171	146.19	128.19	21.92	46.6	329
Methionine	5	149.21	131.21	0.66	1.4	10
Phenylalanine	123	165.19	147.19	18.10	38.4	237
Proline	148	115.13	97.13	14.38	30.5	285
Serine	265	105.09	87.09	23.08	49.0	510
Threonine	270	119.12	101.12	27.30	58.0	519
Tryptophan	1	204.23	186.23	0.19	0.4	2
Tyrosine	74	181.19	163.19	12.08	25.6	142
Valine	262	117.14	99.14	25.97	55.2	504
				470.88	1000.0	
Energy requirement for polymerisation						**19.05**

[a] water is substracted from MW to account for water excretion during peptide bond formation

Protein biosynthesis equation is therefore (in mmol for synthesis of Protein for 1 g Biomass DW):
0.666 ALA + 0.190 ARG + 0.194 ASN + 0.194 ASP + 0.44 CYS + 0.342 GLN + 0.548 GLU + 0.353 GLY + 0.067 HIS + 0.189 ILE + 0.351 LEU + 0.187 LYS + 0.76 MET + 0.128 PHE + 0.159 PRO + 0.245 SER + 0.273 THR + 0.028 TRP + 0.078 TYR + 0.273 VAL + 19.71 ATP -> 19.71 ADP + 19.71 PI + PROTEIN

Table 3. DNA composition:
The composition of DNA was calculated from the genomic sequence of *C. glutamium* ATCC 13032, Biedefeld. Energy requirement for polymerisation of triphosphates was from Neidhardt *et al* ., (1987).

Nucleotide	mol/mol DNA	MW[a], g/mol	mmol/g DNA
dAMP	0.231	313.2	0.748
dCMP	0.269	289.2	0.871
dTMP	0.231	304.2	0.748
dGMP	0.269	329.2	0.871
Energy requirement for polymerisation (ATP):			**4.44**

[a] the molecular weight is the weight of the nucleotide monophosphate substracted 1 water, which is lost during esterification

DNA biosynthesis equation is therefore (in mmol for synthesis of 1 g DNA):
0.748 DAMP + 0.871 DCMP + 0.748 DTMP + 0.871 DGMP + 4.44 ATP -> 4.44 ADP + 4.44 PI + 3.238 PPI + DNA

Table 4. RNA composition:

It was assumed that RNA consisted of 5% mRNA, 75% rRNA and 20% tRNA (molar). The nucleotide composition of mRNA was taken as for genomic DNA. The nucleotide composition of rRNA was calculated from the sequences of 16S, 23S and 5S ribosomal RNA units. tRNA composition was found from sequences of tRNAs. All the sequences were obtained from GenBank (http://www.ncbi.nlm.nih.gov). Energy requirement for polymerisation of triphosphates was from Neidhardt *et al.* , (1987).

Nucleotide	mol/mol RNA			MW[a],	mol/mol	mmol/g RNA		
	mRNA	rRNA	tRNA					
	5%	75%	20%	g/mol	RNA			
AMP	0.231	0.227	0.197	329.2	0.221	0.69	0.221	
GMP	0.269	0.334	0.314	345.2	0.327	1.01	0.327	
CMP	0.231	0.211	0.272	305.2	0.224	0.70	0.224	
UMP	0.269	0.227	0.217	306.2	0.227	0.70	0.227	3.10
Energy requirement for polymerisation (ATP):						1.24	1.000	1.00

[a] the molecular weight is the weight of the nucleotide monophosphate substracted 1 water, which is lost during esterification

RNA biosynthesis equation is therefore (in mmol for synthesis of 1 g RNA):

0.69 ATP + 1.01 GTP + 0.70 CTP + 0.70 UTP + 1.24 ATP -> 1.24 ADP + 1.24 PI + RNA + 3.10 PPI

The two major lipids in *C. glutamicum* are phospholipids and mycolic acids. The ratio between the two were estimated using the data of Puerch *et al*. (2001) (22% phospholipids and 78% mycolic acids of total lipid fraction).

Table 5.1 Composition of total fatty acids in C. glutamicum:
The composition of fatty acids was taken from Collins et al (1982)

Fatty acid	g/g total fatty acids	MW[a], g/mol	mmol/g total fatty acids	mol/mol total fatty acids
C14	0.005	227	0.02	0.006
C15	0.010	241	0.04	0.011
C16	0.415	255	1.63	0.437
C16:1	0.010	255	0.04	0.011
C18	0.010	281	0.04	0.010
C18:1	0.550	281	1.96	0.526
Average molecular weight:		269	SUM:	1.00

Table 5.2 Phospholipids composition:
Data for the composition of phospholipids was taken from Hoichen & Krämer (1990). Biosynthesis of phospholipids components is included in the reaction set. Fatty acids for the biosynthesis are supplied in an activated form - conjugated to acyl-carrier protein (ACP), so no additional ATP was included in the reaction.

Component	g/g phospholipids	mmol/g
Phosphatic acid (PA)	0.03	0.033
Phosphatidylglycerol (PG)	0.87	1.133
Cardiolipin (DPG)	0.01	0.007
Phosphatidyllinositol (PI)	0.032	0.042
Phosphatidyllinositol mannoside (PIM)	0.049	0.065
SUM:	0.99	

Phospholipids biosynthesis equation is therefore (in mmol for synthesis of 1 g phospholipids):
0.033 PA + 1.133 PG + 0.007 CL + 0.042 PIT + 0.065 PIM -> PHOSPHOLIPID

Table 5.3 Molecular weights of phospholipids components:

Constituent	MW, g/mol		
	backbone	# of fatty acids	total
Phosphatic acid (PA)	200	2	756
Phosphatidylglycerol (PG)	212	2	768
Cardiolipin (DPG)	332	4	1444
Phosphatidyllinositol (PI)	200	2	756
Phosphatidyllinositol mannoside (PIM)	200	2	756
Average molecular weight:			896

Table 5.4 Composition of fatty acids in phospholipids:
Data for the composition of fatty acids in phospholipids was taken from (Houchen & Krämer (1990)

Fatty acid	g/g total phospholipid	MW[a] g/mol	mmol/g total fatty acids	mol/mol total fatty acids
C14	0.003	227	0.01	0.004
C15	0.000	241	0.00	0.000
C16:0	0.402	255	1.58	0.438
C16:1	0.004	253	0.02	0.004
C18:0	0.010	283	0.04	0.010
C18:1	0.550	281	1.96	0.544
SUM	0.969			
Average molecular weight:		278	SUM:	1.000

[a] molecular weight without a proton

Example: phosphatidylethanolamine biosynthesis equations are therefore (in mol):
GL3P + 0.004 C140ACP + 0.438 C160ACP + 0.004 C161ACP + 0.010 C180ACP + 0.544 C181ACP -> AGL3P + ACP

AGL3P + 0.004 C140ACP + 0.438 C160ACP + 0.004 C161ACP + 0.01 C180ACP + 0.544 C181ACP -> PA + ACP

PA + CTP <-> CDPDG + PPI

CDPDG + SER <-> CMP + PS

PS -> PE + CO2

Table 5.5 Mycolic acids
No exact data on fatty acid composition of mycolic acids could be found. The composition of fatty acids in mycolic acids were considered to be the same as for total fatty acid composition minus fatty acids used for phospholidids.
Phospholipid fraction of total lipid fraction: **22%**

Fatty acid	g/g total fatty acids	MW[a], g/mol	mmol/g total fatty acids	mol/mol total fatty acids
C14	0.004	227	0.02	0.007
C15	0.010	241	0.04	0.014
C16	0.327	255	1.28	0.437
C16:1	0.009	255	0.04	0.012
C18	0.008	281	0.03	0.009
C18:1	0.429	281	1.53	0.521
Average molecular weight:		341	SUM:	1.00

Free mycolic acid biosynthesis equation is therefore (in mmol for synthesis of 1 g free mycolic acid):
0.007 C140ACP + 0.014 C150ACP + 0.437 C160ACP + 0.012 C161ACP + 0.009 C180ACP + 0.521 C181ACP -> ACP + FREEMYCOLICACID

Table 5.6. Mycolic acid composition:
Data for the composition of mycolic acids was estimated from from Purch *et al*. (2001).

Component	g/g mycolic acid	MW g/mol	mmol/g Mycolic
Trehalose monocyrynomycolate (TMCM)	0.05	822	0.061
Trehalose dicyrynomycolate (TDCM)	0.05	1164	0.043
MYCOLIC ACID Free	0.90	480	1.875
Molecular weight (mycolic acid with C32)		480	

Mycolic acid biosynthesis equation is therefore (in mmol for synthesis of 1 g mycolic acid):
0.061 TMCM + 0.043 TDCM + 1.875 FREEMYCOLICACID -> MYCOLICACID

Table 6.1. Peptidoglycan composition:

Peptidoglycan is one of the main components of the bacterial cell wall. Its composition is the same as for *E. coli*, and data was taken as from Integram *et al.* (1983). This data was corrected so data was for the synthesis of 1 g peptidoglycan. The blocks of the glycan chain are supplied in the activated form (UDP-NAG and UDP-NAM), therefore energy is needed only for the pentapeptide formation (ATP -> ADP per mol of amino acid joined). Half of the alanine in the peptidoglycan was assumed to be D-alanine. D-alanine joins the growing amino acids chain as D-alanyl-D-alanine. The fifth D-alanine residue is cleaved extracellularly to allow bond formation between diaminopimelinic acid and the fourth residue (Integram *et al.* (1983)).

Component	molar ratio in peptidoglycan:	Average	MW[a], g/mol	mmol/g peptidoglycan
N-acetylmuramic acid	1	1.0	275	1.026
N-acetylglucosamine	1	1.0	203	1.026
L-Alanine	1	1.0	71	1.026
Diaminopimelinic acid	1	1.0	154	1.026
D-glutamate	1	1.0	129	1.026
D-Alanine	2	2.0	71	2.052
Energy requirement for polymerisation (ATP):				**5.129**

[a] the molecular weight is substracted water to account for the bond formation

Peptidoglycan biosynthesis equation is therefore (in mmol for synthesis of 1 g peptidoglycan):
1.106 UDPNAM + 1.106 UDPNAG + 1.106 ALA + 1.106 MDAPIM + 1.106 DGLUTAMATE + 2.052 ALAALA + 4.426 ATP -> PEPTIDOGLYCAN + 4.426 ADP + 4.426 PI + 1.106 UDP + 1.106 UMP + 1.026 ALA

Table 6.2. Arabinogalactan composition:

The cell wall carbohydrates composition was assumed to be identical to *C. glutamicum* CGL2005 (Puech et al (2001)). The polysaccharide is made from activated building blocks, therefore there is no need for additional ATP during polymerisation.

Component	Molar ratio	MW[a], g/mol	mmol/g carbohydrate
Arabinose	9	203	4.650
Galactose	1	162	0.498
		183	5.147

[a] the molecular weight is substracted water to account for the bond formation

Arabinogalactan biosynthesis equation is therefore (in mmol for synthesis of 1 g Arabinogalactan):
0.498 UDPGAL + 4.650 UDPARA -> 5.148 UDP + ARABINOGALACTAN

Table 7.1. Energy requirement for polymerisation of macromolecules:
Energy requirements for polymerisation of macromolecules was estimated using values from *E. coli* (Neidhardt *et al*. (1987))

Process	**Energy reqirement**
Protein synthesis and processing	*(mmol ATP · (mmol aminoacid)$^{-1}$)*
Activation and incorporation	4.0
mRNA synthesis	0.2
Proofreading	0.1
Assembley and modification	0.006
SUM	**4.306**
RNA synthesis and processing	*(mmol ATP · (mmol RNA)$^{-1}$)*
Discharging segments	0.38
Modification	0.02
SUM	**0.40**
DNA synthesis and processing	*(mmol ATP · (mmol DNA)$^{-1}$)*
Unwinding helix	1.0
Proofreading	0.36
Discontinous synthesis	0.006
Negative supercoiling	0.005
Methylation	0.001
SUM	**1.372**

Appendix II: References

Cocaign-Bousquet M, Guyonvarch A, Lindley ND. Growth rate-dependent modulation of carbon flux through central metabolism and the kinetic consequences for glucose-limited chemostat cultures of *Corynebacterium glutamicum* .

Collins MD, Goodfellow M, Minnikin DE. Fatty acid composition of some mycolic acid-containing coryneform bacteria. Journal of General Microbiology 1982;128:p 2503-2509.

Daffé M. The Cell Envelope of Corynebacteria, In: Eggeling L, Bott M editors. Handbook of *Corynebacterium glutamicum* . Boca Raton: CRC Press; 2005, p 121-148.

Hoischen C, Krämer R. Membrane alteration is necessary but not sufficient for effective glutamate secretion in *Corynebacterium glutamicum* . Journal of Bacteriology 1990;172:p 3409-3416.

Ingraham JL, Maaløe O, Niedhardt FC. Growth of the Bacterial Cell. Sunderland, Massachusetts: Sinauer Associates, Inc.; 1983.

Keddie RM, Cure GL. Cell-wall Compsition of Coryneform Bacteria, In: Bousfield IJ, Calley AG editors. Coryneform Bacteria. London: Academic Press; 1978, p 47-84.

Marx A, de Graaf AA, Wiechert W, Eggeling L, Sahm H. Determination of the fluxes in the central metabolism of Corynebacterium glutamicum by nuclear magnetic resonance spectroscopy combined with metabolite balancing.

Niedhardt FC, Ingraham JL, Low KB, Magasanik B, Schaechter M, Umbarger HE. *Escherichia coli* and *Salmonella typhimmurium* Cellular and Molecular Biology. Washington DC: ASM; 1987.

Puech V, Chami M, Lemassu A, Laneelle MA, Schiffler B, Gounon P, Bayan N, Benz R, Daffe M. Structure of the cell envelope of corynebacteria: importance of the non-covalently bound lipids in the formation of the cell wall permeability